AN ABSTRACT OF THE DISSERTATION OF

Pallavi A. Phatale for the degree of Doctor of Philosophy in Botany and Plant Pathology presented on December 10, 2012.

Title: Studies on the Centromere-Specific Histone, CenH3, of *Neurospora crassa* and Related Ascomycetes.

Abstract approved:

Michael Freitag

In eukaryotes, the defined loci on each chromosome, the centromeres, accomplish the critical task of correct cell division. In some organisms, centromeres are composed of a euchromatic central core region embedded in a stretch of heterochromatin and the inheritance and maintenance of centromeres are controlled by dynamic epigenetic phenomena. Although the size of centromeres differs between organisms, its organization, and the placement of euchromatic and heterochromatic regions is conserved from the fission yeast, *Schizosaccharomyces pombe*, to humans, *Homo sapiens*. However, relatively little is known about centromeres in the filamentous fungi from the Ascomycota, representing the largest group of fungi and fungal pathogens. Further, studies from humans, flies, yeast and plants have shown

that the inheritance of centromeres is not strictly guided by centromeric DNA content, which is highly AT-rich, repetitive and constantly evolving. Therefore, it is difficult to align ans assemble the sequenced contigs of centromeric regions of higher eukaryotes, including most filamentous fungi. A genetic technique, tetrad (or octad) analysis has helped to map the centromeres of the filamentous fungus *Neurospora crassa* early on. The research presented in this dissertation used *N. crassa* as a model to focus on characterizing different features of centromeres with an emphasis on the centromere-specific histone H3 (CenH3) protein. Data included here represent the first study on centromere-specific proteins in *Neurospora*, and demonstrate that the central core of the centromeres are heterochromatic, showing enrichment of silent histone marks, which is in contrast to the centromere arrangement in fission yeast. The CenH3 protein, whose deposition on the genome licenses formation or maintenance of centromeres, shows highly divergent N-terminal regions and a conserved histone fold domain (HFD) in all eukaryotes. This bipartite nature of CenH3 is also observed in the Ascomycota, which provides an opportunity for functional complementation assays by replacing Neurospora CenH3 (NcCenH3) with CenH3 genes from other species within the Ascomycota. The results from this experimental approach provide good measures for (1) determining the specific regions of CenH3 required for the assembly of centromeres during meiotic and mitotic cell divisions and (2) analyzing the resistance to changes in the organization of centromeres in *N. crassa*.

The genetic analysis showed that the divergent N-terminal region is essential for the proper assembly of centromeres, and that the conserved carboxy-terminus of CenH3 is important for the process of meiosis but not mitotic cell division. ChIP-seq

analyses suggest that the observed loss of *Podospora anserina* CenH3 (PaCenH3-GFP) from certain *N. crassa* centromeres does not result in obvious phenotypic defects, e.g. diminished growth or evidence for aneuploidy. Further, the low enrichment of PaCenH3-GFP at certain centromeres is possibly predetermined during meiosis, which results in irreversible and progressive decreases in enrichment. It remains to be determined if this process is random as far as selection of centromeres is concerned. Together the results presented here suggest that during meiosis more stringent structural requirements for centromere assembly apply and that these are dependent on CenH3, and that depletion of CenH3 from centromeres does not critically affect mitosis in the asynchronously dividing nuclei of *Neurospora* hyphae.

Studies on the Centromere-Specific Histone, CenH3, of *Neurospora crassa* and Related Ascomycetes

by

Pallavi A. Phatale

A DISSERTATION

submitted to

Oregon State University

in partial fulfillment of
the requirements for the
degree of

Doctor of Philosophy

Presented December 10, 2012

Commencement June 2013

Doctor of Philosophy dissertation of Pallavi A. Phatale, presented on December 10, 2012.

APPROVED:

Major Professor, representing Botany and Plant Pathology

Head of the Departmant of Botany and Plant Pathology

Dean of the Graduate School

I understand that my dissertation will become part of the permanent collection of Oregon State University libraries. My signature below authorizes release of my dissertation to any reader upon request.

Pallavi A. Phatale, Author

ACKNOWLEDGEMENTS

First, and foremost, I thank my advisor, Dr. Michael Freitag, for the guidance, encouragement, freedom to follow my interests and career advice you provided to me over the last five years. Your patience and transparency to students made working with you easier.

The challenging discussions with my thesis committee members, Dr. Todd Mockler, Dr.Dan Rockey, Dr.Thomas Wolpert and Dr. Dahong Zhang and their insightful suggestions have been very helpful in improving my scientific thinking and presentation skills. I thank you all for taking time and showing interest in my development. I am thankful to my department for providing me the opportunity to achieve the doctoral training and the financial support.

I express my sincere thanks to Kristina Smith and Lanelle Connolly for their guidance and constant help. Your company always felt like my family. I would like to thank Jonathan Galazka and my peer graduate students Erin Bredeweg, Kyle Pomraning and Steven Friedman.

Most importantly, I thank my parents, my sister Ketaki, my guru Jagdish Subandh, my husband Sangeet Lal and my in-laws for being a constant source of love and encouragement and for providing me the freedom to pursue my passion for science.

Dedicated to my

Grandparents...

CONTRIBUTION OF AUTHORS

Chapter 1: Pallavi A. Phatale wrote the chapter.

Chapter 2: Pallavi A. Phatale performed the bulk of the experiments and data analysis. Minor contributions were from Kristina M. Smith, Joseph Mendoza, Lanelle R. Connolly and Michael Freitag. Pallavi A. Phatale, Kristina M. Smith and Michael Freitag wrote the manuscript.

Chapter 3: Experiments were performed by Pallavi A. Phatale and data were analyzed by Pallavi A. Phatale, Kristina M. Smith and Michael Freitag. Pallavi A. Phatale and Michael Freitag wrote the manuscript.

Chapter 4: Experiments were performed and data were analyzed by Pallavi A. Phatale. Pallavi A. Phatale wrote the chapter.

Chapter 5: Pallavi A. Phatale wrote the chapter.

TABLE OF CONTENTS

Page

INTRODUCTION: COMPARATIVE CENTROMERE BIOLOGY 1
CENTROMERIC DNA 4
CONSERVED FEATURES OF CENTROMERES IN DIVERSE ORGANISMS 6
NEOCENTROMERES AND HOLOCENTROMERES 10
KINETOCHORE PROTEINS 13
NEUROSPORA CENTROMERES 23

THE CARBOXY-TERMINUS OF *NEUROSPORA CRASSA* CENH3 IS REQUIRED FOR MEIOSIS-SPECIFIC FUNCTIONS 36
ABSTRACT 37
INTRODUCTION 39
MATERIALS AND METHODS 43
Strains 43
DNA isolation and Southern analysis 44
Sequence analysis 44
Plasmids and fusion PCR constructs 45
Strain construction 46
Crosses to test meiotic/mitotic function of CenH3s 48
Fluorescence microscopy 49
Assay for linear growth in Ryan ("race") tubes 49
Spot tests on inhibitors 50
RESULTS 50
Phylogenetic analyses of CenH3 from filamentous fungi 50
Is positive selection acting on CenH3 from filamentous fungi? 53
Ectopically inserted CenH3 genes from three different filamentous fungi are targeted to chromocenters in N. crassa 54
Replacement of native CenH3 by CenH3-GFP from three filamentous fungi 57
The CenH3 C-terminal tail is essential during meiosis 59
DISCUSSION 65
Phylogenetic analyses of CenH3 sequences of filamentous fungi 65
Genetic analyses of CenH3 sequences of filamentous fungi 67
PaCenH3 and FgCenH3 complement NcCenH3 function 68
The CenH3 C-terminus has conserved function in kinetochore assembly 70
The N-terminal tail is dispensible for centromere localization but required for meiosis 70
CONCLUSION 71

TABLE OF CONTENTS (Continued)

Page

CENH3-DEFICIENT NEUROSPORA CENTROMERES REMAIN COMPETENT FOR MITOSIS BUT ARE DEFECTIVE DURING MEIOSIS 102
ABSTRACT 103
INTRODUCTION 104
MATERIALS AND METHODS 110
Cloning and fusion PCR constructs 110
Strains and growth media 111
Assay for linear growth in Ryan (race) tubes 111
Assay to detect live cells by AlamarBlue staining 112
Isolation of genomic DNA and Southern analysis 112
Quantitative PCR (qPCR) 112
Chromatin immunoprecipitation and high-throughput sequencing (ChIP-seq) . 113
RESULTS 114
Chimeras of the Nc- or PaCenH3 N-terminal tail with the FgCenH3 HFD are unable to complete meiosis 114
Decreased enrichment of PaCenH3-GFP at some Neurospora centromeres .. 116
Presence of PaCenH3-GFP at Neurospora centromeres causes slightly slower linear growth 117
Loss of PaCenH3-GFP from certain centromeres is irreversible and progressive 120
Epigenetic states of centromeres are maintained in presence of PaCenH3-GFP 124
Centromere DNA sequences are unaltered in the strains having PaCenH3-GFP 126
Depletion of PaCenH3-GFP from certain centromeres does not result in aneuploidy 127
Fertile progeny from backcrosses exclude translocations or chromosome fusions 128
DISCUSSION 129
IN VIVO STUDIES ON THE COMPOSITION OF CENTROMERIC NUCLEOSOMES IN *NEUROSPORA CRASSA* 160
ABSTRACT 161
INTRODUCTION 162
MATERIALS AND METHODS 163
Cloning and strain construction 163
Fluroscence microscopy and Southern blotting 166
ChIP-seq assay 166

TABLE OF CONTENTS (Continued)

Page

Screening strains by western blotting *166*
Co-immunoprecipitation *167*
RESULTS 168
The double tagged N-terminal NcCenH3 co-localize at centromere *168*
NcCenH3 nucleosomes are homotypic dimers *169*
The C-terminal GFP tagged H2AZ is not localized at Neurospora centromeres *172*
DISCUSSION 172
GENERAL SUMMARY AND CONCLUSIONS 187
SUMMARY AND CONCLUSIONS 188
FUTURE WORK 192
SIGNIFICANCE 196
APPENDIX 1: LIST OF ADDITIONAL MANUSCRIPTS PUBLISHED OR ACCEPTED. 197
REFERENCES 198

LIST OF FIGURES

Figure Page

Figure 1.1: Centromere organizations in different organisms. 30
Figure 1.2:Cartoon of chromosome territories on replicated and condensed metaphase chromosomes during mitotic cell division. 31
Figure 1.3: Arrangement of centromere or kinetochore protein complexes. 32
Figure 1.4: Expanded view of ChIP-seq read counts for CenH3 and H3K9me3 aligned to predicted transposon relics in centromeric regions on LG IV. 33
Figure 1.5: Localization of centromere proteins and epigenetic modifications in *Neurospora crassa* centromere II (*Cen-II*) by ChIP-sequencing. 34
Figure 1.6: Changes in centromere size in *dim-5* and *hpo* mutants. 35
Figure 2.1: Phylogenetic relationship between CenH3 genes of filamentous fungi. 84
Figure 2.2: Phylogenetic relationships between CenH3 genes of species in the genera *Neurospora*, *Gelasinospora* and *Sordaria*. 85
Figure 2.3: Positive selection on the N-terminus but negative selection on the histone-fold domain of CenH3 from selected *Neurospora* species and strains. 87
Figure 2.4: Calculation of Pi(a) over Pi(s) ratios within the CenH3 coding regions suggest a small region under positive selection within the N-terminus. 88
Figure 2.5: Gene and protein structure, and sequence alignments of CenH3 from four filamentous fungi used for functional studies. 89
Figure 2.6: Ectopic integration of CenH3-GFP from four filamentous fungi at *his-3* results in proper targeting to centromere foci. 91
Figure 2.7: Integration of CenH3 genes from four filamentous fungi at *N. crassa hH3v* (CenH3) results in proper targeting to centromere foci. 94
Figure 2.8: Linear growth assay in Ryan tubes. 97
Figure 2.9: Fluorescence intensity measurements. 98
Figure 2.10: Growth of tagged and non-tagged CenH3 strains in the presence of various concentrations of TBZ and HU. 99
Figure 2.11: Working model for centromere structure during mitosis and meiosis I in the patches containing CenH3 nucleosomes. 101

LIST OF FIGURES (Continued)

Figure Page

Figure 3.1: General structure of four different fungal CenH3 genes and proteins and chimeric constructs generated for this study....143
Figure 3.2: Sequence alignments of several CenH3 proteins and results of linear growth assays with PaCenH3 strains....145
Figure 3.3: Enrichment of PaCenH3-GFP at *Neurospora* centromeres....147
Figure 3.4: Slight growth defects occur in strains with PaCenH3....149
Figure 3.5: Irreversible loss of PaCenH3-GFP enrichment at certain centromeres after extended vegetative growth....151
Figure 3.6: Progressive loss of PacenH3-GFP enrichment at some centromeres after extended linear growth....153
Figure 3.7: Enrichment of PacenH3-GFP at certain centromeres after extended linear growth....155
Figure 3.8: Epigenetic states of Neurospora centromeres in presence of PaCenH3-GFP....156
Figure 3.9: SNP coverage map for defective centromeres....157
Figure 3.10: qPCR data to test aneuploidy centromere defective strains....159
Figure 4.1: Model depicting homotypic and heterotypic nucleosomes at centromeres....178
Figure 4.2: Maps of various constructs used in this study....180
Figure 4.3: Analysis of correct double-tagged NcCenH3 strains....181
Figure 4.4: Fluorescence microscopy and ChIP-seq data for NcH2AZ-GFP....183
Figure 4.5: Co-immunoprecipitation assay determining homotypic dimer of NcCenH3....185
Figure 4.6: Western blot results for GFP antibody probing on the the immuno-precipitated sample using GFP and RFP magnetic beads....186

LIST OF TABLES

Table Page

Table 2.1: Strains used in this study. 74
Table 2.2: Oligos used in this study. 77
Table 2.3: Accession numbers for H4-2 and CenH3 sequences that were used to build phylogenetic trees. 78
Table 2.4: Results from crosses between strains with tagged and non-tagged versions of different fungal CenH3 genes. 80
Table 2.5: Ascospore germination frequency. 82
Table 3.1: Strains used in this study. 140
Table 3.2: Oligos used for the PCR amplification of genes for chimera cloning and qPCR. ..141
Table 4.1: Neurospora strains used in this study. 176
Table 4.2: Oligonucleotides used as primers for PCR. 177

Introduction: Comparative centromere biology

Pallavi A. Phatale

Genome stability and duplication are essential for the survival of eukaryotic cells and both phenomena require intact centromeres. Initially, the term “centromere” was reserved for the specialized DNA required for chromosome segregation alone, but as we will see below, “centromere” and “kinetochore”, i.e. the protein complex that “moves” chromosomes, have become almost interchangeable terms. In this review, I describe what is known about centromeric DNA in various organisms and discuss the various components of the centromere/kinetochore and how they function during cell division. While many of the proteins involved are generally conserved, fungi – the subjects of my investigations – have many specialized components, and I will discuss differences between vertebrate and fungal biology where appropriate. At the end of this introduction, I discuss what has been learned about centromeres in the filamentous fungi, a large and diverse group of organisms, essential for life on Earth as decayers of biomass, that also includes a large number of destructive plant pathogens and an alarmingly growing set of animal and human pathogens.

Centromeres in many eukaryotes form unique loci on each chromosome whose DNA sequence, size and protein components are organism-specific. In contrast, many eukaryotes have centromere elements distributed along the whole chromosome, resulting in “holocentric” chromosomes (183). While previously considered exclusively a feature of eukaryotic chromosomes, recent studies revealed that prokaryotes also have specialized partitioning systems, Low copy number plasmids contain genes, such as *par* on P1, *sop* on F and *ParA* on R1, to aid in DNA segregation by assembling a specific partitioning complex that mimics some aspects of eukaryotic centromeres. In the R1 plasmid *parA* system the ParR protein binds specific DNA, *parC* repeats, along with ParM, a protein with ATPase activity that is

required for plasmid partitioning (135). Similar functions have been described for the ParA and ParB proteins of the P1 plasmid, and SopA and SopB of the F plasmid (63, 135). These bacterial centromere-like partitioning systems, positioned proximally to the origin of replication (*oriC*) are considered a functional counterpart of eukaryotic centromere (18). A recent hypothesis suggests that circular bacterial plasmids with partitioning systems might have played a role in the evolution of modern centromeres (316). It was proposed that the birth of telomeres to maintain linear plasmids in ancestral proto-eukaryotic cells may have triggered formation of proto-centromeres. During evolution of eukaryotic centromeres, switching from actin filament attachment in PAR systems to microtubule and ribonucleoprotein binding in eukaryotic centromeres may have further increased the specificity of the centromeric loci (316). Of course, one of the major differences between bacterial partitioning systems and modern centromeres is the added complexity generated by the wrapping of DNA around nucleosomes that contain histones, which are presumably of archebacterial origin (61). As we will see below, histone composition and modification regulates the spatio-temporal organization of nucleosomes in eukaryotic centromeres.

The size of modern centromeres in eukaryotes ranges from 0.125 kb in the budding yeast *Saccharomyces cerevisiae* to an average of 1,500 – 3,000 kb in humans and plants, suggesting an overall positive correlation between genome size, and especially the size of the repetitive fraction of a genome, and centromere size (54, 332). Based on the position of the centromeric locus chromosomes are classified into different types, i.e. metacentric, acrocentric and telocentric. When the centromere divides chromosome arms into roughly equal parts, a chromosome is called metacentric, in contrast to submetacentric chromosomes where chromosomal arms

are unequal. In acrocentric chromosomes centomeres are positioned very close to one chromosomal end, whereas in telocentric chromosomes the centromeres are located close to the termini of chromosomes.

Centromeric DNA

Centromeres in the budding yeasts, e.g. *Saccharomyces cerevisiae*, *Candida glabrata*, *Kluyveromyces lactis*, *and Ashbya gossypii* have a single centromeric nucleosome, which results in centromere sizes of 0.125 – 0.225 kb, an arrangement also called “point centromere” (Figure 1.1). The centromeric DNA sequences in these organisms have conserved DNA elements (CDEI, CDEII and CDEIII) that are sufficient to assemble a functional centromere. CDEI and CDEIII are separated by CDEII, which is critical for binding of centromere binding factor 3 (CBF3) and for correct kinetochore assembly (54). Single base mutations in the binding sites within CDEI and CDEIII can cause chromosome loss (118). Thus, in the budding yeasts, DNA sequence determines the genetic locus and guides the organization of centromeres, therefore showing similarity to the features of PAR systems in bacteria mentioned above. Further, based on evolutionary analysis it has been suggested that point centromeres may have emerged from regional centromeres due to loss of the RNAi machinery; however, several studies have determined the presence of the RNAi machinery in Saccharomycetes except *S.cerevisiae* (74, 174, 186). Hence, the question regarding the origin of evolution of point centromeres still remains unanswered. Regional centromeres, characterized by an increasing complexity of AT-rich repeated DNA elements and found in *Schizosaccaromyces pombe*, *Candida albicans* and most higher organisms, contain arrays of centromere-specific

nucleosome interspersed with canonical histone H3 nucleosomes and range in size from 3 kb – 1500 kb (54, 174) (Figure 1.1).

In *S.pombe*, the three regional centromeres (*cen1*, *cen2* and *cen3*) differ drastically in size (38, 65 and 97 kb, respectively) but share a conserved basic structure, each unit consisting of a central core (*cc*) flanked by inverted innermost repeats (*imr*). Adjacent to the *imr* regions lie the outer tandem repeats (*otr*), which consist of three different repeat units, the *dg*, *dh* and *cen253* repeats (Figure 1.1). These repeats vary in their number as well as orientation within each chromosome, suggesting divergence in the centromeric DNA sequences. Further, the *otr* divergence is also seen when individual *cen2 otr* or *cen3 otr* sequences were compared among various strains of *S.pombe*, while this is not true for the *cen1 otr*, which are conserved (2, 219, 275). While there is a high degree of variation between the three centromeres of *S. pombe*, *dg* repeat units are highly conserved (~97%) and are important during meiotic as well as mitotic cell division. The *dg* repeats are not transcribed but there are transcriptionally active tRNA clusters present in the flanking regions of *cen2* and *cen3* that are also found within the *imr* regions of all three centromeres (292). Genetic and biochemical studies show that these tRNA genes might be functioning as boundary elements for centromeres and thus prevent the spreading of specialized chromatin at the centromere locus (213).

Small regional centromeres of *C. albicans* cover ~3 – 5 kb of unique DNA sequences on each of the eight chromosomes (246) (Figure 1.1). The centromeric DNA lacks specific conserved repeats or boundary elements and also differs among closely related *Candida* species (17, 207). Overall, centromeric DNA in the best

studied fungal systems thus shows very well conserved DNA elements in *S. cerevisiae* and less conserved repeats in *S.pombe*, which all bear essential cues for centromere assembly, while this process seems to be completely epigenetic (i.e. independent of DNA sequence) in *C.albicans*.

Similar to *C.albicans* and *S.pombe*, regional centromeres of higher eukaryotes (i.e. humans, invertebrates, and plants) consist of long stretches of repeating satellite DNA monomers along with transposable elements and range between 1-10 Mb in size (22, 81, 111, 192, 262, 283) (Figure 1.1). Due to the repetitive nature of satellite DNA at centromeres, “sequence homogenization” is thought to be a very common phenomenon, occurring by diverse molecular mechanisms such as unequal crossover (179), gene conversion (266), rolling circle replication and reinsertion, and transposon-mediated exchange (295). The eventual outcome of homogenization between centromeric satellite DNA is a new, composite high-order-repeat (HOR), which are supposedly highly conserved and distinct between species, e.g. in humans the alpha satellite HORs are typically 97–100% identical (218). Hence, it is possible that these HORs can be fixed in the population and thus can provide a starting substrate for speciation.

Conserved features of centromeres in diverse organisms

Centromeres are atypical “structural” genetic loci because they are often large specialized chromosomal regions that are essential for guiding cell division and chromosome segregation. Much of the previous section was devoted to underscore how different the actual DNA sequences of centromeres are, even in closely related organisms. This suggests that centromeres are extremely quickly evolving loci. To

maintain genome integrity by preventing the spreading of the centromere over the arms of the chromosomes, which contain protein-coding genes, boundary elements are thought to be present. As mentioned earlier, tRNA clusters mark the boundary of the centromere in *S. pombe*, however, this feature is not conserved in other eukaryotes. Alternatively, the point centromeres from budding yeast, as well as regional centromeres from other organisms except *C.albicans* (17) are enclosed in "pericentric" regions that mark the centromere boundary. The presence of pericentric regions adds to centromere locus specificity by providing an additional "surface" or "anchor" for exclusive protein-protein or protein-DNA interactions, and is known to aid in regulation of centromere functioning during various stages of the cell cycle. Generally, the pericentric regions in fission yeast, plants, mammals and flies are composed of repetitive DNA sequences that are transcriptionally silent, but in budding yeast there are Chromatin Assembly Factor-1 (CAF-1) protein-binding sites within 1-2 kb around the single centromeric nucleosome and kinetochore (263). These CAF-1 binding sites are essential for correct centromere assembly because they help to maintain centromere integrity in *S. cerevisiae* (263). In fission yeast, the centromere DNA bound CAF-1 complex interacts with Hip1, a HirA-like histone chaperone, that helps to recruit Swi6, a homologue of HP1 (Heterochromatin Protein 1) that is necessary for transcriptional silencing of pericentric heterochromatin on regional centromere of fission yeast (26). Similar effects have been seen in human cells (333).

In regional centromeres transcripts are often generated within pericentric regions and these "aberrant transcripts" may - with the help of the RNAi machinery - recruit heterochromatin factors that maintain heterochromatin histone marks on histone H3 and H4 in pericentric region (110). Several specific histone marks have

been identified in the pericentric region of diverse organisms, for example methylation of H3 lysine residue 9 (H3K9me2 and H3K9me3), Lys27 (H3K27me2 and H3K27me3) and H4 Lys20 (H4K20me3) (Figure 1.1) (110). These histone modification marks serve as platforms for sister chromatid cohesin deposition during mitosis and interestingly, loss of H4K20me3 results in aneuploidy (21, 110, 314). Thus, the chromatin silencing function of pericentric regions depends on the RNAi and heterochromatin machinery in fission yeast (230), as well as in other organisms like in *Drosophila*, *Arabidopsis* and rice (167, 198). Moreover, the sequence-specific transcription factors Pax3 and Pax9 that have redundant functions were identified in mouse and seem to play a role in maintaining heterochromatin at the pericentric regions (33) (Figure 1.1).

For a region that was long considered the stereotypical example of silent chromatin, it was surprising that recent studies revealed that H3 nucleosomes of the centromere core have “activating” histone modifications (155, 280), such as methylation of H3 Lys4 (H3K4me1 and H3K4me2) and Lys36 (H3K36me2 and H3K36me3), which are mainly associated with euchromatin (110, 314) (Figure 1.1). However, recent studies in rice and maize centromeres show no enrichment of H3K4me2; instead other histone modifications resembling that of euchromatin are present, e.g. histone H4 acetylation (307, 327, 330). This predominantly euchromatic histone mark, which is absent from fly and human centromeric euchromatin, is present in actively transcribed centromere genes of rice (280, 330). However, transcriptionally active centromeres generating satellite and retroelement transcripts are prevalent in humans, mouse, beetle and tammar wallaby (110). The H3K4me1 and H3K4me2 modifications are thought to be important for the transcription of

aberrant RNA from alpha satellite regions that recruits complexes required for the deposition of the centromere-specific histone H3 (CenH3/CENP-A) at the centromere cores (19).

Recent evidence from budding yeast shows that there is some level of transcritional activity with the help of the transcrition factor Cbf1 and the Ste12 kinase of the MAPK pathway, and that both are required for centromere function (204). In absence of Cbf1 there is chromosome loss and increased sensitivity to benomyl, a widely used inhibitor of microtubule function. Disruption of Ste12 binding sites near CEN3 showed more severe defects of chromosome missegregation rather than a *ste12* deletion strain (204). Nevertheless, the precise role of centromere transcription in budding yeast still remains unanswered.

This is different in *S. pombe*, where RNAPII transcription and non-coding RNAs (ncRNAs) are sufficient to nucleate heterochromatin formation at pericentric regions. This can occur with the help of the exosome RNA degradation machinery in an RNAi-independent pathway (231). Altogether, this evidence suggests that centromeric transcripts are not only essential for regulated deposition of CenH3 as found in humans or mouse but are also involved in localizing other kinetochore protein like CENP-C (one of the inner kinetochore proteins) in maize (75). Further, in fission yeast centromere transcription is necessary for maintaining pericentric heterchromatin that is required for centromere *de novo* assembly, and via the recruitment of cohesins for function, genome stability and accurate cell division.

Neocentromeres and Holocentromeres

"Neocentromeres" are formed *de novo* at ectopic sites when the native centromere locus is disrupted or becomes non-functional. These new centromeres, often formed after alterations in genome structure must be capable to assemble functional kinetochores and able to drive chromosome segregation (35). Formation of neocentromeres is often observed in human cancer cells and their chromosome positions are highly diverse (176). Although newly formed centromeres are not guided by underlying DNA sequences, some of them are defective in their organization because of a loss in balance between euchromatin and heterochromatin (176). Heterochromatin formation by H3K9me3 and HP1 is not required in human neocentromere assembly, but most neocentromeres exhibit slight defects in cohesion binding that might lead to chromosome mis-segregation (4, 6, 128, 176). Neocentromeres are also typically defective in loacalization of Aurora B kinase (Ipl1 in yeast), an essential regulator of kinetochore-microtubule attachments that is also required for scanning and correcting protein connections in kinetochores during cell division (16). On dicentric chromosomes in humans and *S. pombe* one of two centromeres that is either native (on fused chromosomes) or newly formed (by spontaneous neocentromere formation) gets inactivated, however, what exactly triggers this inactivation has been a hot topic of research for 25 years (248, 304). Similarly, poor deposition of CenH3 at maize neocentromeres resulted in genomic instability; nevertheless, after successful deposition of CenH3 genome stability was increased at induced neocentromeres (306).

Experimentally, formation of stable neocentromeres by overexpression of CenH3 and concurrent disruption of endogenous centromere loci by γ-irradiation was

successfully achieved in *Drosophila melanogaster* (171). The new centromere was always formed in proximity to native centromeres at euchromatin-heterochromatin junctions, but the reason for this preference is still not understood. However, the absence of a pericentric heterochromatin boundary at the distal end allowed the spreading of kinetochore protein assemblies into the euchromatin region of this newly formed centromere (171).

In fungi, stable neocentromeres were formed in *S. pombe* by deleting native centromeres with a Cre-loxP system (128), and in *C. albicans* by replacing the entire endogenous centromere on by a selectable marker (146). Under these conditions, new *S. pombe* centromeres were formed at telomeres at the euchromatin - heterochromatin border and in absence of heterochromatin proteins. However, *S. pombe* neocentromeres showed failure of proper chromosome segregation (128). Thus, chromatin structure and location strongly influences formation of neocentromeres in *S. pombe* and *D. melanogaster*. One of the reasons for this preference might be the chromosome conformation, looping and position in the nucleus, in short the chromosome landscape in the nucleus, which has been analyzed in *S. pombe* by HiC, a chromosome conformation capture method coupled to high throughput sequencing (303).

In *C. albicans* native centromeres are devoid of pericentric regions, hence neocentromere formation is not dependent on chromatin context and thus they are formed either proximally or distally in consideration to endogenous centromeres (35). Similar independence of chromatin context was also observed in plant neocentromeres (196, 306). Hence, considering all observations for neocentromere

formation in different organisms, it appears that epigenetic states of the genomic locus are essential rather than the actual DNA sequence. However, the context of epigenetic states in neocentromere formation does not hold true in *C. albicans* and some plants, suggesting different pathways involved in *de novo* centromere assembly. Further, in *C. albicans*, origins of replication are associated with native as well as neocentromeres, suggesting another complex aspect of regulation in centromere assembly and inheritance not solely dependent on DNA content and structure (150).

The second strong line of evidence supporting the hypothesis that DNA sequence does not guide centromere formation is the occurence of "holocentromeres" in many plant and animal species. Instead of single or "monocentric" regions on chromosomes, diffuse centromeres are formed during mitosis along the entire length of holocentric chromosomes. It appears that holocentric chromosomes are much more common in nature than initially considered, and that they have evolved at least on four independent occasions in plants and nine times in animals, providing an excellent example of convergent evolution (183). Conserved features of monocentric centromeres are observed in the holocentromere assembly of *Caenorhabditis elegans* (a nematode worm) and *Luzula nivea* (a grass), e.g. affinity towards heterochromatin (117, 193).

Taken together, all evidence gathered from studies on neocentromere and holocentromere formation suggests that chromatin states, which depend on centromere-specific protein localization in combination with histone modifications, are key processes for centromere assembly rather than the centromeric DNA sequences

alone. Generally, at the native centromeres the underlying DNA sequence is characterized by repetitive sequence with presence of transposable elements. Hence it is possible that after centromere repositioning the immature centromere might eventually accumulate repetitive sequences by integration of transposable elements.

Kinetochore proteins

The “kinetochore” is a large macromolecular proteinaceous knob that connects the centromeric DNA with spindle microtubules and is essential for chromosome segregation during cell division (31, 139). Considerable confusion exists in the literature as to the nature and naming of centromere *versus* kinetochore proteins. Researchers who studied DNA sequences and chromatin tend to talk about “centromere proteins” or “centromere foundation proteins”, while cell biologists who study cell division tend to write about “kinetochore proteins”. Most recently the biochemical analyses of centromere-binding or kinetochore proteins has shed more light on the proteins involved and helped to order the confusing nomenclature into a couple of different large complexes. Proteins that remain attached to the centromeric DNA and chromatin at all times of the cell cycle are now called centromere proteins and – at least in mammals – labeled CENP-A, -B, -C, etc and thought to form the Nucleosome Associated Complex, or NAC (90, 205) or “Constitutive centromere-associated network (CCAN) (121). Proteins that are only temporarily associated with the centromere, e.g. during cell division, are still referred to as kinetochore proteins.

Structures of mitotic kinetochores observed by electron microscopy revealed three discrete kinetochore layers. The inner and outer layers are electron dense and the middle layer is electron translucent and protrudes out from the outer layer in

absence of microtubule attachment (31, 139). These layers are composed of protein complexes, which coordinately regulate cell division (Figure 1.2). As described earlier, there are different arrangements and size variability found in centromeres, i.e. point, regional and holocentromeres along with rapidly evolving underlying centromeric DNA sequences. This suggests less conservation of protein modules that have chromatin interactions in the inner (i.e. DNA-binding) compared to outer kinetochore layers. Outer kinetochore protein complexes are mainly involved in spindle microtubule interactions and whose homologues in diverse eukaryotes carry essential functions (101) (Figure 1.2).

The deposition of centromere specific histone H3 (CenH3), the “centromere identifier”, initiates the process of centromere assembly an epigenetic phenomenon conserved form yeast to humans (117, 191, 203, 211, 290, 312, 318). “CenH3” is referred to by a multitude of monikers, depending on the different organisms, e.g. HTR12 in *Arabidopsis thaliana* (At) (296), Cse4 in *Saccharomyces cerevisiae* (Sc) (184), $Cnp1^{CenpA}$ in *Schizosaccharomyces pombe* (148, 290), Cid in *Drosophila melanogaster* (117), and CENP-A in *Homo sapiens* (80), where it was originally identified (208, 209).

”Licensing” of the centromere locus by deposition of CenH3 is required during or after every round of cell division. The timing or zone of loading of CenH3 is variable in different organisms. In *S. cerevisiae* and *S. pombe* CenH3 is deposited at the centromere during S-phase, i.e. during DNA replication (214, 293). In addition to S-phase, there is also a second time point of deposition of CenH3 during G2 of the cell cycle in *S.pombe*, but the reason for this still remains unanswered (293). However, in

higher eukaryotes like humans, flies and plants, newly synthesized CenH3 is localized at the centromere in a replication-independent manner, i.e. during telophase or early G1 in human cells (115, 134), between G2 and metaphase of somatic cells or during anaphase in fast dividing cells of syncytial embryonic cells of *Drosophila* (1, 255), and CenH3 is loaded during G2 phase in *Arabidopsis thaliana* (159, 160).

Further, this specificity of CenH3 deposition is controlled by the specialized CenH3 chaperone Scm3 in yeast (39, 190, 278, 325), and its homologues, human HJURP (79, 89) and Drosophila CAL1 (84, 182). Structual studies have determined that the N-terminus of HJURP/Scm3 can interact with CenH3 in humans and yeast (52, 126). However, in fission yeast there is another chaperone, Sim3, that is also involved incorporation of CenH3 at centromeres and is proposed to function upstream of Scm3 (78).

Nucleosomes that contain CenH3 or the canonical histone H3 are interspersed within centromeres and thought to form a foundation that allows interaction with inner kinetochore protein modules, now called “CCAN” (Constitutive centromere-associated network; (121)) (Figure 1.3). This network is divided into four sub-complexes: CENP-C, CENP-T-W-S-X, CENP-H-I-K-L-M-N and CENP-O-P-Q-R-U. CENP-C functions as linker protein between centromere chromatin and microtubule binding protein complexes in the outer kinetochore. In sequence analyses, the N- and C-terminal regions of CENP-C have certain stretches of conserved regions that are specific to yeast, animals and plants (294). However, CENP-C from all eukaryotes carries a highly conserved proximal C-terminal “CENP-C motif” that interacts with the CenH3 C-terminus (44, 109, 294). Recent studies used

polynucleosomal and mononucleosomal MNase digests followed by ChIP (chromatin immunoprecipitation) assays and showed that CENP-C interacts with not only with CenH3 but also H3 nucleosomes at centromeres (122). Additionally, the interacting partners with the CENP-C N-terminus vary depending on the organism, yet CENP-C appears functionally conserved as a scaffold protein and helps to maintain the structural integrity of the kinetochore during cell division. For example, during mitosis the human and fly CENP-C N-terminus is involved in direct binding to the Mis12 complex that associates with the microtubule-binding Ndc80 complex (153, 188, 222, 256) (Figure 1.3). In contrast, fission yeast CENP-C (Cnp3) interacts directly with another constitutive centromere protein, CENP-L (Fta1), and the microtubule-clamping protein Pcs1, which is found only in yeast (141, 301). Apart from the conserved regions at the N-and C-terminus the central region of CENP-C has a DNA-binding domain that is highly divergent and differs even within different closely related species (294, 309). Thus, CENP-C sets up a connection between centromeric chromatin and microtubule binding proteins through its direct interaction with the Mis12 complex (49, 55, 222, 235, 256).

Apart from the connection of CENP-C to Ndc80 via the Mis12 complex there is a second way of linking CenH3 nucleosomes to the outer kinetochore, that appears to be conserved from budding yeast to vertebrates. This involves the CEN-T-W-S-X complex that has recently attracted much attention (5, 28, 101, 102, 200, 251). The unstructured CENP-T N-terminus plays an important role of assembly by directly interacting with Ndc80, a microtubule-binding component (101). The C-terminal domain of CENP-T is composed of alpha helices similar to the histone fold domain (HFD) common to canonical histones, and has the potential to interact with DNA to

form non-histone nucleosomes when forming complexes with other CCAN proteins, namely CENP-W, CENP-S and CENP-X (200). The assembly of these proteins forms heterotetrameric “nucleosomes” that are thought to be localized between H3 and CenH3 nucleosomes within centromeres. This increases the uniqueness and specificity of the centromere as a defined genomic locus. In summary, CENP-C interacts indirectly and CENP-T directly with the microtubule-binding Ndc80 complex in two distinct pathways to anchor centromeric chromatin to microtubules.

The components from another two CCAN subcomplexes CENP-H-I-K and CENP-L-M-N are considered to be involved in the incorporation of newly synthesized CenH3 in human as well as fission yeast centromeres (45, 169, 205, 268). In *in vitro* biochemical assays it was shown that CENP-N interacts with the CenH3 nucleosomes and its N-terminal interacts with CENP-L (45), whereas in fission yeast CENP-K (Sim4) is involved in the association of CenH3 with the fungal-specific DASH complex that is present at the microtubule-binding interface (137, 144, 149). A fourth CCAN subcomplex consists of CENP-O-P-Q-R-U, which was found not essential for normal growth in chicken cell lines as deletion alleles proved viable (123). It remains to be seen if a combination of deficiencies will have more drastic effects. The fission yeast homologues of these proteins, Mal2 (CENP-O) and Fta2 (CENP-P) interact with Sim4 (CENP-K), which directly interacts with CenH3, as mentioned above (144).

The inner kinetochore protein complexes that are part of the CCAN directly contact two conserved outer kinetochore complexes, the Mis12 and Ndc80 complex, as well as a single protein, KNL1 (Figure 1.3). Thus, in the species investigated thus far, the outer kinetochore is made up of the “KNL1-Mis12-Ndc80” (KMN) network that

functions as an interface with spindle microtubules and is responsible for multiple vital functions during mitosis (216); the KMN network is equivalent to the NMS complex (Ndc80-MIND-Spc7) in fission yeast (48, 186). The KMN network builds the functional kinetochore that is involved in microtubule binding and chromosome segregation including spindle-assembly-checkpoints (SAC) tied up properly with regulation of chromatid cohesion in the inner centromere (137, 302) (Figure 1.2). A fourth complex, the Dam1/DASH complex is fungal-specific (137) and is discussed separately below.

KNL1 is a large protein, whose N-terminus has microtubule binding activity and functions as signal for spindle-checkpoint silencing. Dephosphorylation of KNL1 as well as Ndc80 by PP1γ (protein phosphatase 1γ) is necessary for their binding to microtubule, which makes them substrates for Aurora B kinase. Phosphorylation of KNL1 and Ndc80 are essential steps for error correction of kinetochore-microtubule attachments. The N-terminus of KNL1 also interacts with the spindle-checkpoint kinases Bub1 and BubR1. Bub1 phosphorylates H2B in centromeric nucleosomes and recruits Shugoshin (Sgo1) and Aurora B to the inner centromere surfaces to establish sister-chromatid cohesion (122, 265, 289, 329). BubR1 modulates the function of Aurora B kinase (157). In vertebrates and fission yeast the C-terminus of KLN1 directly interacts with the Mis12 complex, but direct interaction of KNL1 with Ndc80 has not yet been shown (122, 145).

As stated earlier, the conserved Mis12 and Ndc80 complexes interact directly and thus make the connection of the inner kinetochore with microtubules through CENP-C. The Mis12 complex thus acts as a hub, connecting the outer KMN network with centromeric chromatin. It contains four proteins, Nnf1, Mis12, Dsn1 and Nsl1 that

are arranged in a linear rod shaped unit in which Nnf1 faces towards the inner kinetochore and interacts with CENP-C, while Nsl1 binds directly to the Ndc80 complex and KNL1. Similarly, the Ndc80 complex has four proteins. Spc24 and Spc25 that directly interact with Mis12, while Ndc80 and Nuf 2 are involved in microtubule lattice binding. In fission yeast and vertebrates the microtubule electrostatic interaction of the unstructured Ndc80 N-terminus is regulated by phosphorylation by Aurora B kinase, which serves as a key factor ensuring robust interactions of kinetochores with microtubules (122, 125). However, additional biochemical studies in fission yeast found the internal loop of Ndc80 to be important for stable bipolar spindle microtubule attachment during mitosis by interaction with another transiently localized kinetochore protein Dis1/TOG (125). Taken together genetic, cytological and biochemical studies from the last three decades reveal that interactions of kinetochore proteins present in the CCAN and KMN network, which are residing constitutively at centromeres show remarkable conservation from budding and fission yeast to chicken and human centromeres while the primary protein sequences of many of these proteins is rather ill-conserved.

The assembly of proteins in the KMN network plays an active role at the microtubule interface during mitosis; however, there are several noteworthy intriguing features of fission yeast kinetochores that are common to most of the fungi that have been examined thus far. Most fungi undergo “closed mitosis”, i.e. during mitosis there is no complete breakdown of the nuclear envelope and segregation of chromosomes takes place within the nucleus, resulting in quick turnover of nuclei after mitosis (67, 68, 234). In *S. pombe* the three centromeres cluster in close vicinity with the spindle pole body (SPB) throughout interphase, while during mitosis the SPB provides the

attachment surface for these clustered centromeres (136). Upon entry into mitosis the SPB, which is embedded in the nuclear membrane, divides into two and the daughter SPBs move towards opposite poles of the nucleus after attaching to the dynamic plus ends of spindle microtubules. This movement of SPBs thus establishes a bi-orientation configuration in which sister chromatids linked to the opposite SPBs via kinetochore microtubules move towards opposite poles. Electron microscopy studies show the absence of microtubule between the kinetochores and SPBs suggesting direct tethering of kinetochores to the SPB (169, 217). Live cell imaging studies in fission yeast have shown that the absence of Nuf2 and Mis6 caused declustering of centromeres from the spindle pole body during interphase and prophase in mitosis as well as in meiosis (7, 10). In budding yeast, unlike in fission yeast, the mitotic checkpoint protein Bub2 is localized at the SPB that activates downstream checkpoint pathways via Mad2 (92). Although microscopy provided indirect proof of kinetochore interaction with the SPB, it also suggested the presence of unknown proteins involved in fungal-specific interactions between SPB and kinetochore. Based on these observations, the presence of the Dam1/DASH complex in the outer kinetochore is thought to be essential for successful bi-orientation of chromosomes during mitosis in budding yeast and *C. albicans* (34, 133). In *S. pombe*, although the Dam1/DASH complex is not essential for viability, it is involved in chromosome bi-orientation during mitosis (243). Further, in *S. pombe* it was shown that any unclustered kinetochore during interphase can be timely retrieved in the correct orientation with the help of the Dam1/DASH complex because in fungi centromeres are clustered together at the spindle pole body (SPB), even during interphase (36, 91, 201). Apart from the Dam1/DASH complex there is another recently discovered fungal-specific component

in the otherwise highly conserved tripartite KMN network, Sos7, whose interacting partner is the constitutively kinetochore-localized Spc7, the fission yeast homolog of KLN1. The Sos7 protein is needed for kinetochore targeting of Mis12 components, loss of this gene causes severe chromosomal missegregation and compromised kinetochore microtubule interactions (130). Thus, the closed mitosis in fungi appears to necessitate presence of additional kinetochore components that are specialized and on a practical level might serve as good targets for antifungal drugs.

Once the kinetochore is assembled, various spindle checkpoint-signaling pathways are silenced or activated for screening proper kinetochore-microtubule attachments, helping in recruiting condensins and building microtubule tension during the different phases of the mitotic cell cycle. As mentioned earlier, Ndc80 is a substrate for Aurora B kinase, an enzymatic component of the “chromosomal passenger complex” (CPC) that is made of three additional non-enzymatic components namely, INCENP, Survivin and Borealin (Figure 1.2). Extensive studies in various species from yeast to mammals have determined the pivotal role of the CPC in assembly and stability of a bi-polar spindle, mitotic condensation, spindle assembly checkpoint activation, anaphase spindle stability, and cytokinesis by maintaining proper balance of phosphorylation and dephosphorylation states (237). The catalytic component of CPC, Aurora B kinase, binds to the conserved C-terminus of the scaffold protein INCENP (Sil15 in yeast) and phosphorylates it, which prevents CPC binding to pre-anaphase spindles and central spindles until late anaphase, thus maintaining the spatio-temporal regulation of CPC with the dynamics of microtubules (194).

A second, non- CPC kinase, Cdk1 (Cyclin dependent kinase 1) phosphorylates the other CPC components, i.e. Borealin and Survivin and localizes the complex at the conserved centromere adaptor, Shugoshin. Once the CPC is localized at centromeres, Aurora B kinase phosphorylates its KMN network substrates, i.e. Ndc80, Mis12, KNL1 and in yeasts the subunits of the Dam1/DASH complex, and scans for proper kinetochore connections with microtubules (168, 300, 310, 322). Thus, entry into mitosis is governed by the finely tuned balance and mutual regulation of Cdk1 activating and inhibitory phosphorylation controlled by the Wee1 kinase. Wee1 kinase carries out inhibitory phosphorylation of the Cdk1 catalytic domain and prevents the entry of the cell into mitosis, whereas inactivation of phosphorylated Wee1 kinase removes this inhibition and allows progression of cells into M phase (140, 319). The progression of cell cycle from G2- to M-phase plays a very crucial role in plant pathogenic fungi, e.g. *Ustilago* maydis, *Uromyces appendiculatus* and *Magnaporthe oryzae*, because there is tight coupling of morphogenesis and cell cycle progression that is required for growth and penetration into plant cells (154, 249, 260). Genetic studies indicating mitotic entry arrest caused by inhibitory phosphorylation of Cdk1 plays a pivotal role in *Ustilago maydis* during morphogenesis and pathogenicity and supports the role of Cdk1 as master regulator that controls cell cycle and morphogenesis (83, 260). Similarly, in the human opportunistic pathogen *C. albicans* Swe1-(Wee1)-dependent cell cycle arrest during the G2-M transition triggers polarized filamentous growth responsible for virulence (99). Further, mutation in the SAC component, Mad2 in *C. albicans* does not cause infection in a mouse model, presumably because of the inability of the mutant cells to stop the cell cycle leading to degradation of proteins required for chromosome

segregation by host defenses (13). These studies indirectly suggest the importance of crosstalk between signaling pathways regulating polarized growth and spindle assembly checkpoints that modify assembled kinetochore components in fungal plant and animal pathogens.

In summary, extensive studies on the organization of centromeres, kinetochores and spindle attachment complexes in *S. cerevisiae*, *S. pombe* and *C. albicans* served to improve our understanding of all, and specifically fungal, centromeres. However, we lack understanding of the similarities, and perhaps more importantly differences, of these structures and processes in filamentous fungi, a very diverse group of organisms. Deciphering centromere assembly and maintenance mechanisms in filamentous fungi is essential because most of the fungal pathogens whether infecting animal or plants belong to this group (223).

Neurospora Centromeres

To study centromeres in a new group of organisms is often difficult because of the high repetitive DNA content of the centromeres, which are thus not easy to assemble (272). It was no surprise that the centromeres of many filamentous fungi have been difficult to assemble and are absent or not easily recognizable by bioinformatic tools in the almost completely sequenced and assembled genomes of *Fusarium graminearum* (teleomorph: *Gibberella zeae*) (60), *Aspergillus fumigatus* (86), *A. nidulans* and *A. oryzae* (98), *Nectria haematococca* (56), and even the one filamentous fungus for which there is a predicted “telomere-to-telomere” assembly, *Mycosphaerella graminicola* (107). The one filamentous ascomycete in whose genome sequence centromeres were immediately obvious was *Neurospora crassa*

(97). In this section I discuss what makes Neurospora an excellent model to study centromeres and kinetochores of filamentous fungi.

Neurospora crassa produces octads of ordered ascospores, which made this organism attractive to early geneticists for constructing linkage maps. By relation to other markers on each linkage group (LG), Neurospora centromeres were mapped relatively early by classical genetics (15, 215). Representative centromeric DNA sequences from LG VII obtained from a yeast artificial chromosome (YAC) library revealed a collection of AT-rich, inactivated transposons and simple sequence repeats, e.g., Tsp, Sma, and TTA repeats (41, 47). As mentioned earlier centromeric DNA of mammals (238, 239, 253), plants (267) and flies (283, 284) consists of homogenous repeating units. In contrast, Neurospora centromeric DNA is composed of heterogenous repeats and tandem repeats similar to alpha-satellites are absent, which makes Neurospora an attractive model to study the interplay between, repetitive centromeric DNA and epigenetic deposition of centromere proteins (272).

The hallmarks of Neurospora centromeric DNA are stretches of “near-epeats” (273). These were first discovered by partially sequencing *CenVII* (41). Based on only 16 kb of sequence, it was concluded that Neurospora centromeres are composed of degenerate transposons, mostly retrotransposons, and simple sequence repeats. The degenerate nature of the transposons is due the action of a pre-meiotic process called “Repeat-Induced Point mutation” (RIP), which through an unknown mechanism recognizes repeated DNA and mutates both copies, yielding numerous C:T and G:A transition mutations (42, 259). Since then nearly all centromeric DNA on the seven Neurospora chromosomes has been assembled (30, 97), partly because the genome

has been sequenced to more than one thousand-fold coverage. The early conclusions still hold true but have been refined. The DNA component of each centromere is comprised of 175 - 300 kb of mutated degenerate transposons and other AT-rich sequence that is no longer recognizable as ancestral transposon because of the action of RIP (273). No specific recognizable pattern in the arrangement of these transposon relics has emerged to allow identification of segments that are functionally similar to the *S. pombe otr* and *imr* regions. Indeed, comparing segments of centromeric DNA to segments of DNA that are subject to heterochromatization reveals no obvious compositional or structural bias between core centromeric, pericentric and dispersed heterochromatic DNA in Neurospora (Figure 1.4).

We verified the location of Neurospora centromeres by performing chromatin immunoprecipitation (ChIP) of three reliably centromere-specific proteins, CenH3, CEN-C, and CEN-T, followed by high-throughput sequencing (HTS) of associated DNA, a process called “ChIP-sequencing” (ChIP-seq) (273). As described above, CenH3 is a centromere-specific histone H3 variant, and CEN-C (CENP-C) and CEN-T (CENP-T) are proteins that belong to the CCAN of inner kinetochore complexes (Figure 1.5). We found that Neurospora centromeres occupy approximately 170-300 kb, which is much bigger than *S. pombe* regional centromere.

In order to define the epigenetic organization in Neurospora centromeres we determined enrichment of several histone marks, including H3K9me3 and H3K4me2. To our surprise we found an abundance of H3K9me3 but absence of H3K4me2 within the central centromere cores, exactly the opposite of what has been found in other

regional centromeres (compare Figure 1.1 and Figure 1.5). To test the dependency of CenH3 localization on H3K9me3, ChIP-seq was done in a *dim-5* (H3K9 methyltransferase) mutant, which lacks all, or nearly all, H3K9me3 (162, 297, 298). Enrichment of CenH3 at centromeres in the *dim-5* mutant was greatly reduced except at *Cen-I* and *Cen-IV*, but the reason for subtle differences remains to be determined (Figure 1.6). Additionally, CenH3 enrichment was also checked in an *hpo* mutant, deficient for HP1. HP1 binds to H3K9me3 and is essential for DNA methylation (93). The results showed that, although normal CenH3 localization was dependent on HP1, DNA methylation was overall less abundant within centromere cores than in the neighboring pericentric regions (Figures 1.5 and 1.6). Taken together, these results suggest different un-tapped modes of regulation by HP1 as well as H3K9me3 that may be centromere-specific.

We also analyzed the genome of *N. crassa* and several additional filamentous fungi for the presence of genes for conserved centromere and kinetochore proteins (Table 1.1) (272). Overall, CCAN and KMN networks seem to be very well conserved, but individual proteins are unrecognizable based on sequence conservation or simply not present in the kinetochores of filamentous fungi (272). Our attention has recently shifted to analyzing potential interactions of CenH3 nucleosomes with the proposed CENP-T-W-S-X tetramers.

In summary, we showed that Neurospora centromeres are regional and that normal CenH3 localization depends on H3K9me3 and the presence of HP1, which binds to H3K9me3. We showed that centromere assembly is not simply guided by the centromeric DNA content or the presence of heterochromatin, which was in some

cases found also directly adjacent to regions in which CenH3 was found (Figure 1.4). Based on our knowledge of Neurospora centromeres I concentrated on understanding the exact role CenH3 plays in Neurospora centromeres.

Deposition of CenH3 triggers centromere assembly, a phenomenon conserved in all eukaryotes studied thus far. I wanted to understand specific features of CenH3 that directs it, and not H3, to Neurospora centromeres. In this thesis I collected my studies on the structure and function of CenH3 proteins from four fungi, all expressed in *N. crassa.* With my studies I addressed the following open questions about CenH3:

1) Are centromeric proteins subject to accelerated positive selection that results in adaptive evolution?

I answered this question by in-depth sequence analyses of CenH3 and CEN-C of filamentous fungi. The results are compiled in Chapter 2.

2) What are the sequence-dependent determinants that are responsible for deposition of CenH3 at Neurospora centromeres?

I answered this question through genetic studies that are described in Chapter 2. In this molecular genetic analysis I was able to determine that, during meiosis the histone-fold-domain (HFD) as well as N-terminus tail of CenH3 are essential and any structural perturbation in these two regions causes only meiosis specific inhibition.

3) What are the consequences of replacing Neurospora CenH3 with CenH3 from Podospora anserina (PaCenH3), a relatively closely related fungus?

In addition to the genetic studies described in Chapter 2, I also carried out biochemical ChIP-seq experiments that revealed that Neurospora centromeres progressively and irreversibly lose PaCenH3 from random centromeres.

4) Are centromeric nucleosomes tetramers or octamers, and if they are octamers are they generated from CenH3-H3/H4$_2$ heterotetramers or CenH3$_2$/H4$_2$ homotetramers?

I addressed these questions by co-immunoprecipitation of CenH3 proteins tagged with various antigenic protein sequences. The results of these experiments are described in Chapter 4, and show that centromeric nucleosomes in Neurospora most likely occur as homo-octameric CenH3$_2$/H4$_2$/H2A$_2$/H2B$_2$.nucleosomes.

Table 1.1: Centromere and kinetochore proteins in filamentous fungi. (adapted from (272). Proteins were identified by Blast searches with human or *S.pombe* protein sequences as bait. Current locus numbers are shown. “None”, no homolog was identified by sequence similarity.

H. sapiens	*S. pombe*	*N. crassa*	*F. graminearum*
CENP-A	Cnp1	NCU00145	FGSG_02602.3
HJURP	Scm3	NCU03123	FGSG_00678.3
NPM1	None	None	None
CENP-B	None	None	None
None	None	NCU06592	FGSG_05264.3
None	None	NCU00392	FGSG_07243.3
None	Abp1, Cbh2, Cbh1	None	None
INCENP	None	NCU05211	FGSG_05106.3
Aurora B	Ark1	NCU00108	FGSG_06959.3
CENP-C	Cnp3	NCU09609	FGSG_11834.3
Mis18α/Mis18β	Mis18	None	None
RbAp48/RbAp46	Mis16	NCU06679	FGSG_06798.3:
M18BP1	None	None	None
MgcRacGAP	None	None	None
CENP-T	Cnp20	NCU02161	FGSG_08859.3
CENP-X	Mhf2	NCU09478	FGSG_06022.3
CENP-W	SPAC17G8.15	NCU03400	FGSG_10821.3
CENP-S	SPBC2D10.16	NCU03629	FGSG_07161.3
CENP-H	Fta3	NCU09996	FGSG_00383.3
CENP-I	Mis6	NCU04131	FGSG_07166.3
CENP-K	Sim4	NCU09238	FGSG_01054.3
CENP-L	Fta1	NCU07591	FGSG_04225.3
CENP-M	Mis17	None	None
CENP-N	Mis15	NCU03537	FGSG_05172.3
CENP-O	Mal2	NCU09100	FGSG_08806.3
CENP-P	Fta2	NCU02135	None
CENP-Q	Fta7	NCU06791	FGSG_10762.3
CENP-R	None	None	None
CENP-U	Fta4	NCU01005	FGSG_02626.3
hMis12	Mis12	NCU06463	FGSG_02525.3
DSN1	Mis13	NCU01344	FGSG_10141.3
NNF1	Nnf1	NCU07571	FGSG_05590.3
NSL1	Mis14	NCU02262	FGSG_10778.3
NDC80	Ndc80	NCU03899	FGSG_09262.3
NUF2	Nuf2	NCU06568	FGSG_05288.3
SPC24	Spc24	NCU05312	FGSG_05313.1
SPC25	Spc25	NCU11159	FGSG_01538.3
KNL1	Spc7	NCU03103	FGSG_00672.3
CENP-E	None	NCU02626	FGSG_01004.3
CENP-F	None	NCU03621	FGSG_10111.3

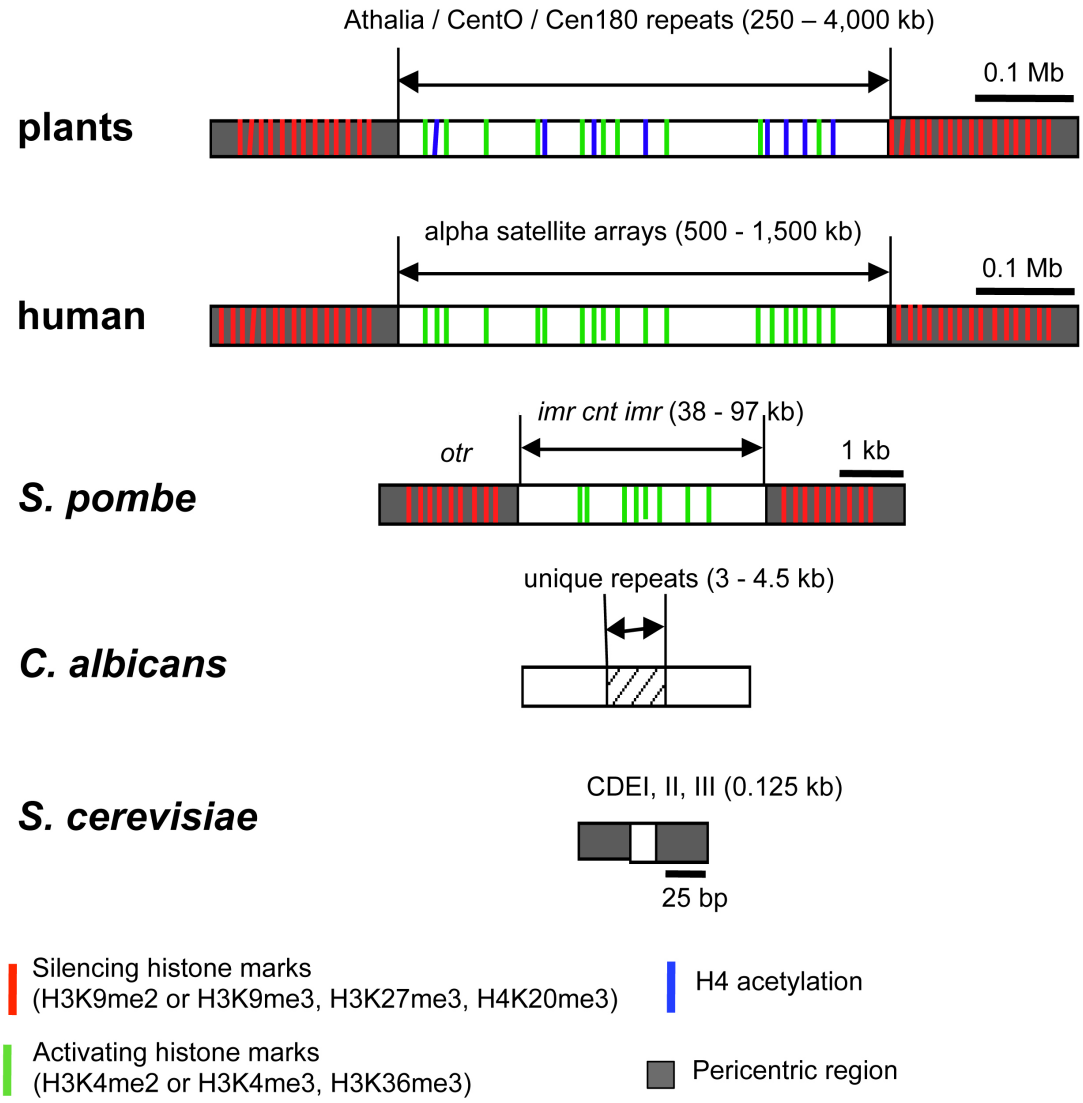

Figure 1.1. Centromere organizations in different organisms.

Shown are plants, human and three hemiascomycete fungi (*S. cerevisiae, C. albicans, S.pombe*). The DNA content of the central core with a mixture of CenH3 and canonical histone H3 nucleosomes is indicated above each arrow, and the number in parentheses indicate centromere size in kilobases (kb). The numbers near the black bar indicates the size of pericentric region. The size of the black bar is not drawn to the scale.

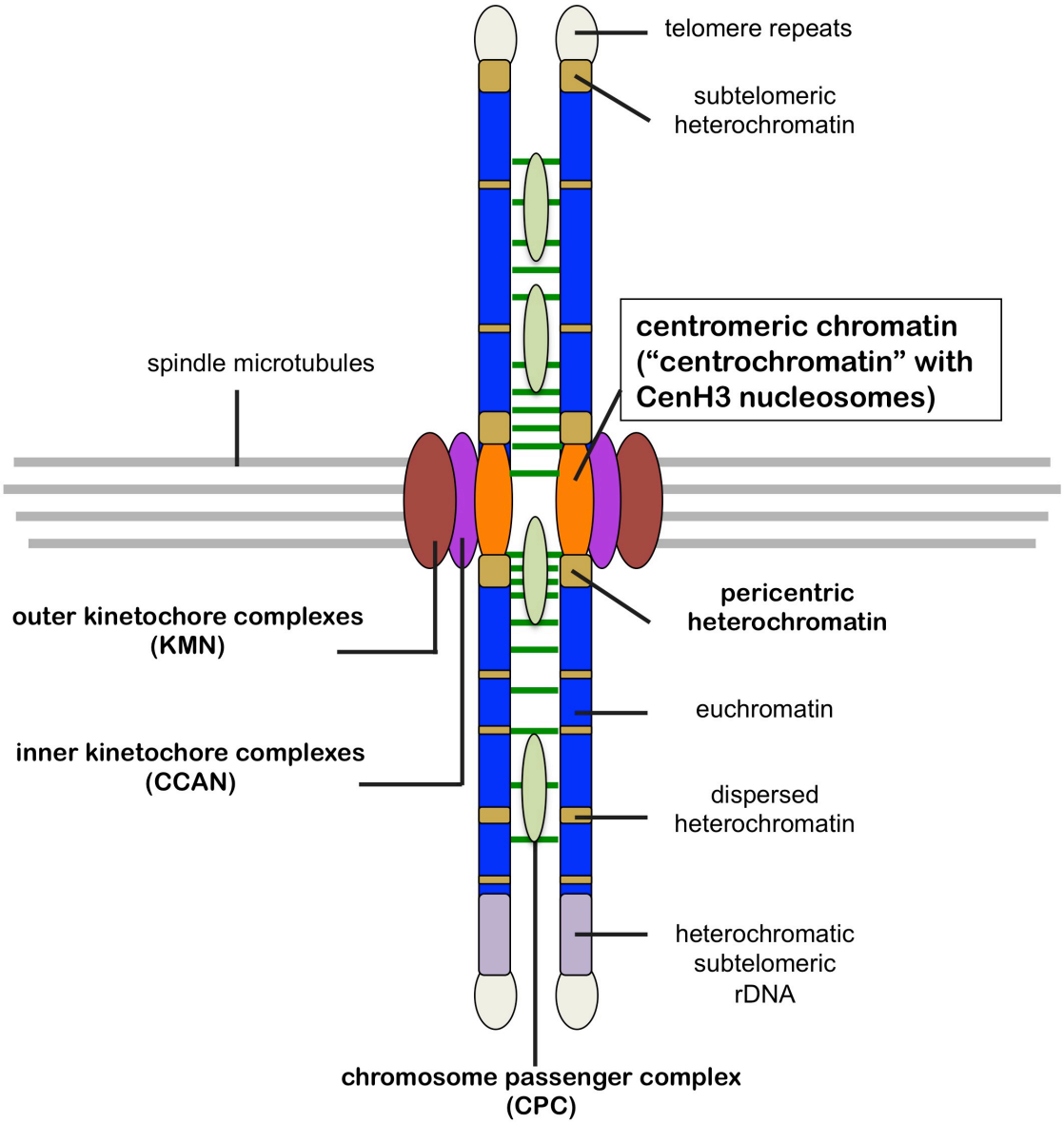

Figure 1.2. Cartoon of chromosome territories on replicated and condensed metaphase chromosomes during mitotic cell division.

The inner kinetochore protein complexes consist of the CCAN (constitutively centromere associated network), whereas the outer kinetochore complex involved in interactions with spindle microtubules consists of the KMN network (KLN1-Mis12-Ndc80 complexes). This kinetochore protein nomenclature is based on the names for human proteins. The green bars connecting the inner surfaces of the chromosome represent cohesins. This is where the CPC (chromosome passenger complex) is located.

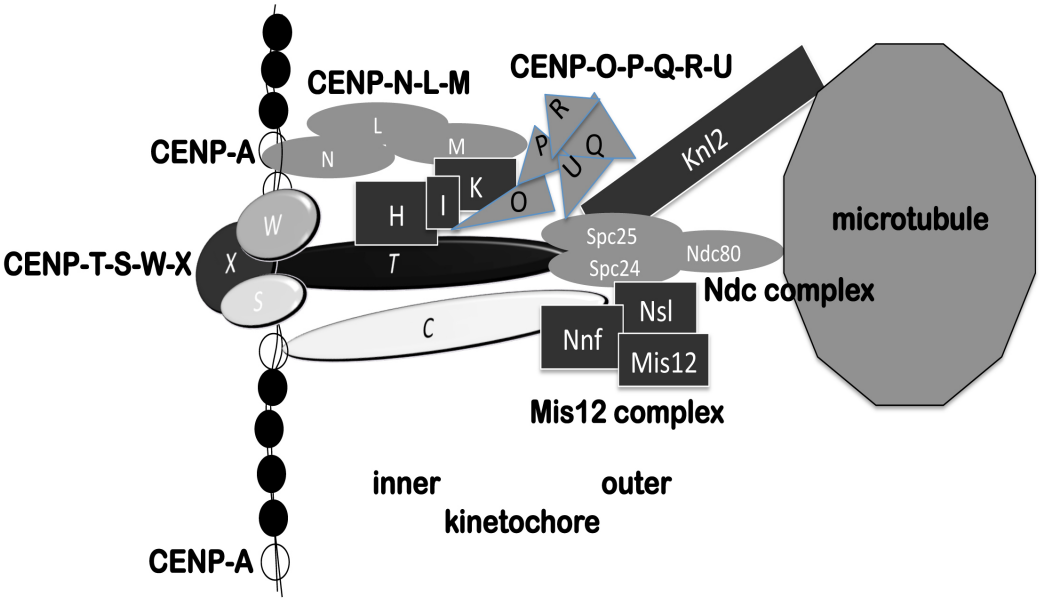

Figure 1.3. Arrangement of centromere or kinetochore protein complexes.

Shown are interactions that have been elucidated from studies in yeasts and vertebrate models. The fungal-specific Dam/Dash complex is omitted for clarity. Adapted from (216).

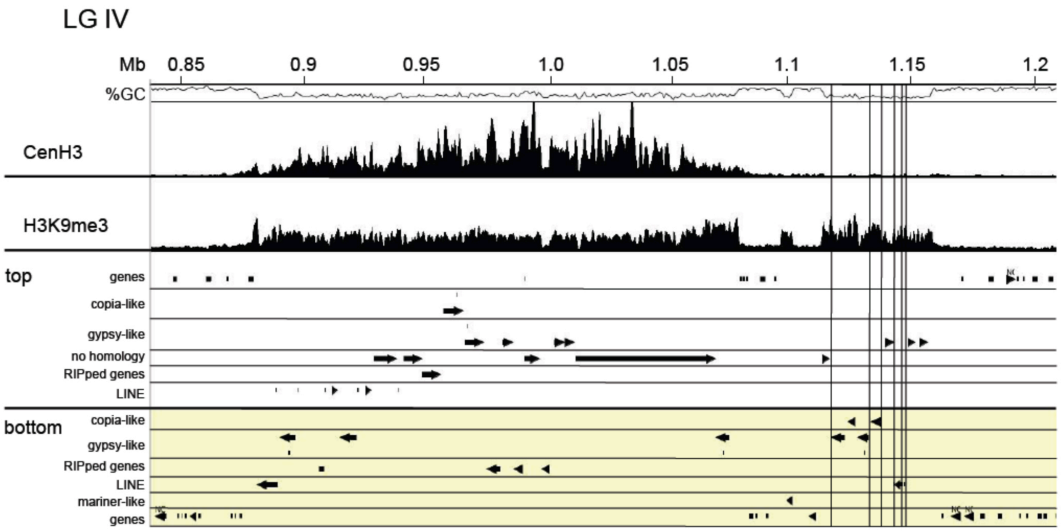

Figure 1.4. Expanded view of ChIP-seq read counts for CenH3 and H3K9me3 aligned to predicted transposon relics in centromeric regions on LG IV.

CenIV is predicted to be on a single contig of ~174 kb. Contig breaks are indicated by vertical lines. Neurospora wildtype strains contain few - if any - active transposable elements (TE). Most duplicated TEs have undergone RIP and are barely recognizable as retrotransposons (copia-, or gypsy-like), DNA transposons (mariner-like) or LINEs after blastx searches. There are large stretches of TA-rich DNA without any matches (no homology) or with poor matches to genes in other organisms (RIPed genes). The scale is in megabasepairs (Mb). Adapted from (273).

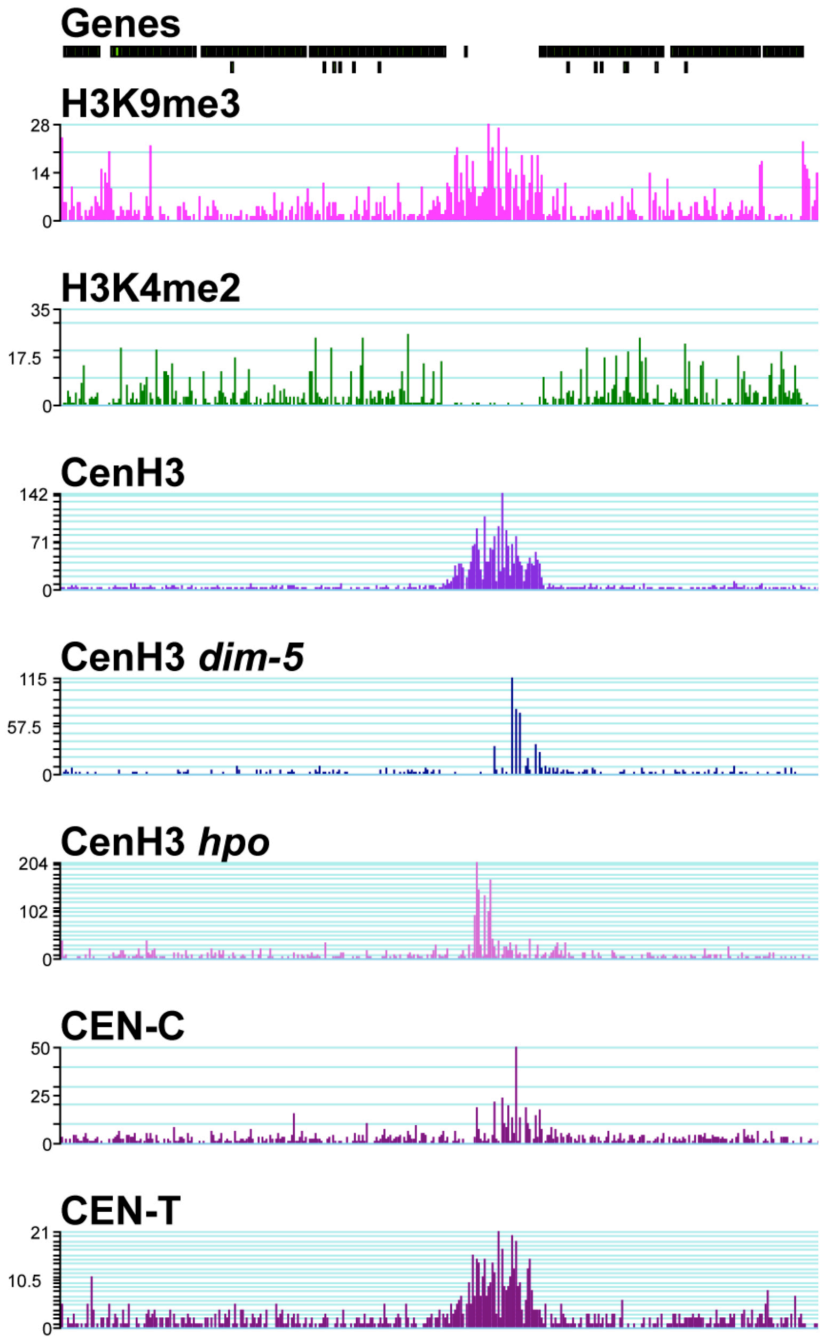

Figure 1.5. Localization of centromere proteins and epigenetic modifications in *Neurospora crassa* centromere II (*Cen-II*) by ChIP-sequencing.

Adapted from (273).

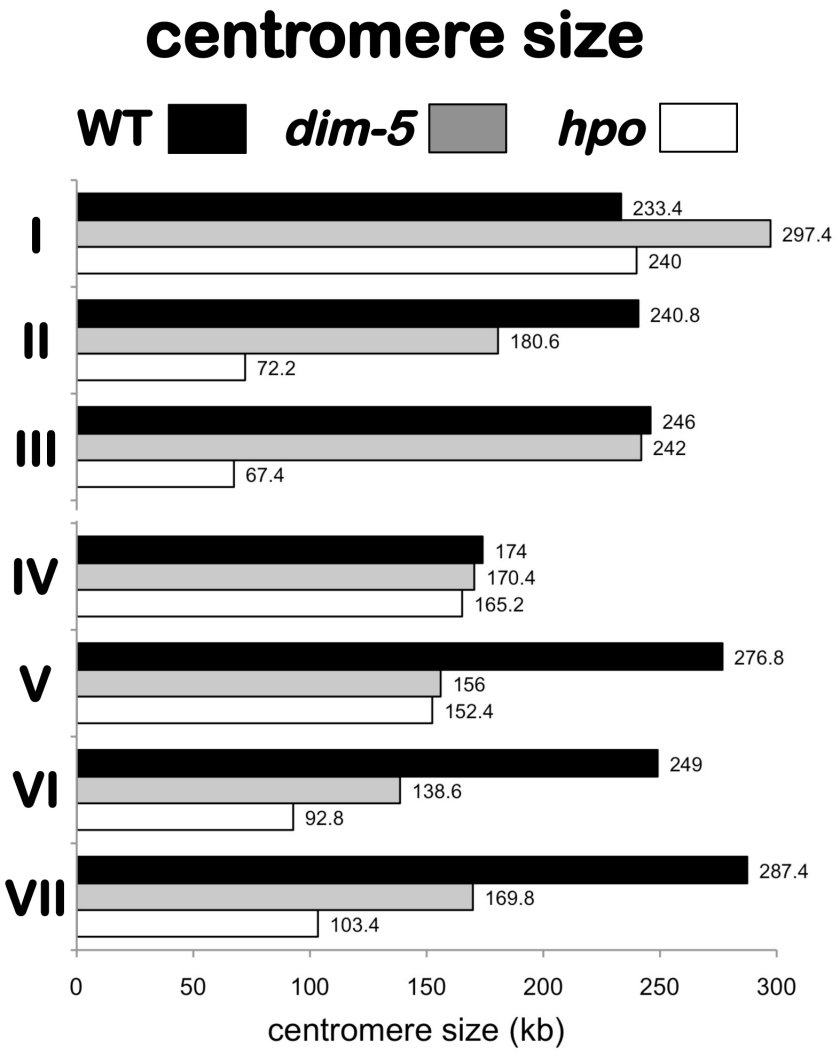

Figure 1.6. Changes in centromere size in *dim-5* and *hpo* mutants.

Adapted from (273).

The carboxy-terminus of *Neurospora crassa* CenH3 is required for meiosis-specific functions

Pallavi A. Phatale, Kristina M. Smith, Lanelle R. Connolly, Joseph Mendoza and Michael Freitag

in preparation for submission to Eukaryotic Cell

Abstract

Centromeric DNA and proteins binding to these regions (centromere foundation and kinetochore proteins) are among the most rapidly evolving elements in eukaryotic genomes. Mechanisms driving this evolution are not well understood. Here we explore the evolution of the centromere-specific histone variant, CenH3 (known as CENPA in mammals), in filamentous fungi, a large, diverse group of organisms that includes medically and economically important species for which public sequence data are rapidly accumulating but that whose centromeres have not been exhaustively studied. By phylogenetic analyses, we examined CenH3 across the fungal kingdom and within the genus *Neuropora* and several closely related genera (*Gelasinospora* and *Sordaria*). These analyses revealed short regions that appear subject to positive or negative selection. To experimentally validate and extend our results, we carried out genetic analyses with CenH3 genes from four species, *Neurospora crassa* (Nc), *Podospora anserina* (Pa), *Fusarium graminearum* (Fg; teleomorph: *Gibberella zeae*) and *Aspergillus nidulans* (An). We replaced the wild type *N. crassa* CenH3 gene (*hH3v*) with tagged and non-tagged alleles of the respective CenH3 genes. All four GFP-tagged CenH3s were properly localized to the centromere, as one clear “chromocenter”, i.e. a single dense heterochomatic region in each nucleus was observed. Additional tagged or untagged CenH3 copies in heterokaryotic transformants did not interfere with growth, spore germination or any other phenotype we tested. To test for complementation, we crossed heterokaryotic transformants to *N. crassa* CenH3 wild type strains. Strains with FgCenH3-GFP or AnCenH3-GFP alone were never recovered from such heterozygous crosses and thus were deemed insufficient to support meiosis and/or post-meiotic mitosis.

PaCenH3-GFP and NcCenH3-GFP were recovered from heterozygous but never from homozygous meioses, where both parents contained CenH3-GFP. This suggested that Pa- and NcCenH3-GFP are able to support mitosis but are unable to support meiosis. Even short tags (e.g. FLAG or a stretch of ten random amino acids) added to the C-terminus disallowed recovery of homokaryotic tagged strains. We conclude that the C-terminal tail of NcCenH3 is required for full meiotic function. We identified mutants in which meiotic or post-meiotic mitotic centromere maintenance is sufficiently affected to stall or abolish further growth. Our results suggest that there is a wide span from non-functional to fully functional centromere-kinetochore assemblies. Taken together, our results support a general model for CenH3 domain function that has emerged over the past five years from studies with yeast, plants and animals.

Introduction

Centromeres are essential for segregation of chromosomes during cell division. Although centromeric DNA is highly diverse, this genetic “locus” is important for correct localization, assembly and maintenance of kinetochores (54). In recent years it has become apparent that it is not the underlying DNA sequence that controls placement of regional centromeres but rather the epigenetic incorporation and inheritance of a histone H3 variant into specialized centromeric nucleosomes. This “centromere identifier”, called CenH3 in *Neurospora crassa* (273), is referred to as HRT12 in *Arabidopsis thaliana* (296), Cse4 in *Saccharomyces cerevisiae* (277) and *Candida spp.* (247), $Cnp1^{CenpA}$ in *Schizosaccharomyces pombe* (290), Cid in *Drosophila melanogaster* (131), and CENPA in *Homo sapiens* (210), where it was first identified. CenH3 proteins have two major domains, an N-terminal region of variable length and composition that is species- or even strain-specific, and a conserved histone fold domain (HFD) that is considered to be under strong negative selection, as are the HFDs of other core histones (282).

To understand why centromeric nucleosomes are different from most other nucleosomes, attention has been focused on CenH3 domains that may have different functions than canonical H3. Studies in *S. cerevisiae*, *Drosophila* and mammals, suggested that the N-terminal region, as well as Loop I and the adjacent α-2 helix within the HFD were sufficiently different from H3 to constitute essential centromere marks for different species or lineages (294). Budding yeast Cse4 is present in perhaps a single nucleosome on each chromosome, forming a “point centromere” (for review see (54, 127). The same arrangement may also hold for closely related species in the Saccharomycetales (14). The N-terminal region of ScCse4 contains an

“essential N-terminal domain”, the END domain, which is necessary for interaction with various centromere complexes (51). Nevertheless, overexpression of an allele of ScCse4 lacking an END domain complemented deletion of wildtype ScCse4 (51, 191). A chimera of the N-terminal domain of ScH3 and the HFD of ScCse4 expressed from the native promoter did, however, not complement a *cse4* null mutation (227). Functional complementation of ScCse4 with orthologues from closely related taxa during mitosis and meiosis has been observed (14, 191).

The ultra-conserved HFD may be even more important to generate the specialized centromeric nucleosomes (23, 258, 286). More than half of all amino acid positions in validated (i.e. centromere-targeting has been experimentally verified) or predicted CenH3 HFD are conserved or identical to those in H3, yet there are clearly functional differences between CenH3 and the canonical H3 proteins, H3.1 and H3.3 (12). Transfection of GFP-tagged chimeric *D. bipectinata* Cid with loop I of the HFD of *D. melanogaster* allows this chimera to be correctly targeted to centromeres in *D. melanogaster* cells (173, 315). Similar studies with human cells showed that chimeric histone H3.3 with loop I and part of the adjacent α-2 helix of CENPA, i.e. the “CENPA-targeting domain” (CATD), is capable of chromosome segregation in cells in which normal CENPA has been depleted by RNAi (25). Similar experiments suggested that HsCENPA was at least partially complemented by ScCse4 (324). At the same time, the N-terminal domain of mammalian CENPA is relatively short and not essential for centromere targeting of CENPA (264, 281). In contrast, an Arabidopsis histone H3.3 chimera with the AtHRT12 CATD failed to localize properly to centromeres, suggesting that in addition to the extended loop I region additional features of AtHRT12 are not required for targeting to centromeres (227).

In vitro and *in vivo* studies with CenH3 from different organisms suggest that it requires dynamic protein interactions during centromere assembly and inheritance, interactions that are expected to be different from those of canonical nucleosomes in non-centromeric regions, and that are likely different from organism to organism. Structural differences between canonical H3 and CenH3 nucleosomes have been studied in great detail (24, 25, 27), culminating with X-ray crystallography on partially or fully reconstituted animal CenH3-containing nucleosomes, which initially suggested that there are important differences in the HFD between H3/H4 and CENPA/H4 tetramers based on the primary amino acid sequence (23, 258), but which were largely absent in the octameric structure (286, 287). Instead, part of loop I appeared to be essential for targeting and maintenance of incorporated CenH3 at the centromere as a double substitution (R80A, G81A) resulted in reduced residence time of CenH3 in nucleosomes (286, 287). A competing structural hypothesis suggests that centromeric nucleosomes of Drosophila may exist as tetramers - “hemisomes“ of just one copy each of Cid, H4, H2A and H2B (61, 62, 72). This idea has gained support through two studies that revealed that the composition of centromeric nucleosomes changes over the course of the cell cycle (32, 271).

Thus, the basic function of CenH3 is apparently conserved among all eukaryotes studied thus far, but differences in centromeric nucleosome assembly and inheritance between different groups of organisms are emerging. Filamentous fungi constitute one of the predominant life forms on Earth. They are of great ecological, clinical and industrial importance and they comprise the major group in the kingdom Mycota. While genetic model systems, e.g. *Neurospora crassa* and *Aspergillus nidulans* are well studied, the sometimes distantly related plant, animal and human pathogens,

e.g. *Fusarium* spp., *Magnaporthe oryzae* and *Aspergillus fumigatus* are presently less well understood. Most centromere studies in fungi have been conducted on yeast species, e.g. *S. cervesiae* and *S. pombe*, and more recently on the dimorphic human commensal *C. albicans*. Thus in-depth knowledge of centromere behavior in filamentous fungi is completely lacking.

Recently we assembled almost all of the Neurospora centromeric DNA regions in two wildtype laboratory strains of *N. crassa* (220, 273), and found that this organism has regional centromeres, as was predicted by earlier genetic (41, 47) and comparative genomic studies (30, 97). To our surprise, we found that trimethylated lysine 9 of H3 serves as the predominant epigenetic mark in the centromeric core regions (273), which differs from what had been found in fission yeast, Drosophila and mammals (38, 155, 280). In all organisms with regional centromeres, the centromere core is flanked by pericentric heterochromatin, e.g. fission yeast (291), plants like rice (*Oryza sativa*), maize (*Zea mays*) and *Arabidopsis thaliana* (58, 152, 156) and animals like humans (*Homo sapiens*) and fruit fly (*Drosophila megalogaster*)(233, 276). This arrangement suggests that targeting of CenH3 to Neurospora centromeric regions may be accomplished in a different manner than has been proposed for mammals, where transcription of alphoid satellite DNA is required for HJURP targeting and CENPA assembly on artificial minichromosomes (19).

Our sequence alignments of CenH3 from publicly available genomes of filamentous fungi revealed hypervariable N-terminal regions and extremely conserved HFDs. To study the plasticity of Neurospora centromere assembly and inheritance, we undertook functional complementation assays where the endogenous NcCenH3

was replaced by the genes encoding CenH3 from *Podospora anserina* (Pa), *F. graminearum* (Fg) and *A. nidulans* (An). All fungal CenH3 proteins tested in this study were correctly localized to the Neurospora centromere when tagged with GFP, which suggests that at least some features of their CATD are conserved. Complementation assays revealed mitotic as well as meiotic defects in the absence of wildtype NcCenH3. The C-terminal GFP tagged PaCenH3 complemented NcCenH3 during mitosis and meiosis, but neither FgCenH3 nor AnCenH3 were sufficient for post-meiotic mitoses. We found that the HFD – and more specifically the very C-terminal tail – of NcCenH3 is required for full meiotic function. Taken together, our studies on CenH3 from filamentous fungi support the general model for CenH3 domain function that has emerged over the past five years. By using CenH3 proteins from closely related species we were able to separate meiotic and mitotic function of the four CenH3 proteins studied. Our results suggest quite an extent of fluidity for centromere nucleosome assembly, maintenance and function.

Materials and Methods

Strains

Neurospora strains (Table 2.1) were maintained and grown according to standard procedures (Davis, 2000). NMF39 was used as the wildtype strain, and N623 and N2240 were used for gene targeting to the *his-3* locus (57, 175). N3011 was the transformation host for gene replacements by homologous recombination. Additional strains were obtained from the Fungal Genetics Stock Center (Kansas City, MO) and grown on Vogel's minimal (VMM), malt extract (ME) or yeast extract/peptone/dextrose

(YEPD) medium to obtain tissue for DNA isolation. To make *Neurospora* grow as colonies, fructose, glucose and sorbose (FGS, 20%, 0.5%, 0.5% [w/v], respectively) were added to VMM (Davis, 2000).

DNA isolation and Southern analysis

Genomic DNA from filamentous fungi was isolated and Southern analyses were carried out as described previously (187, 221).

Sequence analysis

Sequences of *N. crassa* histone H4-2 (*hH4-2*; NCU00212) and CenH3 (*hH3v*; NCU00145) (114) were retrieved from NCBI and the Broad Institute database (http://www.broadinstitute.org/scientific-community/data). The CenH3 (*hH3v*) and *hH4-2* genes from various filamentous fungi were extracted by performing tBLASTn searches with the *N. crassa* sequences as queries. *CenH3* (*hH3v*) and *hH4-2* genes from additional *N. crassa* strains, additional *Neurospora* species, and species from closely related genera (Table 2.1) were amplified by PCR with different combinations of degenerate primers (OMF62, OMF64, OMF1399, OMF1400, OMF1401) and sequenced with OMF1399 at the OSU Center for Genome Research and Biocomputing core labs. Primer sequences are listed in Table 2.2. Accession numbers for DNA sequences used here are listed in Table 2.3.

Multiple sequence alignments and phylogenetic trees for hH4-2 and CenH3 DNA and protein sequences were generated with MEGA software (87, 197, 299). Non-synonymous (Ka) to synonymous (Ks) ratios of coding sequences for amino acid substitutions in aligned CenH3 sequences were calculated using DNASPv2 software (236).

Plasmids and fusion PCR constructs

Throughout the manuscript, NcCenH3 refers to the *N. crassa* CenH3 gene (*hH3v*; (114). The coding regions for CenH3 genes from *N. crassa* (*hH3v*, NcCenH3; NCU00145.5, XP_956658), *P. anserina* (PaCenH3; no GenBank entry), *F. graminearum* (FgCenH3; FGSG_02602.3) and *A. nidulans* (AnCenH3; ANID_06554.1, CBF70976) were amplified by PCR with primers containing *BamH*I and *Pac*I sites for cloning into the *his-3* targeting vector pMF272 (94). The resulting plasmids contain 5'-truncated (pMF319, primers cidBamF and cidPacR) or full-length (pMF320, primers cidBamF2 and cidPacR) NcCenH3, FgCenH3 (pLC2, primers OMF293 and OMF294), PaCenH3 (pLC3, primers OMF299 and OMF300) or AnCenH3 (pLC4, primers OMF297 and OMF298) in frame with the *sgfp* gene.

To generate strains bearing deletions of *hH3v* (NcCenH3), we amplified the 5'- and 3' flanks bordering *hH3v* by PCR with primers OMF63 and NCU00145_5r, or OMF183 and OMF184, respectively. Gene replacement constructs for targeting GFP fusions to *hH3v* were generated by "fusion PCR" (285) based on pZero-GFP-loxP-hph-loxP (120). CenH3 genes were amplified from *N. crassa* (NMF39; FGSC2489), *P. anserina* S *mat-* (NMF113; FGSC6711 *A. nidulans* (FGSC A4) and *F. graminearum* PH1 (FMF1; FGSC9075) genomic DNA with primers OMF1444 and OMF1447, OMF1443 and OMF1446, and OMF1445 and OMF162, respectively (Table 2.2). PCR fragments to generate strains with C-terminal FLAG tags ("CenH3-FLAG"; NMF229 - NMF231) were generated in the same way by amplification with primers OMF180 and OMF182, and OMF181 and OMF188, respectively (273).

To assess the importance of the 3'-untranslated region of *hH3v*, *hph* was introduced immediately downstream of the stop codon of the NcCenH3, PaCenH3,

FgCenH3 and AnCenH3 gene ("NcCenH3-*hph*", "PaCenH3-*hph*", "FgCenH3-*hph*","AnCenH3-*hph*") by fusion PCR with primers OMF1956, OMF1957, OMF1756, OMF2188 and OMF2187. As control, the *hph* gene was also inserted immediately downstream of the 3' end of the transcript, i.e. 1,211 nt downstream of the stop codon by fusion PCR with OMF2019 to OMF2030.

Similarly, the NcCenH3 and PaCenH3 genes were cloned into pPP78, a plasmid for the expression of red fluorescent protein (RFP) with *mCherry-10xGly* (in pBlueScript SKII-). The Nc- or PaCenH3 genes were inserted at the *Nde*I site after amplification with OMF1563 and OMF2218 or OMF2222, respectively, to generate N-terminally tagged RFP-CenH3. The cassette with the hygromycin resistance gene, *hph*, encoding hygromycin phophotransferase, was amplified with primers OMF83 and OMF84 (*hph* cassette). The entire construct resulting in *5'-flank CenH3-mCherry-10xGly-NcCenH3-hph-3'-flank* or *5'-flank CenH3-mCherry-10xGly-PaCenH3-hph-3'-flank* at the NcCenH3 endogenous locus was generated by transformation after split marker fusion PCR with primers OMF180 and OMF182 (5'flank), OMF181 and OMF188 (3'flank), OMF2226 and OMF1956 (NcCenH3), OMF2226 and OMF1957 (PaCenH3), and OMF1053 and OMF1054 (*hph* splitmarker primers).

Strain construction

Constructs targeted to the *his-3* locus were transformed into N623, N2240 or N2928 by electroporation (175). His^+ transformants (5'-truncated NcCenH3-GFP, NMF242; full-length NcCenH3-GFP, NMF243, PaCenH3-GFP, NMF244; AnCenH3-GFP, NMF245; FgCenH3-GFP, NMF246) were selected, grown on slants with VMM and 2 % sucrose, and analyzed by Southern blots for correct integration of the GFP-tagged CenH3 gene. Dominant alleles of *Sad-1* or *Sad-2* repress or abolish "meiotic

silencing by unpaired DNA" in heterozygous crosses (269) and allow unpaired tagged versions of the CenH3 locus to pass through meiosis without being subject to meiotic silencing. Thus, correct integrants were backcrossed to a *Sad-2* mutant (NMF161) to generate homokaryotic strains (NMF296 - NMF305).

A heterokaryotic *hH3v* (NcCenH3) deletion strain was generated by transformation of split marker *hph* fragments fused to *hH3v* flanks (see above) into N3011 by electroporation (57). One heterokaryotic transformant (NMF247) was selected for further studies. The same approach, split marker PCR, was used to generate gene replacements with various tagged constructs at *hH3v* (NMF318 – 323, NMF329 – 332, and NMF421 – 422). Primary transformants were transferred to slants with VMM supplemented with 250 mg/ml histidine and 200 μg/ml of hygromycin B (Hyg). Hyg-resistant (Hyg^R) colonies were confirmed by Southern analyses and subjected to DNA sequencing to verify correct integration. To obtain homokaryotic strains, heterokaryotic transformants were crossed to a *Sad-1* mutant (NMF162), generating strains NMF324 – 327, NMF333, NMF434 – 440, NMF423 – 425. Random ascospores were collected and heat-shocked at 65°C for an hour on plates with VMM and supplements. After 3 days of incubation germinated ascospores were transferred to slants and genotyped by PCR or Southern analysis. To genotype by PCR, a small loopful of conidia was suspended in 100 ul breaking buffer (331). The conidia suspension was microwaved for 90 sec and centrifuged for 2 min at 13,000 rpm. An equal volume of chloroform was added to the supernatant, briefly vortexed and centrifuged for 5 min at 13,000 rpm. Approximately 3 μl of the top aqueous layer was used as a template in PCR for genotype screening.

Split marker constructs for C-terminal GFP or FLAG CenH3 constructs, or N-terminal mCherry-CenH3 constructs (see above) were transformed into N3011 to generate heterokaryotic transformants (e.g., NMF402, NMF486, NMF487) that were crossed (typically to NMF162) to obtain homokaryotic progeny (e.g., NMF406, NMF408, NMF420, NMF484, NMF485; Table 2.1).

To assay for function of CenH3-GFP expressed at *his-3* (NMF243 – 246) we crossed representative strains to a heterokaryotic strain bearing a CenH3 deletion (NMF247). While we obtained *CenH3^{+}; his-3^{+}::CenH3-GFP* progeny, this strategy failed to generate homokaryotic *ΔCenH3^{+}; his-3^{+}::CenH3-GFP* strains. We used an alternative strategy to generate single-copy mutant CenH3-GFP strains. For this the heterokaryotic NMF247 strain was used as transformation host for pMF320, pLC2, pLC3, and pLC4 to yield strains NMF306 – 316, respectively (Table 2.1).

To observe the behavior of nuclei in strains with different CenH3 proteins we generated strains in which the linker histone H1 was tagged by dTomato, a red fluorescent protein (RFP) (261). Plasmid pPP67 (*hH1-dTomato* inserted in pMF272) was transformed into N3011 to generate heterokaryotic transformants that were crossed to NMF162 to obtain homokaryotic NMF427 (Table 2.1). NMF427 was crossed with non-tagged NcCenH3, PaCenH3 and FgCenH3 strains (NMF435, NMF439, and NMF425, respectively) to generate NMF428 – NMF433 (Table 2.1).

Crosses to test meiotic/mitotic function of CenH3s

In order to obtain homokaryotic strains from transformants, crosses were set on modified Synthetic Crossing (SC) medium (240). In most cases, two independent transformants from each transformation were crossed to the *ΔSad-1* mutant NMF162 (Table 2.1). Random ascospores were collected from the lids of each crossing plate,

spread on VMM+FGS plates with required supplements, and heat-shocked at 65°C for one hour. After three days of incubation, typically at room temperature, germinated ascospores were transferred to individual slants. Homozygous crosses were set in the same way, after the mating type of selected progeny was determined either by crosses to *fl* tester strains or by PCR of specific regions within the *mat a* or *mat A* idiomorphs.

Fluorescence microscopy

Asexual spores, germlings and hyphal suspensions of *Neurospora* strains expressing GFP were spotted on slides and observed under a Nikon Eclipse 80i epifluorescence microscope with excitation/emission wavelengths of 490/525 nm for capturing GFP, or 558/583 nm for mCherry. Images were taken and analyzed with the NIS-Elements imaging software and processed in Adopbe Photoshop CS2.

Assay for linear growth in Ryan ("race") tubes

Growth rates were monitored for strains with tagged and non-tagged versions of PaCenH3 and NcCenH3 in race tubes as described previously (65, 241). Approximately 50 μl of conidial suspensions (~10^3 cells/ml) were inoculated at one end of the race tube with VMM or VMM+His with 2% sucrose as carbon source. Growth was monitored for approximately one week or until strains reached the end of the race tube. Strains used were NMF169, NMF327, NMF333, NMF435 (NcCenH3), NMF324, NMF326, NMF439 and NMF440 (PaCenH3) and NMF423 and NMF424 (FgCenH3) along with NMF39 (WT) and N3011 (transformation host).

Spot tests on inhibitors

Sensitivity against various inhibitors was tested by spotting conidial suspensions from 10 -15 day old cultures of strains NMF39 (WT), NMF324 (PaCenH3), NMF408 (NcCenH3-GFP), NMF428 (NcCenH3), NMF429 (NcCenH3) and NMF430 (FgCenH3) on VMM supplemented with the topoisomerase inhibitor camptothecin (CPT; 0.3 μg/ml and 0.5 μg/ml), an inhibitor of DNA synthesis, hydroxyurea (HU; 25 mM and 30 mM), and an inhibitor of microtubule dynamics, thiabendazole (TBZ; 0.1 μg/ml and 0.5 μg/ml). Serial dilutions of 3,000, 300, 30, and three conidia were made and spotted on fresh plates.

Results

Phylogenetic analyses of CenH3 from filamentous fungi

Most filamentous fungi, including *N. crassa*, have a minimal complement of histone genes. In addition to a single linker histone H1 gene, a two-gene cluster of divergently transcribed H2A and H2B genes and an H2AZ gene, they typically have two histone H4 genes that encode identical proteins but have diverged DNA sequences and exon-intron boundaries (114). The *hH4-1* genes (in *N. crassa* locus NCU01634) are always found clustered with *hH3* and the genes are divergently transcribed from an overlapping and shared promoter, as is the case for H2A and H2B. In contrast, the *hH4-2* genes (in *N. crassa* NCU00212) are not near a canonical *hH3* gene, and relatively little is known about their expression patterns or specific functions (82, 114). The Neurospora genome encodes two histone H3 proteins. NCU01635 (*hH3*) on linkage group (LG) II encodes a canonical histone H3.3 and is

clustered with *hH4-1*. NCU00145 (*hH3v*) on LG III encodes CenH3, is not linked to any histone H4 gene (114), and encodes the Neurospora CenH3 protein (273).

We used phylogenetic analyses of publicly available CenH3 gene and protein sequences from filamentous fungi to address if these proteins (1) contain essential conserved regions, and (2) have regions that undergo adaptive evolution. We started by comparing the topology of phylogenetic trees obtained with CenH3 sequences to those obtained with sequences for the *hH4-2* gene, which is considered to be under purifying selection. To do this, we aligned the DNA sequences using MEGA, and generated both Neighbor-Joining (NJ; Figure 2.1) and Maximum-Parsimony (MP) trees for CenH3 and *hH4-2* genes. Based on the bootstrap values for 1000 replicates, minor branches were well resolved for CenH3 genes (Figure 2.1), but less so for the more conserved *hH4-2* genes (data not shown). The NJ tree for CenH3 resolved major branches, especially when intron sequences were retained. Overall, the CenH3 tree topology was similar to the fungal phylogenetic tree constructed with six genes (132). There were a number of important differences, however. While the Sordariomycetes *N.crassa*, *P. anserina* and *F. graminearum* were clustered together as expected, and were found on a different branch from the Eurotiomycetes, e.g. all *Aspergillus* species, they were rather closely associated with some basidiomycetes (e.g. *Laccaria*) and Dothideomycetes (e.g. *Pyrenophora tritici-repentis*), which are not phylogenetically this close to the Sordariomycetes. At the same time, hemiascomycete yeasts (e.g. *Saccharomyces spp.*) clustered closer to the Eurotiomycetes, rather than being basal to all true ascomycetes. This suggests that CenH3 phylogeny does not truly reflect overall phylogeny and lead us to hypothesize that at least parts of CenH3 may be under accelerated positive or adaptive selection.

In contrast, neither external nor internal nodes were well resolved on the *hH4-2* NJ tree, likely because of the high sequence conservation expected from a core histone gene (data not shown). Interior nodes of NJ trees were not resolved any better when we used known or predicted cDNA or protein sequences as input for CenH3 and *hH4-2*. When we compared the MP trees of genomic DNA sequences, cDNA sequences and protein sequences for CenH3 and *hH4-2*, the grouping of taxa was different. Problems with application of maximum parsimony algorithms for this dataset were likely caused by the high conservation of sequences.

We next focused our analyses on the closely related genera *Neurospora* and *Gelasinospora* (71, 100), which are so closely related that some authors place them in the same genus (37). With degenerate primers, we amplified and sequenced CenH3 genes from several species for which cultures are available from the FGSC, and subsequently performed phylogenetic analysis by NJ methods (Figure 2.2). The branching of taxa closely related to and within *Neurospora* showed high bootstrap values, in agreement with phylogenetic analysis of the genus *Neurospora*, which was based on seven nuclear loci from 43 taxa (202, 279). The genus *Neurospora* includes species with three different modes of sexual reproduction, (1) heterothallism, which requires two compatible strains of opposite mating type, (2) homothallism, or self-fertility, which does not require a mating partner, and (3) pseudohomothallism, where nuclei of opposite mating type co-exist in the same individual, which thus typically also does not require mating partners (59, 224). In the CenH3 tree constructed by NJ, three groups of species with different reproductive modes separate in different branches. Thus strains from the heterothallic species *N. crassa*, *N. intermedia*, and *N.*

sitophila grouped together. The pseudohomothallic *N. tetrasperma* produces macroconidia, in contrast to *Gelasinospora tetrasperma* (also known as *N. tetraspora*). We found that *N. tetrasperma* branches within the heterothallic group whereas *G. tetrasperma* groups with *G. cratophora* (*N. cratophora*), and the homothallic *G. reticulospora* and *G. dictyophora* (*N. dictyosphora*). Taken together, our phylogenetic analyses suggest that the relationship of CenH3 genes and proteins from within closely related groups of filamentous fungi and within the genus *Neurospora* mirrors that obtained by phylogenetic reconstructions based on six or seven nuclear loci. The relationships between CenH3 genes and proteins among these larger groups do not, however, reflect true phylogeny. Phylogeny based on the highly conserved *hH4-2* genes was not informative to resolve branches between closely related taxa.

Is positive selection acting on CenH3 from filamentous fungi?

Phylogenetic reconstruction suggested that CenH3 genes from filamentous fungi might be subject to accelerated positive or adaptive selection. For example, high divergence in primary sequence as well as length of the N-terminal region of CenH3 sequences within *Neurospora* and closely related genera of the Sordariaceae was observed. To estimate the degree of negative or positive selection on various domains and motifs of CenH3 (Figure 2.3A), we generated multiple sequence alignments by calculating the ratios of non-synonymous to synonymous replacements in DNA coding sequences of *N. crassa* (Oak Ridge “WT”, NMF39; Mauriceville, NMF37; Emerson, NMF2; Lindegren, NMF4; Louisiana, NMF115; Tamil Nadu, NMF106), *N. intermedia* (NMF49), *N. sitophila* (NMF35, NMF36), *N. tetrasperma* (NMF5), *N. terricola* (NMF29), *G. cerealis* (NMF9), *G. reticulospora* (NMF10), *G.*

cratophora (NMF119), *G. tetrasperma* (NMF11), *G. dictyophora* (NMF121) and *Sordaria macrospora* (NMF107). These analyses required sequence alignments without gaps. To avoid indels and to achieve continuous alignments, two codon positions were masked. The first was codon 8 (CGA, Arg) that was inserted only in *N. terricola* (NMF29) (Figure 2.3B), and the second was codon 26 (GGC, Gly, or CCT, Pro), an insertion found in *G.reticulospora* (NMF10), *G. tetrasperma* (NMF11), *N. terricola* (NMF29), *G. cratophora* (NMF119) and *G. dictyophora* (NMF121).

The masked DNA alignment was used as input for DNASPv2 (236). The DNASP output, obtained after sliding window analysis on the alignment, showed ratios of non-synonymous to synonymous replacements suggesting positive selection [Pi(a)/Pi(s) > 1] in a short region including the first ~100 nucleotides (nt) (Figure 2.4). The values obtained varied from 1 to 1.4, thus suggesting only the slightest prevalence of non-synonymous replacements. By this measure, the remainder of the CenH3 genes are predicted to be under strong negative selection, as Pi(a)/Pi(s) is approaching 0 between ~100-250 nt and equaling 0 between ~250-400 nt (Figure 2.4). Based on this analysis most of CenH3 from *Neurospora spp.* is under strong purifying selection. While there is a “hint” of positive selection in the part of the N-terminus that can be aligned, computational analyses are hampered by the difficulty of aligning sequences without losing resolution caused by masking.

Ectopically inserted CenH3 genes from three different filamentous fungi are targeted to chromocenters in *N. crassa*

Phylogenetic data for CenH3s supports established evolutionary relationships but failed to definitively identify specific regions of CenH3 that are under strong positive selection. To explore the significance of divergent and conserved regions in CenH3

by functional assays, we performed complementation studies with CenH3 genes from three additional filamentous fungi, the closely related *P. anserina* (PaCenH3), and the more distantly related *F. graminearum* (FgCenH3) and the relatively distant *A. nidulans* CenH3 (AnCenH3). The overall domain structure for NcCenH3, FgCenH3, PaCenH3, and AnCenH3 is conserved, although AnCenH3 lacks the second intron found in the other three genes (Figure 2.5A). The N-terminal regions,are highly variable in length and sequence, and the HFD is more conserved (Figure 2.5B).

To keep the endogenous CenH3 gene intact but allow for expression of potentially lethal CenH3-GFP proteins, we began this study by expressing NcCenH3, FgCenH3, PaCenH3 and AnCenH3 as C-terminal GFP fusions at the ectopic *his-3* locus under the control of the inducible Neurospora *ccg-1* promoter (Figure 2.6A). Southern analyses of transformants with the genes encoding different fungal CenH3-GFPs showed integration at *his-3* and retention of the endogenous, untagged copy of NcCenH3 at the native locus (Figure 2.6C). All four proteins were properly targeted to centromeres, as fluorescence was localized in tight foci, one each per nucleus in the typically multinucleate asexual spores or conidia (Figure 2.6D). In addition, we used a *his-3*-targeted truncated version of NcCenH3, which lacks much of the N-terminus as well as the first intron (Figure 2.5A). This construct was also properly targeted to centromeric foci (Figure 2.6D). In combination, these results suggested that a CENPA/CenH3-targeting domain (CATD) of reasonable conservation is all that is required for targeting to chromocenters in *N. crassa*.

To assay for functional complementation of endogenous CenH3 by ectopically expressed CenH3-GFPs, we crossed the heterokaryotic NMF243 [his-3^+::NcCenH3-gfp^+], NMF244, [his-3^+::PaCenH3-gfp^+], NMF245 [his-3^+::AnCenH3-gfp^+], and

NMF246, [his-3$^+$::FgCenH3-gfp$^+$], to a heterokaryotic CenH3 deletion mutant, NMF247 ([ΔNcCenH3::hph$^+$]; Figures 2.6 B and C). In the case of NcCenH3, we expected to recover viable progeny that carried the CenH3 deletion as well as the CenH3-GFP allele at *his-3*. For the three other CenH3 proteins, we expected to isolate viable progeny only if the interspecies CenH3 swap allowed complementation of NcCenH3 deficiency. Based on our previous results (273), we expected that near wildtype levels of CenH3 needed to be deposited at the centromeres to allow completely normal growth. To our surprise, none of the expected progeny (i.e. with presence of fluorescence in tight foci and resistance to hygromycin) were recovered in any of the crosses involving the four CenH3-GFP alleles integrated at *his-3* (Table 2.4). The recovered progeny had two copies of functional CenH3, i.e. wildtype endogenous NcCenH3 and another CenH3 copy at *his-3*, i.e. the C-terminally tagged CenH3 genes from various species, These results suggested that ectopically integrated CenH3 genes under the control of the *ccg-1* promoter and with a C-terminal GFP tag are unable to complement the CenH3 deletion allele.

In Neurospora, unpaired chromosomal regions are silenced during meiosis (8, 269). Thus, it was possible that we were unable to recover the desired progeny from heterozygous CenH3-GFP crosses because of meiotic trans-silencing of all CenH3 copies by the unpaired CenH3-GFP genes at *his-3*. We thus crossed strains with *his-3*-targeted fungal CenH3s to a *ΔSad-2::hph*$^+$ strain (NMF161), a dominant suppressor of meiotic silencing (270). We obtained progeny with *his-3*-targeted CenH3-GFP that were Δ*Sad-2::hph*$^+$ (NMF296-305; Table 2.1), which were crossed to the heterokaryotic CenH3 deletion strain (NMF247). Although all crosses were fertile,

again recombinants with *his-3*-targeted CenH3-GFP and a ΔCenH3 allele were not recovered.

Thus, as a second important result from these crosses we found that we were unable to isolate homokaryotic ΔCenH3 strains, suggesting that Neurospora CenH3 is essential. To validate this finding, we attempted to purify heterokaryotic CenH3 deletion strains by serial plating and isolation of single macroconidia or by generation of uninucleate microconidia. We were unable to obtain homokaryotic strains by either method (data not shown). We therefore conclude that CenH3 is an essential protein in Neurospora.

To generate the desired ΔNcCenH3::hph$^+$; *his-3*$^+$*::CenH3-gfp*$^+$ strains we decided to transform the heterokaryotic ΔNcCenH3::hph$^+$ *his-3* strain directly with pMF320, pLC2, pLC3 and pLC4 plasmids. Correct integration of plasmids was confirmed by Southern analyses (Figure 2.6C) and microscopy showed a single tight focus of fluorescence in each nucleus, indicative of a chromocenter (Figure 2.6D). We next crossed these transformants to a *Sad-1* mutant that is defective in meiotic silencing (NMF162). Again we were unable to obtain the desired *his-3*$^+$*::CenH3-gfp*$^+$; ΔNcCenH3 progeny. In combination, this series of transformations and crosses showed that *his-3*-targeted CenH3-GFP alleles can undergo crosses as heterokaryons, e.g. in the crosses to the *Sad-2* mutant, but that none of the four alleles at the ectopic *his-3* locus were able to complement the CenH3 deletion allele.

Replacement of native CenH3 by CenH3-GFP from three filamentous fungi

From the experiments with ectopically expressed CenH3-GFP it became obvious that gene replacements at the native CenH3 locus were required to properly assay for the effect of different CenH3 alleles. Therefore, we replaced wild type NcCenH3 with

C-terminally GFP tagged NcCenH3, PaCenH3, FgCenH3 and AnCenH3 directly at the native NcCenH3 locus with constructs generated by overlapping PCR (Figure 2.7A). All replacement constructs were transformed into a common host strain (N3011; Table 2.1). Ectopic integration is nearly eliminated in N3011 because the *mus-51* (homologue of ku-70) deletion allele renders it defective for non-homologous end joining (199).

Correct integration of constructs (e.g. transformants NMF318-323 and NMF441; Table 2.1) was verified by Southern analyses (Figure 2.7B, lanes 3-6, 9, 12,17 and 20), and the integrated fusion genes were amplified by PCR and subjected to DNA sequencing (data not shown). Southern analyses of heterokaryotic transformants (NMF320 and NMF440) showed the presence of two bands, i.e. wildtype NcCenH3 and CenH3-GFP genes, when probed with CenH3 gene fragments. Homokaryotic progeny from crosses with NMF162, e.g. for PaCenH3-GFP (NMF324 and NMF326) and NccenH3-GFP (NMF408 and NMF420) showed single CenH3-GFP-specific bands (Figure 2.7B). We also confirmed localization of CenH3-GFP in the original transformants by screening under an epifluorescence microscope, which revealed a single tight focus of fluorescence in each nucleus (typically two or three nuclei per conidium are present), which suggested proper targeting of the four fungal CenH3 proteins at Neurospora centromeric chromocenters (Figure 2.7C).

To test if the single CenH3-GFP fusion genes are able to functionally replace untagged NcCenH3, heterokaryotic transformants (NMF318 to NMF323; Table 2.1) were crossed with a *Sad-1* mutant (NMF162) to obtain homokaryotic CenH3-GFP strains. All heterozygous crosses of heterokaryotic transformants with NMF162

(containing wildtype NcCenH3) were fertile. When we analyzed progeny from these crosses, we found that only PaCenH3-GFP and NcCenH3-GFP were recovered (18/58 and 16/50 germinated ascospores, respectively from crosses XKS122 and XPP14; Table 2.4). This suggests that NcCenH3-GFP and PaCenH3-GFP are able to complement untagged NcCenH3 in heterozygous crosses when some – presumably not nucleus-limited – NcCenH3 from the opposite partner in the cross is present. Ascospores with PaCenH3-GFP and NcCenH3-GFP from heterozygous crosses XPP236 and XPP237 germinated normally and looked identical based on co-localization of H1-dTomato (Figure 2.7D). In contrast, AnCenH3-GFP and FgCenH3-GFP were not recovered from fertile, heterozygous crosses with NMF162 (XPP15, XPP13A and XPP13B, Table 2.4). Ascospores containing AnCenH3-gfp and FgCenH3-gfp germinated on non-selective medium after overnight growth at room temperature but ceased to grow within a day, suggesting that further mitoses were unsuccessful.

The CenH3 C-terminal tail is essential during meiosis

In an attempt to isolate GFP-tagged strains with the Aspergillus or Fusarium CenH3 at the native locus, we carried out heterozygous crosses between strains with either NcCenH3-GFP (NMF169 and NMF327) or PaCenH3-GFP (NMF324 and NMF326) and heterokaryotic transformants that carried nuclei with FgCenH3-GFP (NMF318 and NMF319) or AnCenH3-GFP (NMF321 and NMF322) (Table 2.4). In these crosses any complication caused by potential meiotic silencing should have been alleviated as CenH3 genes in all strains were similarly tagged with the GFP gene and carried the selectable *hph* marker gene in the same location. We screened progeny from these crosses for presence or absence of tagged or wildtype alleles by

PCR. Out of ~120 progeny from crosses with a heterokaryotic AnCenH3-GFP transformant to either a homokaryotic NcCenH3-GFP (XPP39 and XPP40) or a homokaryotic PaCenH3-GFP strain (XPP219, XPP18A and XPP18B) none carried the AnCenH3-GFP gene. Instead, the NcCenH3-GFP gene was recovered in 14/28 progeny, and the PaCenH3-GFP gene was recovered in 35/91 progeny; the remaining strains had the wildtype NcCenH3 gene (Table 2.4). Similarly, out of 85 progeny from crosses with a heterokaryotic FgCenH3-GFP transformant to a homokaryotic NcCenH3-GFP (XPP220, XPP35 and XPP36) or a homokaryotic PaCenH3-GFP strain (XPP219, XPP17A and XPP17B) none were positive for the FgCenH3-GFP gene. The NcCenH3-GFP or PaCenH3-GFP genes compared to the wild type NcCenH3 were recovered at ratios of of 17/12 and 28/28, respectively (Table 2.4). Overall, the PaCenH3-GFP allele was consistently recovered at lower frequencies compared to the NcCenH3-GFP and NcCenH3 alleles, possibly due to subtle meiotic defects.

Neurospora strains in which PaCenH3-GFP or PaCenH3 without a tag replace the wildtype NcCenH3 at the endogenous locus were stable and grew almost normally during extended periods of vegetative growth through “race tubes” (Figure 2.8A). GFP fluorescence from chromocenters in strains with NcCenH3-GFP and PaCenH3-GFP was quantified with the NIS-Elements imaging software. The average fluorescence intensity for NcCenH3-GFP (NMF408) was slightly higher than for PaCenH3-GFP (NMF326) when ~200-300 nuclei of each strain were measured (Figure 2.9). This observation further suggested subtle differences between NcCenH3 and PaCenH3 during kinetochore assembly or maintenance.

Thus we next asked if GFP-tagged PaCenH3 supports completion of meiosis in Neurospora. We set homozygous crosses of PaCenH3-GFP strains (XPP19, Table 2.4). These crosses, done reciprocally and repeated at least once, were all completely barren, i.e. no spores were produced in normally developed perithecia. These results suggested that PaCenH3-GFP does not support normal meiosis in Neurospora. To address if presence of NcCenH3-GFP in the cross would restore normal meiosis in heterozygous crosses, we set crosses between homokaryotic PaCenH3-GFP and NcCenH3-GFP strains (XPP48 and XPP19, Table 2.4). We were surprised to find that these crosses were also completely barren (Table 2.4), suggesting that even a C-terminally GFP-tagged NcCenH3 gene was inadequate for complementation of normal meiosis in Neurospora. Thus homozygous crosses between two NcCenH3-GFP strains (XPP48 and XPP53: Table 2.4) were likewise barren. To test if this defect was specific to the addition of the bulky GFP protein, we generated strains with short C-terminal tags. Homozygous crosses of NcCenH3-FLAG strains (XPP53) and strains with a random string of ten amino acids (XPP99) were also found to be completely barren (Table 2.4). The barrenness of these homozygous crosses with C-terminally tagged CenH3s was confirmed by either repeating the same crosses or setting up new crosses with various different sibling strains from XPP14 and XKS122 crosses (data not shown). From this series of experiments we concluded that the CenH3 C-terminal tail plays an important role during meiosis.

A competing hypothesis to explain our observations is that barreness of homozygous crosses with C-terminally tagged CenH3 is caused by disrupting the CenH3 3'UTR, resulting in dysregulation of CenH3 translation during meiosis. Studies

in mammals have shown that canonical histone mRNAs have stem-loop structures formed by the 3'UTR and that these structures serve as "platforms" for the binding of regulatory proteins important for histone regulation during DNA replication (64, 178). In order to test this hypothesis, we introduced the *hph* gene, which encodes for hygromycin resistance, immediately downstream of the stop codon ("-*hph*") of NcCenH3 and PaCenH3 at the endogenous locus of NcCenH3. The *hph* marker thus disrupted the 3'UTR but the CenH3 protein sequence was no longer altered, allowing us to separate if meiotic defects seen with C-terminally tagged CenH3 are due to the tag or the disruption of 3'UTR-mediated CenH3 regulation. Genotypes of homokaryotic non-tagged NcCenH3 (NMF434-436) and PaCenH3 (NMF437-439) strains (Table 2.1) were confirmed by Southern analyses (data not shown), and strains were used in homozygous crosses (Table 2.4). Both crosses with NcCenH3-*hph* and PaCenH3-*hph*, were fertile and generated as many ascospores as wildtype crosses (data not shown). Genotyping by PCR showed that CenH3 genes were recovered at expected ratios (Table 2.4). Therefore we conclude that the 3'UTR of CenH3 is not important for regulation during meiosis. Rather, access to or folding of the C-terminal tail is important during Neurospora meiosis.

We next performed crosses with FgCenH3-*hph* (XPP188, XPP204, XPP213, XPP212) and AnCenH3-*hph* (XPP184) to determine if the meiotic and mitotic defects observed with previous constructs were caused by differences in CenH3 sequence or presence of the GFP tag (Table 2.4). Neurospora strains with FgCenH3-*hph* were able to undergo homozygous crosses and yielded viable ascospores whose germination frequencies were similar to those from a wildtype cross (Table 2.4 and data not shown). Heterozygous crosses with AnCenH3 alleles produced ascospores

but none of the spores carrying AnCenH3-GFP or AnCenH3-*hph* survived germination (Table 2.4). We conclude that untagged FgCenH3, like PaCenH3, can complement NcCenH3 function in both mitosis and meiosis but that AnCenH3, the most distantly related CenH3, cannot.

Tagging the CenH3 N-terminal tail results in genus-specific meiotic defects

We next asked if the effects observed by tagging the C-terminal tail of CenH3 were domain-specific. We thus inserted the gene for mCherry, encoding a red fluorescent protein, between the native promoter and the N-terminal tail of both NcCenH3 and PaCenH3, while the selectable marker, *hph*, was inserted in the same place as in the constructs with non-tagged strains (Table 2.1). Crosses with heterokaryotic transformants carrying NcCenH3 (XPP201) or PaCenH3 (XBF1) were fertile, and so were homozygous crosses with strains that carried mCherry-NcCenH3 (XPP218; Table 2.4). Conversely, homozygous crosses with strains carrying mCherry-PaCenH3 (XBF1) were barren: just like in the case of C-terminally tagged strains no spores were observed in normally developed perithecia (Table 2.4). These results suggest that tags at the N-terminus can be tolerated by the wildtype NcCenH3 allele, but not by the PaCenH3 allele. In the latter case, addition of peptide sequence appears to cause a complete loss of function for the PaCenH3 allele.

Non-tagged FgCenH3 and PaCenH3 showed vegetative growth defects in the presence of inhibitors

We did not observe obvious growth defects on plates, in slants or during linear growth assays in race tubes with tagged NcCenH3-GFP or PaCenH3-GFP, or in

PaCenH3 and FgCenH3 without tags (Figure 2.8). To observe more subtle defects during mitosis we plated dilutions of Neurospora macroconidia in the presence of hydroxy urea (an inhibitor of DNA synthesis; HU), thiabendazole, (a microtubule destabilizing agent; TBZ) and camptothecin (a topoisomerase I inhibitor; CPT). Growth defects in non-tagged FgCenH3 (NMF431) and PaCenH3 (NMF433), as well as tagged NcCenH3-GFP (NMF408) and PaCenH3-GFP (NMF324) were observed in the presence of 0.5 μg/ml TBZ when compared to WT (NMF39) and non-tagged NcCenH3 (NMF428) (Figure 2.10).

In contrast, non-tagged FgCenH3 (NMF431) and PaCenH3 (NMF433) and tagged NcCenH3-GFP (NMF408) and PaCenH3-GFP (NMF324) strains showed no growth defect at 25 mM and 30 mM of HU when compared to the wild-type NcCenH3 (NMF39) and non-tagged NcCenH3 (NMF428) strains (Figure 2.10). Similarly, CPT did not cause defects (data not shown). These results suggest that DNA replication is not significantly affected in strains with altered CenH3 alleles.

Higher sensitivity to TBZ in strains with altered CenH3 alleles suggested mitotic spindle defects. We thus assayed for differences in mitotic behavior in strains with non-tagged FaCenH3 (NMF431), PaCenH3 (NMF4333) and NcCenH3 (NMF428) that also carry H1-dTomato at *his-3* as a nuclear marker for microscopy studies. We have yet to find conspicuous differences in nuclear behavior throughout the cell cycle or at different incubation temperatures. We found no significant increase in the formation of chromosome bridges that may have formed due to lagging chromosomes during cell division, as has been previously documented for mutants involved in heterochromatin formation and DNA methylation (161).

Discussion

Phylogenetic analyses of CenH3 sequences of filamentous fungi

Earlier reports suggested that domains of CenH3 in some taxa are under positive selection and may thus be adaptively evolving in concert with the centromeric DNA (76, 105, 172, 311). Before this study nothing was known about the level of divergence and adaptation of CenH3 proteins from filamentous fungi. To understand if positive selection may occur across all or parts of CenH3 genes we carried out phylogenetic analyses with all publicly available CenH3 sequences from fungi and compared the resulting phylogenetic trees to published phylogenies (132,Nygren, 2011 #11588, 279). The branching of the CenH3 gene tree largely coincides with fungal phylogenies based on the conserved histone fold domain; high divergence rates are limited to the N-terminal region of CenH3. Thus, by this analysis most of CenH3 from various filamentous fungi is under strong purifying selection, just as the canonical core histones.

Curiously, *Nectria haematococca* appears to have two CenH3 genes. One CenH3 protein clusters with those of the closely related *Fusarium* species, the other clusters with the only distantly related *Tuber melanosporum* (Figure 2.1). Apart from some polyploid plant hybrids, e.g. barley (*Hordeum spp.*) (245), this is the only case where a species has the potential to make two, in this case very different, CenH3 proteins. The *Nectria* CenH3 genes are localized in two functionally distinct compartments of the genome, as the *Fusarium*-type CenH3 gene is localized on a core, or “A”. chromosome, whereas the non-*Fusarium*-type CenH3 is localized on a “dispensable”,

lineage-specific, or “B”, chromosome. This arrangement suggests that lineage-specific chromosomes, which can be maintained stably during crosses in *Nectria*, may require the presence of properly adapted CenH3 proteins, a hypothesis we are currently pursuing further.

A second phylogenetic analysis, based on calculating the relative rates of non-synonymous to synonymous replacements suggested weak positive selection and a slightly higher rate of divergence within the CenH3 N-terminal tail of closely related species of *Neurospora*, *Gelasinospora* and *Sordaria*. Some of the more pronounced differences were found even between strains of the same species that were isolated from geographically distinct regions, e.g. *N. crassa* Mauriceville (NMF37) and *N. crassa* Lindegren (NMF4). In contrast, in *Drosophila* species the N-terminal region was found to be under negative selection (172). Hemiascomycetous yeasts in the genera *Saccharomyces*, *Kluyveromyces*, *Pichia* and *Yarrowia* have defined essential “N-terminal domains” (END) that appear taxon-specific (14), suggesting either fast successive selective sweeps or continuous strong purifying selection in the various genera. While we were able to align CenH3 sequences from closely related genera, a similar analysis was not even attempted here for all filamentous fungi for which CenH3 sequences are available, as the N-terminal tails did not align sufficiently well to retain meaningful sequence information. In summary, CenH3 across the fungal kingdom thus presents as a clearly bipartite protein with an extremely variable N-terminal extension with no clearly identifiable motifs of the END type, and a histone fold domain (HFD) that appears under purifying selection, as is true for the other fungal core histones. The only HFD region with non-conservative substitutions and insertions was loop I, similar to what has been described in studies with

hemiascomycetous yeasts (14), *Drosophila* (173), plants (158, 226, 227) and mammals (25).

Genetic analyses of CenH3 sequences of filamentous fungi

Instead of relying on sequence-derived phylogenetic considerations alone, we wished to determine by functional assays how different CenH3 proteins needed to be before complementation of wildtype Neurospora CenH3 became impossible. This type of assay helps us to understand how diverse centromere and kinetochore maintenance are in different groups of filamentous fungi.

Ectopically expressed CenH3-GFP from *N. crassa*, *P. anserina*, *F. graminearum* and *A. nidulans* were targeted to the Neurospora centromere, likely because of the presence of CenH3 specific loop I regions (Figure 2.5D). These observations agree with studies in fly (315), yeast, and human (25, 264) showing that H3 chimeras containing loop I alone or with part of the adjacent α-2-helix were targeted to the centromere and complemented CENP-A/Cse4 function. However, ectopically expressed C-terminally GFP tagged NcCenH3 genes under control of the *ccg-1* or native CenH3 promoters (data not shown) were unable to complement a CenH3 deletion allele. An ectopically expressed N-terminally tagged NcCenH3 with its native promoter and 3'UTR was, however, was able to complement the CenH3 deletion allele (data not shown). Our observations thus differed from those made with *S. cerevisiae*, *S. pombe* and *C. albicans*, where ectopically expressed C-terminal tagged Cse4 (Cse4-GFP) expressed from a non-native promoter was able to complement the endogenously disrupted Cse4 locus (50, 138, 214). Of course, CenH3 expressed ectopically at the *his-3* locus and from the *ccg-1* promoter (181) might be insufficient

for normal temporal and spatial expression. This promoter is regulated by light, the circadian clock (170) and inducible by glucose repression (181), but without induction generally yields sufficient protein to be considered constitutive expression. One potential reason for not achieving sufficient ectopic expression of CenH3 in Neurospora under a non-native promoter may be the more complex and dynamic nature of regional centromeres, around 150-300 kb in Neurospora (273) in comparison to a mere 150 bp in *Saccharomyces*, 3-4 kb in *Candida* and 38-97 kb in *S. pombe* (127, 146, 186, 291). To alleviate this concern we carried out numerous experiments with CenH3 alleles targeted to the native CenH3 locus.

PaCenH3 and FgCenH3 complement NcCenH3 function

Evolutionarily, *P. anserina* is more closely related to *N. crassa* compared to *F. graminearum* and *A. nidulans* (Figure 2.1 (132). In Neurospora, PaCenH3-gfp, FgCenH3-gfp and AnCenH3-gfp were directly integrated at the endogenous NcCenH3 locus to assay for functional complementation. Only NcCenH3-GFP and PaCenH3-GFP were recovered as single copy alleles from crosses with wildtype NcCenH3 parents, indicating that PaCenH3 can complement NcCenH3, and the GFP tag does not interfere with mitotic function. When these tagged constructs were the only copy of CenH3, and both parents contained the C-terminal GFP tag, neither PaCenH3-GFP nor NcCenH3-GFP were functional in meiosis. This lead us to repeat the functional assays with a smaller FLAG tag, but NcCenH3-FLAG was still not functional in meiosis. Placing a tag at the N-terminus of NcCenH3 restored mitotic and meiotic function to NcCenH3, but not PaCenH3. We conclude that the function of the C-terminal tail of NcCenH3 is more sensitive to perturbations during meiosis than in mitosis.

However, there is decrease in fluorescence intensity in presence of PaCenH3-GFP compared to NcCenH3-GFP in the conidia i.e. during mitosis. Thus, suggesting either the difference in level CenH3 protein incorporated in the centromere nucleosomes or interactions with the kinetochore other proteins for PaCenH3. The actual reason for this variation is yet to be determined.

Since we found that C-terminal tags interfere with function of NcCenH3, we repeated the functional assays for Fg, Pa, and AnCenH3 without the tag. We found that both PaCenH3 and FgCenH3 were able to complement NcCenH3 in both mitosis and meiosis. These alleles passed through crosses with expected frequency in both heterozygous and homozygous conditions where they were the only copy of CenH3 in either parent. Examination of protein alignments show clear similarities between Nc, Pa, and Fg that are absent in An. AnCenH3 has an exceptionally long N-terminal tail as well as two extra amino acids inserted into loop 1 of the HFD. Recent studies in Drosophila showed that an arginine-rich motif within the N-terminus of DmCid (DmCenH3) is required for proper spindle attachment and chromosome orientation during cell division, via interaction with the conserved BubR1 protein (308). The R-rich domain in Drosophila (^{119}RRRKAA^{124}) appears conserved in the same position in Nc, Pa, and Fg CenH3 (^{50}KRRYR^{54}). This region is not conserved in the one fungal protein that did not complement NcCenH3. In AnCenH3 this region is mutated to RHRYK. Disruption of this domain and failure to interact with other Neurospora kinetochore proteins could explain the inability of AnCenH3 to complement NcCenH3.

The domain swap experiment in yeast between *Saccharomyces* Cse4 and *Pichia* Cse4 showed that when 16 or fewer amino acid differences were present within the

HFD region, *Pichia* Cse4 HFD complemented ScCse4 function (14). Therefore, it appeared that the number of differences in HFD determined the functioning of CenH3.

The CenH3 C-terminus has conserved function in kinetochore assembly

In Arabidopsis, a C-terminally GFP-tagged CenH3 did not support meiosis in *cenh3* null mutants even in heterozygous crosses (226, 227). The C-terminus of NcCenH3 has six additional amino acids compared to NcH3. The C-terminal tail of human HsCENP-A is similarly extended compared to HsH3, and the extreme C-terminus of CENP-A is required for CENP-C interaction with CENP-A nucleosomes, at least *in vitro* (44). This interaction is conserved in *Xenopus laevis* (Xl), where H3 chimeras containing only the CENP-A C-terminus were able to recruit CENP-C (109). Both Hs- and XlH3 end in “ERA” and CENP-A end in “LEEGLG”, while NcH3 ends in “ER” and CenH3 ends in “VWGGAGWV”. These sequences are identical in Pa, but mutated to “M/AWGGLG” in Fg and An, possibly explaining why PaCenH3 is the only protein able to complement NcCenH3 during mitosis when the C-terminal GFP tag is present. The shorter C-terminal tail in combination with the GFP tag found in Fg and An CenH3-GFP may disrupt the interaction with NcCEN-C.

The N-terminal tail is dispensible for centromere localization but required for meiosis

Truncation of the NcCenH3 N-terminal tail by 18 amino acids in Fg- and especially PaCenH3 did not interfere with targeting of CenH3 to the chromocenter. Furthermore, all fungal CenH3-GFPs were targeted to the centromere, although they have very different N-termini. Both FgCenH3 and PaCenH3 without the GFP tag were

able to complement NcCenH3 function, but AnCenH3, with the extremely long N-terminus was not. Additionally, placing an N-terminal mCherry tag on PaCenH3 eliminated its ability to complement NcCenH3 function during meiosis. Taken together these results suggest that although sequence content is not crucial for function, unlike at the C-terminus, a certain level of mutation is tolerated up to a threshold beyond which the protein can no longer function. The N-terminal tail in *S. pombe* is essential for centromere nucleosome formation, while the *A. thaliana* CenH3 N-terminal tail is important during meiosis (228, 293). An N-terminal truncation of Arabidopsis HRT12 was properly targeted to centromeres but was not able to complement embryonic lethality in an *hrt12* null mutant (227). In human cells, however, H3 containing loop 1 and the α-2-helix was fully functional although it lacked both the N- and C-terminal tails of CenPA (25). Protein structure studies have concluded that the N-terminal tail and α-N helix are flexible (212).

Conclusion

Neurospora CenH3 is an essential gene and nuclei with a CenH3 deletion participating in heterozygous crosses are not expected to survive unless CenH3 is not nucleus-limited by maintaining the spatial and temporal regulation. The second factor contributing to CenH3 function is the structur of CenH3, there are determinants required for protein and DNA interactions in centromeric nucleosomes. C-terminally GFP-tagged NcCenH3 and PaCenH3 expressed from the endogenous locus resulted in fertile heterozygous crosses but barren homozygous crosses, suggesting a meiotic cell division defect. This experiment also suggests that normal CenH3 can move between parent nuclei and is not nucleus-limited.

Both the tagged and non-tagged AnCenH3 were not able to complement meiosis in *Neurospora* in heterozygous or homozygous crosses. *Aspergillus nidulans* undergos synchronous mitotic cell divisions compared to the asynchronous *N. crassa* (104, 234). Due to this it is possible that spatio-temporal regulation and mechanisms of assembly of kinetochore formation might be different between the Aspergillus and Neurospora clades. Plants, for example barley, can have multiple variants of CenH3 but only one type of CenH3 incorporated into centromeric nuleosomes of hybrids (245). Longer N-terminal tails, as found in AnCenH3, might also act as hindrance for the compact packing of CenH3 nucleosomes (212).

Phenotypic defects in growth were observed in non-tagged and tagged NcCenH3, PaCenH3 and FgCenH3 in the presence of an inhibitor of microtubule dynamics, TBZ, while HU, which inhibits mainly DNA synthesis by inhibiting the enzyme ribonucleotide diphosphate reductase and altering deoxyribonucleotide pools (252) had essentially no effect. TBZ impairs formation of microtubule assembly at the late stage of cell cycle division (317). Recent studies identified some of the essential residues in H2A and H2B histones at centromeres required for bi-orientation of chromosomes during mitosis in budding yeast, and these point mutations were studied based on benomyl (another microtubule inhibitor) and TBZ sentitivity (142). A recent study in Neurospora showed that different deletion strains of genes involved in heterochromatin formation (*hpo*, *dim-5*, *dim-2* and *dim-7*) are also sensitive to TBZ (161). We previously showed that heterochromatin formation is important for normal distribution of CenH3 at Neurospora centromeres (273). In conclusion, our heterologous systems allowed us to generate “poised” or metastable states of CenH3 nucleosomes that can be further explored by site-directed mutagenesis to tease out

small phenotypic differences and will in the future allow us to assign function to non-conserved regions of CenH3

Table 2.1: Strains used in this study.
Transformed heterokaryotic strains are denoted by square brackets in the table and throughout the manuscript. Unless noted otherwise, strains are *N. crassa.* Strains for phylogenetic analyses were obtained from the Fungal Genetics Stock Center (FGSC, University of Missouri, Kansas City, MO). Throughout the table and the manuscript, "*NcCenH3*" refers to the *N. crassa* CenH3 gene, originally called *hH3v* (114); *loxP* indicates recognition sites for the P1 *Cre* recombinase. Strains NMF306 to NMF316 were obtained by transformation of a heterokaryotic strain, NMF247, thus the various CenH3-GFP constructs targeted to *his-3* may have been integrated into the CenH3^{+} or the CenH3^{-} nucleus.

Strains	Known genotypes	Source
FGSCA4	*Aspergillus nidulans*	FGSCA4
FMF1	*Fusarium graminearum*	FGSC9075
NMF9	*Gelasinospora cerealis*	FGSC959
NMF119	*G. cratophora*	FGSC7796
NMF121	*G. dictyophora*	FGSC7798
NMF10	*G. reticulospora*	FGSC960
NMF11	*G. tetrasperma*	FGSC966
NMF39	*N. crassa* ("wild type"; 74-OR23-1VA) *mat A*	FGSC2489
NMF2	*N. crassa* (Emerson 5297) *mat a*	FGSC352
NMF4	*N. crassa* (Lindegren 1) *mat A*	FGSC354
NMF115	*N. crassa* (Louisiana, D113) *mat A*	FGSC8873
NMF37	*N. crassa* (Mauriceville-1-c) *mat A*	FGSC2225
NMF106	*N. crassa* (Tamil Nadu, D98) *mat A*	FGSC8858
NMF49	*N. intermedia mat a*	FGSC3417
NMF35	*N. sitophila mat A*	FGSC2216
NMF36	*N. sitophila mat a*	FGSC2217
NMF5	*N. tetrasperma mat a*	FGSC606
NMF29	*N. terricola*	FGSC1889
NMF113	*Podospora anserina mat s-*	FGSC6711
NMF107	*Sordaria macrospora*) wild type	FGSC4818
N2240	*rid^{RIP1} mat A his-3*	(95)
N623	*mat A his-3*	(95)
N2928	*mat A his-3*; Δ*mus-51*::*bar*$^{+}$	This study
N3011	*mat a his-3*; Δ*mus-51*::*bar*$^{+}$	FGSC9538
NMF160	*mat A;* Δ*Sad-2*::*hph*$^{+}$	(273)
NMF169	*mat a his-3; ΔNcCenH3::NcCenH3-gfp*$^{+}$*-loxP-hph*$^{+}$*-loxP*	(273)
NMF229	*mat A; ΔNcCenH3::NcCenH3-flag*$^{+}$*-loxP-hph*$^{+}$*-loxP*	(273)
NMF230	*mat A; ΔNcCenH3::NcCenH3-flag*$^{+}$*-loxP-hph*$^{+}$*-loxP*; Δ*Sad-2*::*hph*$^{+}$	This study
NMF231	*mat a his-3; ΔNcCenH3::NcCenH3-flag*$^{+}$*-loxP-hph*$^{+}$*-loxP*	This study
NMF161	*mat a;* Δ*Sad-2*::*hph*$^{+}$	This study
NMF162	*mat A* Δ*Sad-1 (partial deletion)*	This study
NMF138	[*mat A his-3* + *mat A his-3*$^{+}$*::P$_{ccg-1}$-tdimerRed*$^{+}$*-hH1*$^{+}$]	This study
NMF242	[*mat A his-3* + *mat A his-3*$^{+}$*::5'ΔNcCenH3-gfp*$^{+}$]	This study
NMF243	[*rid^{RIP1} mat A his-3* + *rid^{RIP1} mat A his-3*$^{+}$*::NcCenH3-gfp*$^{+}$]	This study
NMF244	[*rid^{RIP1} mat A his-3* + *rid^{RIP1} mat A his-3*$^{+}$*::PaCenH3-gfp*$^{+}$]	This study
NMF245	[*rid^{RIP1} mat A his-3* + *rid^{RIP1} mat A his-3*$^{+}$*::AnCenH3-gfp*$^{+}$]	This study
NMF246	[*rid^{RIP1} mat A his-3* + *rid^{RIP1} mat A his-3*$^{+}$*::FgCenH3-gfp*$^{+}$]	This study
NMF247	[*mat a his-3*; Δ*mus-51*::*bar*$^{+}$; *NcCenH3*$^{+}$ + *mat a his-3*; Δ*mus-51*::*bar*$^{+}$ Δ*NcCenH3::hph*$^{+}$]	This study
NMF296, NMF297	*mat A his-3::P$_{ccg-1}$-NcCenH3-gfp*$^{+}$; *ΔSad-2::hph*$^{+}$	This study

NMF298-301	*mat A his-3::P$_{ccg-1}$-PaCenH3-gfp$^+$; ΔSad-2::hph$^+$*	This study
NMF302-304	*mat A his-3::P$_{ccg-1}$-AnCenH3-gfp$^+$; ΔSad-2::hph$^+$*	This study
NMF305	*mat A his-3::P$_{ccg-1}$-FgCenH3-gfp$^+$; ΔSad-2::hph$^+$*	This study
NMF306, NMF307	[*mat a his-3::P$_{ccg-1}$-NcCenH3-gfp$^+$; NcCenH3$^+$; Δmus-51::bar$^+$ + mat a his-3; ΔNcCenH3$^+$::hph$^+$; Δmus-51:: bar$^+$ + mat a his-3; NcCenH3$^+$; Δmus-51::bar$^+$*]	This study
NMF309, NMF310	[*mat a his-3::P$_{ccg-1}$-FgCenH3-gfp$^+$; NcCenH3$^+$; Δmus-51::bar$^+$ + mat a his-3; ΔNcCenH3$^+$::hph$^+$; Δmus-51:: bar$^+$ + mat a his-3; NcCenH3$^+$; Δmus-51::bar$^+$*]	This study
NMF312, NMF313	[*mat a his-3::P$_{ccg-1}$-PaCenH3-gfp$^+$; NcCenH3$^+$; Δmus-51::bar$^+$ + mat a his-3; ΔNcCenH3$^+$::hph$^+$; Δmus-51:: bar$^+$ + mat a his-3; NcCenH3$^+$; Δmus-51::bar$^+$*]	This study
NMF315, NMF316	[*mat a his-3::P$_{ccg-1}$-AnCenH3-gfp$^+$; NcCenH3$^+$; Δmus-51::bar$^+$ + mat a his-3; ΔNcCenH3$^+$::hph$^+$; Δmus-51:: bar$^+$ + mat a his-3; NcCenH3$^+$; Δmus-51::bar$^+$*]	This study
NMF318, NMF319	[*mat a his-3*; Δ*mus-51*::*bar*$^+$; NcCenH3$^+$ + *mat a his-3*; Δ*mus-51*::*bar*$^+$; Δ*NcCenH3::FgCenH3-gfp*$^+$*-hph*$^+$]	This study
NMF320	[*mat a his-3*; Δ*mus-51*::*bar*$^+$; NcCenH3$^+$ + *mat a his-3*; Δ*mus-51*::*bar*$^+$; Δ*NcCenH3::PaCenH3-gfp*$^+$*-hph*$^+$]	This study
NMF321, NMF322, NMF323	[*mat a his-3*; Δ*mus-51*::*bar*$^+$; NcCenH3$^+$ + *mat a his-3*; Δ*mus-51*::*bar*$^+$; Δ*NcCenH3::AnCenH3-gfp*$^+$*-hph*$^+$]	This study
NMF324	*mat a his-3*; Δ*NcCenH3::PaCenH3-gfp*$^+$*-hph*$^+$	This study
NMF325	*mat A* Δ*sad-1 his-3*; Δ*NcCenH3::PaCenH3-gfp*$^+$*-hph*$^+$	This study
NMF326	*mat A* Δ*sad-1*; Δ*NcCenH3::PaCenH3-gfp*$^+$*-hph*$^+$; Δ*mus-51*::*bar*$^+$	This study
NMF327	*mat A*; Δ*NcCenH3::NcCenH3-gfp*$^+$*-hph*$^+$; Δ*mus-51*::*bar*$^+$	This study
NMF329	[*mat a his-3*; Δ*mus-51*::*bar*$^+$; NcCenH3$^+$ + *mat a his-3*; Δ*mus-51*::*bar*$^+$; Δ*NcCenH3::NcCenH3-hph*$^+$]	This study
NMF330	[*mat a his-3*; Δ*mus-51*::*bar*$^+$; NcCenH3$^+$ + *mat a his-3*; Δ*mus-51*::*bar*$^+$; Δ*NcCenH3::PaCenH3-hph*$^+$]	This study
NMF331, NMF332	[*mat a his-3*; Δ*mus-51*::*bar*$^+$; NcCenH3$^+$ + *mat a his-3*; Δ*mus-51*::*bar*$^+$; Δ*NcCenH3::AnCenH3-hph*$^+$]	This study
NMF333	*mat a his-3*; Δ*mus-51*::*bar*$^+$; Δ*NcCenH3::NcCenH3-hph*$^+$	This study
NMF402	[*mat a his-3*; Δ*mus-51*::*bar*$^+$; NcCenH3$^+$ + *mat a his-3*; Δ*mus-51*::*bar*$^+$; Δ*NcCenH3::mCherry*$^+$*-NcCenH3-hph*$^+$]	This study
NMF406	*mat a his-3*; Δ*NcCenH3::mCherry*$^+$*-NcCenH3-hph*$^+$	This study
NMF408	*mat a his-3*; Δ*NcCenH3::NcCenH3-gfp*$^+$*-hph*$^+$	This study
NMF420	*mat A*; Δ*NcCenH3::NcCenH3-gfp*$^+$*-hph*$^+$	This study
NMF421, NMF422	[*mat a*; Δ*mus-51*::*bar*$^+$; NcCenH3$^+$ + *mat a*; Δ*mus-51*::*bar*$^+$; Δ*NcCenH3::FgCenH3-gfp*$^+$*-hph*$^+$]	This study
NMF423	*mat a his-3*; Δ*mus-51*::*bar*$^+$; Δ*NcCenH3::FgCenH3-hph*$^+$	This study
NMF424, NMF425	*mat A*; Δ*NcCenH3::FgCenH3-hph*$^+$	This study
NMF426	*mat A*; Δ*mus-51*::*bar*$^+$; Δ*NcCenH3::mCherry*$^+$*-NcCenH3-hph*$^+$	This study
NMF427	*mat a his-3*$^+$*hH1-dTomato*$^+$; Δ*mus-51*::*bar*$^+$	This study
NMF428, NMF429	*mat a his-3*$^+$*hH1-dTomato*$^+$; Δ*mus-51*::*bar*$^+$; Δ*NcCenH3::NcCenH3-hph*$^+$	This study
NMF430, NMF431	*mat a his-3*$^+$*hH1-dTomato*$^+$; Δ*mus-51*::*bar*$^+$; Δ*NcCenH3::FgCenH3-hph*$^+$	This study
NMF432, NMF433	*mat a his-3*$^+$*hH1-dTomato*$^+$; Δ*mus-51*::*bar*$^+$; Δ*NcCenH3::PaCenH3-hph*$^+$	This study
NMF434	*mat a his-3*; Δ*mus-51*::*bar*$^+$; Δ*NcCenH3::NcCenH3-hph*$^+$	This study
NMF435, NMF436	*mat A* Δ*sad-1* his-3; Δ*NcCenH3::NcCenH3-hph*$^+$	This study
NMF437	*mat a* his-3; Δ*NcCenH3::PaCenH3-hph*$^+$	This study
NMF438	*mat A* Δ*sad-1*; Δ*mus-51*::*bar*$^+$; Δ*NcCenH3::PaCenH3-hph*$^+$	This study
NMF439	*mat A* Δ*sad-1*; Δ*NcCenH3::PaCenH3-hph*$^+$	This study
NMF440	*mat a his-3*; Δ*NcCenH3::PaCenH3-hph*$^+$	This study
NMF441	[*mat a his-3*; Δ*mus-51*::*bar*$^+$; NcCenH3$^+$ + *mat a*; Δ*mus-51*::*bar*$^+$; Δ*NcCenH3::NcCenH3-gfp*$^+$*-hph*$^+$]	This study
NMF442	*mat a his-3*; Δ*NcCenH3::PaCenH3-gfp*$^+$*-hph*$^+$	This study
NMF484	*mat A*; Δ*NcCenH3::mCherry*$^+$*-PaCenH3-hph*$^+$	This study
NMF485	*mat a his-3*; Δ*NcCenH3::mCherry*$^+$*-PaCenH3-hph*$^+$	This study
NMF486, NMF487	[*mat a his-3*; NcCenH3$^+$ + *mat a*; *his-3*; Δ*NcCenH3::mCherry*$^+$*-PaCenH3-hph*$^+$]	This study

NMF614	[*mat a his-3*; Δ*mus-51*::*bar*$^{+}$ + *mat a his-3*$^{+}$*hH1-dTomato*$^{+}$; Δ*mus-51*::*bar*$^{+}$]	This study
NMF615	mat A; Δ*NcCenH3*::*NcCenH3-(QVRIRYAQAYR)-hph*$^{+}$	This study
NMF616	mat a; his-3; Δ*NcCenH3*::*NcCenH3-(QVRIRYAQAYR)-hph*$^{+}$	This study

Table 2.2: Oligos used in this study.

OMF	Sequence (5' to 3')	Other name
63	GCCGAATTCNGGCATYTCCCAGAACCACGTCTC	NCU146R
64	GCCGGATCCTCGCATAATYTNGTNGAAAARCARTA	NCU144F
83	GGCGGAGGCGGCGGAGGCGGAGGCGGAGG	10XGlyF
84	CGAGCTCGGATCCATAACTTCGTATAGCA	loxPR
162	CCTCCGCCTCCGCCTCCGCCGCCTCCGCCACCCAATCCACCCCACATACCGCG	FgCenH3GlyR
180	GATGAATGACTAGATGCCGCGGTG	NcCenH3GlyF
181	TGCTATACGAAGTTATGGATCCGAGCTCGTGTGATTAGCGCATGGCGGTGC	NcCenH3loxF
182	CCTCCGCCTCCGCCTCCGCCGCCTCCGCCTACCCACCCAGCACCTCCCC	NcCenH3GlyR
188	GCCCCCACGCTAAAGCTGTT	NcCenH3loxR3
288	GCCGAATTCYACCCACCCAGCACCNCCCCANACRCC	NCEN3F
289	GCCGGATCCAGCNGGCGAYCCNGTCCCCCARGGC	NCEN5R
290	GCCGAATTCGCCYTGGGGGACNGGRTCGCCNGCT	NCEN5F
293	GCCGGATCCAACATGCCTCCCGCCAAGAAATCCAGA	FGCENBAMF
294	GCCGTTAATTAAACCCAATCCACCCCACATACCGCG	FGCENPACR
297	GCCGGATCCAACATGCCCCCAAAAGGACGAAAGCCA	ANCENBAMF
298	GCCGTTAATTAAGCCAAGACCACCCCAAGCTCCGCG	ANCENPACR
299	GCCGGATCCAACATGCCACCTAAACAGGCTGGCCGT	PACENBAMF
300	GCCGTTAATTAACACCCACCCCGCCCCGCCCCAAAC	PACENPACR
1053	AAAAAGCCTGAACTCACCGCGACG	hph SM-F
1054	TCGCCTCGCTCCAGTCAATGACC	hph SM-R
1399	ATACCCACCCAGCACCTCCCCAC	CidPacR
1400	TTCACCATCATCGATAAACAACA	CenH3_5ATG_1
1401	TTACGGATCATCAATACACAACA	CenH3_5ATG_2
1439	CATTGTTGTTTATCGATGATGGTG	NcCenAdaptR
1443	CAATACATTCACCATCATCGATAAACAACAATGCCCCCAAAAGGACGAAAG	AnCenAdaptF
1444	CAATACATTCACCATCATCGATAAACAACAATGCCACCTAAACAGGCTGGC	PaCenAdaptF
1445	CAATACATTCACCATCATCGATAAACAACAATGCCTCCCGCCAAGAAATCC	FgCenAdaptF
1446	CCTCCGCCTCCGCCTCCGCCGCCTCCGCCGCCAAGACCACCCCAAGCTCCGCG	AnCenH3GlyR
1447	CCTCCGCCTCCGCCTCCGCCGCCTCCGCCCACCCACCCCGCCCCGCCCCAAAC	PaCenH3GlyR
1563	TCCTTACATATGCCACCAAAGAAGGGAGGA	NcCenH3_NdeI
1756	CTCGGATCCCGTCCCCCAGGGCAAGAAGAGGCGT	BamF_C_NcCenH3
1759	CTGGGGATCCTGTACCCGTTCGCGCAAAGCGTCGCTATC	BamF_C_FgCenH3
1760	GATAGCGACGCTTTGCGCGAACGGGTACAGGATCCCCAG	BamF_N_FgCenH3
1818	GTCGGATCCAGAATGCAGCTAACATTGACAAAT	CidBamF
1847	ACGGGATCCCCGGCTGAATTTGTCAAT	NBamR_NcCenH3
1848	ACTGGATCCCCTGCTTTAGGGGGTTTAGT	NBamR_PaCenH3
1849	CAGGGGATCCAGTCCCCCAAGGCCGCAA	CBamF_PaCenH3
1956	GATAAGCTTGATATCGAATTCTTACTTGTTCATACCCACCCAGCACCTCCCCA	Nchph5R2
1957	GATAAGCTTGATATCGAATTCTTACTTGTTCACACCCACCCCGCCCCGCCCCA	Pahph5R2
2188	GATAAGCTTGATATCGAATTCTTACTTGTCTAACCCAATCCACCCCACATACC	Fghph5R2
2187	GATAAGCTTGATATCGAATTCTTACTTGTTCAGCCAAGACCACCCCAAGCTCC	Anhph5R2
2019	GATAAGCTTGATATCGAATTCTTACTTGTCGGCCCCCTTTTTCCTTTTCC	CenH35GRhph
2020	TGCTATACGAAGTTATGGATCCGAGCTCGGGAAAAAGGGGGCCGGCTGTT	CenH33LFhph
2030	TACCAGGAGGTGCTGCTAAGGCCG	CenH33LRhph
2218	TTCATATGCCACCTAAACAGGCTGGCCGTCGC	NdePaCenF
EUS1156	GTCGGATCCAGAATGCAGCTAACATTGACAAAT	cidBamF
N/A	GTCGGATCCACAATGCCACCAAAGAAGGGAGG	cidBamF2
EUS1157	CGGTTAATTAATACCCACCCAGCACCTCCCCAC	cidPacR
N/A	ATCCACTTAACGTTACTGAAATCTCCAACAAGCTGAAGCTAGGTGATCG	NCU00145_5R

Table 2.3: Accession numbers for H4-2 and CenH3 sequences that were used to build phylogenetic trees.

Annotated sequences have specific accession numbers in the NCBI GenBank database. If current accession numbers were not available at NCBI, we are using locus ID numbers from the Broad Institute Fungal Genome Initiative. Some sequences were extracted directly from the genome DNA sequences, as genes were not annotated or incorrectly annotated, some entries need to be changed (bold).

H4-2 gene	Species	CenH3 gene
ARB_05192	*Arthroderma benhamiae CBS112371*	ARB_05193
NC_001146.7	*Saccharomyces cerevisiae S288c*	NC_001143.8
FOXG_13953.2	*Fusarium oxysporum f. sp. lycopersici*	FOXG_10515
FVEG_11375.3	*Fusarium verticillioides*	FVEG_09164.3
NT_086543.1	*Fusarium graminearum (G. zeae) PH-1*	FGSG_02602.3
EEU42757	*Nectria haematococca mpVI 77-13-4*	GG698912.1
NW_001820823.1	*Sclerotinia sclerotiorum*	NW_001820835.1
NCU01634.4	*Neurospora crassa*	NW_001849826.1
SMAC_02364	*Sordaria macrospora*	**No ID**
CU638743.1	*Podospora anserina S mat+*	NS_000198.2
Pc16g12260	*Penicillium chrysogenum WI 54-1255*	**Pc20g11740**
NC_007194.1	*Aspergillus fumigatus Af293*	NC_007199.1
NW_001517094.1	*Aspergillus clavatus NRRL1*	NW_001517095.1
NT_166524.1	*Aspergillus niger*	NT_166530.1
NW_001849580.1	*Aspergillus oryzae RIB40*	NW_001884672.1
CPSG_02568.2	*Coccidioides posadasii Silveira*	CPSG_04648.2
NW_001849862.1	*Malassezia globosa CBS 7966*	NW_001849872.1
NW_003217266.1	*Paracoccidioides brasiliensis Pb01*	NW_003217277.1
NC_012964.1	*Pichia pastoris GS115*	NC_012964.1
NC_009046.1	*Pichia stipitis CBS 6054*	NC_009042.1
NC_006043.2	*Debaryomyces hansenii strain CBS767*	NC_006043.2
NW_003101574.1	*Candida lusitaniae ATCC 42720 =*	NW_003101577.1
NW_001889893.1	*Laccaria bicolor S238N-H82*	NW_001889875.1
NC_012867.1	*Candida dubliniensis CD36*	NC_012862.1
NW_001884552.1	*Phaeosphaeria nodorum SN15*	NW_001884585.1
NC_005785.4	*Ashbya gossypii ATCC 10895*	NC_005783.4
NC_006041.1	*Kluyveromyces lactis NRRL Y-1140*	NC_006039.1
NW_001814466.1	*Botryotinia fuckeliana*	NW_001814570.1
HCBG_03889.2	*Ajellomyces capsulata (Histoplasma c.)*	NW_001813978.1
SPPG_04875.2	*Spizellomyces punctatus*	SPPG_00398.2
CAOG_00754	*Capsaspora_owczarzaki*	CAOG_03668.1
NW_001865073.1	*Monosiga brevicollis MX1*	NW_001865083.1
NW_003307538.1	*Coprinopsis cinerea Okayama7#130*	NW_003307540.1
NW_002990114.1	*Talaromyces stipitatus ATCC 10500*	NW_002990121.1
NW_002196664.1	*Penicillium marneffei ATCC 18224*	NW_002196668.1
NW_001509770.1	*Neosartorya fischeri NRRL 181*	NW_001509760.1
NC_006069.1	*Yarrowia lipolytica CLIB122*	NC_006068.1
NT_165972.1	*Aspergillus terreus*	NT_165933.1
NT_107015.1	*Aspergillus nidulans*	ANID_06554.1
NW_003101679.1	*Ajellomyces dermatitidis SLH14081*	NW_003101673.1

H4-2 gene	Species	CenH3 gene
NW_003052496.1	*Uncinocarpus reesii*	NW_003052499.1
NT_165982.1	*Chaetomium globosum*	NT_165977.1
VDAG_05871.1	*Verticillium dahliae*	VDAG_06605.1
CIRG_07275.1	*Coccidiodes immitis RMSCC 2394*	CIRG_09755.1
TERG_03124.2	*Trichophyton rubrum CBS 118892*	TERG_01202.2
TEQG_08133.1	*Trichophyton equinum CBS127.97*	TEQG_06038.1
TESG_02677.1	*Trichophyton tonsurans CBS112818*	TESG_00928.1
MGYG_08069.1	*Microsporum gypseum CBS 118893*	MGYG_00328.1
MCYG_04838.1	*Microsporum canis CBS 113480*	MCYG_03162.1
AMAG_15239.1	*Allomyces macrogynus ATCC38327*	AMAG_09523.1
NW_001939261.1	*Pyrenophora tritici-repentis*	NW_001939244.1
NW_003298963.1	*Tuber melanosporum Mel28*	NW_003298908.1
NW_001798740.1	*Magnaporthe oryzae 70-15 (MG6)*	NW_001798736.1
NW_001809795.1	*Candida guilliermondii ATCC 6260*	NW_001809797.1
NW_003020038.1	*Candida tropicalis*	NW_003020055.1
CAWG_00969.1	*Candida albicans WO1*	NW_139671.1
AJ249813.1	*Mortierella alpine*	
BDEG_05754.1	*Batrachochytrium dendrobatidis*	BDEG_02571.1
RO3G_08219.3	*Rhizopus oryzae RA 99-880*	**No ID**
SOCG_03366.3	*Schizosaccharomyces octosporus*	SOCG_01254.3
NC_003423.3	*Schizosaccharomyces pombe 927h*	NM_001022392.1
NW_002234919.1	*Schizosaccharomyces japonicas yFS275*	NW_002234916.1
CNAG_07807.2	*Cryptococcus neoformans grubii H99*	CNAG_00673.2
NW_101055.1	*Ustilago maydis*	NW_101156.1
NW_001813682.1	*Lodderomyces elongisporus YB-4239*	NW_001813684.1
PGTG_00392.2	*Puccinia graminis f. sp tritici*	PGTG_01303.2

Table 2.4: Results from crosses between strains with tagged and non-tagged versions of different fungal CenH3 genes.

Neurospora strains (NMF) with NcCenH3, PaCenH3, FgCenH3 and AnCenH3 carry either C-terminal GFP or FLAG, or N-terminal mCherry tags. Non-tagged versions of different fungal CenH3 genes that were targeted to the native NcCenH3 locus are indicated as "-*hph*" because the selectable marker is integrated immediately following the CenH3 stop codon. Progeny were genotyped by PCR. Numbers in brackets indicate total number of spores analyzed. Tag = random string of amino acid "QVRIRYQAYR"

Cross #	Parents		Fertility	progeny recovered	# of progeny
1. Heterozygous crosses with heterokaryotic transformants					
	NcCenH3 (WT)	[NcCenH3-GFP]			
XKS122	NMF160	NMF441	fertile	NcCenH3-GFP/NcCenH3	16/34 (50)
	NcCenH3 (WT)	[PaCenH3-GFP]			
XPP14	NMF162	NMF320	fertile	PaCenH3-GFP/NcCenH3	18/40 (58)
	NcCenH3 (WT)	[FgCenH3-GFP]			
XPP13A	NMF162	NMF318	fertile	FgCenH3-GFP/NcCenH3	0/40 (40)
XPP13B	NMF162	NMF319			
	NcCenH3 (WT)	[AnCenH3-GFP]			
XPP15	NMF162	NMF312	fertile	AnCenH3-GFP/NcCenH3	0/70 (70)
	PaCenH3-GFP	[FgCenH3-GFP]			
XPP17A	NMF325	NMF318	fertile	FgCenH3-GFP/PaCenH3-GFP/NcCenH3	0/28/28 (60)
XPP17B	NMF325	NMF319			
XPP219	NMF326	NMF319			
	PaCenH3-GFP	[AnCenH3-GFP]			
XPP18A	NMF325	NMF321	fertile	AnCenH3-GFP/PaCenH3-GFP/NcCenH3	0/35/56 (100)
XPP18B	NMF325	NMF322			
XPP220	NMF326	NMF323			
	NcCenH3-GFP	[FgCenH3-GFP]			
XPP35	NMF327	NMF318	fertile	FgCenH3-GFP/NcCenH3-GFP/NcCenH3	0/17/12 (30)
XPP36	NMF327	NMF319			
	NcCenH3-GFP	[AnCenH3-GFP]			
XPP39	NMF327	NMF321	fertile	AnCenH3-GFP/NcCenH3-GFP/NcCenH3	0/14/14 (30)
XPP40	NMF327	NMF323			
2. Backcrosses with homokaryotic progeny derived from type 1 heterozygous crosses					
	NcCenH3	NcCenH3-GFP			
XPP49	NMF39	NMF169	fertile	NcCenH3-GFP/NcCenH3	12/18 (30)
	NcCenH3	PaCenH3-GFP			
XPP175	NMF262	NMF571	fertile	PaCenH3-GFP/NcCenH3	20/15 (40)
3. Homozygous crosses with homokaryotic progeny carrying C-terminal tag					
	NcCenH3-GFP	NcCenH3-GFP			
XPP48	NMF169	NMF327	barren	no ascospores in 50 opened asci	
	NcCenH3-FLAG	NcCenH3-FLAG			
XPP53	NMF229	NMF231	barren	no ascospores in 50 opened asci	
	NcCenH3-Tag	NcCenH3-Tag			
XPP99	NMF615	NMF616	barren	no ascospores in 50 opened asci	
	PaCenH3-GFP	PaCenH3-GFP			
XPP19	NMF326	NMF442	barren	no ascospores in 50 opened asci	

Cross #	Parents		Fertility	progeny recovered	# of progeny
4. Homozygous crosses with homokaryotic progeny without C-terminal tag					
	NcCenH3-*hph*	NcCenH3-*hph*			
XPP169	NMF435	NMF333	fertile	NcCenH3-*hph*	28 (30)
	PaCenH3-*hph*	PaCenH3-*hph*			
XPP173	NMF439	NMF440	fertile	PaCenH3-*hph*	24 (30)
	FgCenH3-*hph*	FgCenH3-*hph*			
XPP204	NMF424	NMF423	fertile	FgCenH3-*hph*	42 (50)
	PaCenH3-*hph*	NcCenH3-*hph*			
XPP170	NMF440	NMF436	fertile	PaCenH3-*hph*/NcCenH3-*hph*	17/15 (40)
	NcCenH3-*hph*	PaCenH3-*hph*			
XPP171	NMF438	NMF333	fertile	NcCenH3-*hph*/PaCenH3-*hph*	45/54 (100)
	FgCenH3-*hph*	NcCenH3-*hph*			
XPP213	NMF425	NMF333	fertile	FgCenH3-*hph*/NcCenH3-*hph*	44/55 (100)
	NcCenH3-*hph*	FgCenH3-*hph*			
XPP212	NMF435	NMF423	fertile	NcCenH3-*hph*/FgCenH3-*hph*	37/32 (70)
	NcCenH3	[AnCenH3-*hph*]			
XPP184	NMF162	NMF331	fertile	AnCenH3-*hph*/NcCenH3	0/29 (30)
5. Homozygous crosses with homokaryotic progeny carrying N-terminal tag					
	mCh-NcCenH3	mChNcCenH3			
XPP218	NMF426	NMF406	fertile	mCh-NcCenH3	28 (31)
	mCh-PaCenH3	mCh-PaCenH3			
XBF1	NMF484	NMF485	barren	no ascospores in 70 opened asci	

Table 2.5: Ascospore germination frequency.
Fertile homozygous crosses of non-tagged CenH3s with the hygromycin resistance gene (*hph*) integrated directly behind the stop codon of NcCenH3, PaCenH3 and FgCenH3 gene. Ascospores were heat-shocked on plates supplemented with histidine (His); hygromycin (Hyg), both His and Hyg (His + Hyg) or without supplements (Min). WT CenH3 (NMF162 and N3011). Genotypes of strains used for crossing are shown in Tables 2.1. and 2.4.

Cross	His	His + Hyg	Min	Hyg
PaCenH3 X PaCenH3	215/420 (51%)	337/518 (65%)	107/406 (26%)	126/392 (32%)
PaCenH3 X NcCenH3	233/504 (46%)	81/378 (21%)	183/423 (42%)	257/476 (54%)
NcCenH3 X PaCenH3	386/812 (47%)	297/798 (37%)	106/378 (28%)	211/644 (33%)
FgCenH3 X FgCenH3	166/490 (39%)	168/406 (41%)	139/658 (21%)	108/322 (33%)
FgCenH3 X NcCenH3	158/504 (31%)	192/532 (36%)	131/294 (44%)	94/310 (30%)
NcCenH3 X FgCenH3	195/532 (37%)	127/476 (27%)	117/378 (31%)	212/574 (37%)
NcCenH3 X NcCenH3	399/644 (62%)	291/574 (51%)	150/465 (32%)	169/435 (39%)
WT CenH3 X WT CenH3	160/294 (54%)	----	124/336 (37%)	----

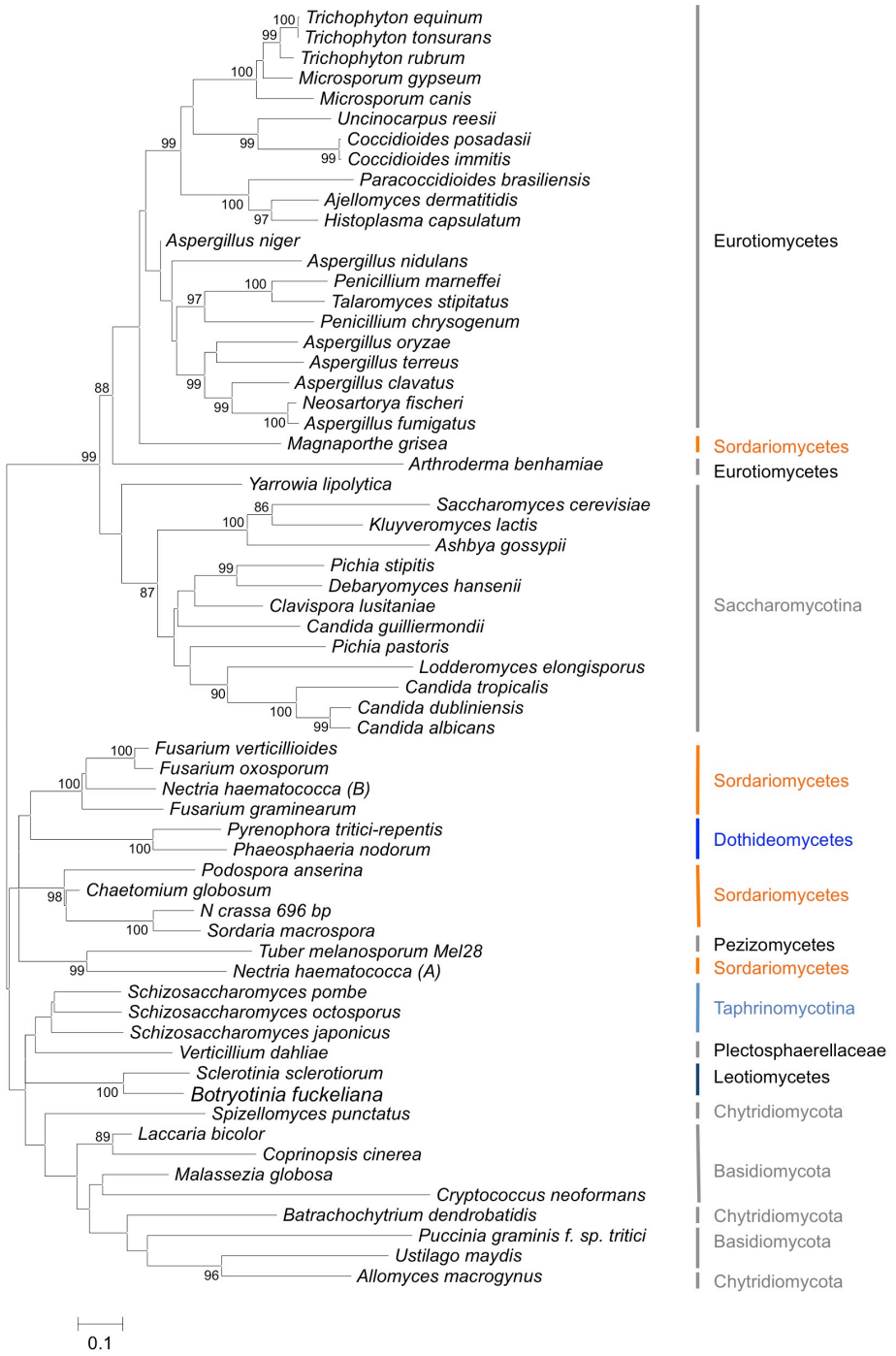
Trichophyton equinum
Trichophyton tonsurans
Trichophyton rubrum
Microsporum gypseum
Microsporum canis
Uncinocarpus reesii
Coccidioides posadasii
Coccidioides immitis
Paracoccidioides brasiliensis
Ajellomyces dermatitidis
Histoplasma capsulatum
Aspergillus niger
Aspergillus nidulans
Penicillium marneffei
Talaromyces stipitatus
Penicillium chrysogenum
Aspergillus oryzae
Aspergillus terreus
Aspergillus clavatus
Neosartorya fischeri
Aspergillus fumigatus
Magnaporthe grisea
Arthroderma benhamiae
Yarrowia lipolytica
Saccharomyces cerevisiae
Kluyveromyces lactis
Ashbya gossypii
Pichia stipitis
Debaryomyces hansenii
Clavispora lusitaniae
Candida guilliermondii
Pichia pastoris
Lodderomyces elongisporus
Candida tropicalis
Candida dubliniensis
Candida albicans
Fusarium verticillioides
Fusarium oxosporum
Nectria haematococca (B)
Fusarium graminearum
Pyrenophora tritici-repentis
Phaeosphaeria nodorum
Podospora anserina
Chaetomium globosum
N crassa 696 bp
Sordaria macrospora
Tuber melanosporum Mel28
Nectria haematococca (A)
Schizosaccharomyces pombe
Schizosaccharomyces octosporus
Schizosaccharomyces japonicus
Verticillium dahliae
Sclerotinia sclerotiorum
Botryotinia fuckeliana
Spizellomyces punctatus
Laccaria bicolor
Coprinopsis cinerea
Malassezia globosa
Cryptococcus neoformans
Batrachochytrium dendrobatidis
Puccinia graminis f. sp. tritici
Ustilago maydis
Allomyces macrogynus
0.1
Eurotiomycetes
Sordariomycetes
Eurotiomycetes
Saccharomycotina
Sordariomycetes
Dothideomycetes
Sordariomycetes
Pezizomycetes
Sordariomycetes
Taphrinomycotina
Plectosphaerellaceae
Leotiomycetes
Chytridiomycota
Basidiomycota
Chytridiomycota
Basidiomycota
Chytridiomycota

Figure 2.1: Phylogenetic relationship between CenH3 genes of filamentous fungi.

This Neighbor-Joining phylogenetic tree for *hH3v* (CenH3) genomic DNA sequences was built without consideration of intron/exon boundaries (i.e. all introns are retained in the sequences analyzed). We used MEGA with the following settings: input, nucleotide sequence from 63 taxa; analysis, phylogeny reconstruction; tree inference, neighbor-joining; phylogeny test and options, bootstrap (1000 replicates, seed=64238); gaps/missing data, pairwise deletion; substitution model, nucleotide/maximum composite likelihood (transitions and transversions included); pattern among lineages, different/heterogeneous; rates among sites, uniform; number of sites, 1346; number of bootstrap replicates, 1000.

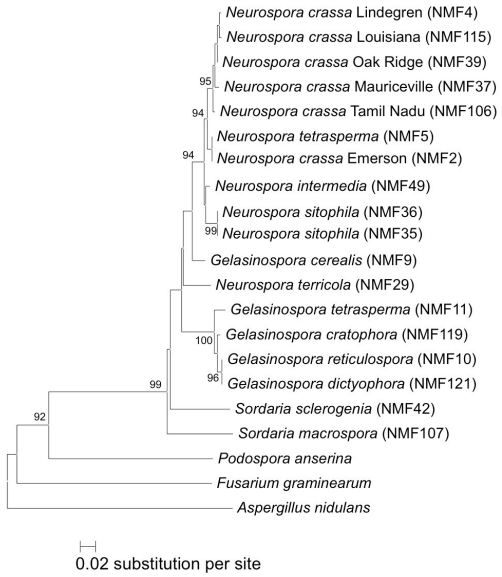

Figure 2.2: Phylogenetic relationships between CenH3 genes of species in the genera *Neurospora*, *Gelasinospora* and *Sordaria*.

Neighbor-Joining phylogenetic tree analysis for partial CenH3 sequences amplified by PCR. The tree was build using the same parameters as in Figure 2.1. In total, 775 positions are considered in the final dataset.

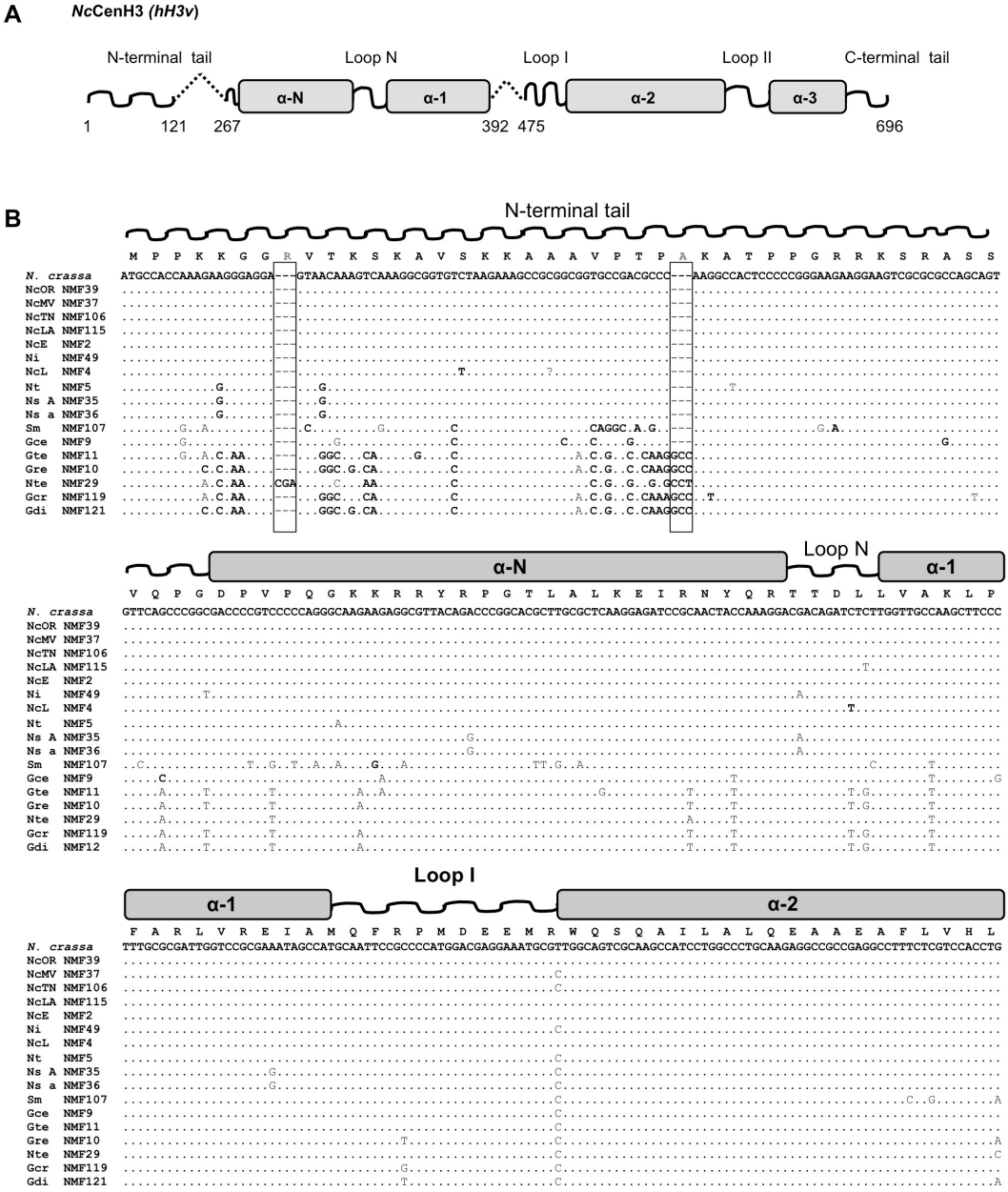
A
NcCenH3 (hH3v)
N-terminal tail
Loop N
Loop I
Loop II
C-terminal tail
α-N
α-1
α-2
α-3
1
121
267
392
475
696
B
N-terminal tail
M P P K K G G R V T K S K A V S K K A A A V P T P A K A T P P G R R K S R A S S
N. crassa ATGCCACCAAAGAAGGGAGGA---GTAACAAAGTCAAAGGCGGTGTCTAAGAAAGCCGCGGCGGTGCCGACGCCC---AAGGCCACTCCCCCGGGAAGAAGGAAGTCGCGCGCCAGCAGT
NcOR NMF39
NcMV NMF37
NcTN NMF106
NcLA NMF115
NcE NMF2
Ni NMF49
NcL NMF4
Nt NMF5
Ns A NMF35
Ns a NMF36
Sm NMF107
Gce NMF9
Gte NMF11
Gre NMF10
Nte NMF29
Gcr NMF119
Gdi NMF121
α-N
Loop N
α-1
V Q P G D P V P Q G K K R R Y R P G T L A L K E I R N Y Q R T T D L L V A K L P
N. crassa GTTCAGCCCGGCGACCCCGTCCCCCAGGGCAAGAAGAGGCGTTACAGACCCGGCACGCTTGCGCTCAAGGAGATCCGCAACTACCAAAGGACGACAGATCTCTTGGTTGCCAAGCTTCCC
Loop I
α-1
α-2
F A R L V R E I A M Q F R P M D E E M R W Q S Q A I L A L Q E A A E A F L V H L
N. crassa TTTGCGCGATTGGTCCGCGAAATAGCCATGCAATTCCGCCCCATGGACGAGGAAATGCGTTGGCAGTCGCAAGCCATCCTGGCCCTGCAAGAGGCCGCCGAGGCCTTTCTCGTCCACCTG

Figure 2.3: Positive selection on the N-terminus but negative selection on the histone-fold domain of CenH3 from selected *Neurospora* species and strains.

(A) Gene and protein structure of *Neurospora* CenH3. The *N. crassa* CenH3 protein is encoded by the 696 nt *hH3v* gene (114); adenine of the predicted start codon is used as position 1). The gene contains two introns, indicated by dashed lines. Predicted α-helices within the conserved histone fold domain are shown as grey boxes and labeled. Unstructured regions or known loops are shown as wavy lines. **(B) Alignment of partial DNA sequence of CenH3 genes from selected strains of *Neurospora Gelanospora* and *Sordaria* species.** Partial DNA sequences aligned to the predicted secondary protein structure and primary amino acid sequence and nucleotide sequence of the reference genome sequence of *N. crassa* CenH3 derived from strain N150 (97), which should be identical to strain NMF39 (FGSC2489). Many more non-synonymous changes occur in the N-terminal region than in the histone-fold domain and DNA sequences for the C-terminal 37 residues are omitted here as there are few additional sequence differences. Identical nucleotides are indicated by a period, synonymous changes are indicated by grey letters and non-synonymous changes are indicated by black letters. Boxes indicate regions of codon insertions in some taxa. Strains and species used: NMF39, *N. crassa* Oak Ridge ("WT", FGSC2489); NMF37, *N. crassa* Mauriceville (FGSC2225); NMF106, *N. crassa* Tamil Nadu (FGSC8858); NMF115*, N. crassa* Louisiana (FGSC8873); NMF2*, N. crassa* Emerson (FGSC352); NMF4, *N. crassa* Lindegren (FGSC354); NMF49*, N. intermedia* (FGSC3417); NMF35*, N. sitophila* (FGSC2216); NMF36*, N. sitophila* (FGSC2217); NMF5*, N. tetrasperma* (FGSC606); NMF9, *Gelasinospora cerealis* (FGSC959); NMF10*, G. reticulosperma* (FGSC960); NMF11, *G. tetrasperma* (FGSC966); NMF29, *N. terricola* (FGSC1889); NMF119, *G. cratophora* (FGSC7796); NMF121*, G. dictyophora* (FGSC7798); NMF107, *S. macrospora* (FGSC4818).

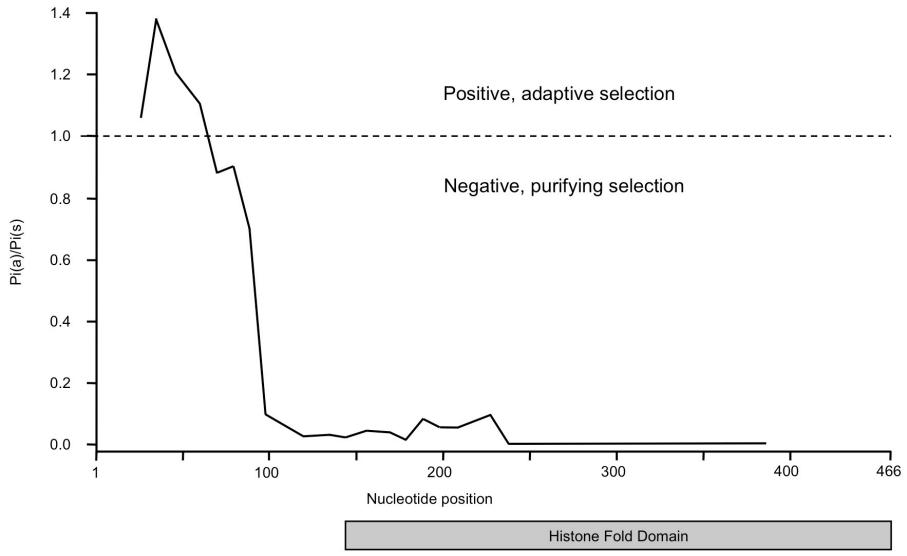

Figure 2.4: Calculation of Pi(a) over Pi(s) ratios within the CenH3 coding regions suggest a small region under positive selection within the N-terminus.

Pi(a)/Pi(s) ratios above 1 suggest that regions are under positive seletion (see dotted line). Only a short section of the N-terminus meets this requirement. Strains and species used for this calculation are the same as in Figure 2.3. The graph was redrawn from an output of the DNAsp program using sliding window analysis (settings: default i.e. window length = 50 and step size=10).

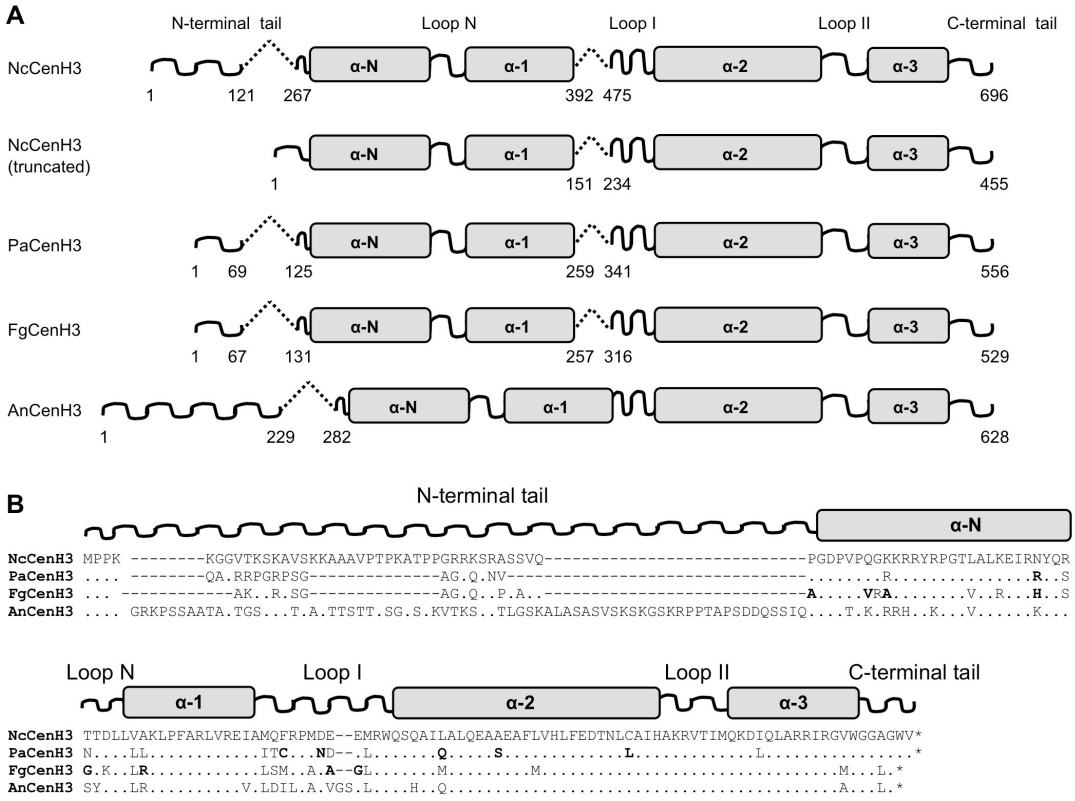

Figure 2.5: Gene and protein structure, and sequence alignments of CenH3 from four filamentous fungi used for functional studies.

(A) Gene and protein structure of CenH3. The *N. crassa* CenH3 (NcCenH3), encoded by *hH3v c*omprises 696 nucleotides (nt), while the version truncated at the N-terminus is 455 nt long. The *Podospora anserina* (PaCenH3), *Fusarium graminearum* (FgCenH3) and *Aspergillus nidulans* (AnCenH3) genes are 556, 529, and 628 nt long, respectively (the adenine of the predicted start codon is used as position 1). The CenH3 genes contain two introns (dashed lines), except for AnCenH3, which lacks the second intron between α-helix 1 and Loop 1 (this is true for CenH3 genes of all *Aspergillus spp*). Predicted α-helices within the conserved histone fold domain are shown as grey boxes and labeled. Unstructured regions or known loops are shown as wavy lines. **(B) Complete sequence alignment of four fungal CenH3.** Abbreviations are as in panel A. Regions of known or predicted secondary structure are indicated above the sequences. In the alignment, identical residues to NcCenH3 are indicated as periods, gaps are indicated as hyphens and substitutions are indicated in one letter amino acid code. Residues indicated in bold are different in PaCenH3 and FgCenH3 when compared to NcCenH3 and may have functional significance.

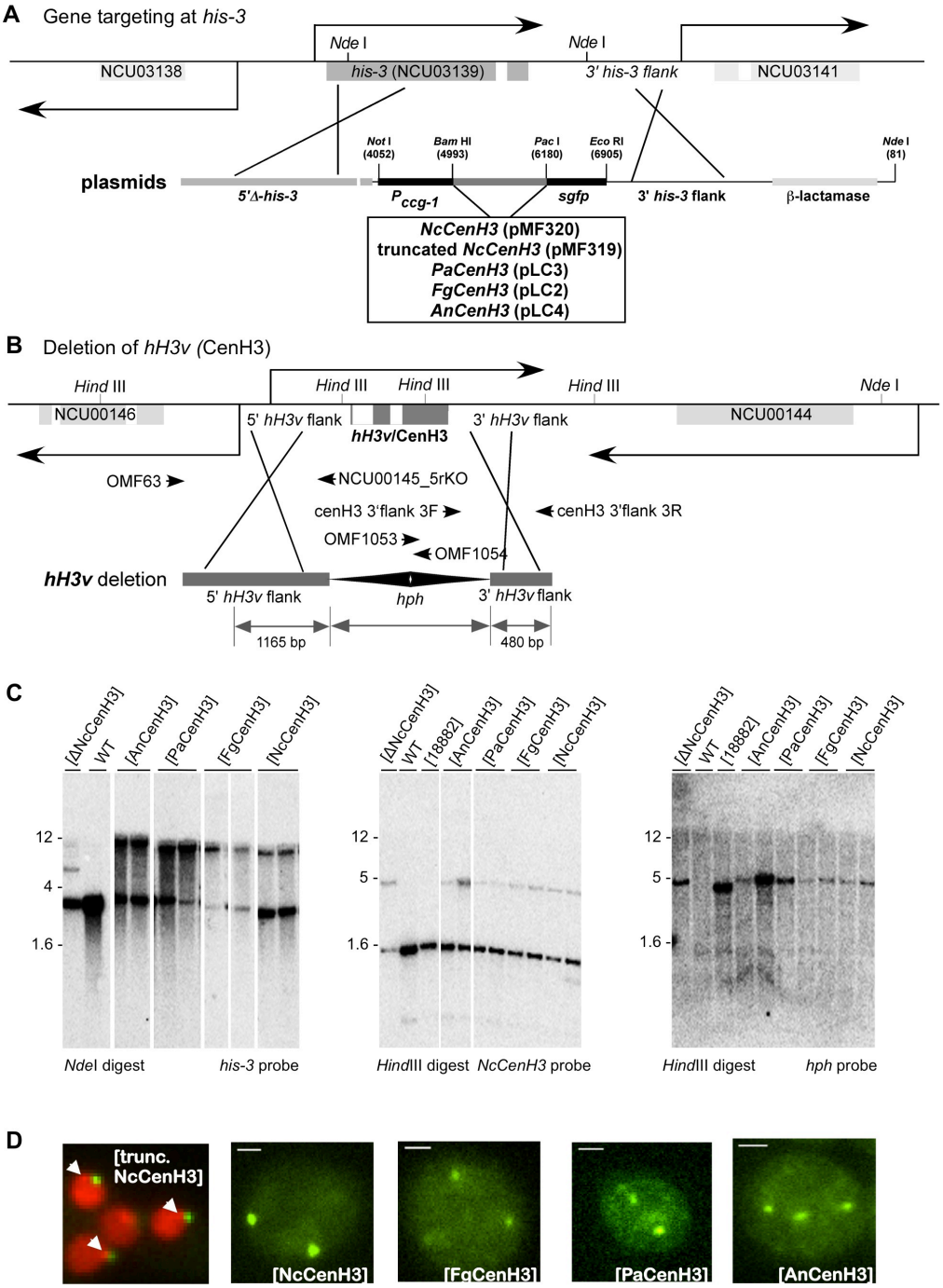
A
Gene targeting at his-3
Nde I
Nde I
NCU03138
his-3 (NCU03139)
3' his-3 flank
NCU03141
Not I (4052)
Bam HI (4993)
Pac I (6180)
Eco RI (6905)
Nde I (81)
plasmids
5'Δ-his-3
P ccg-1
sgfp
3' his-3 flank
β-lactamase
NcCenH3 (pMF320)
truncated NcCenH3 (pMF319)
PaCenH3 (pLC3)
FgCenH3 (pLC2)
AnCenH3 (pLC4)
B
Deletion of hH3v (CenH3)
Hind III
Hind III
Hind III
Hind III
Nde I
NCU00146
5' hH3v flank
hH3v/CenH3
3' hH3v flank
NCU00144
OMF63
NCU00145_5rKO
cenH3 3'flank 3F
cenH3 3'flank 3R
OMF1053
OMF1054
hH3v deletion
5' hH3v flank
hph
3' hH3v flank
1165 bp
480 bp
C
[ΔNcCenH3]
WT
[AnCenH3]
[PaCenH3]
[FgCenH3]
[NcCenH3]
12
4
1.6
NdeI digest
his-3 probe
[ΔNcCenH3]
WT
[18882]
[AnCenH3]
[PaCenH3]
[FgCenH3]
[NcCenH3]
12
5
1.6
HindIII digest
NcCenH3 probe
[ΔNcCenH3]
WT
[18882]
[AnCenH3]
[PaCenH3]
[FgCenH3]
[NcCenH3]
12
5
1.6
HindIII digest
hph probe
D
[trunc. NcCenH3]
[NcCenH3]
[FgCenH3]
[PaCenH3]
[AnCenH3]

Figure 2.6: Ectopic integration of CenH3-GFP from four filamentous fungi at *his-3* results in proper targeting to centromere foci.

(A) Cartoon of gene targeting to *his-3.* The *his-3* gene (NCU03139) has two exons (grey boxes) and one intron (white box); arrows indicate the direction of transcription of *his-3* and neighboring genes. Integration of linearized plasmids pMF320 (full-length NcCenH3-GFP), pMF319 (5'-truncated NcCenH3-GFP), pLC3 (PaCenH3-GFP), pLC2 (FgCenH3-GFP) and pLC4 (AnCenH3-GFP) by homologous recombination allows selection for prototrophy by restoration of the defective *his-3* locus in host strains (see Freitag *et al.*, 2004). The four CenH3 genes were amplified by PCR and inserted at *BamH*I and *Pac*I sites in pMF272 (NcCenH3, 692 nt; truncated NcCenH3, 455 nt; PaCenH3, 553 nt; FgCenH3, 526 nt; AnCenH3, 625 nt). This generates constructs were expression of the *sgfp* fusion genes is driven by the inducible *N. crassa ccg-1* promoter (P_{ccg-1}). and the numbers in the bracket indicate the gene size of CenH3s. **(B) Generation of a deletion allele of *hH3v*, the *N. crassa* CenH3 locus.** The *N. crassa hH3v* (CenH3) gene has three exons (grey boxes) and three introns (white boxes); arrows indicate the direction of transcription of *hH3v* and neighboring genes. The gene was deleted by overlapping PCR to insert *hph*, the gene for hygromycin phosphotransferase, as a selectable marker. Arrowheads indicate primer locations. **(C) Southern analyses shows integration of CenH3 genes at *his-3* in a Neurospora CenH3 deletion mutant (ΔNcCenH3).** Genomic DNA from various strains was digested with *Nde*I (left panel) or *Hind*III (middle and right panel), separated through a 0.8% agarose gel, blotted to nylon membrane and probed with *his-3* (left panel), NcCenH3 (middle panel) or *hph* (right panel) fragments. Two independent heterokaryotic transformants for [NcCenH3-GFP] (NMF306, NMF307), [FgCenH3-GFP] (NMF309, NMF310), [PaCenH3-GFP] (NMF312, NMF313) and [AnCenH3-GFP] (NMF315, NMF316) are shown (left panel). A 12 kb band in addition to the 3.6 kb wildtype *his-3* bands for ΔNcCenH3 (lane 1, NMF247) or WT (lane 2, NMF39) is diagnostic for the presence of nuclei that carry targeted CenH3-GFP genes at *his-3* (lanes 3 to 10, left panel). Two bands are also observed in heterokaryotic transformants when blots were probed with CenH3 sequence (middle panel); the lower band corresponds to the wildtype CenH3 gene, the higher band corresponds to the CenH3 gene at *his-3.* The *hph* gene is present in the heterokaryotic [ΔNcCenH3] strain we constructed (NMF247), the presumed CenH3 deletion strain from the Neurospora Functional Genomics project (FGSC18882), and the two representative transformants for each CenH3 used (see strains for left panel). Note that both strains with deletion alleles still carry the CenH3 locus (middle panel). **(D) Heterokaryotic transformants express CenH3-GFP that is targeted to discrete centromeric foci.** Representative examples of images from four heterokaryotic transformants of [NcCenH3-GFP] (NMF306), [PaCenH3-GFP] (NMF312), [FgCenH3-GFP] (NMF309) and [AnCenH3-GFP] (NMF315) are shown. Neurospora centromeres during interphase are localized in one tight focus per

nucleus. Nuclei are often bi- or trinucletae. The NcCenH3 images is shown at ~1.5 X compared to the other three images (scale bar = 1 μm).

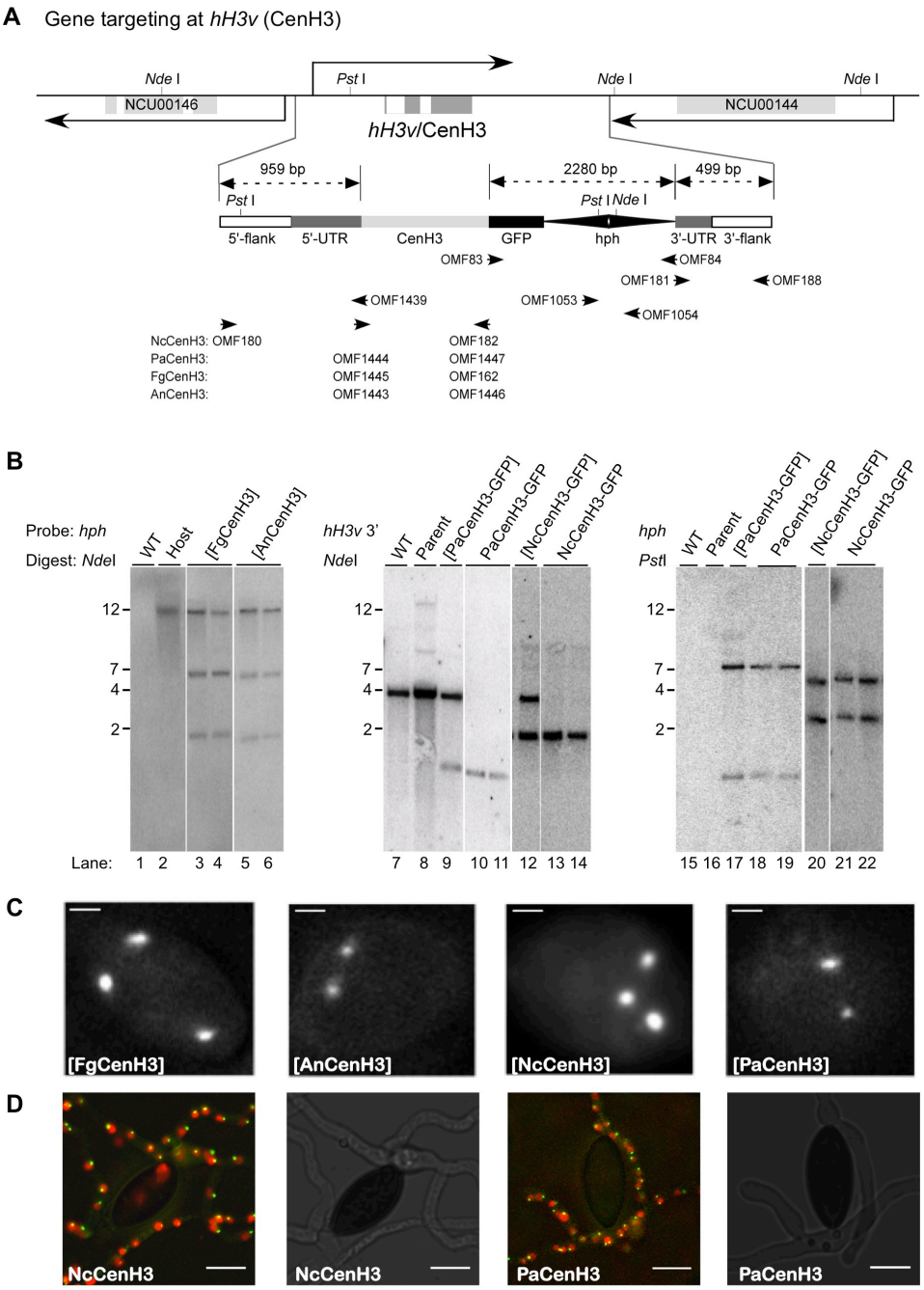
A
Gene targeting at hH3v (CenH3)
Nde I
Pst I
Nde I
Nde I
NCU00146
NCU00144
hH3v/CenH3
959 bp
2280 bp
499 bp
Pst I
Pst I Nde I
5'-flank
5'-UTR
CenH3
GFP
hph
3'-UTR
3'-flank
OMF83
OMF84
OMF181
OMF188
OMF1439
OMF1053
OMF1054
NcCenH3: OMF180
PaCenH3:
FgCenH3:
AnCenH3:
OMF1444
OMF1445
OMF1443
OMF182
OMF1447
OMF162
OMF1446
B
Probe: hph
Digest: NdeI
WT
Host
[FgCenH3]
[AnCenH3]
hH3v 3'
NdeI
WT
Parent
[PaCenH3-GFP]
PaCenH3-GFP
[NcCenH3-GFP]
NcCenH3-GFP
hph
PstI
WT
Parent
[PaCenH3-GFP]
PaCenH3-GFP
[NcCenH3-GFP]
NcCenH3-GFP
12
7
4
2
Lane: 1 2 3 4 5 6 7 8 9 10 11 12 13 14 15 16 17 18 19 20 21 22
C
[FgCenH3]
[AnCenH3]
[NcCenH3]
[PaCenH3]
D
NcCenH3
NcCenH3
PaCenH3
PaCenH3

Figure 2.7: Integration of CenH3 genes from four filamentous fungi at *N. crassa hH3v* (CenH3) results in proper targeting to centromere foci.

(A) Partial map of the *N. crassa* CenH3 locus. *hH3v* (NCU00145) is transcribed convergently with the adjacent NCU00144.Transcripts based on evidence from cDNA and RNA-seq are indicated by arrows. Exons are shown in grey, introns are shown in white. Fusion PCR was used to construct two fragments for split marker transformation of the host strain (N3011). Homologous recombination in *N. crassa* results in generating proper gene replacement constructs with complete flanking regions (5'- and 3'-flanks), untranslated regions (5'- and 3'-UTRs), the four different CenH3 genes (NcCenH3, PaCenH3, FgCenH3, AnCenH3), the GFP or FLAG tags and the *hph* marker gene (see Materials and Methods). Locations of primers are indicated by arrowheads (see Supplemental Table 2), positions of restriction endonuclease recognition sites used in B are indicated. **(B) Southern analyses of transformants and progeny from heterozygous crosses.** Genomic DNA was digested with *Nde*I, separated through a 0.8% agarose gel, blotted to nylon membrane and probed with a fragment containing the *hph* gene and a short region of the *A. nidulans trpC* promoter (left panel). Neither WT (NMF39, lane 1) nor the host strain (N3011, lane 2) show *hph* specific bands (the host has a band at ~12 kb because it carries a *mus-51Δ::trpC-bar*$^{+}$ allele), while both C-terminally GFP-tagged heterokaryotic [FgCenH3-GFP] and [AnCenH3-GFP] transformants (NMF318, NMF319 lanes 3 and 4, and NMF321, NMF322, lanes 5 and 6, respectively) show the expected bands at 3.9 kb and 1.8 kb, respectively. Genomic DNA from WT (NMF39, lane 7), wildtype parent (NMF162, lane 8), heterokaryotic [NcCenH3-GFP] (NMF441, lane 12), and [PaCenH3-GFP] (NMF320, lane 9) were digested with *Nde*I, separated through 0.8% agarose gels, blotted to nylon membrane and probed with a fragment containing the 3' flank of the *hH3v* (CenH3) gene (center panel). Single bands were observed in the WT (lane 7) and wildtype parent (lane 8) for subsequent crosses, while both heterokaryotic transformants carry a mixture of non-transformed and transformed nuclei (indicated by the new bands at 1.2 kb and 2.9 kb in lanes 9 and 12, respectively). Transformants [NcCenH3-GFP] (NMF441) and [PaCenH3-GFP] (NMF320) were crossed to NMF162 to obtain homokaryotic progeny NcCenH3-GFP (NMF408, NMF420) and PaCenH3-GFP (NMF324, NMF326). Southern analyses of these strains shows that only transformed nuclei remain, as the original wildtype *hH3v* band was not detected (compare lanes 9 to 10 and 11, and lanes 12 to 13 and 14, respectively). The blot was reprobed with *hph* (right panel) to show absence of the marker in WT (lane 15) and NMF162 (lane 16) but identical patterns for heterokaryotic transformants (lanes 17 and 20) and homokaryotic progeny (lanes 18, 19, and 21, 22, respectively). **(C) Heterokaryotic transformants express CenH3-GFP that is targeted to a single discrete focus in each nucleus.** Representative images of CenH3-GFP expression in heterokaryotic transformants for NcCenH3-GFP (NMF327), 5'-truncated NcCenH3-GFP (NMF242), PaCenH3-GFP (NMF326),

FgCenH3-GFP (NMF319), AnCenH3-GFP (NMF322) are shown. **(D) CenH3-GFP in homokaryotic progeny with NcCenH3-GFP and PaCenH3-GFP is targeted to centromeric chromocenters.** We obtained progeny from crosses of a strain expressing RFP-tagged nuclear linker histone H1 (NMF427) to [NcCenH3-GFP] (NMF420) or [PaCenH3-GFP] (NMF426). Ascospores were germinated and fluorescence of H1-RFP and CenH3-GFP observed. Crosses with [FgCenH3-GFP] and [AnCenH3-GFP] were barren. Scale bars = 1 μm.

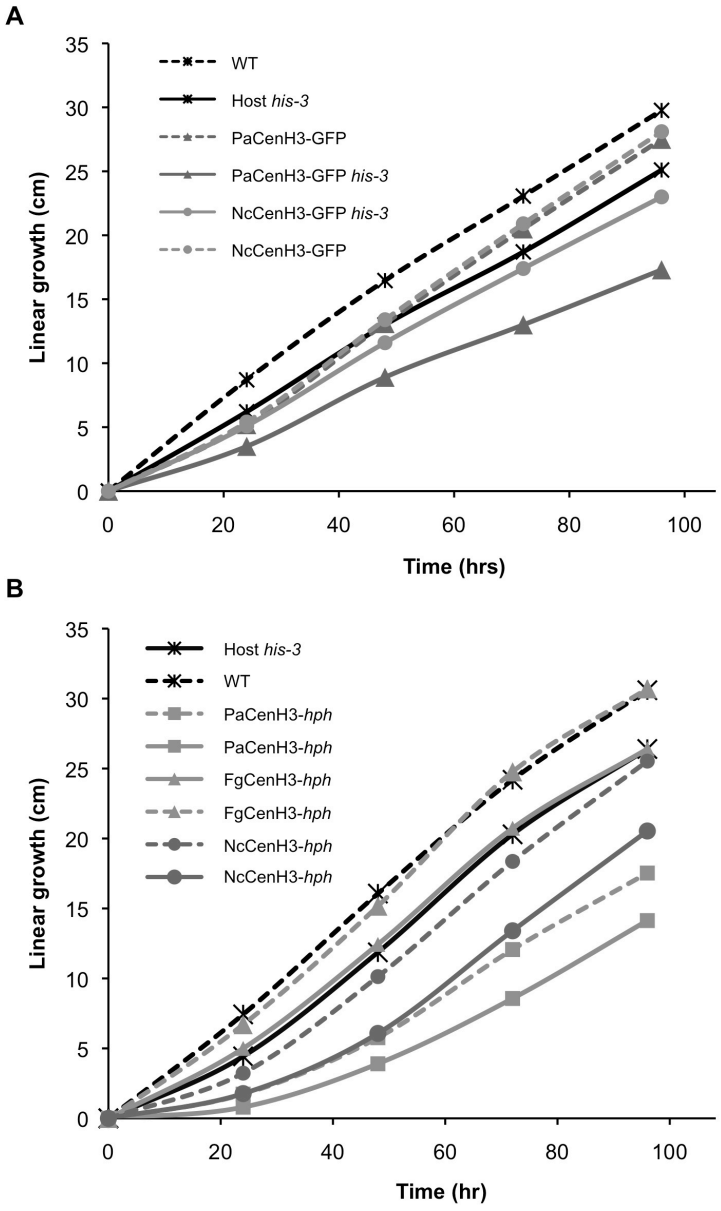
A
WT
Host his-3
PaCenH3-GFP
PaCenH3-GFP his-3
NcCenH3-GFP his-3
NcCenH3-GFP
Linear growth (cm)
Time (hrs)
B
Host his-3
WT
PaCenH3-hph
PaCenH3-hph
FgCenH3-hph
FgCenH3-hph
NcCenH3-hph
NcCenH3-hph
Linear growth (cm)
Time (hr)

Figure 2.8: Linear growth assay in Ryan tubes.

(A) Linear growth for strains tagged with C-terminal GFP in comparison to strains with untagged CenH3. We inoculated Ryan ("race") tubes with spores of PaCenH3-GFP (NMF326, NMF324) and NcCenH3-GFP (NMF169, NMF327) and compared their linear growth to that of WT (NMF39) and the original transformation host (N3011). N3011, NMF169 and NMF324 require histidine as they carry a defective *his-3* allele. NMF324 grows more slowly than NMF169, which grows more slowly than N3011, suggesting that addition of GFP results in slight growth defects and that PaCenH3 inhibits growth slightly more than NcCenH3-GFP. In contrast, NcCenH3-GFP (NMF327) and PaCenH3-GFP (NMF326) showed similar and almost normal growth when compared to WT (NMF39). **(B) Linear growth for strains that carry non-tagged CenH3 followed by a selectable marker.** For strains with PaCenH3-*hph* (NMF439, NMF440), FgCenH3 (NMF423, NMF424) and NcCenH3 (NMF435, NMF333) similar growth defects are observed when compared to the WT (NMF39) or the host (N3011). Much of this difference was based on an extended lag time (0-20 hr).

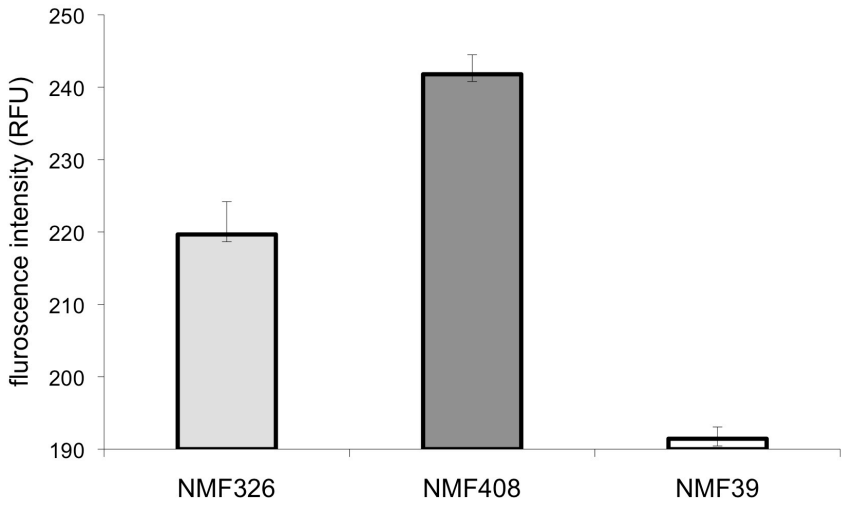

Figure 2.9: Fluorescence intensity measurements.

One PaCenH3-GFP (NMF326) and one NcCenH3-GFP (NMF408), as well as a wildtype strain (NMF39) were used for measurement of fluorescence intensities. Centromeric chromocenter intensities for 200-300 nuclei for each strain were measured using the NIS-Elements BR software and then plotted with the y-axis showing relative fluorescence units (RFU).

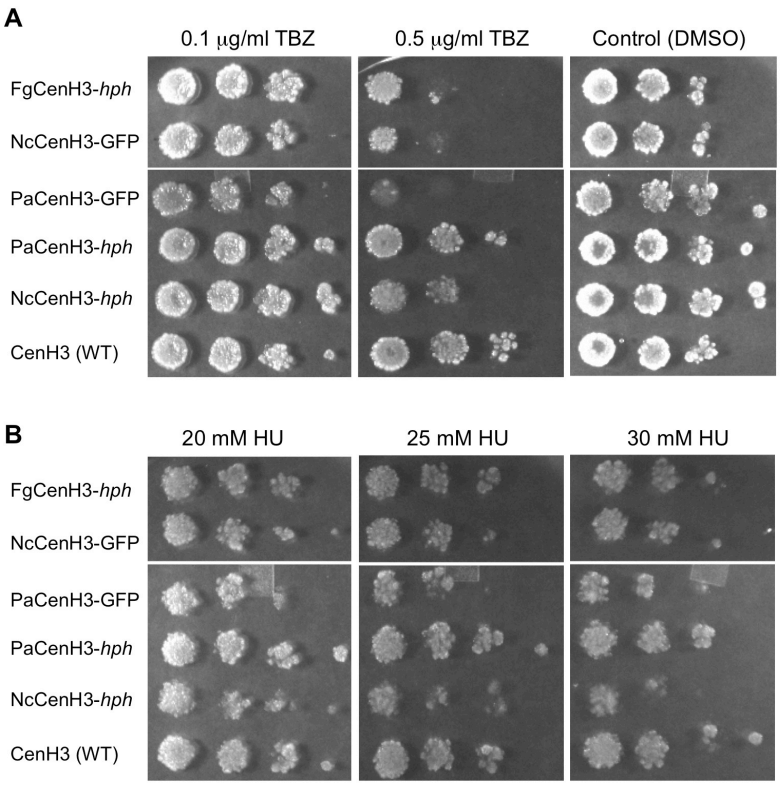

Figure 2.10: Growth of tagged and non-tagged CenH3 strains in the presence of various concentrations of TBZ and HU.

(A) the microtubule function inhibitor thiabendazole (TBZ) or (B) the DNA synthesis inhibitor hydroxyurea (HU). Dilutions of conidia (~3,000, 300, 30 or 3 spores) from FgCenH3-*hph* (NMF431), NcCenH3-GFP (NMF408)),PaCenH3-GFP (NMF324), PaCenH3-*hph* (NMF433), NcCenH3-*hph* (NMF428) and wildtype CenH3 (NMF39) strains were used for spot testing. While there is no effect on growth in the presence of HU, several strains appear to be affected by low concentrations of TBZ.

A **Mitosis: s**ister chromatids with bi-oriented spindles

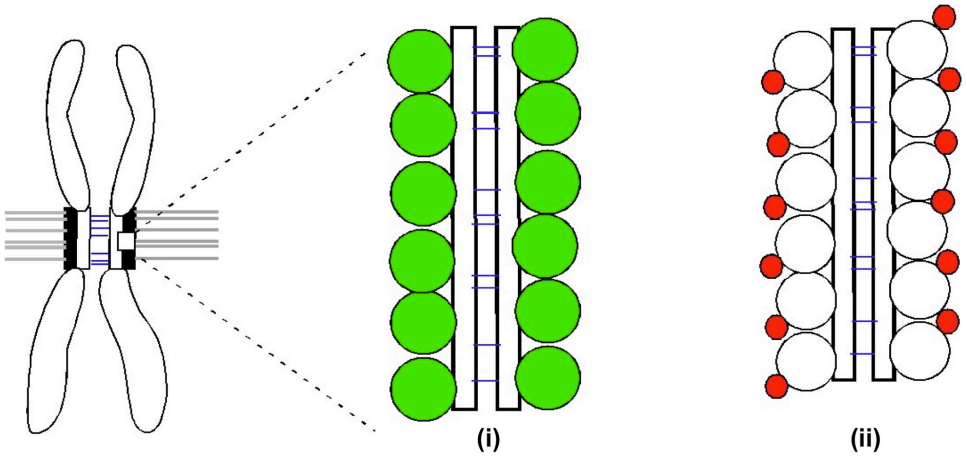

B **Meiosis I:** sister chromatids with mono-oriented spindles

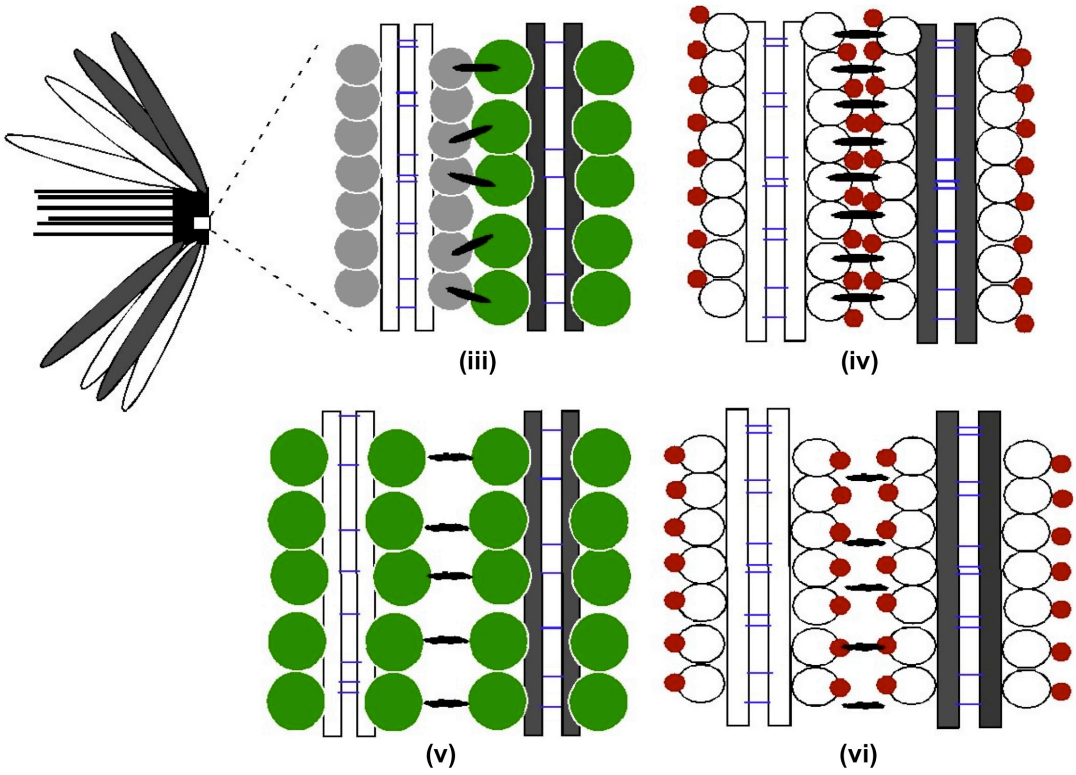

Figure 2.11: Working model for centromere structure during mitosis and meiosis I in the patches containing CenH3 nucleosomes.

(A) The chromosome during mitosis. Black bar represents the outer surface of kinetochores with CenH3 nucleosomes that are attached to spindle microtubules (gray horizontal lines). The white bar represents the inner surface of kinetochores showing interactions with condensins and cohesins (blue horizontal lines). To the right, cartoons of possible arrangements of C-terminally tagged GFP (green circles) (i) and N-terminally tagged CenH3 (red circle: mCherry tag; white circles NcCenH3 or PaCenH3) (ii) nucleosome on sister chromatids during mitosis. (**B) The chromosome during meiosis I.** Black box represents where sister pairs of homologous chromosomes attach during meiosis I. Horizontal lines represent spindle fibers, white and grey ovals are sister pairs of homologous chromosomes. To the right, cartoons of models for centromeric nucleosomes during (iii) heterozygous crosses with one C-terminally GFP tagged PaCenH3 or NcCenH3 parent; meiosis may occur at suboptimal level. Bars represent the sister pair chromosomes attached in presence of C-terminal GFP tagged CenH3 containing nucleosomes (green circles) with meiosis-specific protein complexes (black elongated circles). Red horizontal lines represent the protein complexes holding together sister chromatids. Successful meiosis in the heterozygous cross between C-terminal GFP tagged CenH3 (green circles) and wild type NcCenH3 (grey circles) suggest more severe structural defects during meiosis resulting in barrenness of homozygous crosses. (iv) Homozygous crosses of NcCenH3 tagged with RFP at the N-terminus (mCherry tag, red circles) may not result in any structural hindrance for required interactions of NcCenH3, as the N-terminal tail of NcCenH3 is relatively long. Thus, homozygous crosses are fertile. (v) Centromeric nucleosomes are unable to form properly during meiosis I in homozygous crosses because of severe structural problems with the C-terminally tagged GFP. For NcCenH3-GFP and PaCenH3-GFP homozygous crosses were barren. Severe segregation defects during meiosis may occur because the C-terminal tail tagged with GFP might act as hindrance for proper orientation or holding together of homologous pairs of chromosomes. (vi) Homozygous crosses of N-terminally tagged PaCenH3 (mCherry tag, red circles) may be barren because the PaCenH3 N-terminal tag is too short to avoid hindrance of structural interactions durin meiosis. This suggests that the N-terminal tails also may play key roles during meiosis I.

CenH3-deficient Neurospora centromeres remain competent for mitosis but are defective during meiosis

Pallavi A. Phatale, Kristina M. Smith and Michael Freitag

in preparation for submission to PLoS Genetics

Abstract

CenH3 forms the platform for centromere organization. Structural divergence in this protein, caused by changes in amino acid composition might lead to improper centromere formation. Replacing NcCenH3 (*Neurospora crassa* CenH3) with different fungal CenH3 genes, i.e. from *Podospora anserina* (PaCenH3) or *Fusarium graminearum* (FgCenH3), showed that FgCenH3-GFP was unable to rescue NcCenH3 function during meiosis and mitosis, probably due to amino acid differences in the HFD in comparison with PaCenH3. In *Saccharomyces cerevisiae* there are required stretches of amino acids in the CenH3 HFD rather than single specific amino acid residues that are important for proper CenH3 function. Therefore, we wanted to test the hypothesis that differences in the amino acid composition of the HFD of CenH3 will result in defects in mitotic and meiotic cell divisions. We determined that the HFD of FgCenH3 does not support meiosis in heterozygous crosses, unlike the PaCenH3-GFP HFD. PaCenH3-GFP, however, showed enrichment defects at certain *Neurospora* centromeres. These abnormalities were irreversible and progressive, in absence of gross phenotypic defects. Further, the epigenetic states of these defective centromeres remained unchanged, i.e. H3K9me3 was retained in the central core of centromeres, while H3K4me2 remained absent. We did not observe large difference in centromeric DNA sequences, wholesale translocations or chromosome fusions, and we failed to obtain evidence for aneuploidy. Therefore, the results suggest specific depletion of PaCenH3 from centromeres suggesting a relaxed requirement for CenH3 for mitosis compared to meiosis. The specific mechanism behind these observations remains under investigation.

Introduction

Centromere assembly and inheritance is predominantly under epigenetic control rather than based on the composition of centromeric DNA, even though these gene-poor regions share many similarities, for example being highly AT-rich and of repetitive nature. Enrichment of centromere-specific histone H3 (CenH3) at the genomic locus marks the centromere. Our understanding of the downstream processes for centromere assembly is gaining pace, especially of processes that occur after deposition of CenH3 as the “centromere identifier” (66). Structural studies on human CenH3 nucleosome revealed the importance of differences between CenH3 and canonical histone H3 that might be essential for centromere identity and recognition by inner kinetochore proteins. The specific binding of CENP-C to CenH3 nucleosomes requires the carboxy- or C-terminus of CenH3 (44). Our genetic results presented in Chapter 2 support this essential role of the CenH3 C-terminus during meiosis, but whether CEN-C interactions are important during meiosis remains unanswered. Further, *in vitro* studies of CEN-T, CEN-W, CEN-S and CEN-X showed that due to the presence of histone fold domains (HFD) these inner kinetochore proteins may have the propensity to assemble and form a non-histone nucleosome, called CEN-T-W-S-X (200). The presence of such a “nucleosome” *in vivo* would further add to the structural uniqueness of the centromere locus, however, whether this special nucleosome may guide CenH3 deposition or that of other kinetochore complexes is not yet known.

How CenH3 enrichment at centromeres is accomplished and perhaps guided by pre-existing proteins or protein complexes is still not well understood. However, a

recent series of studies in several organisms has shown that the N-terminus of budding and fission yeast Scm3 and its human homologue HJURP funtions as a CenH3 chaperone and can interact with the HFD of CenH3 and H4 in CenH3:H4 dimers (52, 334). This interaction helps in directing deposition and assembly of newly synthesized CenH3 at the centromere during specific times of the cell cycle. The spatio-temporal regulation of CenH3 deposition takes place by replacement of canonical histone H3 with CenH3 by an as of yet unknown mechanism. In the fission yeast, *Schizosaccharomyces pombe*, CenH3 is loaded during the S and G2 phase of the mitotic cell cycle (292). As one might expect, CenH3 deposition during S phase is replication-coupled, regulated by the GATA-type transcription factor Asm2, but incorporation of CenH3 during G2 depends on protein complexes that generate a "constitutively centromere-associated network" (CCAN), made up of Mis6, Sim4, Mis17 and Mis15, or CENP-I, -K, -M, and -N in human cells (292). This suggests that there are at least two independent pathways that control the deposition of CenH3 at different phases. In the budding yeast, *Saccharomyces cerevisiae*, CenH3 is loaded during S-phase (214). The findings in the two yeasts contrast with those from other organisms, such as plants, flies and humans, where CenH3 is deposited only during mitotic anaphase or the G1/G2 transition (134, 160, 255). One possibility is that these differences in the loading of CenH3 at centromeres is influenced by different interactions of protein complexes involved in the typically "closed" mitosis of fungi, when compared to the "open" mitosis observed in flies, plants and animals (67, 68, 96, 234). It remains a mystery how exactly the phase-specific discrimination of CenH3 loading is accomplished, as at the amino acid sequence level the histone fold domain (HFD) is highly conserved in organisms as different as yeast and humans.

The major difference between CenH3 proteins from even closely related species lies in the highly divergent N-terminal tail (see Chapter 2, Figure 2.1). It is currently not well understood if during CenH3 loading the conserved HFD or the divergent N-terminal tail interacts with the various loading complexes.

Structurally, CenH3 is ~80% identical to histone H3, but the N-terminus varies greatly in length and in amino acid composition (14, 173, 227, 254). Some organisms within the same phylogenetic clade show conserved motifs within the N-terminus that are important during cell division, e.g. the “essential N-terminal domain” (END) domain of Saccharomycotina (51, 308), but this is not a conserved feature as it appears to be absent from the large number of filamentous ascomycetes for which there are CenH3 sequences available (see Chapter 2). In filamentous fungi, the CenH3 N-terminus is highly variable and, as shown in Chapter 2, it appears to undergo adaptive evolution, even within the genera *Neurospora, Gelanospora* and *Sordaria*.

The second major structural difference between CenH3 and canonical histone H3 is the loop I region, which is considered to be necessary for centromere targeting in humans and flies (25). Apart from the divergence in their N-terminal tails, CenH3s with variable loop I sequences from closely related species in the genus *Arabidopsis* were capable of localizing at *A. thaliana* centromeres, but they were unable to complement all of the native CenH3 functions (227). These observations suggested that functional complementation and mere localization of CenH3 to centromeric chromocenters are separable into independent pathways. My genetic data obtained by studying filamentous fungi (see Chapter 2) supported this hypothesis because

loop I amino acid differences in fungal CenH3s did not hinder its localization at centromere. It did not matter if genes were expressed from ectopic inducible or the endogenous promoter in *N. crassa*. Thus, it may be the disruption of an H3-specific sequence feature rather than a CenH3-specific motif that allows default integration of CenH3 into centromeric nucleosomes.

The most conserved region in CenH3 is the HFD, which can interact with the other core histones (i.e., H4, H2A and H2B) in the nucleosomes and has also shown to be required for centromere targeting in plants and budding yeast (160, 191). Domain swapping experiments with budding yeast CenH3 (Cse4) sequences into H3 sequence showed that HFD differences within the N-α-helix and the N-loop resulted in higher likelihood of chromosome loss. Increased chromosomal loss was also observed in domain swaps of the α-2 helix, central and distal regions with the corresponding H3 sequences (143). Further, the α-2 helix of CenH3 is recognized by Scm3; as mentioned above, this protein aids in CenH3 deposition at centromeric nucleosomes during S phase (52, 88, 214, 334). Early studies suggested that there is no single or small stretch of contiguous amino acids in the Cse4 HFD that acts alone to specify Cse4 function at centromeres (143). Taken together, these observations from diverse systems suggest that amino acids distributed throughout the HFD act in combination to impart centromere function to CenH3, a function essential for mitotic chromosome segregation.

In mitosis, spindles on sister chromatids are bi-oriented in contrast to meiosis I, where they are juxta-posed for mono-orientation. Studies in fission yeast have shown that interaction of core centromere regions with cohesins can trigger mono-orientation

in kinetochores during meiosis compared to pericentric interactions with the cohesisns during mitosis (242). Hence, due to this difference in orientation of centromeres it is possible that structural requirements of CenH3 are different in meiosis when compared to mitosis.

This hypotheis was supported by our genetic data in *Neurospora* where, heterozygous crosses with C-terminal GFP tagged *Podospora anserina* CenH3 (PaCenH3-GFP) showed that PaCenH3-GFP was capable to at least partially function in the presence of *N. crassa* CenH3 wildtype and deletion alleles (ΔNcCenH3) (see Chapter 2). At the same time, *Fusarium graminearum* (FgCenH3-GFP) and *Aspergillus nidulans* (AnCenH3-GFP) failed to complement NcCenH3 function. In contrast to C-terminally GFP-tagged versions of FgCenH3, non-tagged alleles could be substituted for wildtype NcCenH3, and thus can support meiosis in *N crassa*. However, some of the strains bearing replacement alleles showed vegetative growth defects, especially in the presence of the microtubule function inhibitor thiabendazole (TBZ; Figure 2.9), hinting at defective assemblies of kinetochores during mitosis.

Pairwise alignments of PaCenH3 or FgCenH3 with NcCenH3 showed 47 or 51 amino acid sequences differences, respectively. Most of the differences lie in HFD domain compared to N-terminus (Figure 3.1A). We considered that differences in HFD sequences might prove sufficient to disrupt meiotic function in the presence of FgCenH3-GFP. We thus began testing the importance of the HFD during meiosis by domain swapping experiments between the N-terminal tail and HFD of three fungal CenH3s (FgCenH3, PaCenH3 and NcCenH3). As mentioned earlier, most differences

in NcCenH3 and PaCenH3 are present in the HFD, so we wanted to analyze differences tolerated by Neurospora centromeres without little disruption in centromere maintenance during vegetative growth. Therefore, to determine centromere assembly in strains with PaCenH3-GFP we next performed chromatin immunoprecipitation followed by high-throughput sequencing (ChIP-seq). We found that after meiosis some centromeres lost PaCenH3-GFP occupancy randomly, progressively and apparently irreversibly in subsequent mitoses. To find unifying mechanisms behind these observations we tested for aneuploidy, chromosome abnormalities or nucleosome-free regions but found none. Our study thus reveals some surprising features of CenH3 depletion from centromeric DNA that underscore the dynamic nature of centromere assembly during mitosis and meiosis (180).

Materials and Methods

Cloning and fusion PCR constructs

The fungal CenH3 genes used for chimeric constructs had been amplified by PCR from *P. anserina*, *F. graminearum* and *N. crassa* for initial genetic analyses (see Chapter 2, Table 2.1). A *BamH*I restriction site was introduced via PCR primers immediately before the N α-helix at the end of the first intron of CenH3 (Figure 3.1A). Primers with *BamH*I sites were used to amplify regions from G=FgCenH3 (OMF1758-OMF1760, OMF1759-OMF162), PaCenH3 (OMF180-OMF1848, OMF1849-OMF1447), and NcCenH3 (OMF180-OMF1847), respectively (Table 3.1). PCR fragments were called “N domain” (N-terminus) or “C domain” (HFD) and cloned into pPP33(NFgcenH3), pPP86(CPaCenH3), pPP87(CNcCenH3) and pPP88 (NPaCenH3) by use of a Zero Blunt TOPO PCR cloning kit (Invitrogen) to generated plasmids pPP51 (NNcCFgCenH3-GFP), pPP52 (NPaCFgCenH3-GFP) and pPP53 (NFgCPaCenH3-GFP), respectively. These plasmids were used for overlap and fusion PCR as described in Chapter 2 to generate full-length fragments of CenH3 genes with 5’- and 3’-overhangs and selectable markers for transformation by electroporation into conidia of host strain N3011 to generate heterokaryotic transformants with CenH3-GFP chimeras (NMF562 - NMF565, Table 3.2). A chimeric NFgCNcCenH3-GFP gene was cloned and transformed into *N. crassa*. However, because of long stretches of homology between the C domain of NcCenH3 and the transforming DNA, homologous recombination resulted in exclusion of the short N domain of FgCenH3 at the endogenous CenH3 locus. Instead, only C-terminal GFP tagged NcCenH3 strains were recovered, so this chimeric construct was not considered in this study. Other strains used in this study, e.g. strains with PaCenH3-

GFP (NMF324, NMF326, NMF327) were constructed as part of studies reported in Chapter 2 (Table 2.1).

Strains and growth media

All strains used for this study are listed in Table 3.1. Strains were maintained on Vogel's Minimal Medium (VMM) with supplements as necessary (see Chapter 2).

Assay for linear growth in Ryan (race) tubes

Conidia from PaCenH3-GFP (NMF324, NMF326), NcCenH3-GFP (NMF327), WT (NMF39), one transformation host (N3011) and a wildtype sibling of CenH3-GFP strains (NMF568) were inoculated at on end of race tubes with VMM. When the strains reached the opposite end of the tube, conidiate were collected and re-inoculated into fresh race tubes. This was repeated four times, for a total of five length or race tubes (~150 cm) and with triplicates of each strain. Conidia from every strain were collected after each race tube and stored in 25% glycerol at -80C. During the entire growth period readings for linear growth extension were collected at marked on the tubes at regular intervals. Strains collected after the first race tube run were labeled "START", samples collected after the fifth run were labeled "STOP". The START samples of three biological replicates of NMF324 (NMF569, NMF575, NMF579) and NMF326 (NMF571, NMF577 and NMF581) along with STOP samples for NMF324 (NMF570, NMF576 and NMF580) and NMF326 (NMF572, NMF578 and NMF582) strains were used for ChIP-seq experiments and phenotypic anlyses. Only one biological replicate for NcCenH3-GFP was used for ChIP-seq as START (NMF573) and STOP (NMF574) strain, as previous experiments did not reveal major changes in enrichment patterns (273).

Assay to detect live cells by AlamarBlue staining

Conidia from 10-day old cultures of NMF569, NMF570, NMF571, NMF572, NMF573, NMF574, NMF583 and NMF584 were harvested and diluted to 20,000 or 2,000 conidia in 20 μl. Fewer conidia in a given sample volume appear to result in comparatively synchronous growth (177). In 96-well plates, 20 μl of conidial suspensions were added to 180 μl of VMM and incubated for 8 hrs at 32C, followed by addition of 20 μl undiluted AlamarBlue dye (Invitrogen). The samples were incubated for another 4hrs at 32 degrees C. Fluorescence readings were taken on a Synergy 2 Plate Reader (BioTek, Winooski, VT) at 530 – 560 nm excitation and 590 nm emission wavelengths (147). The length of incubation to obtain reproducible readings was determined by trial and error. A total incbation of 8+4 hrs was arrived at because it typically takes ~3 - 4 hrs for *Neurospora* macroconidia to develop a germ tube. In addition, nuclear division cycles in non-germinated spores are approximately five times longer compared to divisions in germ tube (234). Therefore, in order to capture the start point for log-phase growth the optimal incubation time considered was between 8 – 12 hrs.

Isolation of genomic DNA and Southern analysis

Genomic DNA from filamentous fungi was isolated and Southern analyses were carried out as described previously (187, 221).

Quantitative PCR (qPCR)

The concentration of genomic DNA used as template for qPCR reactions was first estimated by a pico-green fluorescene method using high-range standard curve as described in the Quant-iT PicoGreen dsDNA reagents and Kits (Invitrogen). Then, 20

μl PCR reactions with Fermentas master mix were run on the CGRB core lab's ABI PRISM 7500 Realtime PCR machine. The Ct-values for each sample (in triplicate) was measured, differences were calculated for each sample and plotted. Primers OMF2063 and OMF2064 for G2 mitotic specific cyclin (NCU01242) on LG V, along with primers OMF2037 and OMF2060 for 5,6 phosphofructose kinase (NCU01728) on LG II were used as internal control primers for each genomic DNA template (e.g. NMF39, NMF569 and NMF570; Tables 3.1 and 3.2). The test primer set was tel1 (OMF1085, OMF1086), NCU01998 (OMF2033, OMF2057) and Cen1L (OMF2661, OMF2662) for LG I. For LG V the test primer set used was Cen5L, Cen5C, and Cen5R (OMF2681 to OMF2686; Table 3.2).

Chromatin immunoprecipitation and high-throughput sequencing (ChIP-seq)

The procedures for ChIP and ChIP-seq were the same as previously described (273).

Results

Chimeras of the Nc- or PaCenH3 N-terminal tail with the FgCenH3 HFD are unable to complete meiosis

In my previous work (see Chapter 2) I showed that strains with FgCenH3-GFP were never recovered from heterozygous crosses, in contrast to strains containing PaCenH3-GFP. Strains with non-tagged FgCenH3, however, were recovered, even from homozygous crosses, showing that complete gene swaps can be carried out even between somewhat distantly related taxa. Nevertheless, even these strains showed growth defects in presence of thiabendazole (TBZ), a microtubule-destabilizing agent, which suggests defective centromere or kinetochore assembly. Similar results had been obtained on studes with fission yeast, showing that thiabendazole interferes with clustering of centromeres at the spindle pole body (SPB) (108). Thus both results suggest the probability of abnormal centromere assembly when FgCenH3 replaces NcCenH3. In order to determine the cause of meiotic defects and to differentiate if they stem from N-terminus divergence or differences in the Histone Fold Domain (HFD) of FgCenH3, we build chimeric Fg- and NcCenH3-GFP proteins. This was accomplished by introducing a unique *BamH*I site between the N-terminal tail and HFD (Figure 3.1A). Swapping the N-terminal tail of FgCenH3 with that of NcCenH3 and PaCenH3 (NNc-CFgCenH3-GFP and NPa-CFgCenH3-GFP) resulted in two chimeras with the FgCenH3 HFD; the third chimera carried the N-terminal tail of FgCenH3 and the HFD of PaCenH3 (NFg-CPaCenH3-GFP).

All three chimeras, when transformed into *Neurospora*, were properly targeted to centromeric chromocenters (in strains NMF562 NMF564 and NMF565; Figure 3.1B). When screened by epifluorescence microscopy, tight foci of fluorescence were observed, one per nucleus, where all seven *Neurospora* centromeres cluster together. However, ascospores from heterozygous crosses XPP124 and XPP126 (NMF162 X NMF562 and NMF162 X NMF564, respectively), both of which had constructs with FgCenH3 HFDs, failed to germinate. This was in contrast to ascospores from cross XPP132 (NMF162 X NMF565), which contained constructs with the PaCenH3 HFD; these ascospores germinated in the expected frequency. Homozygousity for two of these NFgCPaCenH3-GFP chimeric strains (NMF566 and NMF567) was checked by genotyping the strains by Southern blotting (Figure 3.1C). Absence of the wildtype NcCenH3 band but presence of *hph* (the gene for hygromycin resistance, encoding hygromcyin phosphotransferase) as selectable marker in the progeny suggests proper gene replacements. Production of viable ascospores demonstrates that the PaCenH3 HFD aids in supporting meiosis in *Neurospora*.

Mitotic defects in the presence of non-tagged or tagged CenH3 were difficult to discern (see Chapter 2) suggesting that mitosis was normal or almost normal. Observing no phenotypic defects caused by perturbation of centromere assembly may be explained because of the flexibility and plasticity observed in centromere assembly systems in many organisms (20, 106). However, the small mitotic and more drastic meiotic defects we detected based on tagging with C- or N-terminal fluorescent proteins, should in the end depend on the merely 16 amino acid differences in the HFD of Pa- compared to NcCenH3-GFP, which did not show any

prominent growth defects (Figure 3.2). Curiously, the small defects we detected were more noticeable in strains of *his-3* background. The reason for this is not understood at present, but defects in histidine biosynthesis have long been correlated with defects in *Neurospora* DNA repair (65).

Decreased enrichment of PaCenH3-GFP at some Neurospora centromeres

It is know that epigenetic phenomena drive centromere assembly and maintenance, hence it is possible that in strains with PaCenH3-GFP there might be changes in various pathways involved in centromere maintenance that do not reveal phenotypic defects. We determined that the PaCenH3 HFD in combination with the FgCemH3 N-terminal tail supports meiosis in *Neurospora*, thus we wished to compare proper maintenance of centromeric nucleosomes in the presence of PaCenH3-GFP during mitosis. This can be accomplished by mapping of the localization of CenH3 itself, as it is the characteristic marker of centromere chromatin.

We thus compared PaCenH3-GFP enrichment to that with NcCenH3-GFP control strains we had previously used to determine where *Neurospora* centromeres are localized (273). ChIP-seq data obtained with these strains showed overall similar enrichment of PaCenH3-GFP at most centromeres when compared to that of NcCenH3-GFP (Figure 3.3, *CenII* and *CenV*). The enrichment peaks of both PaCenH3-GFP strains (NMF324 and NMF326) overlapped very closely with NcCenH3-GFP peaks. There were no contractions or expansions of the original centromeric regions we observed with NcCenH3-GFP, or global changes in localization patterns, i.e. to ectopic sites elsewhere on chromosomes. To our surprise, we noticed that in two independently obtained progeny certain centromeres showed

depletion of PaCenH3, suggesting incomplete centromere maintenance. This happened after one meiotic event, i.e. after a single cross at *CenI* (NMF324) or *CenVI* (NMF326). For this experiment we randomly picked two strains of ~20 progeny. That both strains should have defects at one centromere each suggests that this is not a rare phenomenon; genome-wide tests with additional strains from the same and additional crosses are in progress (data will be available at the time of the defense seminar).

Because the homokaryotic PaCenH3-GFP strains stemmed from a heterozygous cross with a strain in which wildtype NcCenH3 was present, these results may imply the presence of previously bound wildtype NcCenH3 enriched at *CenI* and *CenVI* that may have generated functional centromeric nucleosomes, similar to *CenII* and *CenV* (Figure 3.3). We thus decided to carry out a long-term growth experiment, which would assure that any potential wildtype NcCenH3 would be subject to protein turnover.

Presence of PaCenH3-GFP at *Neurospora* centromeres causes slightly slower linear growth

As mentioned in the introduction, CenH3 loading happens during or after each mitotic cell cycle. Therefore we wished to test if the enrichment patterns observed at *CenI* and *CenVI* (Figure 3.3) were maintained after many more mitotic divisions. We grew the strains with PaCenH3-GFP for up to a month in an extended growth assay that involved Ryan (or “race”) tubes that are typically used for studies on circadian rhythms (65, 241).

We inoculated tubes with wild type CenH3 (NMF39 and NMF568, a NcCenH3 sibling from XPP14), NcCenH3 *his-3* (N3011), NcCenH3-GFP (NMF327), PaCenH3-GFP (NMF326) and PaCenH3-GFP *his3* (NMF324) in parallel and in triplicate (Figure 3.4A). Initially similar growth rates were observed for all strains (days 0-5), as evidenced by tight clustering. By day 11 of growth (in the third race tube) we observed separation of strains along the y-axis: strains with PaCenH3-GFP (NMF324 and NMF326) were noticeably slower, suggesting a slight defect in growth rate that was not observed on plates or in culture tubes (Figure 3.4A). NcCenH3-GFP (NMF327) and NcCenH3 strains (NMF39, NMF568, N3011) grew similar, but strains with *his-3* mutations were again growing more slowly than true wildtype strains.

Next, we tried to quantify the growth of these strains using an AlamarBlue assay (see Materials and Methods). AlamarBlue assays use resazurin, an initially non-fluorescent dye that is converted to the red–fluorescent resorufin by reduction reactions of metabolically active cells. The amount of relative fluorescence produced in each reaction is thus proportional to the number of living cells. Initially we standardized growth conditions of germlings for this assay by using wildtype conidia (NMF584) as controls (Figure 3.4B). We found that incubation for 8 hrs correlated with the beginning of log-phase growth. Next, these experiments were repeated using 20,000 (Figure 3.4C) and 2,000 (Figure 3.4D) conidia of control and test strains. Based on the relative fluorescence obtained we found no major differences in the number of live cells after 8 hrs of pre-incubation followed by 4hrs of incubation in the presence of AlamarBlue dye when we used 2,000 conidia as inoculum, at least for wildtype NcCenH3 (NMF583, NMF584), NcCenH3-GFP (NMF574) and PaCenH3-GFP (NMF571) (Figure 3.4D). Under identical conditions, we found am unexplained

higher reading for one NcCenH3-GFP strain (NMF573). At the same time, three of the PaCenH3-GFP test strains showed reproducibly lower readings (NMF572, NMF569, NMF579). While there was a clear tendency for reduced number of viable cells in samples that contained PaCenH3-GFP we propose that the difference in the readings of the PaCenH3-GFP strains can be again explained by the presence of a mutant *his-3* allele (in NMF569 and NMF570 compared to NMF571 and NMF572). We also doubted the reliabilityof this assay and thus repeated the experiments with 20,000 conidida as inoculum; all other conditions were identical as to the first set of experiments. Under these conditions, the PaCenH3-GFP *his-3* strains (NMF569 and NMF570) again had the lowest number of live cells, when compared to all other strains (Figure 3.4C). The results for the six wildtype NcCenH3, NcCenH3-GFP and PaCenH3-GFP strains suggest that there is large variability in this assay and that it may be difficult to tease reliable differences from this assay.

One possible explanation for our observation of very subtle growth defects described in Figure 3.4 is that some kind of selection occurs at the level of nuclei, where the healthiest nuclei undergo mitosis first, and thus shelter defective nuclei. This “checkpoint” may provide time for correction of potentially lethal events in other nuclei. This underscores one of the advantages of maintaining asynchrony of nuclear division in coenocytic *Neurospora* hyphae. To refine the assay AlamarBlue assay described above, we also used shorter incubation times of 4 hrs, but under these conditions the AlamarBlue dye was not sensitive enough to detect the much lower cell mass. This experiment was also tried in the presence of TBZ because it was helpful in differentiating subtle growth defects in strains with GFP-tagged CenH3 (see Chapter 2). Nevertheless, even in these assays the relative fluorescence always

fluctuated and no clear correlation between type of CenH3 protein present and live cell numbers was observed,

Loss of PaCenH3-GFP from certain centromeres is irreversible and progressive

Two of the original ascospore progeny obtained from cross XPP14 were first grown in slants, transferred to liquid medium, and analyzed by an initial ChIP-seq experiment (NMF324 and NMF326, Figure 3.2). ChIP-seq analyses suggested that PaCenH3 was lost frequently and perhaps randomly from centromeric DNA. We next wished to address if this loss was random and/or irreversible and/or progressive. Different scenarios can be imagined: (1) The changes in PaCenH3 occupancy observed in the two strains, though observed at two different centromeres were random and can occur at any centromere at any time ("random centromere defect"), (2) changes were initiated during the cross (i.e. in meiosis), and thus observations made in initial experiments NMF324 and NMF326 (Figure 3.2) will not change ("conservative meiotic defect"), and (3) changes were initiated during meiosis but changes can occur after meiosis in successive cell divisons ("cumulative division defect").

To differentiate between these possibilities, we used the long-term linear growth experiment (Figure 3.4A) to obtain strains that allowed us to determine PaCenH3-GFP occupancy by ChIP-seq. We collected conidia after each of the successive runs through race tubes but initially focused our attention on the very initial strains obtained after the first linear growth through race tubes. These strains are from now on called "START (equivalent to the 0 day time point, Figure 3.4A). Strains obtained after four additional linear growth experiments through fresh race tubes were called

“STOP” (equivalent to the 31 day time point, Figure 3.4A). In addtion to NMF324 and NMF326, we thus tested six independent vegetatively derived strains by START ChIP-seq analyses (on NMF569, NMF575, NMF579, all derived from NMF324, and NMF571, NMF573, NMF581, all derived from NMF326, respectively) and STOP ChIP-seq analyses (on NMF570, NMF576, NMF580, all derived from NMF324, and NMF572, NMF574, NMF582, all derived from NMF326, respectively).

We grew the originally obtained and derived strains for long periods of times to differentiate between Scenarios 1 to 3. Scenario 1, where the changes observed are random or perhaps even experimental noise (and thus not meaningful), predicts that the same strains, when re-examined, would exhibit different patterns of changes, and that these changes would be different in each of the triplicate START and STOP strains. Scenario 2 predicts that the original changes are maintained faithfully, and are thus irreversible, as all changes in PaCenH3 distribution or recruitment were pre-determined during meiosis in cross XPP14. Scenario 3 predicts that the original defect was predetermined in meiosis but that defects will be not only irreversible but also progressive, i.e. over time PaCenH3 will be depleted from additional centromeric regions.

The enrichment patterns for PaCenH3-GFP START (NMF569, NMF575, NMF579, NMF571, NMF573, NMF581) and STOP strains (NMF570, NMF576, NMF580, NMF572, NMF574, NMF582) matched with NcCenH3-GFP START (NMF573) and STOP (NMF574) strains at *CenII*, *CenIII* and *CenV* (Figure 3.5A, and data not shown). The initial loss of PaCenH3-GFP enrichment at *CenI* for NMF324 and *CenVI* for NMF326 (Figure 3.2) did not change, even after duplicating the

experiment (*CenI* in START strains NMF569, NMF575, NMF579, and *CenVI* in START strains NMF571, NMF573, NMF581, respectively) or using extended growth periods (*CenI* in STOP strains NMF570, NMF576, NMF580, and *CenVI* in STOP strains NMF572, NMF574, NMF582, respectively; Figure 3.5B). Biological replicates for NcCenH3-GFP strains (e.g. NMF573 and NMF574) had been done for a previous study (Smith 2011) that revealed no prominent differences in enrichment of NcCenH3-GFP at any centromere. No changes in enrichment of PaCenH3-GFP at centromeres that had previously shown no defects, or where the original defect was not altered (Figure 3.2) suggested that Scenario 2 applies, i.e. conservative and likely irreversible defects that were predetermined in meiosis, as all strains behave similarly.

Examination of the remaining centromeric regions, however, revealed additional changes. Enrichment of PaCenH3-GFP at *CenIV* and *CenVII* progressively decreased from the original NMF324 and the START strains NMF569, NMF575 and NMF579 when compared to the STOP strains NMF570, NMF576, and NMF580 (top six strains shown in red in Figure 3.6). In contrast, PaCenH3-GFP enrichment in the original NMF326 and the START strains NMF571, NMF577 and NMF581, as well as the STOP strains NMF572, NMF578 and NMF582 was comparable to that of NcCenH3-GFP at both centromere *CenIV* and *CenVII* (compare two strains in black to bottom six strains in red in Figure 3.6). These observations suggest that Scenario 3 (“cumulative division defect”) applies, as in addition to irreversible conservative changes observed at *CenI* and *CenVI* in two different lineages progressive loss of PaCenH3-GFP from additional centromeric regions (*CenIV* and *CenVII*) was observed

Taken together, these observations suggest that PaCenH3-GFP localization and loading at centromere although defective in long-term growth studies is not lethal (when compared to deletion of NcCenH3, see Chapter 2). Secondly, although there is some randomness in PaCenH3-GFP depletion from centromeres, the overall pattern appears to be set during meiosis, as depletion appears irreversible (i.e., gain of PaCenH3-GFP in a previously depleted region has not been observed) and progressive (i.e., centromeric regions with initially low occupancy remain low in PaCenH3 or PaCenH3 occupancy is further reduced). This is more clearly illustrated when reads per bp are normalized for each run (Figure 3.7). Our observations thus suggest that during mitosis in filamentous fungi CenH3 is required at minimal levels at centromeres. In *Neurospora* germ tubes the time per mitosis is reduced by about five times compared to non-germinated conidia (234). Thus mitosis may be too fast during polarized growth of filaments to allow for loading of new PaCenH3-GFP after each mitotic division.

It seems amazing that specific centromeres are essentially free of PaCenH3-GFP, the only CenH3 available in the cell, yet these strains can grow almost normally for extend periods of time. We thus attempted to elucidate the mechanism underlying this behavior. We considered four potential ways for the cell to avoid death because of insufficient CenH3-GFP at specific centromeres: (1) epigenetic regulation and influx of H3 nucleosomes into regions normally occupied by CenH3 nucleosomes, (2) rapid and drastic changes in the underlying centromeric DNA, (3) aneuploidy with maintenance of some few normal chromosomes that may shelter the deficient nuclei, and (4) large translocations or chromosome fusions that would make some

centromeres unnecessary. The following experiments addressed each of these four possibilities.

Epigenetic states of centromeres are maintained in presence of PaCenH3-GFP

We wondered how centromeres without normal levels of CenH3 might function to keep the cells alive. One possibility we considered were changes in epigenetic regulation of neighboring H3-containing nucleosomes. Regional centromeres from fission yeast, flies, human and plants show pericentric regions enriched with nucleosomes that carry H3K9me3 (histone H3 lysine 9 trimethylation), a typical mark for heterochromatic regions. In contrast, the core or central regions of centromeric DNA that are embedded in pericentric regions has alternating arrays of CenH3 and histone H3 nucleosomes, which in fission yeast, flies and humans are enriched with H3K4me2, a typical mark for euchromatin that is found in transcriptionally active regions of the genome (3). Studies with human cells have shown that induction of heterochromatin by H3K9me3 on alpha-satellite repeats results in loss of CenH3, inactivating functional centromeres (195, 206) and that expression of alpha-satellite DNA is required for proper loading of CenH3 on human artificial chromosomes (19). Contradictory to these observations, our data on *Neurospora* centromere characterization showed that pericentric and central core regions are enriched with H3K9me3 and that the core regions are devoid of H3K4me2, suggesting that centromeres are truly heterochromatic in *Neurospora* (273).

We examined whether the defective centromeres in presence of PaCenH3-GFP showed any alterations in enrichment of these two telltale histone marks. We did ChIP-seq assays with H3K9me3 and H3K4me2 antibodies (as described in the

Materials and Methods). Our ChIP-seq data for PaCenH3-GFP START strains (NMF569, NMF571) and STOP strains (NMF570, NMF572) matched those for NcCenH3-GFP strains (NMF573 and NMF574), and showed conservation of localization of both histone marks, i.e. the centromere core regions were enriched with H3K9me3 and H3K4me2 was absent from this region (Figure 3.8A). This observation suggests that centromeres with PaCenH3-GFP have specifically lost CenH3 at some centromeres (i.e. *CenI*, *CenIV*, *CenVI* and *CenVII* in the various strains discussed above and shown in Figures 3.5 to 3.7), possibly because of disruption in DNA interactions in the presence of PaCenH3-GFP during nucleosome formation. Alternatively, PaCenH3-GFP might not be loaded efficiently at *Neurospora* centromeres either due to structural defects or due to alteration of spatio-temporal regulation, the reason for which is yet to be determined.

Looking more closely at the enrichment data presented in Figure 3.8, there seem to be overall small differences in enrichment of H3K9me3 in the STOP strain of NcCenH3-GFP (NMF574) in comparison to the START strain (NMF573); there are fewer purple bars that represent enrichment scores greater then the cutoff of >10 reads/bp. Similarly, peak enrichment of H3K9me3 as well as H3K4me2 did not change much in the PaCenH3-GFP START and STOP strains NMF571 and NMF572 (Figure 3.8). However, in the somewhat more growth-defective strains NMF569 and NMF570 (PaCenH3-GFP *his-3*), the enrichment of H3K9me3 at centromere in NMF569 seemed to be much decreased in the STOP strain NMF570. Compared to the NcCenH3-GFP strains and the euchromatic regions in the PaCenH3-GFP strains, H3K4me2 enrichment in the centromeres was greatly reduced in the PaCenH3-GFP strains. There is quite a bit of variability in these normalized ChIP-seq data, and the

enrichment was relatively low overall (maximum ~30, compared to CenH3 peak values at centromeres, which are >100; Figures 3.5, 3.6 and 3.8A). Taken together, our data suggest that there are insufficiently large changes in epigenetic marks that could explain why centromeres depleted for CenH3 function almost like normal centromeres in the PaCenH3 strains we analyzed by ChIP-seq.

Centromere DNA sequences are unaltered in the strains having PaCenH3-GFP

Masive rearrnagement or deletion of centromeric DNA would be another way to account for the viability of strains with deficient centromeres. Recent work with maize centromeres has shown that nucleosome positions were distinct for the three major centromeric DNA elements, which might be influenced by chromatin structure at centromere (103). The periodicity of nucleosome positioning on tandem repeats of *CentC* was dependent on AA/TT dimers in contrast to retroelements *CRM1* and *CRM2*, which lacked the correlation of AA/TT dimer periodicity. But, nucleosomes on *CRM2* still showed a strong phasing effect that was absent in *CRM1* (103). Secondly, high rates of mitotic recombination were observed both in fission yeast and human centromeres (129, 166). Hence there is a possibility that mitotic recombination may cause rapid changes in centromeric DNA sequences and thus decrease enrichment or change localization of CenH3, which probably depends on chromatin confirmation or recognition that may at least to some extent be guided by the underlying DNA sequence.

Therefore, we performed a SNP (single nucleotide polymorphism) analysis, comparing the parent strains used in heterozygous crosses (i.e. N1961 and N3011) (Table 3.1) to determine if there are any differences in centromeric DNA sequences

between the strains. This SNP analysis showed hardly any differences in the centromeric sequences for *CenI*, *CenVI* and *CenVII*, except for some little divergence observed in *CenIV* (Figure 3.9). Thus it is difficult to predict if the underlying DNA plays any role for CenH3 localization or is the defect due to nucleosome postioning at Neurospora centromeres. We did notice, however, that in the homokaryotic strains with PaCenH3-GFP some short regions of centromeric DNA had been removed, perhaps by recombination. This can be deduced from an absence of ChIP-seq reads in certain regions. ChIP in *Neurospora* always results in some background reads. If no such backgrouns is detected that means that the region in questions has been deleted from the genome of the strain analyzed. This pattern can be observed in *CenI* of NMF326 and its derivatives (Figures 3.2, 3.5 and 3.7). This region is present in both parent strains (Figure 3.9)

Depletion of PaCenH3-GFP from certain centromeres does not result in aneuploidy

One of the potential outcomes in the presence of defective centromeres is aneuploidy due to improper chromosome segregation. Initally, in order to test whether there is aneuploidy in PaCenH3-GFP containing strains, regular semiquantitative PCR amplification for a limited number of cycles was attempted, as one would expect large differences in DNA content for chromosomes with normal *versus* CenH3-deficient centromeres (expected ratios would be ~10-100:1). No difference was observed. Hence we tried to use a more sensitive technique to detect anueploidy, i.e. qPCR on DNA, which was previously carefully adjusted to the same concentration by a pico-green-based method. We quantified genomic DNA samples from wild type (NMF39) and two PaCenH3-GFP strains (NMF569, NMF570. The result did not

reveal any obvious differences between the START (NMF569) and STOP (NMF570) strains (Figure 3.9) that would match the large differences in CenH3 occupancy (Figure 3.7). However, the accuracy of this experiment is difficult to evaluate and it is possible that experimental errors occurred. Two internal control primer pairs were used; one was to amplify a fragment of the gene for G2 mitotic specific cyclin (NCU01242) on LG V and the other was to amplify a fragment of the gene for 5,6 phospho-fructose kinase (NCU01728) on LG II. Both gave overall similar results, which would suggest no aneuploidy based on these data. However, the standard deviations for these assays are too high to be conclusive and also suggest experimental error.

Fertile progeny from backcrosses exclude translocations or chromosome fusions

One additional way to avoid death in the presence of defective centromeres is to generate large translocations or even chromosome fusions that would render some centromeres unnecessary. In *Neurospora*, this idea is most easily tested by crossing the defective strains back to wildtype strains. If the strains with depleted PaCenH3-GFP at certain centromeres contained large translocations that fused whole chromosome arms of LG I or LG VI to the other chromosomes, crosses to wild type would result in a relatively large fraction of dead, white or misshapen spores, as meiosis would result in missegregation. If random viable progeny of these crosses are again crossed to wild type, some crosses will be normal. Crossed with strains that originally carried large translocations or chromosome fusion will now likely contain large regions that are duplicated (i.e. that are partially diploid). Such crosses are essentially barren in *Neurospora*. In our backcrosses XPP182 (NMF39 X NMF570)

XPP235 (NMF262 X NMF572), we did not observe these phenotypes for either the first or the second backcross, thus very likely the strains that are depleted in PaCenH3 at certain centromeres do not carry large duplications.

Discussion

Results from our previous genetic approach (see Chapter 2) showed that PaCenH3-GFP strains can be recovered from heterozygous crosses whereas FgCenH3-GFP strains are not recovered, likely because of more severe meiotic defects. Nevertheless, non-tagged FgCenH3 seemed to complement *Neurospora* CenH3 during meiosis, even though they showed growth defects in the presence of the microtubule inhibitor, thiabendazole (TBZ), which suggested mitotic defects. Thus, FgCenH3 – either non-tagged or tagged at the C-terminus – alters *Neurospora* centromeres sufficiently to results in meiotic or mitotic defects. Accordingly, in our experiments with chimeras, we found that the HFD of FgCenH3 failed to support meiosis, as no viable ascospores were obtained, again signifying the importance of HFD during meiosis. Likely this is caused by differences in centromere interaction surfaces in meiosis and mitosis (see Fig. 11 in Chapter 2). In mitosis there is back-to-back assembly of sister kinetochores, in contrast to juxtaposed side-to-side attachment for mono-orientation of sister chromatids during meiosis (320, 321).

The plasticity of centromere assembly has made it difficult to predict specific structural determinants of CenH3 essential for its function. However, recently lysine residue (K79) in the α-3 helix within the HFD of human CenH3 has been shown to be acetylated, presumably to neutralize the negatively charged DNA wrapped around the nucleosomes, thus maintaining stability of nucleosome structure (32). This lysine

residue is conserved in all fungal CenH3 proteins we studied (Figure 3.2A) but is expected to be buried inside the nucleosome. Further, deuterium ion exchange studies have determined another important lysine residue, K49 within the α-N helix that appears necessary for CenH3 nucleosome array condensation at human centromeres (212). The corresponding lysine residue, K61 (according to NcCenH3) in NcCenH3 and PaCenH3 is conserved in contast to FgCenH3 that shows presence of arginine similar to histone H3. In humans, presence of this lysine residue (K49) instead of arginine (R49) in CenH3 provides flexibility to nucleosome stucture that improves easy exchange of CenH3 within the nucleosome. This process might be necessary in some unknown regulatory events during centromere assembly. In another structural study of human CenH3 nucleosomes, important residues involved in targeting of CenH3 to centromeric regions lie within the α-2 helix (258). The corresponding residues in fungal CenH3s are identical or more similar to those in canonical histone H3 rather than human CenH3 (Figure 3.2A). This suggests different structural requirements for fungal CenH3 that allow for targeting to centromeric regions or nucleosome formation. It certainly seems that there are few absolutely required amino acid residues for centromeric targeting that are conserved over long periods of evolutionary time.

Alternatively, the dynamics of nucleosome formation with fungal CenH3 or CenH3 loading at fungal centromeres might not be determined by primary sequence alone but rather share features of chaperone pathways that are involved in histone H3 and human CenH3 assembly. In our studies to determine structural requirements of NcCenH3 by using molecular genetics, we showed that along with the conserved HFD the length of the N-terminal tail appears essential for meiosis (see Chapter 2).

The N-terminal tail, the loop I region and the C-terminus of CenH3 all are exposed at the surface of nucleosomes, thus providing possible CenH3 nucleosomal binding sites for trans-acting factors (286-288). In FgCenH3, PaCenH3 and NcCenH3 the N-terminal regions are highly divergent (Figure 3.2A). Thus, these observations suggest that the balance and flexibility is maintained in centromere assembly depending on the CenH3 amino acid residue differences where unlike HFD of FgCenH3-GFP, PaCenH3-GFP can support meiosis.

Overall differences between the fugal CenH3s are not specific to certain regions but rather are spread out across the whole protein, which may help explain the different results obtained by tagged or non-tagged whole proteins (Chapter 2) and the chimeric proteins used here. It seems that meiosis is overall more vulnerable to CenH3 defects than mitosis. Reasons for this stricter specificity may lie in the basic difference of sister chromatid orientation in mitosis and meiosis. In mitosis, spindles are bi-oriented whereas in meiosis I they are mono-oriented for segregation of replicated homologous chromosomes instead of sister chromatids (321). Therefore, the interaction surfaces at centromeres change during mitosis *versus* meiosis, suggesting perhaps that different protein networks and complexes are involved in centromere mechanics. In conclusion, requirements for CenH3 structural determinants during meiosis are not fulfilled in the presence of FgCenH3-GFP compared to PaCenH3-GFP in *Neurospora*.

The genus *Podospora* is more closely related to *Neurospora* and hence it is possible that these two genera share similarity in their centromere assembly. We also found that non-tagged PaCenH3 functionally complements NcCenH3, and that

PaCenH3-GFP can be recovered from heterozygous crosses (see Chapter 2). Thus, divergence at the amino acid level in the HFD of PaCenH3 is tolerated during *Neurospora* centromere assembly without any drastic phenotypic defects. These results support the idea that centromere organization and regulation may be highly flexible, dynamic and guided by epigenetic phenomena as seen in plants, animals, flies and fission yeast. The parasite *Plasmodium falciparum* serves as another good example. In this organism the centromeres cluster in a single nuclear location prior to and during mitosis and in cytokinesis but dissociate soon after invasion of the host (119). Hence it is possible that due to this dynamic nature of centromere assembly the perturbation in these systems can last for only short times and not result in obvious phenotypic defects.

We wondered is this may be also true in the presence of PaCenH3-GFP for *Neurospora* centromeres. To observe subtle molecular defects we made use of ChIP-seq, which allows us to precisely map the location of CenH3 and other centromeric proteins, something that is still difficult in many other eukaryotes, including plants and animals. Although the enrichment of PaCenH3-GFP overlapped that of NcCenH3-GFP at most centromeres when comparing NMF324 and NMF 326 to NMF327, we found virtually no PaCenH3-GFP at *CenI* or *CenVI* in NMF324 or NMF326, respectively. Initially we thought that one reason for our observations might be skewed inheritance of preassembled NcCenH3 at these centromeres. The PaCenH3-GFP strains were obtained from a heterozygous cross with wldtype NcCenH3 present. It seemed possible that sufficient NcCenH3 would be maintained for a few mitotic divisions until complete loading of PaCenH3 at centromeres *CenI* and *CenVI* would be accomplished. In support of this reasoning, there are studies that show high

stability and slow turnover of incorporated CenH3 at centromeres (115, 134). After S-phase of mitosis already existing CenH3 gets diluted to one half in sister chromatids but once new CenH3 has been incorporated into centromeric nucleosomes it shows very slow turnover (115, 134). Further, stepwise centromere disintegration studies of human artificial chromosomes (HAC) have shown that CenH3 is the last protein to be removed from centromeres, again suggesting high stability of CenH3 nucleosomes (43). Thus, overall human CenH3 bound to mature centromeres seems fairly stable, Another perhaps less likely scenario, includes the possibility of low enrichment of PaCenH3-GFP caused by specific chromosome architecture where the *CenI* and *CenVI* are comparatively less accessible than other chromosomes while all centromeres are clustered together at the spindle pole body (96, 234).

We tested if the first idea could be true by subjecting the two PaCenH3-GFP strains to continous growth for a month or more. We argued that this would allow for sufficient divisions to dilute out any wildtype NcCenH3 that may have been deposited in the PaCenH3-GFP strains during meiosis. When we tried to quantify growth defects with the AlamarBlue live cell assay we found at best minor differences in cell survival, largely due to the presence of the mutant *his-3* allele rather than different versions of CenH3. We performed ChIP-seq on NcCenH3-GFP and PaCenH3-GFP strains that were passed through longer growth cycles. The following three outcomes were observed in these ChIP data of three replicates for each of the two PaCenH3-GFP strains: (1) Both the START and STOP samples with PaCenH3-GFP showed irreversible loss of PaCenH3 at *CenI* and *Cen VI* in all the replicates of either strains (Figure 3.5). (2) At other centromeres, i.e. *CenIV* and *CenVII* for one of the PaCenH3-GFP strains (NMF324) the START samples showed higher enrichment of PaCenH3-

GFP compared to its STOP replicates, suggesting progressive loss of PaCenH3 from some centromeres. (3) At *CenII*, *CenIII* and *CenV* enrichment levels in both the PaCenH3 strains remained unchanged for STOP and START strains of all replicates. Taken together, these extended growth assay ChIP-seq results report for the first time drastic variability in CenH3 enrichment within *bona fide* centromeres without any substantial growth defects. This was a surprising finding, as one would expect cells without sufficient CenH3 to be nonviable.

We considered several possibilities that would help explain why PaCenH3-GFP strains grow in absence of drastic phenotypes. The loss of PaCenH3, which may also be considered a mutant NcCenH3, is irreversible and progressive in some centromeres whereas others show normal enrichment. One possible reason for loss of PaCenH3-GFP from some centromeres is translocation during or shortly following meiosis. This would allow maintenance of chromosome arms, or whole chromosomes in the case of teomere-telomere fusions, if single centromeres would be rendered nonfunctional. However, this possibility was eliminated because backcrosses between wild type (NMF39 and NMF262) and STOP samples (NMF570 and NMF572) were all fertile; translocations or chromosome fusions would have resulted in less fertile or sterile crosses. We are still investigating the possibility that in such backcrosses PaCenH3-GFP and NcCenH3 can be reacquired at previously CenH3-deficient centromeres.

A second hypothesis to explain survival of cells with reduced PaCenH3-GFP at certain centromeres involved epigenetic features of the neighboring H3 nucleosomes. We had previously shown that *Neurospora* centromeres are truly heterochromatic

(273). To date, *Neurospora* centromeres are the only ones that show exclusive enrichment of H3K9me3 and a complete absence of H3K4me2 in their centromere core. We had also shown that normal CenH3 localization depends on the presence of H3K9me3 and the methyl-binding protein HP1 (273). Based on centromere studies in other organisms it is difficult to predict the pathways that might rely on hetrochromatic histone mark required for regulation of CenH3 at *Neurospora* centromere, although studies with chicken centromeres have shown CenH3 nucleosomes to be interspersed with H3K9me3 nucleosomes and lower amounts of H3K4me2 nucleosomes (232). It has also been suggested that CenH3 assembly and maintenance is not simply based on the balance of heterochromatic or euchromatic marks in the region, but that there may be diverse, as of yet unknown pathways involved (195). Here we showed that neither H3K9me3 nor H3K4me2 distribution, or amounts of the histone marks were drastically altered in PaCenH3-GFP strains. While we have not tested other histone marks, we consider changes in epigenetic profiles at the CenH3-deficient centromeres in NMF324 and NMF326 unlikely. Similarly, we did not observe overproportional enrichment of these marks in the centromeric regions, suggesting that normal H3 nucleosomes do not simply replace CenH3 nucleosomes in the deficient regions.

A third possibility included rapid changes in the underlying centromeric DNA, i.e. a rapid shrinkage or acquisition of nocel sequence. We first analyzed the parent strains involved in the generation of the homokaryotic PaCenH3-GFP strains and found few changes when these strains were compared to the *Neurospora* reference genome. Moreover, few large changes, as evidenced by wholesale deletions or insertions, were observed in NMF234 and NMF236, even though a few shorter regions in

individual centromeres appeared variable. Thus we conclude that the structure of centromeric DNA is not responsible for either the defects in CenH3 localization or in a failure to measure PaCenH3-GFP because different centromeric sequences are present.

The last possibility we considered was aneuploidy in many nuclei. Based on semiquantitative and qPCR analyses we do not believe this to be the case. The differences in PaCenH3-GFP localization are large, i.e. in the centromeric regions were the protein is depleted there may be 1-5% of the normal PaCenH3-GFP present. Such drastic differences, if indeed based on aneuploidy should be easily detectable by regular end-point PCR with 22-24 cycles of amplification on genomic DNA, which we often use to ascertain that ChIP assays have been successful. While the qPCR results are inconclusive, semiquantitative PCR and Southern analyses do not support the idea of wide-spread aneuploidy.

PaCenH3 loss from specific *Neurospora* centromeres may supports the idea of different chromosome conformations, as observed in budding yeast (305) but we observed neither centromere nor chromosome length correlation between defective and normal centromeres in our study. However, it is possible that centromere interactions and chromosome confirmations might indirectly guide the accessibility of different centromeric regions for proper CenH3 loading.

CenH3 is loaded into centromere-specific nucleosomes by the CenH3-specific chaperone Scm3 in fission and budding yeast (39, 190, 278, 325). HJURP in human and Cal1 in flies are Scm3 homologues (79, 84, 89, 182). Over expression studies of Scm3 in budding yeast and in humans have diminished localization of Scm3 at

centromere, which renders chromosome loss, and also shows reduction of CenH3 and H4 at centromere. This conclusion was made based on the results obtained in synchronous growth of cells in yeast and human cells, however synchronously growing Neurospora conidia culture is not still achieved. Each conidium of Neurospora is made up of 3-4 nuclei on an average and they all divide asynchronously, additionally as mentioned above the nuclear division timings in non-germinated conidia are longer than found in germ tube of germinated conidia (4-5 hrs culture) (177, 234).

Further, Scm3 is approximately half the size of HJURP (748 aa), but the N-terminal motif that specifically interacts with CenH3 is evolutionary highly conserved (70, 244). However, Cal1 in Drosophila is a huge protein (979 aa) with conserved N-terminal motif sequences that function to interact with CenH3 (250). Similarly, the Scm3 orthologs from the true Ascomycota are much longer (800-1300 aa) than yeast Scm3. They contain the conserved N-terminal helix that is supposed to mediate association with CenH3 but the rest of the sequences is enriched mostly in DNA binding motifs, such as AT-hooks, which may prove essential for centromere DNA interactions and are absent in budding and fission yeast Scm3. Thus the architecture of filamentous fungi Scm3 based on computationally defined motifs shows similarity with Cal1 that can locally alter DNA and chromatin structure at the centromere (9). Deletion of the putative Scm3 ortholog from Neurospora is lethal (data not shown); however, there is currently not enough experimental data to annotate the actual Scm3 coding sequence, as it is very poorly expressed. Very low amount of these proteins are required to perform their function (189, 250). Hence it is difficult to predict

whether the loading of PaCenH3 at Neurospora centromere is improper due to defective Scm3 interactions or functioning.

The inner kinetochore proteins directly interact with CenH3 nucleosomes. Studies have determined the stepwise assembly and maturation in human centromeres with the CCAN (Constitutively Centromere associated Network) complexes (85). Two important components in this CCAN complex are CENP-T and CENP-C, which are considered to be scaffolding protein showing multiple interactions with other inner kinetochore proteins (216). Further, the CENP-T has potential of forming non-histone nucleosome *in-vitro* (200). If this kind of non-histone nucleosome actually exists at centromere then indirect distortion of H3 nucleosome array at the centromere may be caused in presence of improper formation of CenH3 nucleosomes in presence PaCenH3 or FgCenH3 based on their sequence differences. The ChIP-seq data for CENP-T-GFP pull down in strains having non-tagged PaCenH3, FgCenH3 and NcCenH3 showed loss of nucleosome phasing effect (data not shown), suggesting either changes in the nucleosome positioning, nucleosome content or chromatin structure. Moreover, the studies in Drosophila have shown that C-terminal of Cal1 shows binding to CENP-C and thus helps in bridging the interaction between CenH3 and CENP-C (250). Hence comparing the wild type localization pattern for these inner kinetochore proteins (CENP-C and CENP-T) with the strains having PaCenH3 and FgCenH3 would help us determine the effects for the loss of CenH3 from centromere based on structural determinants.

Finally, the centromere nucleosome structure is similar to histone H3 nucleosome (286). The CenH3 is incorporated at centromere by replacement of histone H3 in a

cell cycle dependent manner. On the other hand during centromere inactivation process there is enrichment of the H3K9me3 histone mark in the central core because of replacement of CenH3 with histone H3 (20). Thus these replacement tendencies of histone H3 with CenH3 and vice versa is common feature, hence it is possible that the observed defect in presence of PaCenH3 might be due to changes in the centromere nucleosome content i.e. there is enrichment of hetrotypic dimers in nucleosomes made up of histone H3 and CenH3 instead of homodimers. Our CoIP data for NcCenH3 suggest presence of homotypic dimers at Neurospora centromeres (data not shown) so whether this observation is matched in presence of PaCenH3 is yet to be determined and we are currently trying to address this question.

Table 3.1: Strains used in this study.
Transformed heterokaryotic strains are denoted by square brackets. Fungal Genetics Stock Center (FGSC).

Strains	Genotypes	Reference or Source
NMF39	*mat A; 74-OR23-1VA*	FGSC2489
N3011	*mat a his-3; mus-51::bar*$^+$	FGSC9538
NMF162	*mat A ΔSad-1 (partial deletion)*	Chapter 2
NMF262	*mat a; 74-OR23-1VA*	Chapter 2
NMF324	*mat a; his-3; ΔNcCenH3::PaCenH3-gfp*$^+$*-hph*$^+$	Chapter 2
NMF326	*mat A; ΔNcCenH3::PaCenH3-gfp*$^+$*-hph*$^+$*; Δmus-51:: bar*$^+$	Chapter 2
NMF327	*mat A; ΔNcCenH3::NcCenH3-gfp*$^+$*-hph*$^+$*; Δmus-51:: bar*$^+$	Chapter 2
NMF562, NMF563	*[mat a; his-3; ΔNcCenH3::NNcCFg-gfp*$^+$*-hph*$^+$*; Δmus-51:: bar*$^+$ *+ mat a; his-3; NcCenH3; Δmus-51:: bar*$^+$*]*	This study
NMF564	*[mat a; his-3; ΔNcCenH3::NPaCFg-gfp*$^+$*-hph*$^+$*; Δmus-51:: bar*$^+$ *+ mat a; his-3; NcCenH3; Δmus-51:: bar*$^+$*]*	This study
NMF565	*[mat a; his-3; ΔNcCenH3::NFgCPa-gfp*$^+$*-hph*$^+$*; Δmus-51:: bar*$^+$ *+ mat a; his-3; NcCenH3; Δmus-51:: bar*$^+$*]*	This study
NMF566	*ΔNcCenH3:: NFgCPa-gfp*$^+$*-hph*$^+$	This study
NMF567	*ΔNcCenH3:: NFgCPa-gfp*$^+$*-hph*$^+$	This study
NMF568	*NcCenH3; mat A*	This study
NMF569	*mat a; his-3; ΔNcCenH3::PaCenH3-gfp*$^+$*-hph*$^+$ (START 1)	This study
NMF570	*mat a; his-3; ΔNcCenH3::PaCenH3-gfp*$^+$*-hph*$^+$ (STOP 1)	This study
NMF571	*mat A; ΔNcCenH3::PaCenH3-gfp*$^+$*-hph*$^+$ (START 1)	This study
NMF572	*mat A; ΔNcCenH3::PaCenH3-gfp*$^+$*-hph*$^+$ (STOP 1)	This study
NMF573	*mat A ΔNcCenH3::NcCenH3-gfp*$^+$*-hph*$^+$ (START 1)	This study
NMF574	*mat A; ΔNcCenH3::NcCenH3-gfp*$^+$*-hph*$^+$ (STOP 1)	This study
NMF575	*mat a; his-3; ΔNcCenH3::PaCenH3-gfp*$^+$*-hph*$^+$ (START 2)	This study
NMF576	*mat a; his-3; ΔNcCenH3::PaCenH3-gfp*$^+$*-hph*$^+$ (STOP 2)	This study
NMF577	*mat A; ΔNcCenH3::PaCenH3-gfp*$^+$*-hph*$^+$ (START 2)	This study
NMF578	*mat A; ΔNcCenH3::PaCenH3-gfp*$^+$*-hph*$^+$ (STOP 2)	This study
NMF579	*mat a; his-3; ΔNcCenH3::PaCenH3-gfp*$^+$*-hph*$^+$ (START 3)	This study
NMF580	*mat a; his-3; ΔNcCenH3::PaCenH3-gfp*$^+$*-hph*$^+$ (STOP 3)	This study
NMF581	*mat A; ΔNcCenH3::PaCenH3-gfp*$^+$*-hph*$^+$ (START 3)	This study
NMF582	*mat A; ΔNcCenH3::PaCenH3-gfp*$^+$*-hph*$^+$ (STOP 3)	This study
NMF583	*mat A; NcCenH3* (STOP 1)	This study
NMF584	*mat A; 74-OR23-1VA* (STOP 1)	This study

Table 3.2: Oligos used for the PCR amplification of genes for chimera cloning and qPCR.
Primer sequences reported here are from 5' to 3' direction.

Number	Name	Sequence (5' -> 3')
162	FgCenH3GlyR	CCTCCGCCTCCGCCTCCGCCGCCTCCGCCACCCAATCCACCCCACATACCGCG
180	NcCenH3GlyF	GATGAATGACTAGATGCCGCGGTG
1085	TEL_lLF	CTTCTTGCGTCTTGCCTGCTC
1086	TEL_lLR	CCTTTTCGTTCGGTTGACAGC
1447	PaCenH3GlyR	CCTCCGCCTCCGCCTCCGCCGCCTCCGCCCACCCACCCCGCCCCGCCCCAAAC
1758	NdeI_FgCenH3	ATCATATGCCTCCCGCCAAGAAATCCAGA
1759	BamF_C_FgCenH3	CTGGGGATCCTGTACCCGTTCGCGCAAAGCGTCGCTATC
1760	BamF_N_FgCenH3	GATAGCGACGCTTTGCGCGAACGGGTACAGGATCCCCAG
1846	NBamR_NcCenH3	ACGGGATCCCCGGCTGAATTTGTCAAT
1848	NBamR_PaCenH3	ACTGGATCCCCTGCTTTAGGGGGTTTAGT
1849	CBamF_PaCenH3	CAGGGGATCCAGTCCCCCAAGGCCGCAA
2033	NCU01998_R	TTCGACAACTTTGACGAGGA
2037	NCU01728_R	GTTGGGGAGATGAGAAGCAG
2057	NCU01998_F	CAGCTCCTACCTGCTTCGAG
2060	NCU01728_F	ACATCTTCCCGACAGACCAG
2063	G2cyc_i2F	GAGCATCAAACGGAGGAAGA
2064	G2cyc_i2R	GGGAGAAGACTGAAGCGATG
2661	cen1rf	AGCGGTAAGGCTAGTTGTTTGCC
2662	cen1rr	TTGCCAGGGACCCCTCGAGG
2681	cen5lf	TCGGCGACCGTTTACGATGC
2682	cen5lr	CTAGAGCCCGCGTGCAAGCT
2683	cen5cf	CAATGTGCGACGAGGGCGCT
2684	cen5cr	CGGCGACCGCTGGCAGAATC
2685	cen5rf	TCGCGAGCGTTACTGCACCC
2686	cen5rr	GTTCCCCACCGGAGCGTGTC

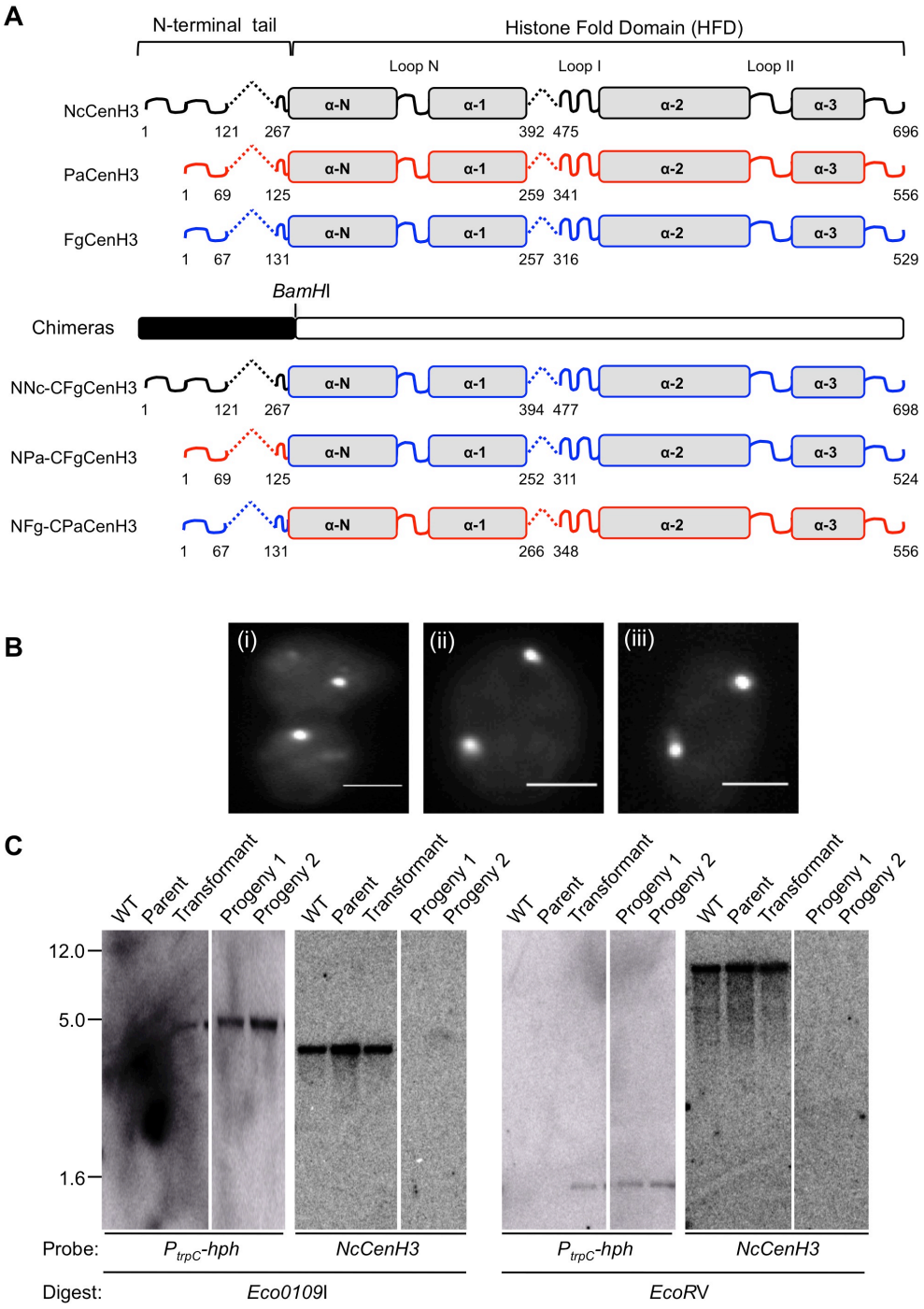
A
N-terminal tail
Histone Fold Domain (HFD)
Loop N
Loop I
Loop II
NcCenH3
PaCenH3
FgCenH3
α-N
α-1
α-2
α-3
1
121
267
392
475
696
69
125
259
341
556
67
131
257
316
529
BamHI
Chimeras
NNc-CFgCenH3
NPa-CFgCenH3
NFg-CPaCenH3
394
477
698
252
311
524
266
348
B
(i)
(ii)
(iii)
C
WT
Parent
Transformant
Progeny 1
Progeny 2
12.0
5.0
1.6
Probe:
PtrpC-hph
NcCenH3
Digest:
Eco0109I
EcoRV

Figure 3.1: General structure of four different fungal CenH3 genes and proteins and chimeric constructs generated for this study.

(**A) Schematic representation of secondary structure of NcCenH3, PaCenH3 and FgCenH3.** Boxes are the helices the solid lines are coiled regions and stippled lines are introns. The numbers represent the base pairs of CenH3 genes and the colors show different fungal CenH3 (black represents NcCenH3, red is PaCenH3, blue is FgCenH3). The different chimeras were constructed by introducing BamHI site where black bars represent the N-terminal tail domain swapped during construction of chimeras. The different chimeras with secondary structure along intron position are shown. **(B) Chimeric CeH3-GFP constructs are targeted to centromeric chromocenters.** The epi-fluorescence data for the NNcCFg (i), NPaCFg (ii) and NFgCPa (iii) strains NMF562, NMF564 and NMF566 respectively. NFgCPa is the homozygous strain whereas, NNcCFg and NPaCFg are hetrokaryotic transformants. **(C) The NFgCPaCenH3-GFP gene was integrated into the *Neurospora* genomes as expected.** The NFgCPaCenH3-GFP gene is shown as an example. Southern analyses of genomic DNA digested with *Eco0109*I and *EcoRV* probed with *hph* and *NcCenH3* gene fragments revealed correct integration as the expected 4.2 kb and 1.2 kb fragments were found. Strains are as follows: WT (NMF39, wild type); Parent (NMF162); Transformant with the NFgCPaCenH3-GFP chimera (NMF565); Progeny 1 and 2, two independent Hyg^{+} progeny obtained after a cross to NMF162 (NMF566, NMF567).

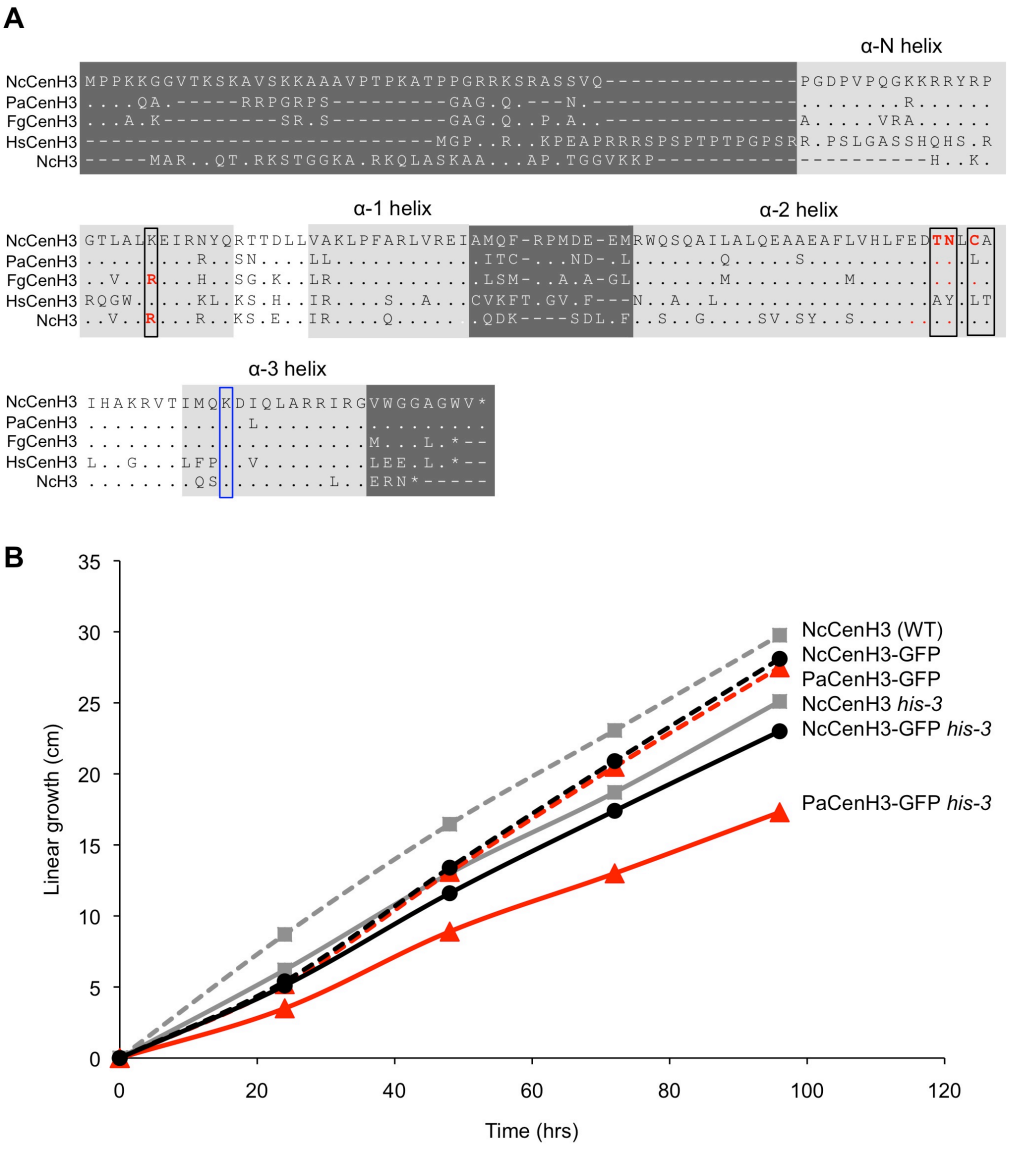
A
α-N helix
NcCenH3 MPPKKGGVTKSKAVSKKAAAVPTPKATPPGRRKSRASSVQ----------PGDPVPQGKKRRYRP
PaCenH3 ....QA.-----RRPGRPS---------GAG.Q.---N.----------.....R.....
FgCenH3 ...A.K---------SR.S---------GAG.Q..P.A..----------A.....VRA.....
HsCenH3 -------------------------MGP..R..KPEAPRRRSPSPTPTPGPSRR.PSLGASSHQHS.R
NcH3 -----MAR..QT.RKSTGGKA.RKQLASKAA...AP.TGGVKKP----------H..K.
α-1 helix
α-2 helix
NcCenH3 GTLALKEIRNYQRTTDLLVAKLPFARLVREIAMQF-RPMDE-EMRWQSQAILALQEAAEAFLVHLFEDTNLCA
PaCenH3 .....R..SN....LL.....ITC-...ND-.L.....Q.....S.....L.
FgCenH3 ..V..R...H..SG.K..LR.....LSM-..A.A-GL.....M.....M.....
HsCenH3 RQGW...KL.KS.H..IR....S..A...CVKFT.GV.F---N..A..L.....AY.LT
NcH3 ..V..R...R..KS.E..IR....Q.....QDK----SDL.F..S..G....SV.SY..S.....
α-3 helix
NcCenH3 IHAKRVTIMQKDIQLARRIRGVWGGAGWV*
PaCenH3 .....L.....
FgCenH3 .....M...L.*--
HsCenH3 L..G...LFP..V.....LEE.L.*--
NcH3 .....QS..L..ERN*-----
B
Linear growth (cm)
Time (hrs)
0
5
10
15
20
25
30
35
0
20
40
60
80
100
120
NcCenH3 (WT)
NcCenH3-GFP
PaCenH3-GFP
NcCenH3 his-3
NcCenH3-GFP his-3
PaCenH3-GFP his-3

Figure 3.2: Sequence alignments of several CenH3 proteins and results of linear growth assays with PaCenH3 strains.

(A) Sequence alignment of CenH3 and H3 proteins. Regions exposed to surface of centromeric nucleosome are highlighted in dark gray boxes, indicating the N-terminus, loop I and the C-terminal tail. CenH3 from several species are shown: *N. crassa* (NcCenH3), *P. anserina* (PaCenH3), *F. graminearum* (FgCenH3), and *Homo sapiens* (HsCenH3, human CenH3 is also called CENP-A) and compared to *Neurospora* canonical histone H3 (NcH3). The four α-helices that are part of the HFD domain are represented as light gray boxes. In the sequence alignment, periods signify residues identical to the *Neurospora* sequence, whereas hyphens signify absence of residues. Black boxes represent important residues determining centromeric nucleosome structure in humans (Panchenko *et al* PNAS; 2011 and Sekulic *et. al.* NATURE; 2010, NISHIKI, 2011 CELL). The residue highlighted in red show differences in residues between H3 and CenH3. The lysine residue in the blue box has been shown to be acetylated in human CenH3 (Bui *et al* Cell; 2012). This residue is conserved in all the fungal CenH3's. **(B) Linear growth assays with PaCenH3-GFP strains.** Linear growth of a wild type (NMF39) and transformation host strain (NMF3011; *his-3*) was compared to that of NcCenH3-GFP (NMF327), NcCenH3-GFP *his-3* (NMF169), PaCenH3-GFP (NMF326) and PaCenH3-GFP *his-3* (NM324) strains. Note that presence of the mutant *his-3* allele reduced linear growth in all strains, even on supplemented medium.

CenI

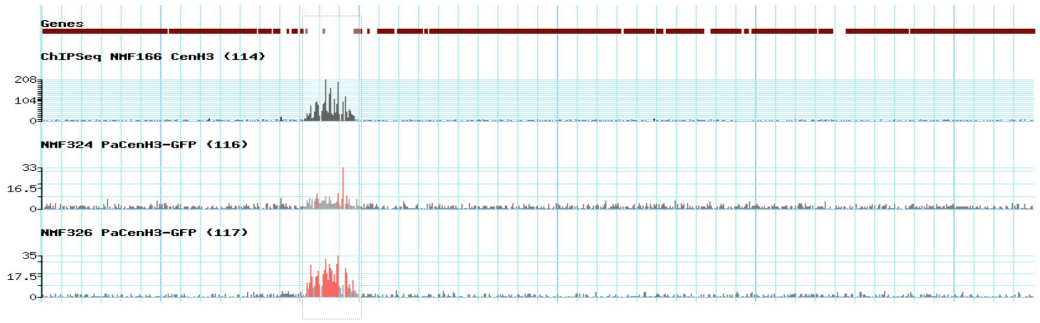

CenII

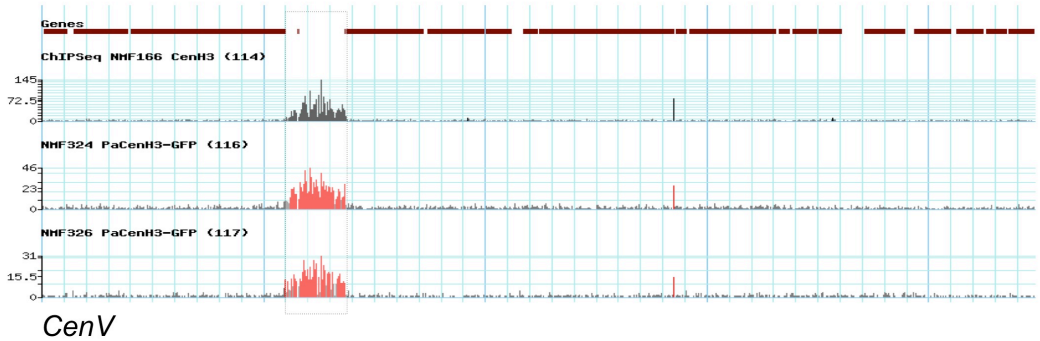

CenV

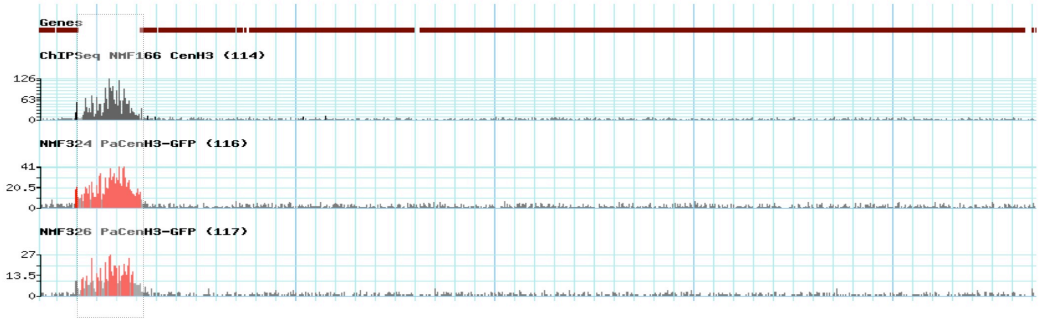

CenVI

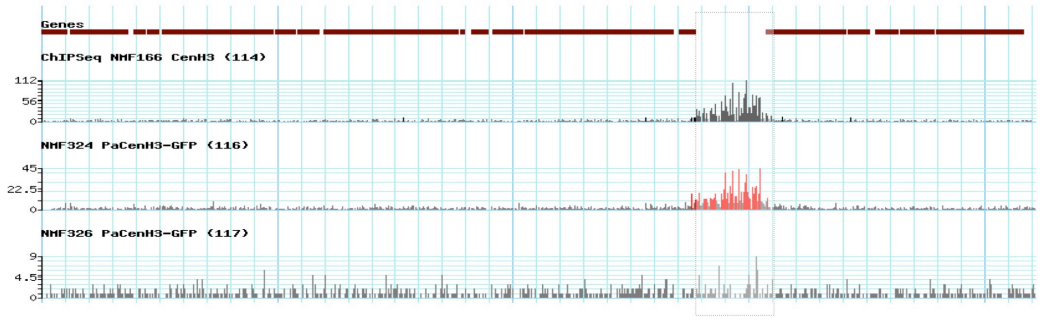

Figure 3.3: Enrichment of PaCenH3-GFP at *Neurospora* centromeres.

PaCenH3-GFP and NcCenH3-GFP strains were subjected to ChIP-seq to determine precise CenH3 location and levels in the cell. Strains were grown for approximately 6 hrs before harvest. The maroon boxes represent genes on linkage groups I, II, V and VI near the centromeric region (the x-axis shows 5Mb regions on the respective chromosomes) near the centromere. The y-axis gives the enrichment as reads bp after mapping all reads obtained by ChIP-seq with BWA (163). The stippled boxes shows almost perfectly overlapping enrichment of NcCenH3 and PaCenH3 in gene-deficient regions that had been previously identified as centromeric (273). Color of the CenH3 peaks represents mapping scores, i.e. >10 reads/bp are indicated in black for NcCenH3 (NMF166) and in red for PaCenH3 (NMF324, NMF326), while scores <10 reads/bp are represented by gray. Tracks in the dedicated gbrowse ChIP-seq browser are labeled by protein precipitated, strain number, and unique lab highthroughput sequencing ID number for ChIP-seq runs. Here, *CenII* and *CenV* centromeres show normal maintenance of PaCenH3-GFP when compared to NcCenH3-GFP enrichment, while enrichment at *CenI* was decreased in NMF324 compared to NMF326, whereas the sitution is reversed for *CenVI*.

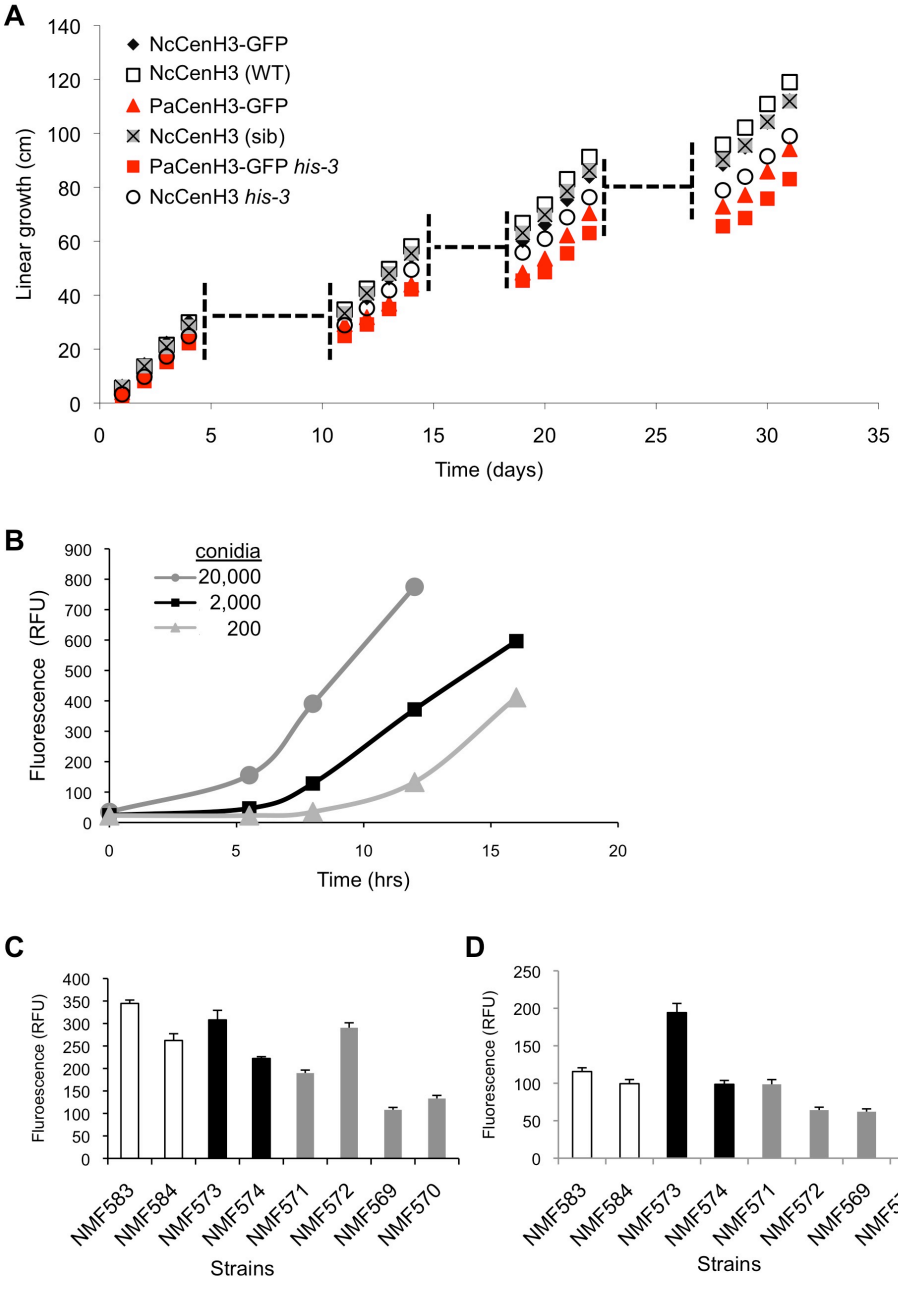
A
Linear growth (cm)
Time (days)
NcCenH3-GFP
NcCenH3 (WT)
PaCenH3-GFP
NcCenH3 (sib)
PaCenH3-GFP his-3
NcCenH3 his-3
B
Fluorescence (RFU)
Time (hrs)
conidia
20,000
2,000
200
C
Fluroescence (RFU)
Strains
NMF583
NMF584
NMF573
NMF574
NMF571
NMF572
NMF569
NMF570
D
Fluorescence (RFU)
Strains

Figure 3.4: Slight growth defects occur in strains with PaCenH3.

(A) Long-term linear growth assay thorugh serial Ryan (or "race") tubes. Two wildtype CenH3 strains (NMF39, NMF568), a *his-3* CenH3 strain (N3011), NcCenH3-GFP (NMF327) and PaCenH3-GFP (NMF326), NcCenH3-GFP *his-3* (NMF169) and PaCenH3-GFP *his-3* (NMF324) strains were grown through four race tubes and linear growth (in cm) recorded at regular intervals. The gaps with the stippled lines indicate the conidiation period, after which inoculum was used to inoculate a new race tube. **(B) Standardization of incubation times for AlamarBlue live cell assay.** We used three different dilutions of conidia from a wild type CenH3 strain (NMF584) to optimize the incubation time (in hours). We fund that carrying out the assay between 8-12 hrs gave the most reproducible results in this assay. **(C) AlamarBlue assay with 20,000 conidia in single reactions.** Each measurement of relative fluorescence units (RFU) represents the average of five replicates. Strains used: PaCenH3-GFP *his-3* (grey; NMF569, NMF570) PaCenH3-GFP (grey; NMF571 and NMF572); NcCenH3-GFP (black; NMF573, NMF574); wild type siblings (white; NMF583 and NMF584) were used as control strains. **(D) AlamarBlue assay with 2,000 conidia in single reactions.** The same strains as in C were used. ***Note*:** The graph in (A) shows only four race tube readings because of experimental error in the fifth run for two replicates. This last run was thus not included in the graph.

CenII

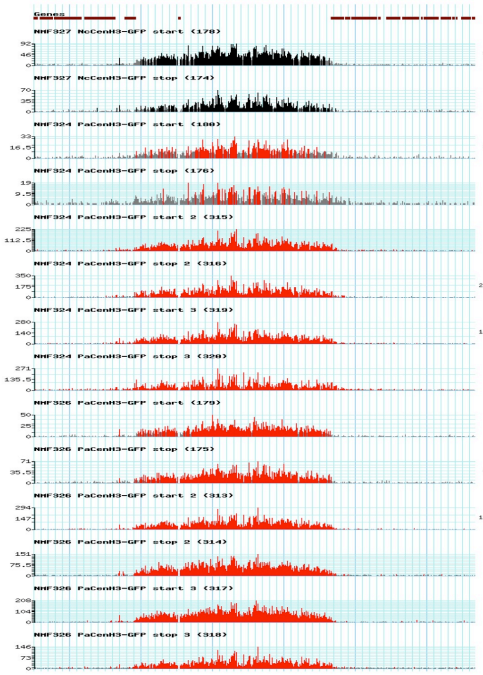

CenV

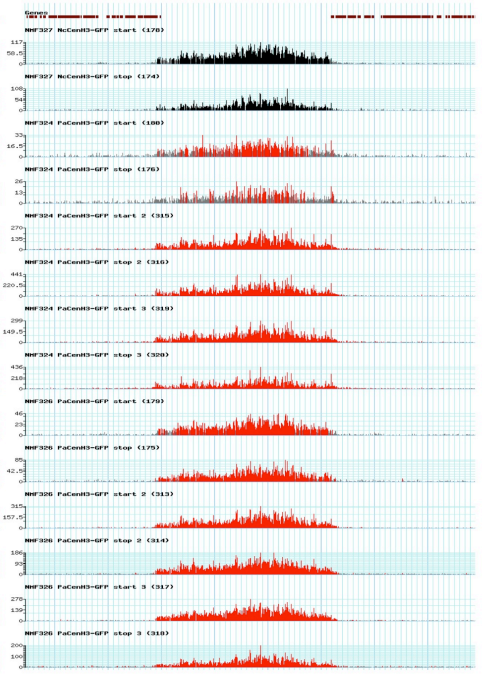

CenI

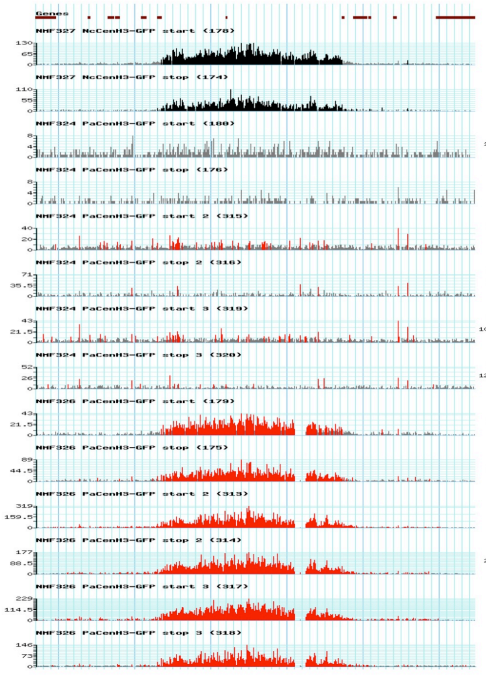

CenVI

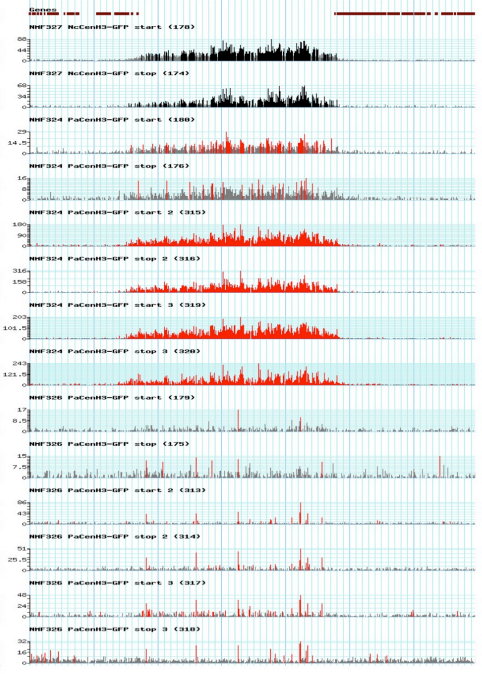

Figure 3.5: Irreversible loss of PaCenH3-GFP enrichment at certain centromeres after extended vegetative growth.

Maroon boxes represent the genes on Linkage Groups (LG) I, II, V and VI near the centromeric region (x-axis, chromosome zoomed into 1Mb region near the centromere. The y-axis shows enrichment as reads/bp. The black highlighted histogram shows derivatives of the NcCenH3-GFP strain (NMF327) after extended linear growth as START,(NMF573) and STOP (NMF574) strains. The red highlighted regions are for two PacenH3-GFP (NMF324 and NMF326) strains with three biological replicates of each, where START samples for NMF324 are NMF569, NMF575, NMF579, and NMF571, NMF577, NMF581, respectively. The STOP samples for NMF324 are NMF570, NMF576, NMF580 and those for NMF326 are NMF572, NMF578, NMF582. *CenII* and *CenV* have normally assembled centromeres in the presence of PacenH3-GFP because the enrichment is comparable to that of NcCenH3-GFP (NMF573 and NMF574). There is irreversible loss of PaCenH3-GFP enrichment at *CenI* for NMF324-derived strains (NMF575, NMF576, NMF579 and NMF580) whereas the NMF326-derived strains are normal. This permanent loss of enrichment is also observed at centromere *CenVI* for NMF326-derived strains (NMF571, NMF572, NMF577, NMF578, NMF581 and NMF582) while the NMF324-derived strains were normal. The localization pattern is diminished for NMF569 and NMF570, perhaps because of slightly poorer growth.

CenIV *CenVII*

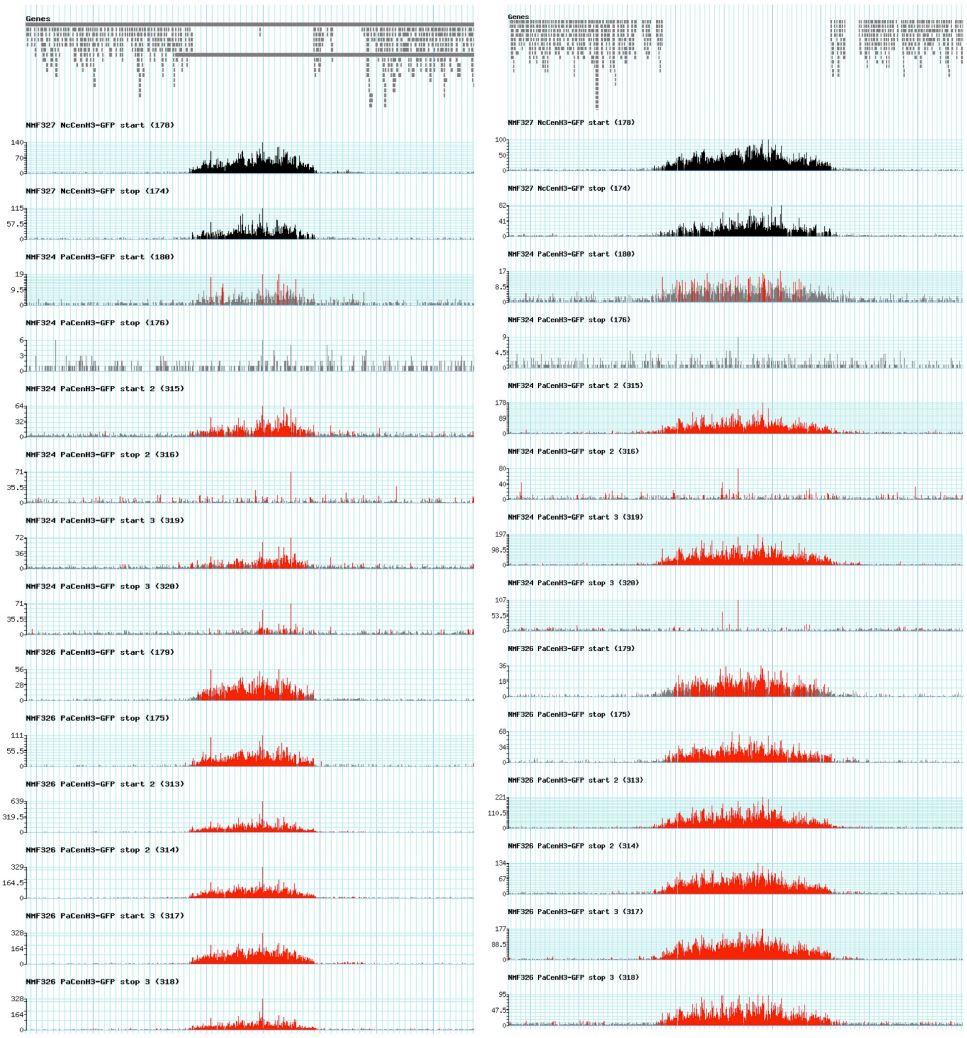

Figure 3.6: Progressive loss of PacenH3-GFP enrichment at some centromeres after extended linear growth.

The gray boxes represent reads from RNA-seq data mapped to LG IV and VII near the centromeric regions. The y-axis gives the score for the reads/bp enrichment. As shown the enrichment pattern for the NMF324-derived START strains (NMF569, NMF575 and NMF579) shows some enrichment in contrast to the STOP strains (NMF570, NMF576, NMF580). All NMF326-derived strains (NMF571, NMF572, NMF577, NMF578, NMF581 and NMF582) show comparable enrichment pattern as the NcCenH3-GFP; black START (NMF573) and STOP (NMF574) samples. The localization pattern is diminished for NMF569 and NMF570, perhaps because of slightly poorer growth.

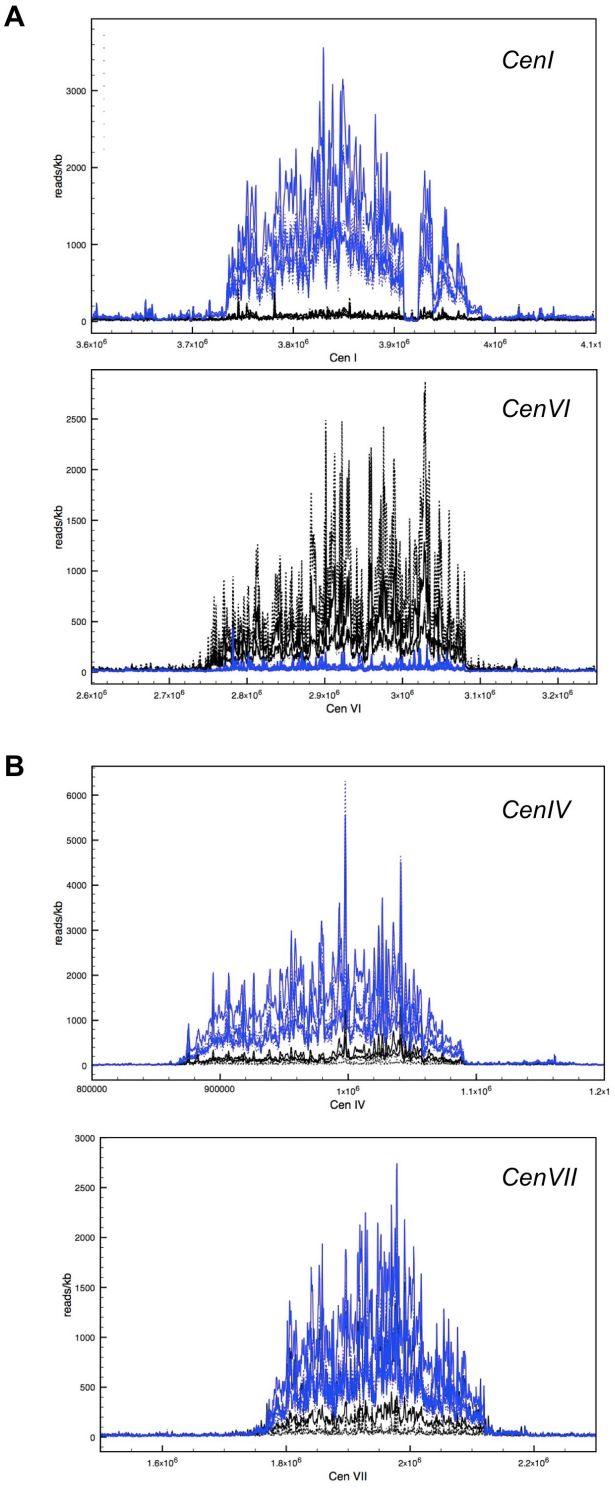
A
CenI
reads/kb
Cen I
CenVI
reads/kb
Cen VI
B
CenIV
reads/kb
Cen IV
CenVII
reads/kb
Cen VII

Figure 3.7: Enrichment of PacenH3-GFP at certain centromeres after extended linear growth.

Enrichment for the different strains is shown here as reads/kb to emphasize differences between the strains. All strains derived from NMF324 are shown in black (NMF569, NMF575, NMF579, NMF570, NMF576, NMF580) and all strains derived from NMF326 are shown in blue (NMF571, NMF572, NMF577, NMF578, NMF581 and NMF582). **(A) Initial defects at *CenI* or *CenVI* are maintained in the NMF324- or NMF326-derived strains.** Enrichment obtained with original strains was so low that no further reduction was observed, i.e. all black lines (top panel) or blue lines (bottom panel) fall on top of each other, while there are some differences in the control strains obtained from the other strain that did not show lack of enrichment. **(B) Enrichment defects are irreversible and progressive.** Enrichment at *CenIV* or *CenVII* in NMF3240-derived strains continued to be reduced after long-term growth. START strains are shown in black and STOP strains in grey; note how enrichment in STOP strains is lower at both centromeres in STOP strains.

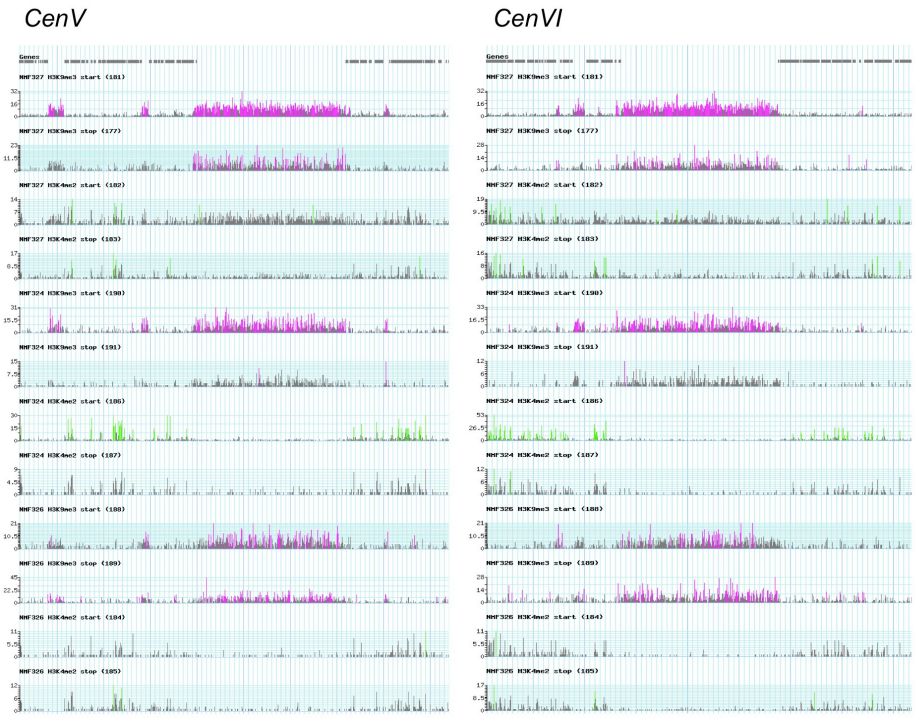

Figure 3.8: Epigenetic states of Neurospora centromeres in presence of PaCenH3-GFP.

The x-axis represents chromosome location and the y-axis shows reads /bp over a region of 1Mb near the centromere. The gray boxes represent the genes adjacent to centromere regions of LG V and VI. The centromeric region corresponds to the gene-deficient region. These ChIP-seq data are for H3K9me3 (pink) and H3K4me2 (green) for the START and STOP samples of only the first replicate strains. The top two panels are for NcCenH3-GFP START (NMF573) and STOP (NMF574), where the pink lines represent read scores >10 and the gray lines reads/bp <10. H3K4me2 panels in green and gray are for the same strains. There is overall enrichment of H3K9me3 at centromeres and in neighboring gene-deficient heterochromatic regions, but deficiency of H3K4me2. These patterns were conserved for four PaCenH3-GFP strains (fifth and sixth panel, START NMF569 and STOP NMF570 strains, H3K9me3 (pink) and H3K4me2 (green); ninth and tenth panel, START NMF571 and STOP NMF572 strains, H3K9me3 (pink) and H3K4me2 (green).

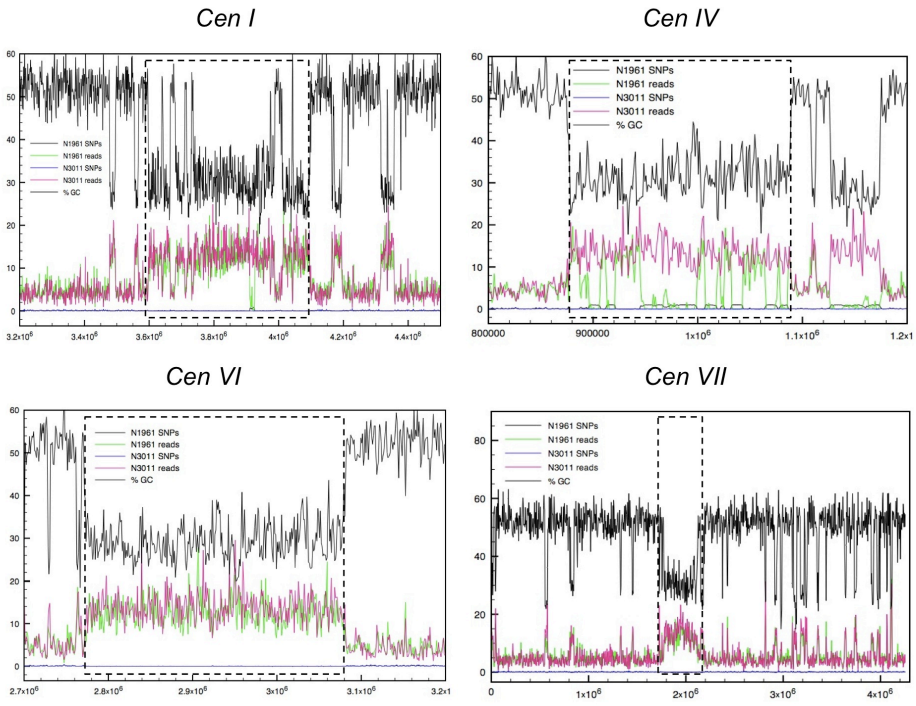

Figure 3.9: SNP coverage map for defective centromeres.

The genomes from the host strain (N3011, *mat a his-3*) into which the PaCenH3-GFP construct was transformed, and a strain used for backcrosses, N1961 (NMF162, *mat A Sad-1*), were sequenced to examine variability of centromeric DNA. Shown are the tracks for LG I, IV, VI and VII, in which low enrichment of PaCenH3-GFP had been discovered in ChIP-seq data. The black graph on the top depicts GC content (%GC), which drops significantly at the AT-rich centromeres, shown enclosed in stippled boxes. The green and pink graphs correspond to the total reads obtained by Illumina sequencing for N1961 and N3011, respectively. The black and blue lines close to the x-axis represent the SNP ratios for N3011 and N1961. For all centromeres there is hardly any deviation observed accept for small regions at *CenIV*, suggesting no large scale variability between centromeric DNAs of these strains. The x-axis shows the centromere locus at different resolution, i.e. for *CenI* at 0.2 Mb, *CenIV* and *CenVI* at 0.1 Mb, whereas *CenVII* is shown at 1 Mb.

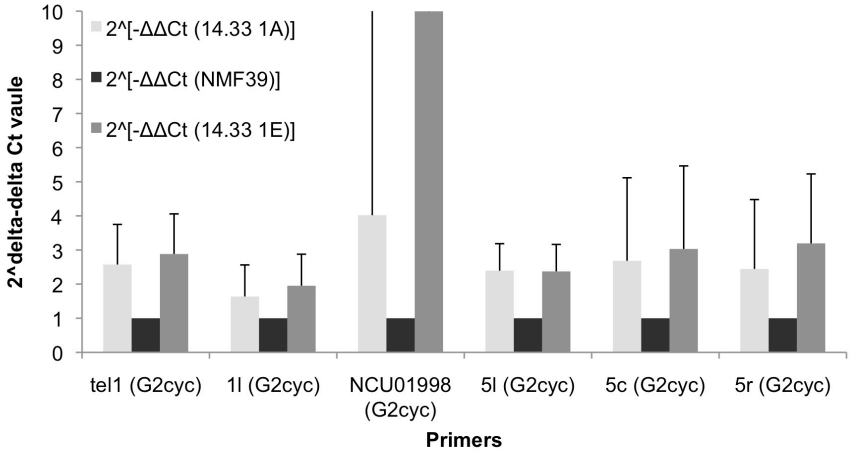
2^[-ΔΔCt (14.33 1A)]
2^[-ΔΔCt (NMF39)]
2^[-ΔΔCt (14.33 1E)]
2^delta-delta Ct vaule
10
9
8
7
6
5
4
3
2
1
0
tel1 (G2cyc)
1l (G2cyc)
NCU01998 (G2cyc)
5l (G2cyc)
5c (G2cyc)
5r (G2cyc)
Primers

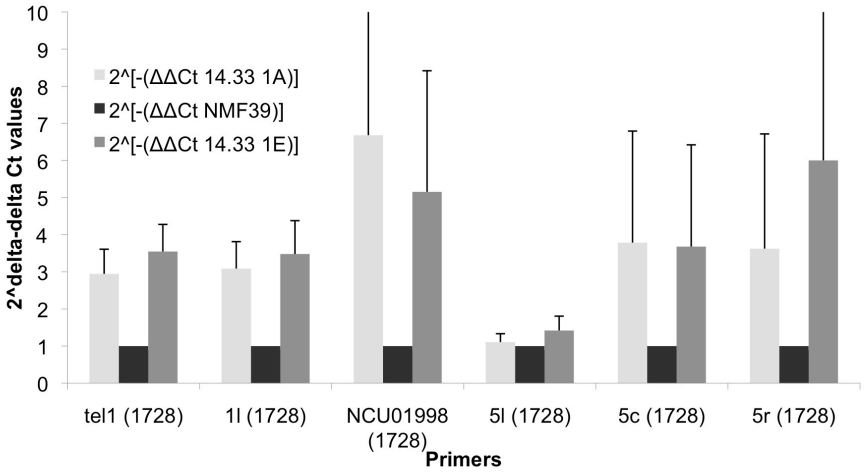
2^[-(ΔΔCt 14.33 1A)]
2^[-(ΔΔCt NMF39)]
2^[-(ΔΔCt 14.33 1E)]
2^delta-delta Ct values
10
9
8
7
6
5
4
3
2
1
0
tel1 (1728)
1l (1728)
NCU01998 (1728)
5l (1728)
5c (1728)
5r (1728)
Primers

Figure 3.10: qPCR data to test aneuploidy centromere defective strains.

The genomic DNA of one of the PaCenH3-GFP START (NMF569) and STOP (NMF570) with drastic differences in PaCenH3-GFP enrichment were used. The data shown here are for *CenI* where ChIP data showed irreversible CenH3 loss in both strains. The standard deviation for three replicate qPCR readings is represented as error bar. The x-axis shows names of primer pairs used for amplification: left arm telomere I (tel1), left side *CenI* (1l) and right arm NCU01998 of LG I, which were compared to a set of *CenV* primers (left side, 5l; center, 5c; right side, 5r) where ChIP-seq data showed normal enrichment of PaCenH3-GFP. Two sets of internal control primers were used, “G2cyc” and “1728” (shown in brackets).

In vivo studies on the composition of centromeric nucleosomes in *Neurospora crassa*

Pallavi A. Phatale

Abstract

Two highly divergent regions in centromere-specific histone H3 (CenH3) are the N-terminus and loop I, and it has been shown that they assign uniqueness to the nucleosome structure at centromeres. In contrast, the canonical histone H3 is ubiquitously found, even alternating with CenH3 nucleosomes in centromeric regions, and H3 shows strong negative selection in structure as well as amino acid composition. In humans, CenH3 nucleosomes are supposed to occur as octamers, composed of dimers of CenH3, histone H4, H2A and H2B. In budding yeast, however, the presence of this octameric CenH3 nucleosome is debated as recent studies support the existence of non-histone protein Scm3 in the CenH3 nucleosome. Furthermore, a histone H2A variant, H2AZ, is supposedly localized in human and fission yeast centromeres; however, whether H2AZ is associated with CenH3 is not yet determined in any organism. Finally recent studies showed that centromeric nucleosomes may exist as tetramers in budding yeast, Drosophila and human. Based on these, mostly *in vitro*, studies on CenH3 nucleosome composition and H2AZ localization at centromere we attempted to analyze the composition of CenH3 nuceleosome in *Neurospora in vivo*. Our biochemical analyses suggest that NcCenH3 (*N. crassa* CenH3) exists as a CenH3 dimer. Secondly, C-terminally GFP-tagged Neurospora H2AZ fails to localize to centromeres, which excludes the option of interactions between CenH3 and H2AZ. However, further investigation is necessary to confirm these results to help determine the uniqueness and similarities in nucleosome content of NcCenH3 when compared to yeast and human CenH3 nucleosomes.

Introduction

Dimers of the human core histone proteins CenH3, H4, H2A and H2B can be assembled *in vitro* into what should be centromere-specific nucleosome octamers, and their crystal structure has been solved (286). Previously, tetrameric CenH3/H4 particles had been generated to solve their crystal structure (258). The exact composition of the centromere-specific nucleosomes containing CenH3 in *S. cerevisiae*, however, remains unresolved. Reports from several labs suggested that CenH3 (Cse4 in *S. cerevisiae*) containing octamers are similar in composition to human CenH3 nucleosomes (70, 334), whereas another study showed that CenH3-containing nucleosomes include the non-histone protein Scm3, which interacts with its N-terminal motif with CenH3 and gets deposited at the centromere (190, 328). The HJURP protein in *H. sapiens* is analogous to Scm3 in *S. cerevisiae.* HJURP also interacts with CenH3 protein via the N-terminal region, however, HJURP is not considered part of the human CenH3 nucleosomes. The results of these studies were largely inferred from *in vitro* assays with reconstituted protein complexes. The *in vivo* conformation of homodimeric octamers of CenH3 nucleosomes was recently confirmed in both humans and budding yeast (32, 271). Surprisingly, these studies also revealed that at certain times during the cell cycle centromeric nucelosomes exist as tetramers, rather than as octamers, something that had been suggested earlier based on studies with centromeric nucleosomes from flies (62, 72).

We generated tagged Neurospora strains with two different types of CenH3 (NcCenH3) proteins, one copy with an N-terminal GFP gene fused in frame to the CenH3 gene integrated at an ectopic locus, *his-3*, and another copy with an N-terminal mCherry gene fused in frame to the CenH3 gene integrated at its

endogenous locus. Another set of NcCenH3 double-tagged strains with a FLAG tag and HA tag was constructed for co-immunoprecipitation assays (co-IPs) to examine whether NcCenH3 nucleosomes contain homotypic or heterotypic dimmers of CenH3 and H3 (Figure 4.1).

Apart from the presence of CenH3, we were interested in determining if there exists any other histone variant in centromere-specific nucleosomes in *N. crassa.* We focused our studies on H2AZ, a variant of histone H2A that is generally found in actively transcribed regions of the genome and counteracts gene silencing, at least in budding yeast (185, 229). Moreover, H2AZ protein has been shown previously to localize in centromeres in a number of organisms, such as *S. cerevisiae*, *S. pombe* and *H. sapiens* (124, 151, 225). These studies showed that H2AZ at the centromere is essential for contributing unique structural specificities and is also necessary for proper chromosome segregation. Therefore, we became interested in three main questions, namely, if (1) H2AZ is localized at the centromeres in *N. crassa*, if (2) H2AZ is a member of the canonical histone H3 nucleosomes that are enriched with H3K9me3, a silencing mark, and if (3) there may be CenH3/H2A occupancy in centromeric nucleosomes. We addressed these questions by co-immunoprecipitated and ChIP-seq assays in non-synchronized *N. crassa* cultures to begin to determine the precise structure and composition of *N. crassa* centromeric nucleosomes.

Materials and Methods

Cloning and strain construction

The NcCenH3 gene along with the 3'UTR was amplified from N3011 (Table 4.1) using OMF1563 and OMF2019 (Table 4.2) and cloned using intp pCR4 with a TOPO

blunt-end cloning kit (Invitrogen) to generate pPP84.7 (see maps in Figure 4.2). The CenH3 fragment was cloned into pPP77.7 to generate GFP-NcCenH3-3'UTR in pBSKII(-), yielding pPP85.4. The entire GFP-CenH3 fragment from pPP85.4 was then amplified with OMF2226 and OMF2019 with overhangs that overlapped with the NcCenH3 promoter (P_{CenH3}) that was amplified by using OMF2238 and OMF182. The P_{CenH3}-GFP-NcCenH3-3'UTR fragment obtained from the overlapping PCR amplification was cloned into the *his-3* targeting vector pBM60, yielding pPP74.55. Similarly, the N-terminally tagged mCherry-NcCenH3 fragment constructed by overlapping PCR amplification was integrated at the endogenous locus. For this, the desired sequences were amplified with primers OMF2238 and OMF182 for the CenH3 promoter and OMF2226 and OMF1956 for the mCherry-10xGly-NcCenH3 fragment from pPP80.17. The fragment with the hygromycin split marker and the 3'UTR were amplified using the same primer pairs as described in the Chapter 2 for the splitmarker transformation.

Further, using the same strategy of PCR amplification as described above, the N-terminal tagged FLAG and HA tagged NcCenH3 strains were prepared. In this cloning, the primers OMF2701 and OMF2700 or OMF2701 and OMF2699 were used to amplify 3xFLAG-10xGly and 3xHA-10xGly fragments from the pQA-N-3xFLAG-hph-loxP and pQA-N-3xHA-hph-lopP plasmids (120), respectively. The NcCenH3 gene was amplified using primers OMF2702 and OMF1956 and was fused with the NcCenH3 promoter-3xFLAG (or 3xHA)-10xGly-NcCenH3 fragment without the NcCenH3 3'UTR. Both amplified fragments were cloned into the *his-3* targeting vector pBM60 by blunt-end cloning after the fusion PCR reaction.

Plasmids pPP70.6 (3xHA-NcCenH3) and pPP71.24 (3xFLAG-NcCenH3) were for integration at the *his-3* locus. The construct that was integrated at the endogenous CenH3 locus, was built using the same set of primers as described above for the mCherry-NcCenH3 construct. After making the fragments for targeting to the endogenous CenH3 locus, they were transformed into N3011 for homologous recombination via electroporation (57) to generate transformants NMFxxx (*his-3+::*P_{CenH3}*-GFP-10xGly-NcCenH3-3'UTR*; *NcCenH3::mCherry-10xGly-NcCenH3*), NMFxxx (*his-3+::*P_{CenH3}*-FLAG-10xGly-NcCenH3-3'UTR*; *NcCenH3::HA-10xGly-NcCenH3*) and NMFxxx (*his-3+::*P_{CenH3}*-HA-10xGly-NcCenH3-3'UTR*; *NcCenH3::FLAG-10xGly-NcCenH3*). These transformants were crossed with N162 (XPP264 = N162 X NMF605 and XPP251 = N162 X NMF608) and homozygous progeny NMF606, NMF607 and NMF603 were obtained (Table 4.2).

The C-terminally GFP-tagged H2AZ construct was generated by overlapping PCR fragments. The 5' flank fragment of H2AZ was PCR-amplified from wildtype NMF39 genomic DNA with primers OMF1499 and OMF1483, and the 3' flank fragment was amplified using OMF1562 and OMF1501. This construct was then transformed into strain N3011, and the transformants were screened for GFP fluorescence as described previously (94). Transformants with correct integration (checked by Southern and PCR, data not shown) and good fluorescence intensity were selected (NMF595 and NMF600) for ChIP-seq assays as described earlier. NMF595 was re-transformed to integrate the N-terminal–mCherry tagged NcCenH3 at the *his-3* locus (pPP68.11). The re-transformed strain NMF596 was screened again by microscopy and correct strains were selected for co-IP assays. Similarly, the C-terminal GFP tagged H2A was constructed using primers OMF1495 and OMF1523 for the 5' flank

fragment, and OMF1496 and OMF1524 for the 3' flank fragment. Again, a correct transformant (NMF597) was re-transformed with pPP68.10 and re-transformants were screened by microscopy to yield NMF599.

Fluroscence microscopy and Southern blotting

The strains were screened by fluorescence microscopy as described in Chapter 2. The excitation/emission wavelength of 490/525 nm was used for capturing GFP, whereas 558/583 nm was used for mCherry fluorescence.

ChIP-seq assay

The procedures for ChIP and ChIP-seq were the same as previously described (273).

Screening strains by western blotting

Tissue from NMF606 and NMF607 strains was lyophilized overnight and ground using a metal spatula while vortexing, followed by the addition of 200 µl of urea-SDS loading buffer (1% SDS, 9 M urea, 25 mM Tris-HCl pH 6.8, 1 mM Na-EDTA pH 8.0, 10 mM βME). The suspension was transferred to a 1.5 ml Eppendorf tube, mixed by vortexing and boiled for 3 min. This was repeated twice and then the tube was cooled on ice. After clearing the lysates by centrifugation at 14,000 rpm for 2 mins, 20 µl of the supernatant was separated by SDS-PAGE. The proteins were transferred onto a PVDF membrane according to manufacturer's protocols. The membrane was washed briefly in TBST buffer (1xTBS + 0.05% Tween-20) followed by blocking with 2% nonfat milk in TBST for 1-2 hr at room temperature (RT). The membrane was incubated overnight with mouse monoclonal anti-FLAG (Sigma) or rat monoclonal anti-HA (Roche) antibodies at 1:5,000 dilution at 4 C. The membrane was washed 4x,

10 mins each with TBST. The appropriate secondary antibody, goat anti-mouse (Life Technologies) or goat anti-rat (Roche) was used at 1:3,300 dilution in TBST buffer for 2 hrs at RT. After washing the membrane for 3x for 10 min each with TBST, chemiluminescence was detected using 1 ml of pico substrate (Pierce ECL, Thermo Scientific) diluted in 25 ml TBST.

Co-immunoprecipitation

For co-IP on the NMF603 strain, the NMF426 (mCherry-NcCenH3) strain was used as the positive control and for NMF606 co-IPs, single tag FLAG (NMF229) and HA (NMF607) stains were used as positive controls. In both co-IPs, NMF39 was used as the negative control. In the co-IP procedure, tissue was grown for 5 hrs at 30 C using approximately 10^9 conidia in 200 ml Vogel's liquid media (see Chapter 2). The germinated conidia were harvested, flash frozen in liquid nitrogen, and the tissue ground under liquid N_2. The ground tissue was suspended in 15 ml ice-cold lysis buffer (1x TBS; 2 mM EDTA; 10% glycerol; 0.5% Triton X-100) along with protease inhibitors (PMSF, leupeptin, pepstatin and E-64). Then, proteins were dissolved by incubation on a rotary shaker at 4 C for 1.5 hrs. After incubation, lysate was cleared by centrifugation in a swinging bucket rotor at 2,000 rpm at 4 C for 5 min. The supernatant was transferred to a fresh tube and centrifuged again for 10 min at 8,000 rpm. The supernatant was aspirated and 100 µl saved as the input fraction and the rest of the supernatant was incubated with 30 µl FLAG resin (Sigma) at 4 C overnight. On the next day, the resin was centrifuged at 1,000 rpm and washed 5-7 times with 500 µl wash buffer (1x TBS, 10% glycerol, 1 mM EDTA) at 4 C. After washes, the bound proteins were eluted from the resin by adding 300 µl of 200 µg/ml anti-FLAG peptide (3xFLAG peptide, New England Peptide). The proteins were concentrated by

TCA precipitation by adding 1 volume of TCA stock to 4 volumes of protein sample and incubation for 10 min at 4 C. The samples were centrifuged at 14,000 rpm for 5 min and the supernatant was aspirated, leaving the protein pellet intact. The pellet was washed twice with 200 µl cold acetone and centrifuged at 14,000 rpm for 5 min. The remaining acetone was evaporated and the pellet was dried by heating tubes in a 95 C heat block for 5-10 min. For SDS-PAGE, the samples were mixed with 2x or 4x sample loading dye and boiled for 5 mins at 100 C before loading an SDS-PAGE gel for western blotting.

The same protocol was followed for immunoprecipitating mCherry tag with anti-RFP magnetic beads (RFP-Trap, Chromotek). However, in this experiment, the elution was done by glycine extraction. In this method of extraction, the proteins from the beads were eluted by adding 100 µl of 100 mM glycine (pH 3.0), incubating for 3 min followed by neutralizing the low pH glycine with 1 mM Tris-HCl (pH 8.0). The western blotting was done using anti-mouse GFP antibody (Santa Cruz).

Results

The double tagged N-terminal NcCenH3 co-localize at centromere

In the double-tagged fluorescence NcCenH3 strains when screened under an epifluorescence microscope, both GFP-NcCenH3 and mCherry-NcCenH3 tags appeared co-localized at centromeres in strain NMF603 (Figure 4.3A). However, this does not allow us to determine if both tagged proteins occupied the same nucleosome. To begin to answer this question, we carried out co-immunoprecipitation analyses. In addition, in strains NMF596 and NMF597 mCherry-NcCenH3 was

localized at the chromocenter as red fluorescence, whereas H2AZ-GFP and H2A-GFP fluoresced throughout the entire nucleus (Figure 4.4).

NcCenH3 nucleosomes are homotypic dimers

Western blotting was used for screening FLAG- and HA-tagged strains NMF606 and NMF607 (Figure 4.3B). The FLAG- and HA-tagged NcCenH3 bands were observed in double-tagged NMF606, whereas only the HA-tagged NcCenH3 band was seen in the single-tagged NMF607 strain (Table 4.1). Our goal was to determine whether the NcCenH3 nucleosome octamers contain homotypic or heterotypic dimers H3 variants, i.e. either two copies of CenH3 or one copy each of CenH3 and the canonical histone H3, respectively (Figure 4.1). This was analyzed by performing co-IP on NMF606, NMF607 and NMF229. In Neurospora, the chances of Scm3 occupying the nucleosome as seen in budding yeast (Scm3, 233 amino acids long) (328) is rather remote, as the predicted Scm3 homolog in Neurospora is a large protein of 1355 amino acids (data not shown). Further, our co-IP results, using the FLAG resin for the pull down and the FLAG antibody for initial probing in western blotting (Figure 4.5A), shows a band for the 3xFLAG-CenH3 tag protein (~25 KD) in eluted sample of the double-tagged (NMF606) and single-tagged FLAG strain (NMF229); i.e. compare lane 4 and 8 as well as in the whole cell extract (WCE) sample, lane 3 and lane 7, respectively Figure 4.5A). This band of ~25 kDa is absent in WCE as well as in the eluted samples from negative controls, i.e. the single-tagged HA strain (NMF607), lane 5 and 6 and wild type strain (NMF39), lane 1 and 2, respectively. Further, the western blot probed with the HA antibody (Figure 4.5A) showed a band of 3xHA-CenH3 (~25 KD) only in the double-tagged strain (NMF606), lanes 7 and 8, whereas the 3xHA-CenH3 band was present only in the WCE sample

of the single HA tagged strain (NMF607), as shown in the lane 5 (Figure 4.5A). These co-IP results suggest tight interactions between the FLAG- and HA-tagged NcCenH3 proteins, as pull-down with the FLAG tag antibody and then probing with HA antibody on Western blot shows bands of 3xHA-CenH3 in double-tagged strain NMF606 (Table 4.1).

In western blots for H3K9me3, anti-mouse Ab (Active Motif) was used on the FLAG pull down samples for the single HA tagged strain (NMF607), double tagged strain (NMF606), single FLAG tagged strain (NMF229) and wildtype strain (NMF39) (Figure 4.5B). In the “IP” lane 2 (NMF607), lane 4 (NMF606), lane 6 (NMF613) and lane 8 (NMF39), no bands were present at ~20KD (expected size of H3K9me3), but in the WCE, lane 1 (NMF607) and 7 (NMF39), the band of ~20 kDa suggested that H3K9me3 was observed. Altogether, these observations for H3K9me3 western blotting suggest that there is absence of interaction between histone H3 and 3xHA-CenH3. However, no band was observed in WCE (lane 3) for the double-tagged strain NMF606 and also in lane 5 of the single FLAG tagged strain NMF613 (Figure 4.5B). This may either be due to the lack of sufficient starting material, i.e. tissue, or the incomplete lysis of tissues or fragmentation of chromatin structures to extract the histone complexes. On the other hand, it is possible that there are no H3K9me3 histone marks present in the nucleosomes where histone H3 and CenH3 exist together as a heterotypic dimer in the centromere nucleosome octamers in *N. crassa*. Alternatively, it is also possible that getting the histone H3 complexes in suspension is difficult due to the rigid nucleosome structures formed with DNA. This is because structural studies have shown that CenH3 protein is more loosely packed in the nucleosome compared to histone H3 (212). Hence, getting CenH3 dimers from the

centromere nucleosome into the suspension might be much easier than canonical histone H3 with an H3K9me3 histone mark. The western blotting with other specific antibodies, for example the N-terminus and C-terminus of histone H3, H4, H2A and H2B did not work. Further standardization of the technique for the complete lysis of tissues and successful complete extraction of the protein complexes of the entire centromere nucleosome is required.

The results suggesting presence of homotypic dimers of NcCenH3 were confirmed by co-IP of GFP and mCherry on a double-tagged NcCenH3 strain (NMF603). In this co-IP assay, NMF603 CenH3 was pulled down with both RFP and GFP magnetic beads. The single tag mCherry-NcCenH3 strain (NMF426) was used as the positive control and NMF39 wild type as a negative control. The glycine elution protocol mentioned in the materials and methods for extracting proteins associated with the -GFP and -RFP beads did not work and therefore no bands were observed (lane 2, 4, 6 and 9) on the Western blot probed with the monoclonal anti-mouse GFP antibody (SantaCruz) (Figure 4.6). The GFP and the RFP beads used directly in the co-IP assay were loaded onto the SDS-PAGE gel to check if the tagged CenH3 are bound to the beads. As shown in Figure 4.6, beads were loaded in lane 1 and 3 and the expected band of ~50 KD (NcCenH3+GFP) was obtained for both GFP as well RFP magnetic beads used for the pull downs in the double-tagged NMF603 strain. No band was observeded for the single mCherry (RFP) tagged NMF426 strain (lane 5; Figure 4.6) and in the wild type NMF39 control strain. Combined analysis of these results suggests interaction between GFP- and mCherry-tagged NcCenH3 proteins.

The C-terminal GFP tagged H2AZ is not localized at Neurospora centromeres

In the ChIP-seq assay with H2AZ-GFP, we found that H2AZ appearsto be excluded from centromeres, suggesting that the heterochromatic centromeres of Neurospora are different in organization. Epifluorescence microscopy showed that GFP-CenH3 and mCherry-NcCenH3 are co-localized (Figure 4.3A) in comparison to H2AZ-GFP and mCherry-NcCenH3 in NMF596 (Figure 4.5B). Curiously, H2A-GFP appeared in tight foci as well, which seemed to overlap with mCherry-CenH3, but it is possible that these signals are bleed-through from the RFP channel (Figure 4.5B). The microscopy overall supports H2AZ-GFP ChIP-seq data, suggesting no enrichment at centromere nucleosomes specifically. Whether H2AZ is present in canonical histone H3 or CenH3 nucleosomes can be addressed by performing co-IP experiments in the future.

Discussion

The co-IP results suggest that NcCenH3 nucleosomes exist as homotypic dimer at the centromere and are similar to human CenH3 nucleosomes in their composition. However, the important amino acid residues in the structural studies of human CenH3 that impart specificity to the CenH3 nucelosomes structure are not conserved in the fungal CenH3 used in these studies. The residues in the α-N helix and in the distal end of the α -2 helix that impart specificity to CenH3 nucleosome have identical residues to canonical histone H3 (see Figure 3.2). This observation suggests the possibility that the structural aspects of NcCenH3 nucleosome must be more similar to canonical histone H3 nuceolsome and/or there might be different structural determinants of CenH3 nucleosomes in *Neurospora* that play a role in guiding the NcCenH3 nucleosome specificity at the centromere. In order to determine the

presence of heterotypic nucleosomes at Neurospora centromeres, we probed western blots with H3K9me3 antibody on the FLAG pull down immuno-precipitated samples. However, the results were inconclusive (Figure 4.5C), suggesting two possible reasons for this observation. First, there might be no H3K9me3 histone marks present on histone H3, if it should exist together with CenH3 as a heterotypic ocatmer at the Neuropsora centromere. Second, due to rigidity in the histone H3 nucleosomal structures, there might be difficulty in getting the H3 into the cell extract suspension. Apart from these two reasons, it is most likely that NcCenH3 gets loaded into centromeric nucleosomes as homotypic dimer. In this case interactions with H4 should be observed, but we have yet to show these. We note that the two most recent papers on human and yeast centromeres also failed to show western data that proved H4 present in their preparations (32, 271). In yeast nucleosomes Scm3 is supposed to assume the role of H2A and H2B (190), although this is controversial (40).. In both yeast and human, CenH3 and H4 dimers interact at least temporarily with the Scm3/HJURP chaperone and this complex gets deposited at the centromere. To truly understand the uniqueness of the CenH3 deposition mechanism in *Neurospora*, further analysis in this direction is required.

Our ChIP-seq data for H2AZ-GFP show no localization of H2AZ at the centromere. However, recent data from the lab of Eric Selker at the University of Oregon in Eugene (personal communcation) suggest that H2AZ is localized at Neurospora centromeres. The H2AZ strain used in their ChIP-seq analysis contained a FLAG tag at the C-terminus. The contradiction in our ChIP-seq output is still unresolved. Our ChIP-seq data is generated by analyzing a single transformant (NMF595), hence this result should be further confirmed by analyzing another strain.

Alternately, this contradictory data output can be explained by performing co-IPs on the double-tagged strains NMF595 and NMF600 (H2AZ-GFP + mCherry-NcCenH3) to see if H2AZ and CenH3 can occur in the same nucleosome. On the other hand, the co-IPs on the double-tagged strains NMF599 and NMF602 (H2A-GFP + mCherry-NcCenH3) will help in determining other histone members from the CenH3 nucleosomes; this would refute the earlier yeast data (190). A recent study showed that the C-terminus of H2AZ is very important for regulating its association with the nucleosomes (326). Hence, it is possible that the bulkier C-terminal GFP tag used in our ChIP-seq might inhibit H2AZ localization at the centromere. Therefore, these negative data suggest that the C-terminus of H2AZ is required for its centromere localization. However, to confirm this observation, more strain construction and additional experiments are required.

Performing co-IPs on strains with double-tagged PaCenH3 that substitutes for NcCenH3 will help determine whether the nucleosome content remains the same in the presence of PaCenH3 at Neurospora centromere, and will tie in with results presented in Chapter 3. Although the FLAG tag strain of PaCenH3 showed no bands in the IP (lane 6 of Figure 4.5B, compared to the light band in lane 5, i.e. WCE), these results need to be confirmed because the dynamics for the nucleosome composition in presence of NcCenH3 is still not well understood. We need supporting data for the presence of other histones in the nucleosomes, e.g. histone H4, H2A and H2B. However, generation of double-tagged strain with tagged PaCenH3 and NcCenH3 may be useful in future assays for testing the propensity of PaCenH3 getting loaded in the Neurospora centromere nucleosome in comparison to NcCenH3. Therefore, studies in this direction will provide important information about the differences and

uniqueness of Neurospora centromeres that will serve as the platform for studying centromeres in other filamentous fungi.

Table 4.1: Neurospora strains used in this study.
Transformed heterokaryotic strains are denoted by square brackets. Neurospora strains used for phylogenetic analysis were used from Fungal Stock Center (FGSC).

Strains	Genotypes	Reference or Source
NMF39	*74-OR23-1VA*	FGSC2489
NMF229	*mat A; ΔNcCenH3::NcCenH3-3xflag^{+}-hph^{+}*	(273)
NMF426	*mat A; ΔNcCenH3:: mCherry^{+}-NcCenH3-hph^{+}; Δmus-51::trpc-bar^{+}*	Chapter 2
NMF595	*[mat a; his-3; ΔH2AZ::H2AZ-gfp^{+}-hph^{+}; Δmus-51:: bar^{+} + mat a; his-3; H2AZ; Δmus-51:: bar^{+}]*	This study
NMF596	*[mat a; his-3::P_{CenH3}-mCherry^{+}-NcCenH3 ;ΔH2AZ::H2AZ-gfp^{+}-hph^{+}; Δmus-51:: bar^{+} + mat a; his-3; ΔH2AZ::H2AZ-gfp^{+}-hph^{+}; Δmus-51:: bar^{+} + mat a; his-3::P_{CenH3}-mCherry^{+}-NcCenH3 ;H2AZ; Δmus-51:: bar^{+} + mat a; his-3; Δmus-51:: bar^{+}; H2AZ]*	This study
NMF597	*[mat a; his-3; ΔH2A::H2A-gfp^{+}-hph^{+}; Δmus-51:: bar^{+} + mat a; his-3; H2A; Δmus-51:: bar^{+}]*	This study
NMF599	*[mat a; his-3::P_{CenH3}-mCherry^{+}-NcCenH3 ; ΔH2A::H2A-gfp^{+}-hph^{+}; Δmus-51:: bar^{+} + mat a; his-3; ΔH2A::H2A-gfp^{+}-hph^{+}; Δmus-51:: bar^{+} + mat a; his-3::P_{CenH3}-mCherry^{+}-NcCenH3 ;H2A; Δmus-51:: bar^{+} + mat a; his-3; Δmus-51:: bar^{+}; H2A]*	This study
NMF603	*mat a; his-3::P_{CenH3}-gfp^{+}-NcCenH3-3'UTR; ΔNcCenH3::mCherry^{+}-NcCenH3-hph^{+}*	This study
NMF604	*[mat a; his-3::P_{CenH3}-3xflag^{+}-NccenH3; Δmus-51:: bar^{+} + mat a; his-3; Δmus-51:: bar^{+}]*	This study
NMF605	*[mat a; his-3::P_{CenH3}-3Xflag^{+}-NccenH3; NcCenH3; Δmus-51:: bar^{+} + mat a; his-3; ΔNcCenH3:: 3XHA-NcCenH3-hph^{+}; Δmus-51:: bar^{+} + mat a; his-3 ::P_{CenH3}-3Xflag^{+}-NccenH3; ΔNcCenH3:: 3XHA^{+}-NcCenH3-hph^{+}; Δmus-51:: bar^{+} + mat a; his-3; Δmus-51:: bar^{+}]*	
NMF606	*mat a; his-3::P_{CenH3}-3xflag^{+}-NcCenH3; ΔNcCenH3::3xHA-NcCenH3-hph^{+}*	This study
NMF607	*mat A; ΔNcCenH3::3xHA^{+}-NcCenH3-hph^{+}*	This study
NMF608	*[mat a; his-3::P_{CenH3}-gfp^{+}-NccenH3-3'UTR; ΔNcCenH3:: mCherry^{+}-NcCenH3-hph^{+}; Δmus-51:: bar^{+} + mat a; his-3; ΔNcCenH3:: mCherry^{+}-NcCenH3-hph^{+}; Δmus-51:: bar^{+}]*	This study
NMF613	*mat a; his-3; ΔNcCenH3::3Xflag^{+}-PaCenH3-hph^{+}; Δmus-51:: bar^{+} + mat a; his-3; NcCenH3; Δmus-51:: bar^{+}]*	This study

Table 4.2: Oligonucleotides used as primers for PCR.

OMF	Name	Sequence (5' -> 3')
180	NcCenH3GlyF	GATGAATGACTAGATGCCGCGGTG
181	NcCenH3loxF	TGCTATACGAAGTTATGGATCCGAGCTCGTGTGATTAGCGCATGGCGGTGC
182	NcCenH3GlyR	CCTCCGCCTCCGCCTCCGCCGCCTCCGCCTACCCACCCAGCACCTCCCC
188	NcCenH3loxR3	GCCCCCACGCTAAAGCTGTT
509	FPPacF	CGCTTAATTAACATGGTGAGCAAGGGCGAGGAG
1483	H2AZGlyR	CCTCCGCCTCCGCCTCCGCCGCCTCCGCCAGCCTCCTGAGCCTTGGCCTTCTT
1495	H2AGlyR	CCTCCGCCTCCGCCTCCGCCGCCTCCGCCAAGTTCTTGACTCGCGTTCTTGCC
1496	H2AloxF	TGCTATACGAAGTTATGGATCCGAGCTCGCCCTTTTTTCTGGTTGGCACGTTG
1499	H2AzGlyF	GCAGAGCCATTCTGCTCGCGCTGG
1501	H2AZloxR	GGGTATCAGTGTCGTCCGAAACAG
1523	H2AGlyF	AGCTGACGAAAGCCCTGACTTGTT
1524	H2AloxR	CTCGACTGGGCTGTCAATCGCCAA
1562	H2AZloxF	TGCTATACGAAGTTATGGATCCGAGCTCGCGCACACGTTTCGCACACTGTCTT
1563	NcCenH3_NdeI	TCCTTACATATGCCACCAAAGAAGGGAGGA
1956	Nchph5R2	GATAAGCTTGATATCGAATTCTTACTTGTTCATACCCACCCAGCACCTCCCCA
2019	CenH35GRhph	GATAAGCTTGATATCGAATTCTTACTTGTCGGCCCCCTTTTTCCTTTTCC
2226	AdapCenApaCherryR	CAATACATTCACCATCATCGATAAACAACAGGGCCCATGGTGAGCAAGGGCGAG
2238	NotCenH3GlyF	CGTTGCGGCCGCGATGAATGACTAGATGCCGCGGTG
2699	HAadaptCenF	CAATACATTCACCATCATCGATAAACAACAATGATCTTTTACCCATACGAT
2700	FLadaptCenF	CAATACATTCACCATCATCGATAAACAACAATGGACTACAAAGACCATGAC
2701	N10XGlyR	ATGGCCTCCGCCGCCTCCGCCGCCTCC
2702	N10XGlyF	GGAGGCGGCGGAGGCGGCGGAGGCCAT

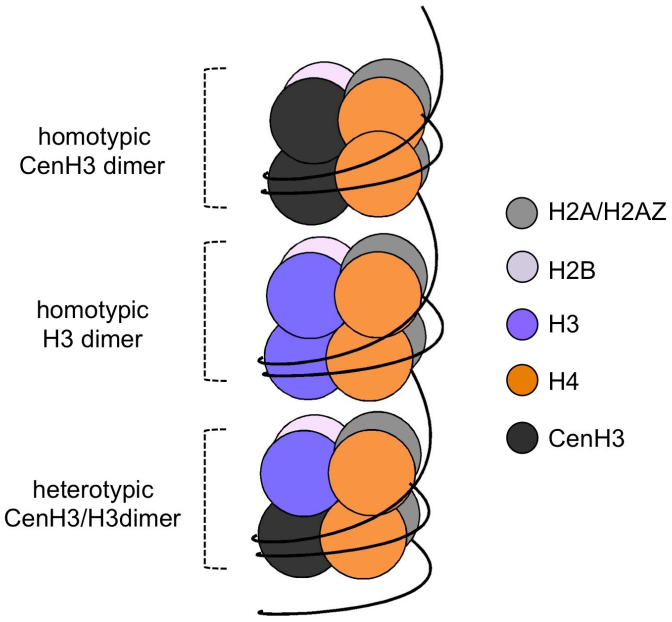

Figure 4.1: Model depicting homotypic and heterotypic nucleosomes at centromeres.

The first and second nucleosomes represents homotypic CenH3 or H3 dimers within an octameric core particle. The third nucleosome contains a heterotypic CenH3/H3 dimer within the otherwise canonical octamer. Under certain circumstances centromeric nucleosomes may contain H2AZ.

A

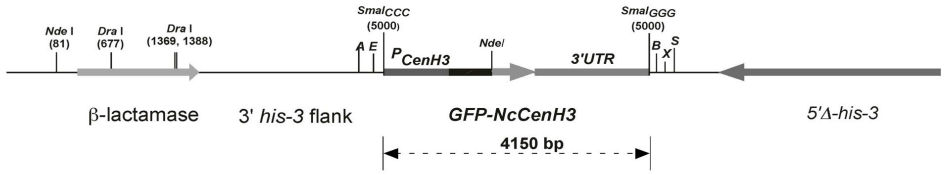

B

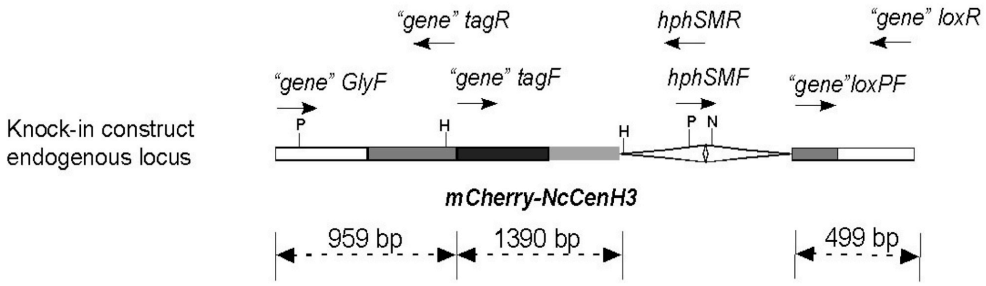

C

Knock-in C-terminal GFP tag

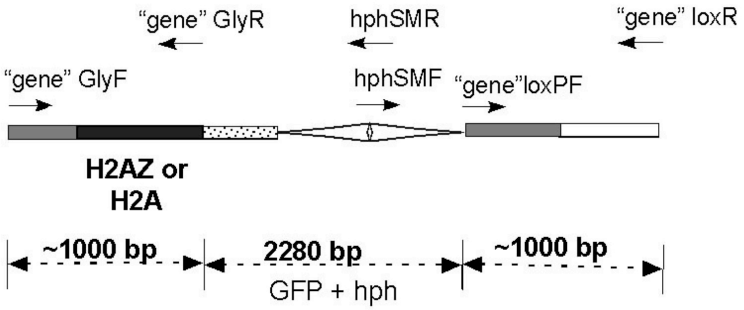

Figure 4.2: Maps of various constructs used in this study.

(A) pPP74.55. The *his-3* targeted pBM60 vector backbone representing *AmpR* marker beta-lactamase along with his-3 flanking regions. The blunt end cloning was done for the construct having CenH3 promoter-GFP-NcCenH3-3'UTR at SmaI site, depicted as $SmaI_{CCC}$ is first half of site and $SmaI_{GGG}$ other half of the site. *SmaI* site is present in multiple cloning sites (MCS) of the pBM60 vector, hence A = *ApaI,* E = *EcoRI*, B = *BamHI*, X = *XbaI* and S = *SpeI* are various restriction sites at MCS. *DraI* site was used for linearizing the vector during transformation because *NdeI* site was already present in the construct at the junction of GFP and start of NcCenH3 gene. **(B) Construct build using overlapping PCR amplification strategy for N-terminal tagged NcCenH3 with mCherry.** This construct was targeted at the endogenous locus of CenH3. P= *PstI*; H = *HindIII*; N = *NdeI* restriction enzyme site used for southern blots. The white box on the left hand side represent the 5'flank and one on the right hand site represent the 3'flank of the locus; the left hand gray box is promoter region of NcCenH3 from endogenous locus and the right hand gray box is 3'UTR of NcCenH3 endogenous locus. The black box represent the mCherry tag followed by NcCenH3 gene (gray box). The triangles represent the split-marker of hygromycin (hph) amplified using; hphSMF = OMF1053; hphSMR = OMF1054. The black arrows represent the primers used in the construct "gene" here refers to NcCenH3; "gene"GlyF = OMF180; "gene"tagR = OMF2226; "gene"tagF = OMF509 ; "gene"loxF = OMF181; "gene" loxR = OMF188. **(C) Knock-in construct generated by overlapping PCR amplification strategy for H2A and H2AZ with the C-terminal GFP tag.** The gray box on the right side represent the promoter region of H2A or H2AZ; Black box is H2A/H2AZ gene; the spotted box shows the GFP tag attached at the C-terminal of H2A or H2AZ gene. The triangles represent the spilt marker hygromycin (hph) same as before. The gray and white box on the right hand side represent the 3'UTR and 3'flank region of the endogenous locus of H2A or H2AZ. Note: the maps are not drawn to the scale. In this map "gene" refers either to H2AZ or H2A. Primers (black arrows): "gene"GlyF = OMF1499/1523; "gene"GlyR = OMF1483/1495; "gene" loxPF = OMF1496/1562; "gene"loxR = OMF1501/1524.

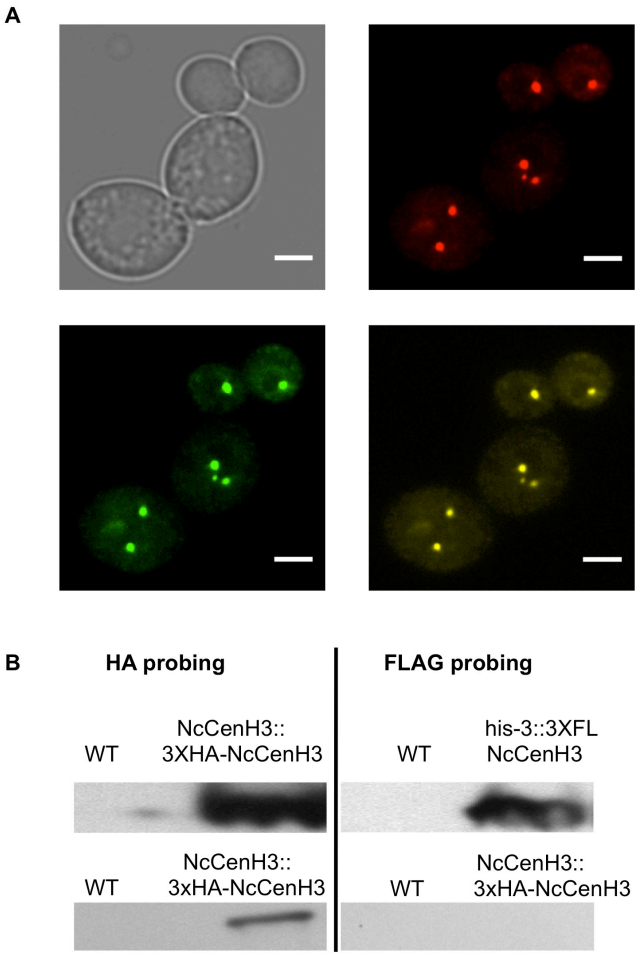

Figure 4.3: Analysis of correct double-tagged NcCenH3 strains.

(A) Fluorescence microscopy. Top panel left shows the bright field exposure of conidia from NMF603 (*his-3*::P_{CenH3}-GFP-NcCenH3-3'UTR; NcCenH3::mCherry-NcCenH3-*hph*). Top right shows the tight foci of mCherry-NcCenH3 fluorescence within the nuclei from DS-Red filter. Bottom left side is the tight foci of GFP-NcCenH3 fluorescence within the nuclei from FITC filter. Bottom right side is the merge of the top right (red) and bottom left (green) and hence shows the yellow foci of fluorescence suggesting the co-localization of GFP-NcCenH3 and mCherry-NcCenH3. (scale bar = 5um). **(B) Screening of FLAG- and HA-tagged strain by western blot.** The double tagged strain NMF606 showed bands at ~25 KDa when probed with HA as well FLAG antibodies, whereas a single tagged HA strain NMF607 shows no band in FLAG probing.

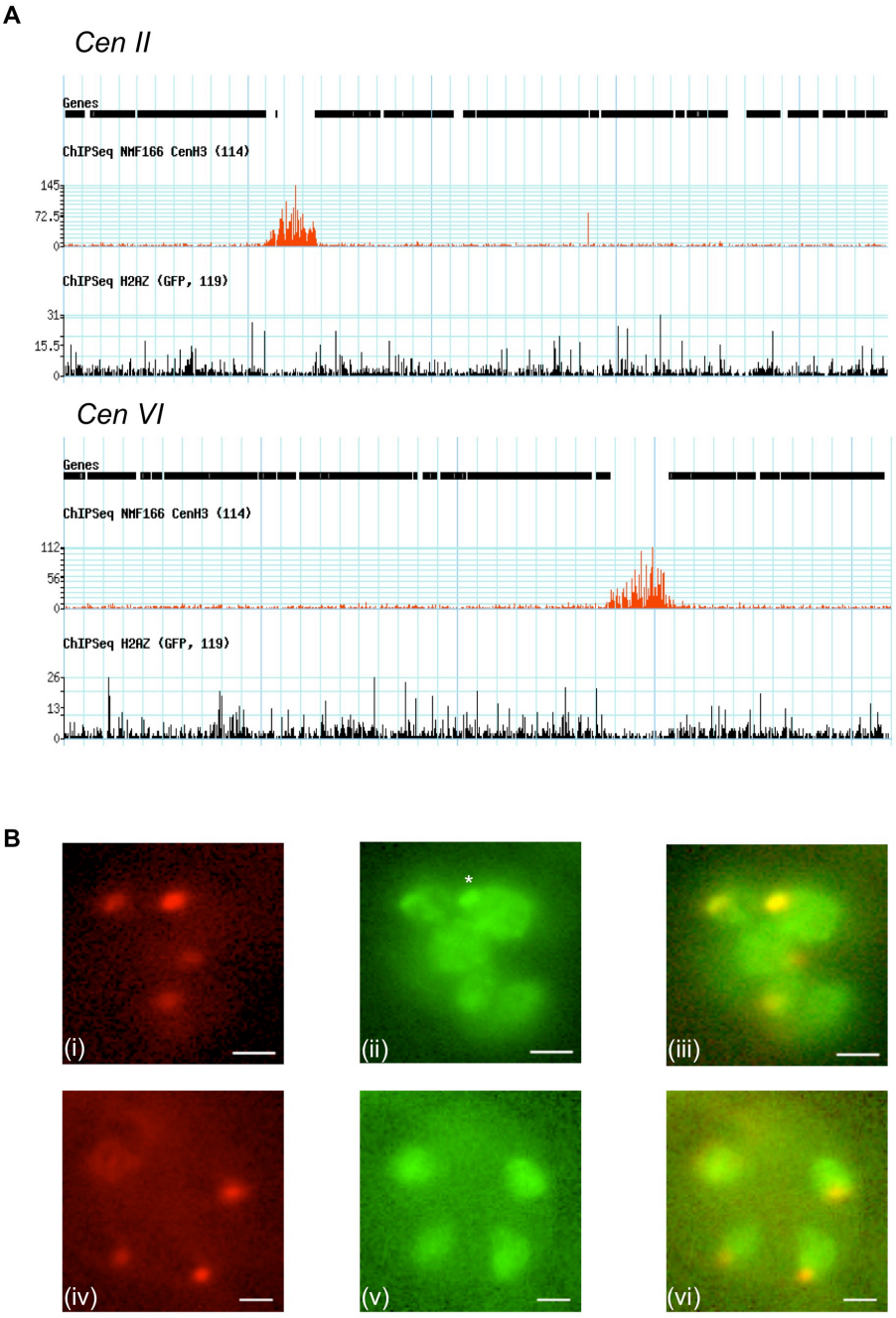
A
Cen II
Genes
ChIPSeq NMF166 CenH3 (114)
145
72.5
0
ChIPSeq H2AZ (GFP, 119)
31
15.5
0
Cen VI
Genes
ChIPSeq NMF166 CenH3 (114)
112
56
0
ChIPSeq H2AZ (GFP, 119)
26
13
0
B
(i)
(ii)
*
(iii)
(iv)
(v)
(vi)

Figure 4.4: Fluorescence microscopy and ChIP-seq data for NcH2AZ-GFP.

(A) Snapshot of ChIP-seq data for H2AZ-GFP for *Cen II* and *CenVI*. The black boxes represent the genes on the chromosome 2 and 6. ChIP-seq data for the NcCenH3-GFP (NMF166) enriched at centromere which is the gene deficient region. H2AZ-GFP (NMF595) localization (black) is absent at the centromere in comparison to the chromosomes arms. **(B) Fluorescence microscopy for NMF596 and NMF599.** DS-Red filter shows the tight foci of florescence for mCherry-NcCenH3 localization in NMF596 and NMF599 (i) and (iv); GFP-Quad filter shows GFP florescence localized in the entire nuclei in presence of H2A-GFP (ii) in NMF599 and for H2AZ-GFP (v) in NMF596. Tight foci of fluorescence in (ii) compared to (v) suggests localization of H2A-GFP at the centromere (*). Panel (iii) and (vi) are the merge images. (scale bar = 1um)

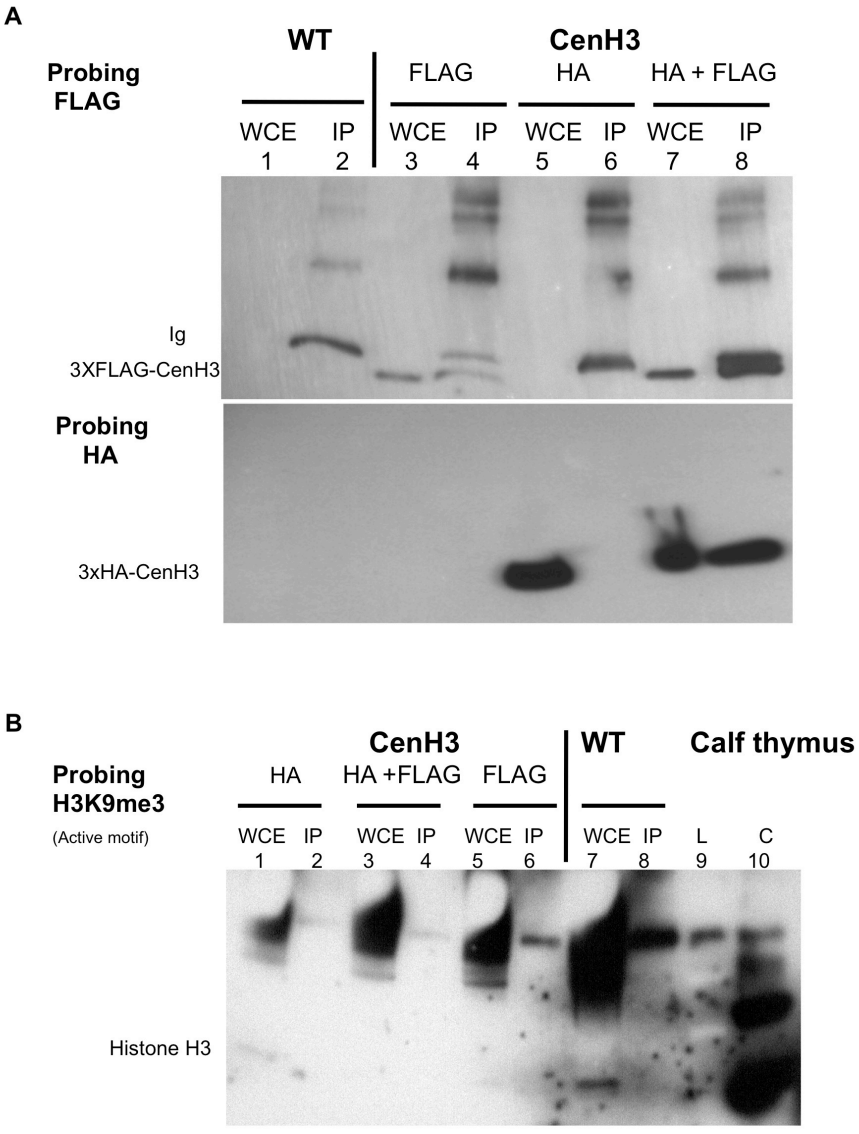
A
WT
CenH3
Probing FLAG
FLAG
HA
HA + FLAG
WCE IP WCE IP WCE IP WCE IP
1 2 3 4 5 6 7 8
Ig
3XFLAG-CenH3
Probing HA
3xHA-CenH3
B
CenH3
WT
Calf thymus
Probing H3K9me3
(Active motif)
HA
HA +FLAG
FLAG
WCE IP WCE IP WCE IP WCE IP L C
1 2 3 4 5 6 7 8 9 10
Histone H3

Figure 4.5: Co-immunoprecipitation assay determining homotypic dimer of NcCenH3.

(A) Western blot probed with FLAG and HA antibody on the immuno-precipitated sample using FLAG resin. The first (top) blot shows the results for FLAG antibody where 3xFLAG-CenH3 band ~25KD is absent in WT lane 1 and 2 (wild type NMF39) and in HA strain lane 5 and 6 (NMF607). Whereas, in C-terminal tagged FLAG strain lane 3 and 4 (NMF229) and HA+FLAG strain lane 7 and 8 (NMF606) the 3xFLAG-CenH3 band is present. WCE (Whole Cell Extract); IP = Immuno-precipitated sample and Ig = immunoglobulin (in this case mouse light chain). The second (bottom) blot is probed with HA antibody where no band is present in WT NMF39 (lane 1 and 2) and FLAG NMF229 (lane 3 and 4). For HA strain NMF607 (lane 5) band was present for WCE but band is absent in lane 6 i.e. for an IP sample. Band ~25 KDa is observed in WCE as well as in IP lanes 7 and 8 for double tag strain NMF606. **(B) Western blot for H3K9me3 antibody probing on the the immuno-precipitated sample using FLAG resin.** HA strain is NMF607, HA+FLAG strain is NMF606, FLAG is NMF613 which is 3xFLAG-PaCenH3 (Table 1) and WT is wild type NMF39. L= ladder; C= control (Calf thymus). The expected band sized for histone H3 is ~20 KD which is seen in lane 10, lane 7 and lane 1.

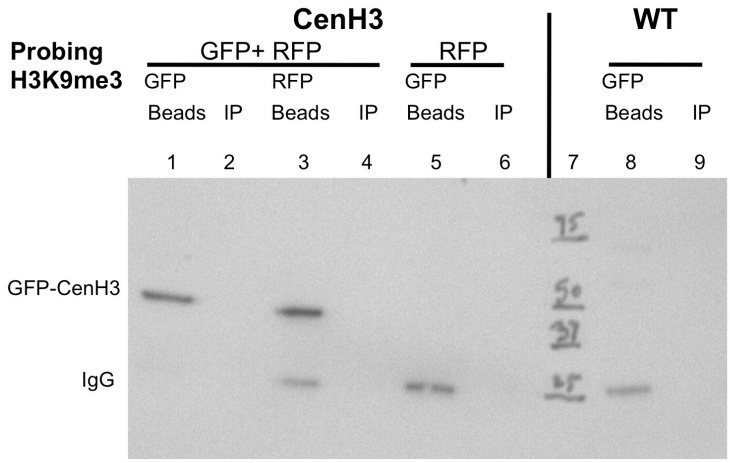

Figure 4.6: Western blot results for GFP antibody probing on the the immuno-precipitated sample using GFP and RFP magnetic beads.

WT = wild type NMF39; GFP+RFP strain is NMF603 and RFP strain is NMF426. The expected band size for GFP-NcCenH3 is ~50 KD as seen in lanes 1,and lane 3. Ig = immunoglobulin (light chain of mouse). Beads = magnetic beads either RFP/GFP that are directly loaded on the SDS-PAGE gel.

General summary and conclusions

Pallavi A. Phatale

Summary and conclusions

The centromere-specific histone H3 (CenH3), a variant of the canonical histone H3, uniquely localizes at centromeres and plays an essential role during cell division (20). Centromeres exist in a wide range of sizes and the organization patterns in different organisms, from a point centromere in budding yeast to regional centromeres in plants, fission yeast, flies, and humans (3, 332). A point centromere is defined by the presence of a single nucleosome in the centromere, whereas the regional centromeres are made up of interspersed arrays of histone H3 and CenH3 nucleosomes. Generally, the central core of centromeres is embedded in heterochromatic silenced regions called pericentric regions that are enriched with closely spaced histone H3 nucleosomes. These nucleosomes possess H3K9me3 (histone H3 lysine 9 trimethylation), a histone mark occurs that along with other complexes, including HP1 (heterochromatin protein 1). In contrast, the central core is a euchromatic region characterized by the presence of H3K4me2 as the dominant histone mark (3). This balance of heterochromatic and euchromatic regions is important for kinetochore assembly and microtubule attachment during cell division (106, 110).

Saccharomyces cerevisiae and *Schizosaccharomyces pombe* have been widely used in centromer research and have hence been accepted, in general, as the representatives of fungi. However, given the great diversity in the fungal world, this seems unreasonable (113, 274, 323). *Neurospora crassa* is a filamentous fungus belonging to the Ascomycota, and many members of this group are pathogenic in nature, e.g. *Fusarium graminearum*, *Aspergillus fumigatus*, *Magnaporthe grisea*

(223). *Neurospora crassa* is a well-studied organism and is considered a model organism for studying genetic phenomena such as recombination, crossing over and gene conversions using tetrad analysis (11, 46, 164, 257).

Based on earlier genetic analyses, centromere positions were precisely mapped in Neurospora, which makes it a very useful organism for studies on centromere assembly and inheritance. Therefore, I used Neurospora as the model for centromere studies presented in this dissertation. In my studies, I characterized Neurospora centromeres that have contrasting features compared to centromere organization in many other organisms. The central core region of Neurospora centromeres is enriched with H3K9me3 instead of H3K4me2 that has generally been found in other organisms. Thus, Neurospora centromeres are truly heterochromatic in organization, which may help explain some basic differences in the assembly and maintenance of centromeres in Neurospora compared to other organisms (273). Mounting evidence suggests that centromeric DNA in higher eukaryotes does not guide centromere assembly, although the DNA has specific characteristics like AT-enriched regions, gene-poor regions, presence of transposable elements and repeated regions (116). This observation of the centromere assembly being independent of the underlying DNA sequence is also true in Neurospora, suggesting that centromere assembly and maintenance is driven by epigenetic phenomena (273).

In order to increase our understanding of centromere organization in filamentous fungi, I analyzed the sequences of CenH3 from different fungi. CenH3 has a highly divergent N-terminus and loop I region but a conserved histone fold domain (HFD) (14, 173, 296). Using CenH3 phylogenetic analysis, I determined that the evolution of

the CenH3 gene appeared to be grouped largely according to the evolutionary relationship derived from the six-genes fungal phylogenetic tree (132) suggesting that the CenH3 locus evolved at same pace as the entire genome. Further CenH3 sequence analysis within the genus *Neurospora* and close relatives showed divergent N-termini but conserved loop I regions. Recent studies in budding yeasts, flies and humans showed that the loop I region of CenH3 is important for centromere targeting (25, 143, 315). Hence, to determine if this is true in filamentous fungi, we used the CenH3 protein possessing divergent loop I and N-terminus regions from fungi that showed various degrees of divergence to Neurospora. For example, the *Podospora anserina* CenH3 (PaCenH3) is closely related to Neurospora compared to *Fusarium graminearum* CenH3 (FgCenH3), whereas *Aspergillus nidulans* CenH3 (AnCenH3) is more divergent than the other two. These different fungal CenH3 proteins were tagged with GFP at the C-terminus (PaCenH3-GFP, FgCenH3-GFP, AnCenH3-GFP and NcCenH3-GFP), expressed under the inducible Neurospora promoter *ccg-1* and targeted for integration at the ectopic *his-3* locus. Interestingly, all four fungal CenH3 proteins localized at the centromere suggesting that the divergence in the loop I region does not affect the centromere localization of CenH3 in filamentous fungi, consistent with findings in Arabidopsis (227). Further, the data from genetic studies showed that the C-terminal tagged PaCenH3-GFP was able to support meiosis in Neurospora, but strains carrying FgCenH3-GFP and AnCenH3-GFP failed to undergo meiosis. I also found that the 3'UTR region, which is important for transcriptional regulation in canonical histone H3 (73), is not required for meiosis in CenH3 because the non-tagged versions of NcCenH3, PaCenH3 and FgCenH3 supported mitosis as well as meiosis. However, in presence of the microtubule inhibitor TBZ, strains with

FgCenH3 were more sensitive than PaCenH3 and NcCenH3. In fission yeast, it is shown that TBZ acts by disrupting the centromere clustering (108). So, it can be suggested that in the presence of FgCenH3, Neurospora centromere assembly may be distorted and be more sensitive to TBZ. Altogether, these genetic studies suggest that the process of centromere assembly and maintenance in Neurospora is partially resistant to the structural distortion that may be attributed to the amino acid composition in PaCenH3 and FgCenH3 during mitosis. During meiosis, the carboxy-terminus of the CenH3 might be essential and requires more stringent structural specificity hence any modification at the C-terminus shows the lethal phenotype during meiosis.

I determined three major graded phenotypic differences in our genetic analysis, i.e. PaCenH3-GFP supports meisosis in NcCenH3 unlike FgCenH3-GFP and drastic growth defects occur in strains with non-tagged FgCenH3 in the presence of TBZ. In the follow-up experiments of domain swapping of the N-terminus and the HFD between FgCenH3, NcCenH3 and PaCenH3, I found that chimeras with FgCenH3 HFD were unable to rescue meiosis, supporting the results obtained from studies in plants and budding yeast (143, 227). Importantly, PaCenH3 was capable of replacing NcCenH3 function without any noticeable phenotypic defect, in spite of the difference in the HFD when compared to NcCenH3. This can be possible because the centromere assembly system in Neurospora is flexible enough to adjust the differences caused by PaCenH3-GFP HFD in comparison to the defects caused by FgCenH3-GFP HFD. However, I have been so far unable to determine whether this difference was due to any specific residues or a particular region in the HFD of

CenH3 that is essential during meiosis. Overall, we deduce some plasticity in centromere assembly and regulation.

Next, I confirmed the correct localization of PaCenH3-GFP at Neurospora centromeres by performing ChIP-seq assays. Interestingly, I observed an unprecedented loss of PaCenH3-GFP enrichment at specific centromeres after a single meiois in a heterozygous cross, namely at *CenI* and *CenVI* in two different strains (NMF324 and NMF326). I considered three likely scenarios and it seems likely that this deficiency of PaCenH3-GFP was determined during the initial meiosis but that loss of PaCenH3-GFP over time is progressive and irreversible. I attempted to elucidate the mechanisms behind these observations. I found that neither major rearrangements of centromeric DNA, translocations nor chromosomes fusions are likely to have occurred, that strains do not seem aneuploid and that epigenetic characteristics of centromeres seem unchanged. The results may thus best be explained by the existence of a centromere-licensing checkpoint. In a multinucleate compartment, like that of Neurospora hyphae, a few actively dividing nuclei may be sufficient to keep the strains growing almost normally. At the same time, nuclei in which certain centromeres have insufficient amounts of CenH3 deposited may enter an arrest, which can only be overcome if additional CenH3 is provided.

Future Work

From my genetic data, I determined that the entire HFD of the CenH3 is important for supporting meiosis because without any conserved differences or similarities, PaCenH3-GFP HFD supported meiosis whereas FgCenH3-GFP did not. I also observed that, although the N-terminus of CenH3 is evolutionarily under positive

selection pressure, a long, perhaps genus-specific N-terminus of CenH3 is required during meiosis in Neurospora. My data show that the N-terminally tagged NcCenH3 was able to undergo meiosis in homozygous crosses, whereas mCherry-PaCenH3 failed to produce ascospores. The N-termini of fungal CenH3s are different in length and amino acid composition, so additional genetic assays can be used to answer the question what specifically is required in the N-termini, by constructing another set of chimeras that includes AnCenH3 N-terminus instead of PaCenH3 and NcCenH3 to generate NAnCPaCenH3 and NAnCNcCenH3 (N-terminal of AnCenH3 and HFD, i.e. C-domain of either PaCenH3 or NcCenH3), respectively. The N-terminus of the AnCenH3 is longer but divergent from NcCenH3 and PaCenH3; hence if the test cross with NAnCPaCenH3 is fertile, it will suggest that the length of the N-terminus is essential during meiosis. On the other hand, if the control test cross with NAnCNcCenH3 were barren it would suggest that the composition of amino acids in the N-terminus of CenH3 is also necessary. This would be helpful to narrow down the scanning region to determine the important residues in the N-terminus of the CenH3 required for meiosis.

To understand whether normal centromeres are assembled in the presence of non-tagged PaCenH3 and FgCenH3, tagged inner kinetochore proteins can be introduced in these Neurospora strains. This can be achieved by crossing non-tagged PaCenH3 and FgcenH3 strains with tagged inner kinetochore protein CEN-T or CEN-C strains that are already available from work in this study. This can be followed by ChIP-seq analyses on the progeny and results can be compared with the initial pull down of CEN-T and CEN-C.

The packed chromosomes in the nucleus have defined territories and are organized in specific pattern, e.g. as seen in the human nucleus by using 3D-fluorescence *in situ* hybridization (FISH) technique (29). However, the resolution of this technique is limited, one can predict the changes in the chromosome localization pattern associated with the analysis but it does not provide the idea of the actually involved DNA regions. On other hand, the “Hi-C” technique was successful in capturing the long-range interaction in human and yeast genome (165, 313). In this technique, first the genomic interactions are fixed using agents such as formaldehyde followed by the digestion of the fixed chromatin with restriction enzymes generating overhangs. The sticky ends generated from the digested fixed chromatin having crosslinked DNA are ligated. Because of the ligation, the genomic regions lying in close proximity in the 3D space may come together and these captured interactions are then characterized by quantitative PCR technique by designing primers close to restriction site for the area of interest or mapped on the genome by using high-throughput sequencing (69). Applying this technique on the strains that shows defective PaCenH3-GFP loading might provide important clues as to whether centromere organization is important in leading to a bias in CenH3 loading at different centromeres. In Neurospora, all seven centromeres are attached together at the spindle pole body (SPB), and that may be a reason for the loss of CenH3 at certain centromeres due to the three -dimensional centromere architechture.

The CenH3 nucleosome structural studies in humans have shown that there exist a homodimer of CenH3 in a centromere nucleosome octamer (32, 271). However, the CenH3 nucleosome content in budding yeast is still under debate, because one study showed CenH3 forming a tetramer with its non-histone chaperone Scm3 to generate

atypical centromere nucleosome, whereas the other study showed that CenH3 nucleosomes are exclusive of Scm3 and are similar to human CenH3 nucleosome content, i.e. dimers of CenH3, H4, H2A and H2B (70, 334). Further, it has been shown that the entry of the CenH3 into centromeric nucleosomes is by the replacement of the canonical histone H3; however there is lack of knowledge elucidating this mechanism (77, 212). Considering these results from different studies, it is possible that the observed defects at certain centromeres in the presence of PaCenH3-GFP might be caused by differences in the CenH3 nucleosome content due to a potential reduction of replacement of the canonical histone H3 with CenH3. To precisely determine this possibility, I wanted to know what kind of dimers exists in Neurospora centromeres in presence of NcCenH3. Therefore, we transformed the Neurospora strain with two constructs having different N-terminal tags at two different locus one at endogenous and another at ectopic locus of *his-3*. The doubly tagged strain having mCherry (red) and GFP (green) fluorescent tags showed co-localization at the centromere, suggesting both the tagged CenH3 localized at the centromere. Next, co-immunoprecipitation experiments were performed on another set of doubly tagged strains with -3xHA (hemagglutinin tag) and 3xFL (Flag tag). The results suggested that the NcCenH3 might exist as a homodimer in the Neurospora centromere nucleosome. Based on this knowledge, I will test whether similar condition exists in the presence of PaCenH3. To further confirm the biochemical analysis in presence of PaCenH3 and NcCenH3, nanofluidic channels can be used to detect the content in each nucleosome (53). On the other hand, the failure in loading PaCenH3 might generate nucleosome deficient regions at the centromere region that can be detected by mapping the mono-nucleosomes

generated after micrococcal digestions form the PaCenH3-GFP strains showing defective centromeres.

Significance

The research presented in this dissertation is the first study of characterizing centromeres in filamentous fungi using Neurospora as the working model. In general, understanding the dynamics of centromeres is itself challenging, however, the data in this dissertation has high potential to help deciphering the network of pathways and associated mechanisms during different stages of cell division in filamentous fungi. Most of the plant pathogens belonging to this group of organisms undergo various morphogenesis phases during their infectious mode that are closely linked to cell division (112, 249). Therefore the knowledge gained in this field is not only exciting but also necessary for understanding the plant-pathogen interactions and finding ways to inhibit the attack by fungal plant pathogens.

Appendix 1: List of additional manuscripts published or accepted.

R. Karimi-Aghcheh, J. W. Bok, **P. A. Phatale**, K. M. Smith, S. E. Baker, A. Lichius, M. Omann, S. Zeilinger, B. Seiboth, C. Rhee, N. P. Keller, M. Freitag and C. P. Kubicek (2012) Functional analyses of *Trichoderma reesei* LAE1 reveal conserved and contrasting roles of this regulator. G3 (accepted pending revision).

K. R. Pomraning, K. M. Smith, E. L. Bredeweg, **P. A. Phatale**, L. R. Connolly and M. Freitag (2012) Paired-end library preparation for rapid genome sequencing. Methods Mol. Biol. 944: 1-22. (doi: 10.1007/978-1-62703-122-6_1) PMID: 23065605.

K. M. Smith, J. M. Galazka, **P. A. Phatale**, L. R. Connolly, M. Freitag (2012) Centromeres of filamentous fungi. Chromosome Research, 20: 635-656. PMID: 22752455

K. M. Smith, **P. A. Phatale**, E. L. Bredeweg, K. R. Pomraning and M. Freitag (2012) Epigenetics of filamentous fungi, in: “EPIGENETIC REGULATION AND EPIGENOMICS”, Encyclopedia of Molecular Biology and Molecular Medicine, Wiley-Blackwell

B. Seiboth, R. Karimi-Aghcheh, **P.A. Phatale**, R. Linke, D.G. Sauer, K.M. Smith, S.E. Baker, M. Freitag and C.P. Kubicek (2012) The putative protein methyltransferase LAE1 controls 1 cellulase gene expression in *Trichoderma reesei.* Mol. Microbiol. 84: 1150-1164. (doi: 10.1111/j.1365-2958.2012.08083.x) PMID: 22554051

K. M. Smith, **P. A. Phatale**, C. M. Sullivan, K. R. Pomraning and M. Freitag (2011) Heterochromatin is required for normal distribution of Neurospora CenH3. Molecular and Cellular Biology 31: 2528-2542 (doi:10.1128/MCB.01285-10) PMID: 21505064.

References

1. **Ahmad, K., and S. Henikoff.** 2001. Centromeres are specialized replication domains in heterochromatin. J Cell Biol **153:**101-110.
2. **Allshire, R.** 2001. Dissecting Fission Yeast Centromeres via Silencing.
3. **Allshire, R. C., and G. H. Karpen.** 2008. Epigenetic regulation of centromeric chromatin: old dogs, new tricks? Nat Rev Genet **9:**923-937.
4. **Alonso, A., D. Hasson, F. Cheung, and P. E. Warburton.** 2010. A paucity of heterochromatin at functional human neocentromeres. Epigenetics Chromatin **3:**6.
5. **Amano, M., A. Suzuki, T. Hori, C. Backer, K. Okawa, I. M. Cheeseman, and T. Fukagawa.** 2009. The CENP-S complex is essential for the stable assembly of outer kinetochore structure. J Cell Biol **186:**173-182.
6. **Amor, D. J., K. Bentley, J. Ryan, J. Perry, L. Wong, H. Slater, and K. H. Choo.** 2004. Human centromere repositioning "in progress". Proc Natl Acad Sci U S A **101:**6542-6547.
7. **Appelgren, H., B. Kniola, and K. Ekwall.** 2003. Distinct centromere domain structures with separate functions demonstrated in live fission yeast cells. J Cell Sci **116:**4035-4042.
8. **Aramayo, R., and R. L. Metzenberg.** 1996. Meiotic transvection in fungi. Cell **86:**103-113.
9. **Aravind, L., L. M. Iyer, and C. Wu.** 2007. Domain architectures of the Scm3p protein provide insights into centromere function and evolution. Cell Cycle **6:**2511-2515.
10. **Asakawa, H., A. Hayashi, T. Haraguchi, and Y. Hiraoka.** 2005. Dissociation of the Nuf2-Ndc80 complex releases centromeres from the spindle-pole body during meiotic prophase in fission yeast. Mol Biol Cell **16:**2325-2338.
11. **Asch, D. K., G. Frederick, J. A. Kinsey, and D. D. Perkins.** 1992. Analysis of junction sequences resulting from integration at nonhomologous loci in *Neurospora crassa*. Genetics **130:**737-748.
12. **Ausio, J.** 2006. Histone variants--the structure behind the function. Brief Funct Genomic Proteomic **5:**228-243.
13. **Bai, C., N. Ramanan, Y. M. Wang, and Y. Wang.** 2002. Spindle assembly checkpoint component CaMad2p is indispensable for Candida albicans survival and virulence in mice. Mol Microbiol **45:**31-44.
14. **Baker, R. E., and K. Rogers.** 2006. Phylogenetic analysis of fungal centromere H3 proteins. Genetics **174:**1481-1492.
15. **Barratt, R. W., D. Newmeyer, D. D. Perkins, and L. Garnjobst.** 1954. Map construction in Neurospora crassa. Adv Genet **6:**1-93.
16. **Bassett, E. A., S. Wood, K. J. Salimian, S. Ajith, D. R. Foltz, and B. E. Black.** 2010. Epigenetic centromere specification directs aurora B accumulation but is insufficient to efficiently correct mitotic errors. J Cell Biol **190:**177-185.

17. **Baum, M., K. Sanyal, P. K. Mishra, N. Thaler, and J. Carbon.** 2006. Formation of functional centromeric chromatin is specified epigenetically in Candida albicans. Proc Natl Acad Sci U S A **103:**14877-14882.
18. **Bendich, A. J., and K. Drlica.** 2000. Prokaryotic and eukaryotic chromosomes: what's the difference? Bioessays **22:**481-486.
19. **Bergmann, J. H., M. G. Rodriguez, N. M. Martins, H. Kimura, D. A. Kelly, H. Masumoto, V. Larionov, L. E. Jansen, and W. C. Earnshaw.** 2011. Epigenetic engineering shows H3K4me2 is required for HJURP targeting and CENP-A assembly on a synthetic human kinetochore. EMBO J **30:**328-340.
20. **Bernad, R., P. Sanchez, and A. Losada.** 2009. Epigenetic specification of centromeres by CENP-A. Exp Cell Res **315:**3233-3241.
21. **Bernard, P., J. F. Maure, J. F. Partridge, S. Genier, J. P. Javerzat, and R. C. Allshire.** 2001. Requirement of heterochromatin for cohesion at centromeres. Science **294:**2539-2542.
22. **Birchler, J. A., and F. Han.** 2009. Maize centromeres: structure, function, epigenetics. Annu Rev Genet **43:**287-303.
23. **Black, B. E., and D. W. Cleveland.** 2011. Epigenetic centromere propagation and the nature of CENP-a nucleosomes. Cell **144:**471-479.
24. **Black, B. E., D. R. Foltz, S. Chakravarthy, K. Luger, V. L. Woods, Jr., and D. W. Cleveland.** 2004. Structural determinants for generating centromeric chromatin. Nature **430:**578-582.
25. **Black, B. E., L. E. Jansen, P. S. Maddox, D. R. Foltz, A. B. Desai, J. V. Shah, and D. W. Cleveland.** 2007. Centromere identity maintained by nucleosomes assembled with histone H3 containing the CENP-A targeting domain. Mol Cell **25:**309-322.
26. **Blackwell, C., K. A. Martin, A. Greenall, A. Pidoux, R. C. Allshire, and S. K. Whitehall.** 2004. The Schizosaccharomyces pombe HIRA-like protein Hip1 is required for the periodic expression of histone genes and contributes to the function of complex centromeres. Mol Cell Biol **24:**4309-4320.
27. **Blower, M. D., B. A. Sullivan, and G. H. Karpen.** 2002. Conserved organization of centromeric chromatin in flies and humans. Dev Cell **2:**319-330.
28. **Bock, L. J., C. Pagliuca, N. Kobayashi, R. A. Grove, Y. Oku, K. Shrestha, C. Alfieri, C. Golfieri, A. Oldani, M. Dal Maschio, R. Bermejo, T. R. Hazbun, T. U. Tanaka, and P. De Wulf.** 2012. Cnn1 inhibits the interactions between the KMN complexes of the yeast kinetochore. Nat Cell Biol **14:**614-624.
29. **Bolzer, A., G. Kreth, I. Solovei, D. Koehler, K. Saracoglu, C. Fauth, S. Muller, R. Eils, C. Cremer, M. R. Speicher, and T. Cremer.** 2005. Three-dimensional maps of all chromosomes in human male fibroblast nuclei and prometaphase rosettes. PLoS Biol **3:**e157.
30. **Borkovich, K. A., L. A. Alex, O. Yarden, M. Freitag, G. E. Turner, N. D. Read, S. Seiler, D. Bell-Pedersen, J. Paietta, N. Plesofsky, M. Plamann, M. Goodrich-Tanrikulu, U. Schulte, G. Mannhaupt, F. E. Nargang, A. Radford, C. Selitrennikoff, J. E. Galagan, J. C. Dunlap, J. J. Loros, D. Catcheside, H. Inoue, R. Aramayo, M. Polymenis, E. U. Selker, M. S. Sachs, G. A. Marzluf, I. Paulsen, R. Davis, D. J. Ebbole, A. Zelter, E. R. Kalkman, R. O'Rourke, F. Bowring, J. Yeadon, C. Ishii, K. Suzuki, W.**

Sakai, and R. Pratt. 2004. Lessons from the Genome Sequence of Neurospora crassa: Tracing the Path from Genomic Blueprint to Multicellular Organism. Microbiol Mol Biol Rev **68:**1-108.

31. **Brinkley, B. R., and E. Stubblefield.** 1966. The fine structure of the kinetochore of a mammalian cell in vitro. Chromosoma **19:**28-43.
32. **Bui, M., E. K. Dimitriadis, C. Hoischen, E. An, D. Quenet, S. Giebe, A. Nita-Lazar, S. Diekmann, and Y. Dalal.** 2012. Cell-cycle-dependent structural transitions in the human CENP-A nucleosome in vivo. Cell **150:**317-326.
33. **Bulut-Karslioglu, A., V. Perrera, M. Scaranaro, I. A. de la Rosa-Velazquez, S. van de Nobelen, N. Shukeir, J. Popow, B. Gerle, S. Opravil, M. Pagani, S. Meidhof, T. Brabletz, T. Manke, M. Lachner, and T. Jenuwein.** 2012. A transcription factor-based mechanism for mouse heterochromatin formation. Nat Struct Mol Biol **19:**1023-1030.
34. **Burrack, L. S., S. E. Applen, and J. Berman.** 2011. The requirement for the Dam1 complex is dependent upon the number of kinetochore proteins and microtubules. Curr Biol **21:**889-896.
35. **Burrack, L. S., and J. Berman.** 2012. Neocentromeres and epigenetically inherited features of centromeres. Chromosome Res **20:**607-619.
36. **Buttrick, G. J., and J. B. Millar.** 2011. Ringing the changes: emerging roles for DASH at the kinetochore-microtubule Interface. Chromosome Res **19:**393-407.
37. **Cai, L., R. Jeewon, and K. D. Hyde.** 2006. Phylogenetic investigations of Sordariaceae based on multiple gene sequences and morphology. Mycol Res **110:**137-150.
38. **Cam, H. P., T. Sugiyama, E. S. Chen, X. Chen, P. C. FitzGerald, and S. I. Grewal.** 2005. Comprehensive analysis of heterochromatin- and RNAi-mediated epigenetic control of the fission yeast genome. Nat Genet **37:**809-819.
39. **Camahort, R., B. Li, L. Florens, S. K. Swanson, M. P. Washburn, and J. L. Gerton.** 2007. Scm3 is essential to recruit the histone h3 variant cse4 to centromeres and to maintain a functional kinetochore. Mol Cell **26:**853-865.
40. **Camahort, R., M. Shivaraju, M. Mattingly, B. Li, S. Nakanishi, D. Zhu, A. Shilatifard, J. L. Workman, and J. L. Gerton.** 2009. Cse4 is part of an octameric nucleosome in budding yeast. Mol Cell **35:**794-805.
41. **Cambareri, E. B., R. Aisner, and J. Carbon.** 1998. Structure of the chromosome VII centromere region in *Neurospora crassa*: degenerate transposons and simple repeats. Mol Cell Biol **18:**5465-5477.
42. **Cambareri, E. B., B. C. Jensen, E. Schabtach, and E. U. Selker.** 1989. Repeat-induced G-C to A-T mutations in *Neurospora*. Science **244:**1571-1575.
43. **Cardinale, S., J. H. Bergmann, D. Kelly, M. Nakano, M. M. Valdivia, H. Kimura, H. Masumoto, V. Larionov, and W. C. Earnshaw.** 2009. Hierarchical inactivation of a synthetic human kinetochore by a chromatin modifier. Mol Biol Cell **20:**4194-4204.
44. **Carroll, C. W., K. J. Milks, and A. F. Straight.** 2010. Dual recognition of CENP-A nucleosomes is required for centromere assembly. J Cell Biol **189:**1143-1155.

45. **Carroll, C. W., M. C. Silva, K. M. Godek, L. E. Jansen, and A. F. Straight.** 2009. Centromere assembly requires the direct recognition of CENP-A nucleosomes by CENP-N. Nat Cell Biol **11:**896-902.
46. **Case, M. E., and N. H. Giles.** 1958. EVIDENCE FROM TETRAD ANALYSIS FOR BOTH NORMAL AND ABERRANT RECOMBINATION BETWEEN ALLELIC MUTANTS IN Neurospora Crassa. Proc Natl Acad Sci U S A **44:**378-390.
47. **Centola, M., and J. Carbon.** 1994. Cloning and characterization of centromeric DNA from *Neurospora crassa*. Mol. Cell. Biol. **14:**1510-1519.
48. **Cheeseman, I. M., J. S. Chappie, E. M. Wilson-Kubalek, and A. Desai.** 2006. The conserved KMN network constitutes the core microtubule-binding site of the kinetochore. Cell **127:**983-997.
49. **Cheeseman, I. M., S. Niessen, S. Anderson, F. Hyndman, J. R. Yates, 3rd, K. Oegema, and A. Desai.** 2004. A conserved protein network controls assembly of the outer kinetochore and its ability to sustain tension. Genes Dev **18:**2255-2268.
50. **Chen, E. S., S. Saitoh, M. Yanagida, and K. Takahashi.** 2003. A cell cycle-regulated GATA factor promotes centromeric localization of CENP-A in fission yeast. Mol Cell **11:**175-187.
51. **Chen, Y., R. E. Baker, K. C. Keith, K. Harris, S. Stoler, and M. Fitzgerald-Hayes.** 2000. The N terminus of the centromere H3-like protein Cse4p performs an essential function distinct from that of the histone fold domain. Mol Cell Biol **20:**7037-7048.
52. **Cho, U. S., and S. C. Harrison.** 2011. Recognition of the centromere-specific histone Cse4 by the chaperone Scm3. Proc Natl Acad Sci U S A **108:**9367-9371.
53. **Cipriany, B. R., R. Zhao, P. J. Murphy, S. L. Levy, C. P. Tan, H. G. Craighead, and P. D. Soloway.** 2010. Single molecule epigenetic analysis in a nanofluidic channel. Anal Chem **82:**2480-2487.
54. **Cleveland, D. W., Y. Mao, and K. F. Sullivan.** 2003. Centromeres and kinetochores: from epigenetics to mitotic checkpoint signaling. Cell **112:**407-421.
55. **Cohen, R. L., C. W. Espelin, P. De Wulf, P. K. Sorger, S. C. Harrison, and K. T. Simons.** 2008. Structural and functional dissection of Mif2p, a conserved DNA-binding kinetochore protein. Mol Biol Cell **19:**4480-4491.
56. **Coleman, J. J., S. D. Rounsley, M. Rodriguez-Carres, A. Kuo, C. C. Wasmann, J. Grimwood, J. Schmutz, M. Taga, G. J. White, S. Zhou, D. C. Schwartz, M. Freitag, L. J. Ma, E. G. Danchin, B. Henrissat, P. M. Coutinho, D. R. Nelson, D. Straney, C. A. Napoli, B. M. Barker, M. Gribskov, M. Rep, S. Kroken, I. Molnar, C. Rensing, J. C. Kennell, J. Zamora, M. L. Farman, E. U. Selker, A. Salamov, H. Shapiro, J. Pangilinan, E. Lindquist, C. Lamers, I. V. Grigoriev, D. M. Geiser, S. F. Covert, E. Temporini, and H. D. Vanetten.** 2009. The genome of Nectria haematococca: contribution of supernumerary chromosomes to gene expansion. PLoS Genet **5:**e1000618.
57. **Colot, H. V., G. Park, G. E. Turner, C. Ringelberg, C. M. Crew, L. Litvinkova, R. L. Weiss, K. A. Borkovich, and J. C. Dunlap.** 2006. A high-

throughput gene knockout procedure for Neurospora reveals functions for multiple transcription factors. Proc Natl Acad Sci U S A.

58. **Copenhaver, G. P., K. Nickel, T. Kuromori, M. I. Benito, S. Kaul, X. Lin, M. Bevan, G. Murphy, B. Harris, L. D. Parnell, W. R. McCombie, R. A. Martienssen, M. Marra, and D. Preuss.** 1999. Genetic definition and sequence analysis of Arabidopsis centromeres. Science **286:**2468-2474.
59. **Coppin, E., R. Debuchy, S. Arnaise, and M. Picard.** 1997. Mating types and sexual development in filamentous ascomycetes. Microbiol Mol Biol Rev **61:**411-428.
60. **Cuomo, C. A., U. Guldener, J. R. Xu, F. Trail, B. G. Turgeon, A. Di Pietro, J. D. Walton, L. J. Ma, S. E. Baker, M. Rep, G. Adam, J. Antoniw, T. Baldwin, S. Calvo, Y. L. Chang, D. Decaprio, L. R. Gale, S. Gnerre, R. S. Goswami, K. Hammond-Kosack, L. J. Harris, K. Hilburn, J. C. Kennell, S. Kroken, J. K. Magnuson, G. Mannhaupt, E. Mauceli, H. W. Mewes, R. Mitterbauer, G. Muehlbauer, M. Munsterkotter, D. Nelson, K. O'Donnell, T. Ouellet, W. Qi, H. Quesneville, M. I. Roncero, K. Y. Seong, I. V. Tetko, M. Urban, C. Waalwijk, T. J. Ward, J. Yao, B. W. Birren, and H. C. Kistler.** 2007. The Fusarium graminearum genome reveals a link between localized polymorphism and pathogen specialization. Science **317:**1400-1402.
61. **Dalal, Y., T. Furuyama, D. Vermaak, and S. Henikoff.** 2007. Structure, dynamics, and evolution of centromeric nucleosomes. Proc Natl Acad Sci U S A **104:**15974-15981.
62. **Dalal, Y., H. Wang, S. Lindsay, and S. Henikoff.** 2007. Tetrameric structure of centromeric nucleosomes in interphase Drosophila cells. PLoS Biol **5:**e218.
63. **Dam, M., and K. Gerdes.** 1994. Partitioning of plasmid R1. Ten direct repeats flanking the parA promoter constitute a centromere-like partition site parC, that expresses incompatibility. J Mol Biol **236:**1289-1298.
64. **Davila Lopez, M., and T. Samuelsson.** 2008. Early evolution of histone mRNA 3' end processing. RNA **14:**1-10.
65. **Davis, R. H.** 2000. Neurospora: Contributions of a Model Organism. Oxford University Press.
66. **De Rop, V., A. Padeganeh, and P. S. Maddox.** 2012. CENP-A: the key player behind centromere identity, propagation, and kinetochore assembly. Chromosoma.
67. **De Souza, C. P., A. H. Osmani, S. B. Hashmi, and S. A. Osmani.** 2004. Partial nuclear pore complex disassembly during closed mitosis in Aspergillus nidulans. Curr Biol **14:**1973-1984.
68. **De Souza, C. P., and S. A. Osmani.** 2007. Mitosis, not just open or closed. Eukaryot Cell **6:**1521-1527.
69. **de Wit, E., and W. de Laat.** 2012. A decade of 3C technologies: insights into nuclear organization. Genes Dev **26:**11-24.
70. **Dechassa, M. L., K. Wyns, M. Li, M. A. Hall, M. D. Wang, and K. Luger.** 2011. Structure and Scm3-mediated assembly of budding yeast centromeric nucleosomes. Nat Commun **2:**313.
71. **Dettman, J. R., F. M. Harbinski, and J. W. Taylor.** 2001. Ascospore morphology is a poor predictor of the phylogenetic relationships of Neurospora and Gelasinospora. Fungal Genet Biol **34:**49-61.

72. **Dimitriadis, E. K., C. Weber, R. K. Gill, S. Diekmann, and Y. Dalal.** 2010. Tetrameric organization of vertebrate centromeric nucleosomes. Proc Natl Acad Sci U S A **107:**20317-20322.
73. **Dominski, Z., and W. F. Marzluff.** 2007. Formation of the 3' end of histone mRNA: getting closer to the end. Gene **396:**373-390.
74. **Drinnenberg, I. A., D. E. Weinberg, K. T. Xie, J. P. Mower, K. H. Wolfe, G. R. Fink, and D. P. Bartel.** 2009. RNAi in budding yeast. Science **326:**544-550.
75. **Du, Y., C. N. Topp, and R. K. Dawe.** 2010. DNA binding of centromere protein C (CENPC) is stabilized by single-stranded RNA. PLoS Genet **6:**e1000835.
76. **Dubin, M., J. Fuchs, R. Graf, I. Schubert, and W. Nellen.** 2010. Dynamics of a novel centromeric histone variant CenH3 reveals the evolutionary ancestral timing of centromere biogenesis. Nucleic Acids Res **38:**7526-7537.
77. **Dunleavy, E. M., G. Almouzni, and G. H. Karpen.** 2011. H3.3 is deposited at centromeres in S phase as a placeholder for newly assembled CENP-A in G(1) phase. Nucleus **2:**146-157.
78. **Dunleavy, E. M., A. L. Pidoux, M. Monet, C. Bonilla, W. Richardson, G. L. Hamilton, K. Ekwall, P. J. McLaughlin, and R. C. Allshire.** 2007. A NASP (N1/N2)-related protein, Sim3, binds CENP-A and is required for its deposition at fission yeast centromeres. Mol Cell **28:**1029-1044.
79. **Dunleavy, E. M., D. Roche, H. Tagami, N. Lacoste, D. Ray-Gallet, Y. Nakamura, Y. Daigo, Y. Nakatani, and G. Almouzni-Pettinotti.** 2009. HJURP is a cell-cycle-dependent maintenance and deposition factor of CENP-A at centromeres. Cell **137:**485-497.
80. **Earnshaw, W., B. Bordwell, C. Marino, and N. Rothfield.** 1986. Three human chromosomal autoantigens are recognized by sera from patients with anti-centromere antibodies. J Clin Invest **77:**426-430.
81. **Edwards, N. S., and A. W. Murray.** 2005. Identification of xenopus CENP-A and an associated centromeric DNA repeat. Mol Biol Cell **16:**1800-1810.
82. **Ehinger, A., S. H. Denison, and G. S. May.** 1990. Sequence, organization and expression of the core histone genes of *Aspergillus nidulans*. Mol Gen Genet **222:**416-424.
83. **Enserink, J. M., and R. D. Kolodner.** 2010. An overview of Cdk1-controlled targets and processes. Cell Div **5:**11.
84. **Erhardt, S., B. G. Mellone, C. M. Betts, W. Zhang, G. H. Karpen, and A. F. Straight.** 2008. Genome-wide analysis reveals a cell cycle-dependent mechanism controlling centromere propagation. J Cell Biol **183:**805-818.
85. **Eskat, A., W. Deng, A. Hofmeister, S. Rudolphi, S. Emmerth, D. Hellwig, T. Ulbricht, V. Doring, J. M. Bancroft, A. D. McAinsh, M. C. Cardoso, P. Meraldi, C. Hoischen, H. Leonhardt, and S. Diekmann.** 2012. Step-Wise Assembly, Maturation and Dynamic Behavior of the Human CENP-P/O/R/Q/U Kinetochore Sub-Complex. PLoS One **7:**e44717.
86. **Fedorova, N. D., N. Khaldi, V. S. Joardar, R. Maiti, P. Amedeo, M. J. Anderson, J. Crabtree, J. C. Silva, J. H. Badger, A. Albarraq, S. Angiuoli, H. Bussey, P. Bowyer, P. J. Cotty, P. S. Dyer, A. Egan, K. Galens, C. M. Fraser-Liggett, B. J. Haas, J. M. Inman, R. Kent, S. Lemieux, I. Malavazi, J. Orvis, T. Roemer, C. M. Ronning, J. P. Sundaram, G. Sutton, G. Turner,**

J. C. Venter, O. R. White, B. R. Whitty, P. Youngman, K. H. Wolfe, G. H. Goldman, J. R. Wortman, B. Jiang, D. W. Denning, and W. C. Nierman. 2008. Genomic islands in the pathogenic filamentous fungus Aspergillus fumigatus. PLoS Genet **4:**e1000046.

87. **Felsenstein, J.** 1985. Confidence limits on Phylogenies: An approach using the Bootstrap. Evolution **39:**783-791.
88. **Feng, H., Z. Zhou, B. R. Zhou, and Y. Bai.** 2011. Structure of the budding yeast Saccharomyces cerevisiae centromeric histones Cse4-H4 complexed with the chaperone Scm3. Proc Natl Acad Sci U S A **108:**E596; author reply E597.
89. **Foltz, D. R., L. E. Jansen, A. O. Bailey, J. R. Yates, 3rd, E. A. Bassett, S. Wood, B. E. Black, and D. W. Cleveland.** 2009. Centromere-specific assembly of CENP-a nucleosomes is mediated by HJURP. Cell **137:**472-484.
90. **Foltz, D. R., L. E. Jansen, B. E. Black, A. O. Bailey, J. R. Yates, 3rd, and D. W. Cleveland.** 2006. The human CENP-A centromeric nucleosome-associated complex. Nat Cell Biol **8:**458-469.
91. **Franco, A., J. C. Meadows, and J. B. Millar.** 2007. The Dam1/DASH complex is required for the retrieval of unclustered kinetochores in fission yeast. J Cell Sci **120:**3345-3351.
92. **Fraschini, R., E. Formenti, G. Lucchini, and S. Piatti.** 1999. Budding yeast Bub2 is localized at spindle pole bodies and activates the mitotic checkpoint via a different pathway from Mad2. J Cell Biol **145:**979-991.
93. **Freitag, M., P. C. Hickey, T. K. Khlafallah, N. D. Read, and E. U. Selker.** 2004. HP1 is essential for DNA methylation in Neurospora. Mol Cell **13:**427-434.
94. **Freitag, M., P. C. Hickey, N. B. Raju, E. U. Selker, and N. D. Read.** 2004. GFP as a tool to analyze the organization, dynamics and function of nuclei and microtubules in Neurospora crassa. Fungal Genet Biol **41:**897-910.
95. **Freitag, M., R. L. Williams, G. O. Kothe, and E. U. Selker.** 2002. A cytosine methyltransferase homologue is essential for repeat-induced point mutation in *Neurospora crassa*. Proc Natl Acad Sci U S A **99:**8802-8807.
96. **Funabiki, H., I. Hagan, S. Uzawa, and M. Yanagida.** 1993. Cell cycle-dependent specific positioning and clustering of centromeres and telomeres in fission yeast. J Cell Biol **121:**961-976.
97. **Galagan, J. E., S. E. Calvo, K. A. Borkovich, E. U. Selker, N. D. Read, D. Jaffe, W. FitzHugh, L. J. Ma, S. Smirnov, S. Purcell, B. Rehman, T. Elkins, R. Engels, S. Wang, C. B. Nielsen, J. Butler, M. Endrizzi, D. Qui, P. Ianakiev, D. Bell-Pedersen, M. A. Nelson, M. Werner-Washburne, C. P. Selitrennikoff, J. A. Kinsey, E. L. Braun, A. Zelter, U. Schulte, G. O. Kothe, G. Jedd, W. Mewes, C. Staben, E. Marcotte, D. Greenberg, A. Roy, K. Foley, J. Naylor, N. Stange-Thomann, R. Barrett, S. Gnerre, M. Kamal, M. Kamvysselis, E. Mauceli, C. Bielke, S. Rudd, D. Frishman, S. Krystofova, C. Rasmussen, R. L. Metzenberg, D. D. Perkins, S. Kroken, C. Cogoni, G. Macino, D. Catcheside, W. Li, R. J. Pratt, S. A. Osmani, C. P. DeSouza, L. Glass, M. J. Orbach, J. A. Berglund, R. Voelker, O. Yarden, M. Plamann, S. Seiler, J. Dunlap, A. Radford, R. Aramayo, D. O. Natvig, L. A. Alex, G. Mannhaupt, D. J. Ebbole, M. Freitag, I. Paulsen, M.**

S. Sachs, E. S. Lander, C. Nusbaum, and B. Birren. 2003. The genome sequence of the filamentous fungus Neurospora crassa. Nature **422:**859-868.

98. **Galagan, J. E., S. E. Calvo, C. Cuomo, L. J. Ma, J. R. Wortman, S. Batzoglou, S. I. Lee, M. Basturkmen, C. C. Spevak, J. Clutterbuck, V. Kapitonov, J. Jurka, C. Scazzocchio, M. Farman, J. Butler, S. Purcell, S. Harris, G. H. Braus, O. Draht, S. Busch, C. D'Enfert, C. Bouchier, G. H. Goldman, D. Bell-Pedersen, S. Griffiths-Jones, J. H. Doonan, J. Yu, K. Vienken, A. Pain, M. Freitag, E. U. Selker, D. B. Archer, M. A. Penalva, B. R. Oakley, M. Momany, T. Tanaka, T. Kumagai, K. Asai, M. Machida, W. C. Nierman, D. W. Denning, M. Caddick, M. Hynes, M. Paoletti, R. Fischer, B. Miller, P. Dyer, M. S. Sachs, S. A. Osmani, and B. W. Birren.** 2005. Sequencing of Aspergillus nidulans and comparative analysis with A. fumigatus and A. oryzae. Nature **438:**1105-1115.

99. **Gale, C. A., M. D. Leonard, K. R. Finley, L. Christensen, M. McClellan, D. Abbey, C. Kurischko, E. Bensen, I. Tzafrir, S. Kauffman, J. Becker, and J. Berman.** 2009. SLA2 mutations cause SWE1-mediated cell cycle phenotypes in Candida albicans and Saccharomyces cerevisiae. Microbiology **155:**3847-3859.

100. **Garcia, D., A. M. Stchigel, J. Cano, J. Guarro, and D. L. Hawksworth.** 2004. A synopsis and re-circumscription of Neurospora (syn. Gelasinospora) based on ultrastructural and 28S rDNA sequence data. Mycol Res **108:**1119-1142.

101. **Gascoigne, K. E., and I. M. Cheeseman.** 2012. T time for point centromeres. Nat Cell Biol **14:**559-561.

102. **Gascoigne, K. E., K. Takeuchi, A. Suzuki, T. Hori, T. Fukagawa, and I. M. Cheeseman.** 2011. Induced ectopic kinetochore assembly bypasses the requirement for CENP-A nucleosomes. Cell **145:**410-422.

103. **Gent, J. I., K. L. Schneider, C. N. Topp, C. Rodriguez, G. G. Presting, and R. K. Dawe.** 2011. Distinct influences of tandem repeats and retrotransposons on CENH3 nucleosome positioning. Epigenetics Chromatin **4:**3.

104. **Gladfelter, A. S.** 2006. Nuclear anarchy: asynchronous mitosis in multinucleated fungal hyphae. Curr Opin Microbiol **9:**547-552.

105. **Glynn, M., A. Kaczmarczyk, L. Prendergast, N. Quinn, and K. F. Sullivan.** 2010. Centromeres: assembling and propagating epigenetic function. Subcell Biochem **50:**223-249.

106. **Gonzalez-Barrios, R., E. Soto-Reyes, and L. A. Herrera.** 2012. Assembling pieces of the centromere epigenetics puzzle. Epigenetics **7:**3-13.

107. **Goodwin, S. B., B. M'Barek S, B. Dhillon, A. H. Wittenberg, C. F. Crane, J. K. Hane, A. J. Foster, T. A. Van der Lee, J. Grimwood, A. Aerts, J. Antoniw, A. Bailey, B. Bluhm, J. Bowler, J. Bristow, A. van der Burgt, B. Canto-Canche, A. C. Churchill, L. Conde-Ferraez, H. J. Cools, P. M. Coutinho, M. Csukai, P. Dehal, P. De Wit, B. Donzelli, H. C. van de Geest, R. C. van Ham, K. E. Hammond-Kosack, B. Henrissat, A. Kilian, A. K. Kobayashi, E. Koopmann, Y. Kourmpetis, A. Kuzniar, E. Lindquist, V. Lombard, C. Maliepaard, N. Martins, R. Mehrabi, J. P. Nap, A. Ponomarenko, J. J. Rudd, A. Salamov, J. Schmutz, H. J. Schouten, H. Shapiro, I. Stergiopoulos, S. F. Torriani, H. Tu, R. P. de Vries, C. Waalwijk, S. B. Ware, A. Wiebenga, L. H. Zwiers, R. P. Oliver, I. V.**

Grigoriev, and G. H. Kema. 2011. Finished genome of the fungal wheat pathogen Mycosphaerella graminicola reveals dispensome structure, chromosome plasticity, and stealth pathogenesis. PLoS Genet **7:**e1002070.

108. **Goto, B., K. Okazaki, and O. Niwa.** 2001. Cytoplasmic microtubular system implicated in de novo formation of a Rabl-like orientation of chromosomes in fission yeast. J Cell Sci **114:**2427-2435.
109. **Guse, A., C. W. Carroll, B. Moree, C. J. Fuller, and A. F. Straight.** 2011. In vitro centromere and kinetochore assembly on defined chromatin templates. Nature **477:**354-358.
110. **Hall, L. E., S. E. Mitchell, and R. J. O'Neill.** 2012. Pericentric and centromeric transcription: a perfect balance required. Chromosome Res **20:**535-546.
111. **Hall, S. E., G. Kettler, and D. Preuss.** 2003. Centromere satellites from Arabidopsis populations: maintenance of conserved and variable domains. Genome Res **13:**195-205.
112. **Hansjakob, A., M. Riederer, and U. Hildebrandt.** 2012. Appressorium morphogenesis and cell cycle progression are linked in the grass powdery mildew fungus Blumeria graminis. Fungal Biol **116:**890-901.
113. **Harris, S. D., and M. Momany.** 2004. Polarity in filamentous fungi: moving beyond the yeast paradigm. Fungal Genet Biol **41:**391-400.
114. **Hays, S. M., J. Swanson, and E. U. Selker.** 2002. Identification and characterization of the genes encoding the core histones and histone variants of *Neurospora crassa*. Genetics **160:**961-973.
115. **Hemmerich, P., S. Weidtkamp-Peters, C. Hoischen, L. Schmiedeberg, I. Erliandri, and S. Diekmann.** 2008. Dynamics of inner kinetochore assembly and maintenance in living cells. J Cell Biol **180:**1101-1114.
116. **Henikoff, S., K. Ahmad, and H. S. Malik.** 2001. The centromere paradox: stable inheritance with rapidly evolving DNA. Science **293:**1098-1102.
117. **Henikoff, S., K. Ahmad, J. S. Platero, and B. van Steensel.** 2000. Heterochromatic deposition of centromeric histone H3-like proteins. PNAS **97:**716-721.
118. **Hennemuth, B., and K. A. Marx.** 2006. DNA deformability changes of single base pair mutants within CDE binding sites in S. Cerevisiae centromere DNA correlate with measured chromosomal loss rates and CDE binding site symmetries. BMC Mol Biol **7:**12.
119. **Hoeijmakers, W. A., C. Flueck, K. J. Francoijs, A. H. Smits, J. Wetzel, J. C. Volz, A. F. Cowman, T. Voss, H. G. Stunnenberg, and R. Bartfai.** 2012. Plasmodium falciparum centromeres display a unique epigenetic makeup and cluster prior to and during schizogony. Cell Microbiol **14:**1391-1401.
120. **Honda, S., and E. U. Selker.** 2009. Tools for fungal proteomics: multifunctional neurospora vectors for gene replacement, protein expression and protein purification. Genetics **182:**11-23.
121. **Hori, T., M. Amano, A. Suzuki, C. B. Backer, J. P. Welburn, Y. Dong, B. F. McEwen, W. H. Shang, E. Suzuki, K. Okawa, I. M. Cheeseman, and T. Fukagawa.** 2008. CCAN makes multiple contacts with centromeric DNA to provide distinct pathways to the outer kinetochore. Cell **135:**1039-1052.
122. **Hori, T., and T. Fukagawa.** 2012. Establishment of the vertebrate kinetochores. Chromosome Res **20:**547-561.

123. **Hori, T., M. Okada, K. Maenaka, and T. Fukagawa.** 2008. CENP-O class proteins form a stable complex and are required for proper kinetochore function. Mol Biol Cell **19:**843-854.
124. **Hou, H., Y. Wang, S. P. Kallgren, J. Thompson, J. R. Yates, 3rd, and S. Jia.** 2010. Histone variant H2A.Z regulates centromere silencing and chromosome segregation in fission yeast. J Biol Chem **285:**1909-1918.
125. **Hsu, K. S., and T. Toda.** 2011. Ndc80 internal loop interacts with Dis1/TOG to ensure proper kinetochore-spindle attachment in fission yeast. Curr Biol **21:**214-220.
126. **Hu, H., Y. Liu, M. Wang, J. Fang, H. Huang, N. Yang, Y. Li, J. Wang, X. Yao, Y. Shi, G. Li, and R. M. Xu.** 2011. Structure of a CENP-A-histone H4 heterodimer in complex with chaperone HJURP. Genes Dev **25:**901-906.
127. **Ishii, K.** 2009. Conservation and divergence of centromere specification in yeast. Curr Opin Microbiol **12:**616-622.
128. **Ishii, K., Y. Ogiyama, Y. Chikashige, S. Soejima, F. Masuda, T. Kakuma, Y. Hiraoka, and K. Takahashi.** 2008. Heterochromatin integrity affects chromosome reorganization after centromere dysfunction. Science **321:**1088-1091.
129. **Jaco, I., A. Canela, E. Vera, and M. A. Blasco.** 2008. Centromere mitotic recombination in mammalian cells. J Cell Biol **181:**885-892.
130. **Jakopec, V., B. Topolski, and U. Fleig.** 2012. Sos7, an essential component of the conserved Schizosaccharomyces pombe Ndc80-MIND-Spc7 complex, identifies a new family of fungal kinetochore proteins. Mol Cell Biol **32:**3308-3320.
131. **James, T. C., and S. C. Elgin.** 1986. Identification of a nonhistone chromosomal protein associated with heterochromatin in Drosophila melanogaster and its gene. Mol Cell Biol **6:**3862-3872.
132. **James, T. Y., F. Kauff, C. L. Schoch, P. B. Matheny, V. Hofstetter, C. J. Cox, G. Celio, C. Gueidan, E. Fraker, J. Miadlikowska, H. T. Lumbsch, A. Rauhut, V. Reeb, A. E. Arnold, A. Amtoft, J. E. Stajich, K. Hosaka, G. H. Sung, D. Johnson, B. O'Rourke, M. Crockett, M. Binder, J. M. Curtis, J. C. Slot, Z. Wang, A. W. Wilson, A. Schussler, J. E. Longcore, K. O'Donnell, S. Mozley-Standridge, D. Porter, P. M. Letcher, M. J. Powell, J. W. Taylor, M. M. White, G. W. Griffith, D. R. Davies, R. A. Humber, J. B. Morton, J. Sugiyama, A. Y. Rossman, J. D. Rogers, D. H. Pfister, D. Hewitt, K. Hansen, S. Hambleton, R. A. Shoemaker, J. Kohlmeyer, B. Volkmann-Kohlmeyer, R. A. Spotts, M. Serdani, P. W. Crous, K. W. Hughes, K. Matsuura, E. Langer, G. Langer, W. A. Untereiner, R. Lucking, B. Budel, D. M. Geiser, A. Aptroot, P. Diederich, I. Schmitt, M. Schultz, R. Yahr, D. S. Hibbett, F. Lutzoni, D. J. McLaughlin, J. W. Spatafora, and R. Vilgalys.** 2006. Reconstructing the early evolution of Fungi using a six-gene phylogeny. Nature **443:**818-822.
133. **Janke, C., J. Ortiz, T. U. Tanaka, J. Lechner, and E. Schiebel.** 2002. Four new subunits of the Dam1-Duo1 complex reveal novel functions in sister kinetochore biorientation. Embo J **21:**181-193.
134. **Jansen, L. E., B. E. Black, D. R. Foltz, and D. W. Cleveland.** 2007. Propagation of centromeric chromatin requires exit from mitosis. J Cell Biol **176:**795-805.

135. **Jensen, R. B., R. Lurz, and K. Gerdes.** 1998. Mechanism of DNA segregation in prokaryotes: replicon pairing by parC of plasmid R1. Proc Natl Acad Sci U S A **95:**8550-8555.
136. **Jin, Q. W., J. Fuchs, and J. Loidl.** 2000. Centromere clustering is a major determinant of yeast interphase nuclear organization. J Cell Sci **113 (Pt 11):**1903-1912.
137. **Joglekar, A. P., K. S. Bloom, and E. D. Salmon.** 2010. Mechanisms of force generation by end-on kinetochore-microtubule attachments. Curr Opin Cell Biol **22:**57-67.
138. **Joglekar, A. P., D. Bouck, K. Finley, X. Liu, Y. Wan, J. Berman, X. He, E. D. Salmon, and K. S. Bloom.** 2008. Molecular architecture of the kinetochore-microtubule attachment site is conserved between point and regional centromeres. J Cell Biol **181:**587-594.
139. **Jokelainen, P. T.** 1967. The ultrastructure and spatial organization of the metaphase kinetochore in mitotic rat cells. J Ultrastruct Res **19:**19-44.
140. **Jorgensen, P., and M. Tyers.** 2004. How cells coordinate growth and division. Curr Biol **14:**R1014-1027.
141. **Kalitsis, P., and K. H. Choo.** 2009. Orchestrating twosome and foursome chromosome parties. Dev Cell **17:**305-307.
142. **Kawashima, S., Y. Nakabayashi, K. Matsubara, N. Sano, T. Enomoto, K. Tanaka, M. Seki, and M. Horikoshi.** 2011. Global analysis of core histones reveals nucleosomal surfaces required for chromosome bi-orientation. EMBO J **30:**3353-3367.
143. **Keith, K. C., R. E. Baker, Y. Chen, K. Harris, S. Stoler, and M. Fitzgerald-Hayes.** 1999. Analysis of primary structural determinants that distinguish the centromere-specific function of histone variant Cse4p from histone H3. Mol Cell Biol **19:**6130-6139.
144. **Kerres, A., V. Jakopec, C. Beuter, I. Karig, J. Pohlmann, A. Pidoux, R. Allshire, and U. Fleig.** 2006. Fta2, an essential fission yeast kinetochore component, interacts closely with the conserved Mal2 protein. Mol Biol Cell **17:**4167-4178.
145. **Kerres, A., V. Jakopec, and U. Fleig.** 2007. The conserved Spc7 protein is required for spindle integrity and links kinetochore complexes in fission yeast. Mol Biol Cell **18:**2441-2454.
146. **Ketel, C., H. S. Wang, M. McClellan, K. Bouchonville, A. Selmecki, T. Lahav, M. Gerami-Nejad, and J. Berman.** 2009. Neocentromeres form efficiently at multiple possible loci in Candida albicans. PLoS Genet **5:**e1000400.
147. **Kiso, T., K. Fujita, X. Ping, T. Tanaka, and M. Taniguchi.** 2004. Screening for microtubule-disrupting antifungal agents by using a mitotic-arrest mutant of Aspergillus nidulans and novel action of phenylalanine derivatives accompanying tubulin loss. Antimicrob Agents Chemother **48:**1739-1748.
148. **Kniola, B., E. O'Toole, J. R. McIntosh, B. Mellone, R. Allshire, S. Mengarelli, K. Hultenby, and K. Ekwall.** 2001. The domain structure of centromeres is conserved from fission yeast to humans. Mol Biol Cell **12:**2767-2775.
149. **Kobayashi, Y., S. Saitoh, Y. Ogiyama, S. Soejima, and K. Takahashi.** 2007. The fission yeast DASH complex is essential for satisfying the spindle

assembly checkpoint induced by defects in the inner-kinetochore proteins. Genes Cells **12:**311-328.

150. **Koren, A., H. J. Tsai, I. Tirosh, L. S. Burrack, N. Barkai, and J. Berman.** 2010. Epigenetically-inherited centromere and neocentromere DNA replicates earliest in S-phase. PLoS Genet **6:**e1001068.
151. **Krogan, N. J., K. Baetz, M. C. Keogh, N. Datta, C. Sawa, T. C. Kwok, N. J. Thompson, M. G. Davey, J. Pootoolal, T. R. Hughes, A. Emili, S. Buratowski, P. Hieter, and J. F. Greenblatt.** 2004. Regulation of chromosome stability by the histone H2A variant Htz1, the Swr1 chromatin remodeling complex, and the histone acetyltransferase NuA4. Proc Natl Acad Sci U S A **101:**13513-13518.
152. **Kumekawa, N., N. Ohmido, K. Fukui, E. Ohtsubo, and H. Ohtsubo.** 2001. A new gypsy-type retrotransposon, RIRE7: preferential insertion into the tandem repeat sequence TrsD in pericentromeric heterochromatin regions of rice chromosomes. Mol Genet Genomics **265:**480-488.
153. **Kwon, M. S., T. Hori, M. Okada, and T. Fukagawa.** 2007. CENP-C is involved in chromosome segregation, mitotic checkpoint function, and kinetochore assembly. Mol Biol Cell **18:**2155-2168.
154. **Kwon, Y. H., Hoch, H.C.** 1991. Temporal and spatial dynamics of ap-pressorium formation in Uromyces appendiculatus. Experimental Mycology **15:**116 - 131.
155. **Lam, A. L., C. D. Boivin, C. F. Bonney, M. K. Rudd, and B. A. Sullivan.** 2006. Human centromeric chromatin is a dynamic chromosomal domain that can spread over noncentromeric DNA. Proc Natl Acad Sci U S A **103:**4186-4191.
156. **Lamb, J. C., W. Yu, F. Han, and J. A. Birchler.** 2007. Plant chromosomes from end to end: telomeres, heterochromatin and centromeres. Curr Opin Plant Biol **10:**116-122.
157. **Lampson, M. A., and T. M. Kapoor.** 2005. The human mitotic checkpoint protein BubR1 regulates chromosome-spindle attachments. Nat Cell Biol **7:**93-98.
158. **Lermontova, I., O. Koroleva, T. Rutten, J. Fuchs, V. Schubert, I. Moraes, D. Koszegi, and I. Schubert.** 2011. Knock down of CENH3 in Arabidopsis reduces mitotic divisions and causes sterility by disturbed meiotic chromosome segregation. Plant J.
159. **Lermontova, I., T. Rutten, and I. Schubert.** 2011. Deposition, turnover, and release of CENH3 at Arabidopsis centromeres. Chromosoma **120:**633-640.
160. **Lermontova, I., V. Schubert, J. Fuchs, S. Klatte, J. Macas, and I. Schubert.** 2006. Loading of Arabidopsis centromeric histone CENH3 occurs mainly during G2 and requires the presence of the histone fold domain. Plant Cell **18:**2443-2451.
161. **Lewis, Z. A., K. K. Adhvaryu, S. Honda, A. L. Shiver, M. Knip, R. Sack, and E. U. Selker.** 2010. DNA methylation and normal chromosome behavior in Neurospora depend on five components of a histone methyltransferase complex, DCDC. PLoS Genet **6:**e1001196.
162. **Lewis, Z. A., S. Honda, T. K. Khlafallah, J. K. Jeffress, M. Freitag, F. Mohn, D. Schubeler, and E. U. Selker.** 2009. Relics of repeat-induced point

mutation direct heterochromatin formation in Neurospora crassa. Genome Res **19:**427-437.

163. **Li, H., and R. Durbin.** 2009. Fast and accurate short read alignment with Burrows-Wheeler transform. Bioinformatics **25:**1754-1760.
164. **Li, Y. Y., and Y. Z. Zhao.** 2003. [A simple method to correct genetic distance between linked genes and a correction of calculating data in tetrad analysis in Neurospora crassa]. Yi Chuan **25:**330-332.
165. **Lieberman-Aiden, E., N. L. van Berkum, L. Williams, M. Imakaev, T. Ragoczy, A. Telling, I. Amit, B. R. Lajoie, P. J. Sabo, M. O. Dorschner, R. Sandstrom, B. Bernstein, M. A. Bender, M. Groudine, A. Gnirke, J. Stamatoyannopoulos, L. A. Mirny, E. S. Lander, and J. Dekker.** 2009. Comprehensive mapping of long-range interactions reveals folding principles of the human genome. Science **326:**289-293.
166. **Liebman, S. W., L. S. Symington, and T. D. Petes.** 1988. Mitotic recombination within the centromere of a yeast chromosome. Science **241:**1074-1077.
167. **Lippman, Z., and R. Martienssen.** 2004. The role of RNA interference in heterochromatic silencing. Nature **431:**364-370.
168. **Liu, D., G. Vader, M. J. Vromans, M. A. Lampson, and S. M. Lens.** 2009. Sensing chromosome bi-orientation by spatial separation of aurora B kinase from kinetochore substrates. Science **323:**1350-1353.
169. **Liu, X., I. McLeod, S. Anderson, J. R. Yates, 3rd, and X. He.** 2005. Molecular analysis of kinetochore architecture in fission yeast. EMBO J **24:**2919-2930.
170. **Loros, J. J., S. A. Denome, and J. C. Dunlap.** 1989. Molecular cloning of genes under control of the circadian clock in *Neurospora*. Science **243:**385-388.
171. **Maggert, K. A., and G. H. Karpen.** 2001. The activation of a neocentromere in Drosophila requires proximity to an endogenous centromere. Genetics **158:**1615-1628.
172. **Malik, H. S.** 2009. The centromere-drive hypothesis: a simple basis for centromere complexity. Prog Mol Subcell Biol **48:**33-52.
173. **Malik, H. S., and S. Henikoff.** 2001. Adaptive evolution of Cid, a centromere-specific histone in Drosophila. Genetics **157:**1293-1298.
174. **Malik, H. S., and S. Henikoff.** 2009. Major evolutionary transitions in centromere complexity. Cell **138:**1067-1082.
175. **Margolin, B. S., M. Freitag, and E. U. Selker.** 1997. Improved plasmids for gene targeting at the *his-3* locus of *Neurospora crassa* by electroporation. Fungal Genetics Newsl. **44:**34-36.
176. **Marshall, O. J., A. C. Chueh, L. H. Wong, and K. H. Choo.** 2008. Neocentromeres: new insights into centromere structure, disease development, and karyotype evolution. Am J Hum Genet **82:**261-282.
177. **Martegani, E., F. Tome, and F. Trezzi.** 1981. Timing of nuclear division cycle in Neurospora crassa. J Cell Sci **48:**127-136.
178. **Marzluff, W. F., E. J. Wagner, and R. J. Duronio.** 2008. Metabolism and regulation of canonical histone mRNAs: life without a poly(A) tail. Nat Rev Genet **9:**843-854.

179. **Mashkova, T., N. Oparina, I. Alexandrov, O. Zinovieva, A. Marusina, Y. Yurov, M. H. Lacroix, and L. Kisselev.** 1998. Unequal cross-over is involved in human alpha satellite DNA rearrangements on a border of the satellite domain. FEBS Lett **441:**451-457.
180. **McClelland, S. E., S. Borusu, A. C. Amaro, J. R. Winter, M. Belwal, A. D. McAinsh, and P. Meraldi.** 2007. The CENP-A NAC/CAD kinetochore complex controls chromosome congression and spindle bipolarity. EMBO J **26:**5033-5047.
181. **McNally, M. T., and S. J. Free.** 1988. Isolation and characterization of a Neurospora glucose-repressible gene. Curr Genet **14:**545-551.
182. **Mellone, B. G., K. J. Grive, V. Shteyn, S. R. Bowers, I. Oderberg, and G. H. Karpen.** 2011. Assembly of Drosophila centromeric chromatin proteins during mitosis. PLoS Genet **7:**e1002068.
183. **Melters, D. P., L. V. Paliulis, I. F. Korf, and S. W. Chan.** 2012. Holocentric chromosomes: convergent evolution, meiotic adaptations, and genomic analysis. Chromosome Res **20:**579-593.
184. **Meluh, P. B., P. Yang, L. Glowczewski, D. Koshland, and M. M. Smith.** 1998. Cse4p is a component of the core centromere of Saccharomyces cerevisiae. Cell **94:**607-613.
185. **Meneghini, M. D., M. Wu, and H. D. Madhani.** 2003. Conserved histone variant H2A.Z protects euchromatin from the ectopic spread of silent heterochromatin. Cell **112:**725-736.
186. **Meraldi, P., A. D. McAinsh, E. Rheinbay, and P. K. Sorger.** 2006. Phylogenetic and structural analysis of centromeric DNA and kinetochore proteins. Genome Biol **7:**R23.
187. **Miao, V. P., M. Freitag, and E. U. Selker.** 2000. Short TpA-rich segments of the zeta-eta region induce DNA methylation in *Neurospora crassa*. J. Mol. Biol. **300:**249-273.
188. **Milks, K. J., B. Moree, and A. F. Straight.** 2009. Dissection of CENP-C-directed centromere and kinetochore assembly. Mol Biol Cell **20:**4246-4255.
189. **Mishra, P. K., W. C. Au, J. S. Choy, P. H. Kuich, R. E. Baker, D. R. Foltz, and M. A. Basrai.** 2011. Misregulation of Scm3p/HJURP causes chromosome instability in Saccharomyces cerevisiae and human cells. PLoS Genet **7:**e1002303.
190. **Mizuguchi, G., H. Xiao, J. Wisniewski, M. M. Smith, and C. Wu.** 2007. Nonhistone Scm3 and Histones CenH3-H4 Assemble the Core of Centromere-Specific Nucleosomes. Cell **129:**1153-1164.
191. **Morey, L., K. Barnes, Y. Chen, M. Fitzgerald-Hayes, and R. E. Baker.** 2004. The histone fold domain of Cse4 is sufficient for CEN targeting and propagation of active centromeres in budding yeast. Eukaryot Cell **3:**1533-1543.
192. **Nagaki, K., Z. Cheng, S. Ouyang, P. B. Talbert, M. Kim, K. M. Jones, S. Henikoff, C. R. Buell, and J. Jiang.** 2004. Sequencing of a rice centromere uncovers active genes. Nat Genet **36:**138-145.
193. **Nagaki, K., K. Kashihara, and M. Murata.** 2005. Visualization of diffuse centromeres with centromere-specific histone H3 in the holocentric plant Luzula nivea. Plant Cell **17:**1886-1893.

194. **Nakajima, Y., A. Cormier, R. G. Tyers, A. Pigula, Y. Peng, D. G. Drubin, and G. Barnes.** 2011. Ipl1/Aurora-dependent phosphorylation of Sli15/INCENP regulates CPC-spindle interaction to ensure proper microtubule dynamics. J Cell Biol **194:**137-153.
195. **Nakano, M., S. Cardinale, V. N. Noskov, R. Gassmann, P. Vagnarelli, S. Kandels-Lewis, V. Larionov, W. C. Earnshaw, and H. Masumoto.** 2008. Inactivation of a human kinetochore by specific targeting of chromatin modifiers. Dev Cell **14:**507-522.
196. **Nasuda, S., S. Hudakova, I. Schubert, A. Houben, and T. R. Endo.** 2005. Stable barley chromosomes without centromeric repeats. Proc Natl Acad Sci U S A **102:**9842-9847.
197. **Nei, M., and S. Kumar.** 2000. Molecular evolution and phylogenetics. Oxford University Press, Oxford, U.K.
198. **Neumann, P., H. Yan, and J. Jiang.** 2007. The centromeric retrotransposons of rice are transcribed and differentially processed by RNA interference. Genetics **176:**749-761.
199. **Ninomiya, Y., K. Suzuki, C. Ishii, and H. Inoue.** 2004. Highly efficient gene replacements in Neurospora strains deficient for nonhomologous end-joining. Proc Natl Acad Sci U S A **101:**12248-12253.
200. **Nishino, T., K. Takeuchi, K. E. Gascoigne, A. Suzuki, T. Hori, T. Oyama, K. Morikawa, I. M. Cheeseman, and T. Fukagawa.** 2012. CENP-T-W-S-X forms a unique centromeric chromatin structure with a histone-like fold. Cell **148:**487-501.
201. **Nogales, E., and V. H. Ramey.** 2009. Structure-function insights into the yeast Dam1 kinetochore complex. J Cell Sci **122:**3831-3836.
202. **Nygren, K., R. Strandberg, A. Wallberg, B. Nabholz, T. Gustafsson, D. Garcia, J. Cano, J. Guarro, and H. Johannesson.** 2011. A comprehensive phylogeny of Neurospora reveals a link between reproductive mode and molecular evolution in fungi. Mol Phylogenet Evol **59:**649-663.
203. **Oegema, K., A. Desai, S. Rybina, M. Kirkham, and A. A. Hyman.** 2001. Functional analysis of kinetochore assembly in Caenorhabditis elegans. J Cell Biol **153:**1209-1226.
204. **Ohkuni, K., and K. Kitagawa.** 2011. Endogenous transcription at the centromere facilitates centromere activity in budding yeast. Curr Biol **21:**1695-1703.
205. **Okada, M., I. M. Cheeseman, T. Hori, K. Okawa, I. X. McLeod, J. R. Yates, 3rd, A. Desai, and T. Fukagawa.** 2006. The CENP-H-I complex is required for the efficient incorporation of newly synthesized CENP-A into centromeres. Nat Cell Biol **8:**446-457.
206. **Okada, T., J. Ohzeki, M. Nakano, K. Yoda, W. R. Brinkley, V. Larionov, and H. Masumoto.** 2007. CENP-B controls centromere formation depending on the chromatin context. Cell **131:**1287-1300.
207. **Padmanabhan, S., J. Thakur, R. Siddharthan, and K. Sanyal.** 2008. Rapid evolution of Cse4p-rich centromeric DNA sequences in closely related pathogenic yeasts, Candida albicans and Candida dubliniensis. Proc Natl Acad Sci U S A **105:**19797-19802.

208. **Palmer, D. K., and R. L. Margolis.** 1985. Kinetochore components recognized by human autoantibodies are present on mononucleosomes. Mol Cell Biol **5:**173-186.
209. **Palmer, D. K., K. O'Day, and R. L. Margolis.** 1989. Biochemical analysis of CENP-A, a centromeric protein with histone-like properties. Prog Clin Biol Res **318:**61-72.
210. **Palmer, D. K., K. O'Day, M. H. Wener, B. S. Andrews, and R. L. Margolis.** 1987. A 17-kD centromere protein (CENP-A) copurifies with nucleosome core particles and with histones. J Cell Biol **104:**805-815.
211. **Panchenko, T., and B. E. Black.** 2009. The epigenetic basis for centromere identity. Prog Mol Subcell Biol **48:**1-32.
212. **Panchenko, T., T. C. Sorensen, C. L. Woodcock, Z. Y. Kan, S. Wood, M. G. Resch, K. Luger, S. W. Englander, J. C. Hansen, and B. E. Black.** 2011. Replacement of histone H3 with CENP-A directs global nucleosome array condensation and loosening of nucleosome superhelical termini. Proc Natl Acad Sci U S A.
213. **Partridge, J. F., B. Borgstrom, and R. C. Allshire.** 2000. Distinct protein interaction domains and protein spreading in a complex centromere. Genes & Development **14:**783-791.
214. **Pearson, C. G., E. Yeh, M. Gardner, D. Odde, E. D. Salmon, and K. Bloom.** 2004. Stable kinetochore-microtubule attachment constrains centromere positioning in metaphase. Curr Biol **14:**1962-1967.
215. **Perkins, D. D.** 1953. The Detection of Linkage in Tetrad Analysis. Genetics **38:**187-197.
216. **Perpelescu, M., and T. Fukagawa.** 2011. The ABCs of CENPs. Chromosoma **120:**425-446.
217. **Pidoux, A. L., S. Uzawa, P. E. Perry, W. Z. Cande, and R. C. Allshire.** 2000. Live analysis of lagging chromosomes during anaphase and their effect on spindle elongation rate in fission yeast. J Cell Sci **113 Pt 23:**4177-4191.
218. **Plohl, M., A. Luchetti, N. Mestrovic, and B. Mantovani.** 2008. Satellite DNAs between selfishness and functionality: structure, genomics and evolution of tandem repeats in centromeric (hetero)chromatin. Gene **409:**72-82.
219. **Polizzi, C., and L. Clarke.** 1991. The chromatin structure of centromeres from fission yeast: Differentiation of the central core that correlates with function. J Cell Biol **112:**191-201.
220. **Pomraning, K. R., K. M. Smith, and M. Freitag.** 2011. Bulk segregant analysis followed by high-throughput sequencing reveals the Neurospora cell cycle gene, ndc-1, to be allelic with the gene for ornithine decarboxylase, spe-1. Eukaryot Cell.
221. **Pomraning, K. R., K. M. Smith, and M. Freitag.** 2009. Genome-wide high throughput analysis of DNA methylation in eukaryotes. Methods **47:**142-150.
222. **Przewloka, M. R., Z. Venkei, V. M. Bolanos-Garcia, J. Debski, M. Dadlez, and D. M. Glover.** 2011. CENP-C is a structural platform for kinetochore assembly. Curr Biol **21:**399-405.
223. **Raffaele, S., and S. Kamoun.** 2012. Genome evolution in filamentous plant pathogens: why bigger can be better. Nat Rev Microbiol **10:**417-430.

224. **Raju, N. B., and D. D. Perkins.** 1994. Diverse programs of ascus development in pseudohomothallic species of *Neurospora, Gelasinospora*, and *Podospora*. Dev Genet **15:**104-118.
225. **Rangasamy, D., L. Berven, P. Ridgway, and D. J. Tremethick.** 2003. Pericentric heterochromatin becomes enriched with H2A.Z during early mammalian development. EMBO J **22:**1599-1607.
226. **Ravi, M., and S. W. Chan.** 2010. Haploid plants produced by centromere-mediated genome elimination. Nature **464:**615-618.
227. **Ravi, M., P. N. Kwong, R. M. Menorca, J. T. Valencia, J. S. Ramahi, J. L. Stewart, R. K. Tran, V. Sundaresan, L. Comai, and S. W. Chan.** 2010. The rapidly evolving centromere-specific histone has stringent functional requirements in Arabidopsis thaliana. Genetics **186:**461-471.
228. **Ravi, M., F. Shibata, J. S. Ramahi, K. Nagaki, C. Chen, M. Murata, and S. W. Chan.** 2011. Meiosis-specific loading of the centromere-specific histone CENH3 in Arabidopsis thaliana. PLoS Genet **7:**e1002121.
229. **Redon, C., D. Pilch, E. Rogakou, O. Sedelnikova, K. Newrock, and W. Bonner.** 2002. Histone H2A variants H2AX and H2AZ. Curr Opin Genet Dev **12:**162-169.
230. **Reinhart, B. J., and D. P. Bartel.** 2002. Small RNAs correspond to centromere heterochromatic repeats. Science **297:**1831. Epub 2002 Aug 1822.
231. **Reyes-Turcu, F. E., K. Zhang, M. Zofall, E. Chen, and S. I. Grewal.** 2011. Defects in RNA quality control factors reveal RNAi-independent nucleation of heterochromatin. Nat Struct Mol Biol **18:**1132-1138.
232. **Ribeiro, S. A., P. Vagnarelli, Y. Dong, T. Hori, B. F. McEwen, T. Fukagawa, C. Flors, and W. C. Earnshaw.** 2010. A super-resolution map of the vertebrate kinetochore. Proc Natl Acad Sci U S A **107:**10484-10489.
233. **Riddle, N. C., A. Minoda, P. V. Kharchenko, A. A. Alekseyenko, Y. B. Schwartz, M. Y. Tolstorukov, A. A. Gorchakov, J. D. Jaffe, C. Kennedy, D. Linder-Basso, S. E. Peach, G. Shanower, H. Zheng, M. I. Kuroda, V. Pirrotta, P. J. Park, S. C. Elgin, and G. H. Karpen.** 2011. Plasticity in patterns of histone modifications and chromosomal proteins in Drosophila heterochromatin. Genome Res **21:**147-163.
234. **Roca, M. G., H. C. Kuo, A. Lichius, M. Freitag, and N. D. Read.** 2010. Nuclear dynamics, mitosis and the cytoskeleton during the early stages of colony initiation in Neurospora crassa. Eukaryot Cell.
235. **Roy, B., L. S. Burrack, M. A. Lone, J. Berman, and K. Sanyal.** 2011. CaMtw1, a member of the evolutionarily conserved Mis12 kinetochore protein family, is required for efficient inner kinetochore assembly in the pathogenic yeast Candida albicans. Mol Microbiol **80:**14-32.
236. **Rozas, J., and R. Rozas.** 1995. DnaSP, DNA sequence polymorphism: an interactive program for estimating population genetics parameters from DNA sequence data. Comput Appl Biosci **11:**621-625.
237. **Ruchaud, S., M. Carmena, and W. C. Earnshaw.** 2007. Chromosomal passengers: conducting cell division. Nat Rev Mol Cell Biol **8:**798-812.
238. **Rudd, M. K., M. G. Schueler, and H. F. Willard.** 2003. Sequence organization and functional annotation of human centromeres. Cold Spring Harb Symp Quant Biol **68:**141-149.

239. **Rudd, M. K., and H. F. Willard.** 2004. Analysis of the centromeric regions of the human genome assembly. Trends Genet **20:**529-533.
240. **Russo, V. E. A., T. Sommer, and J. A. A. Chambers.** 1985. A modified Vogel's medium for crossings, mating-type tests, and the isolation of female-sterile mutants of *Neurospora crassa*. Neurospora Newsl. **32:**10-11.
241. **Ryan, F. J., G. W. Beadle, and E. L. Tatum.** 1943. The tube method of measuring the growth rate of Neurospora. Am. J. Botany. **30:**784-799.
242. **Sakuno, T., K. Tada, and Y. Watanabe.** 2009. Kinetochore geometry defined by cohesion within the centromere. Nature **458:**852-858.
243. **Sanchez-Perez, I., S. J. Renwick, K. Crawley, I. Karig, V. Buck, J. C. Meadows, A. Franco-Sanchez, U. Fleig, T. Toda, and J. B. Millar.** 2005. The DASH complex and Klp5/Klp6 kinesin coordinate bipolar chromosome attachment in fission yeast. EMBO J **24:**2931-2943.
244. **Sanchez-Pulido, L., A. L. Pidoux, C. P. Ponting, and R. C. Allshire.** 2009. Common ancestry of the CENP-A chaperones Scm3 and HJURP. Cell **137:**1173-1174.
245. **Sanei, M., R. Pickering, K. Kumke, S. Nasuda, and A. Houben.** 2011. Loss of centromeric histone H3 (CENH3) from centromeres precedes uniparental chromosome elimination in interspecific barley hybrids. Proc Natl Acad Sci U S A **108:**E498-505.
246. **Sanyal, K., M. Baum, and J. Carbon.** 2004. Centromeric DNA sequences in the pathogenic yeast Candida albicans are all different and unique. Proc Natl Acad Sci U S A **101:**11374-11379.
247. **Sanyal, K., and J. Carbon.** 2002. The CENP-A homolog CaCse4p in the pathogenic yeast Candida albicans is a centromere protein essential for chromosome transmission. Proc Natl Acad Sci U S A **99:**12969-12974.
248. **Sato, H., F. Masuda, Y. Takayama, K. Takahashi, and S. Saitoh.** 2012. Epigenetic inactivation and subsequent heterochromatinization of a centromere stabilize dicentric chromosomes. Curr Biol **22:**658-667.
249. **Saunders, D. G., Y. F. Dagdas, and N. J. Talbot.** 2010. Spatial uncoupling of mitosis and cytokinesis during appressorium-mediated plant infection by the rice blast fungus Magnaporthe oryzae. Plant Cell **22:**2417-2428.
250. **Schittenhelm, R. B., F. Althoff, S. Heidmann, and C. F. Lehner.** 2010. Detrimental incorporation of excess Cenp-A/Cid and Cenp-C into Drosophila centromeres is prevented by limiting amounts of the bridging factor Cal1. J Cell Sci **123:**3768-3779.
251. **Schleiffer, A., M. Maier, G. Litos, F. Lampert, P. Hornung, K. Mechtler, and S. Westermann.** 2012. CENP-T proteins are conserved centromere receptors of the Ndc80 complex. Nat Cell Biol **14:**604-613.
252. **Schroeder, A. L.** 1986. Chromosome instability in mutagen sensitive mutants of *Neurospora*. Curr. Genet. **10:**381-387.
253. **Schueler, M. G., A. W. Higgins, M. K. Rudd, K. Gustashaw, and H. F. Willard.** 2001. Genomic and genetic definition of a functional human centromere. Science **294:**109-115.
254. **Schueler, M. G., W. Swanson, P. J. Thomas, and E. D. Green.** 2010. Adaptive evolution of foundation kinetochore proteins in primates. Mol Biol Evol **27:**1585-1597.

255. **Schuh, M., C. F. Lehner, and S. Heidmann.** 2007. Incorporation of Drosophila CID/CENP-A and CENP-C into centromeres during early embryonic anaphase. Curr Biol **17:**237-243.
256. **Screpanti, E., A. De Antoni, G. M. Alushin, A. Petrovic, T. Melis, E. Nogales, and A. Musacchio.** 2011. Direct Binding of Cenp-C to the Mis12 Complex Joins the Inner and Outer Kinetochore. Current Biology **21:**391-398.
257. **Sealse, T. W.** 1972. Super suppressors in Neurospora crassa I. Induction, genetic localization and relationship to a missense suppressor. Genetics **70:**385-396.
258. **Sekulic, N., E. A. Bassett, D. J. Rogers, and B. E. Black.** 2010. The structure of (CENP-A-H4)(2) reveals physical features that mark centromeres. Nature **467:**347-351.
259. **Selker, E. U.** 1990. Premeiotic instability of repeated sequences in *Neurospora crassa*. Annu. Rev. Genet. **24:**579-613.
260. **Sgarlata, C., and J. Perez-Martin.** 2005. Inhibitory phosphorylation of a mitotic cyclin-dependent kinase regulates the morphogenesis, cell size and virulence of the smut fungus Ustilago maydis. J Cell Sci **118:**3607-3622.
261. **Shaner, N. C., R. E. Campbell, P. A. Steinbach, B. N. Giepmans, A. E. Palmer, and R. Y. Tsien.** 2004. Improved monomeric red, orange and yellow fluorescent proteins derived from Discosoma sp. red fluorescent protein. Nat Biotechnol **22:**1567-1572.
262. **Shang, W. H., T. Hori, A. Toyoda, J. Kato, K. Popendorf, Y. Sakakibara, A. Fujiyama, and T. Fukagawa.** 2010. Chickens possess centromeres with both extended tandem repeats and short non-tandem-repetitive sequences. Genome Res **20:**1219-1228.
263. **Sharp, J. A., A. A. Franco, M. A. Osley, and P. D. Kaufman.** 2002. Chromatin assembly factor I and Hir proteins contribute to building functional kinetochores in S. cerevisiae. Genes Dev **16:**85-100.
264. **Shelby, R. D., O. Vafa, and K. F. Sullivan.** 1997. Assembly of CENP-A into centromeric chromatin requires a cooperative array of nucleosomal DNA contact sites. J Cell Biol **136:**501-513.
265. **Shepperd, L. A., J. C. Meadows, A. M. Sochaj, T. C. Lancaster, J. Zou, G. J. Buttrick, J. Rappsilber, K. G. Hardwick, and J. B. Millar.** 2012. Phosphodependent recruitment of Bub1 and Bub3 to Spc7/KNL1 by Mph1 kinase maintains the spindle checkpoint. Curr Biol **22:**891-899.
266. **Shi, J., S. E. Wolf, J. M. Burke, G. G. Presting, J. Ross-Ibarra, and R. K. Dawe.** 2010. Widespread gene conversion in centromere cores. PLoS Biol **8:**e1000327.
267. **Shibata, F., and M. Murata.** 2004. Differential localization of the centromere-specific proteins in the major centromeric satellite of Arabidopsis thaliana. J Cell Sci **117:**2963-2970.
268. **Shiroiwa, Y., T. Hayashi, Y. Fujita, A. Villar-Briones, N. Ikai, K. Takeda, M. Ebe, and M. Yanagida.** 2011. Mis17 is a regulatory module of the Mis6-Mal2-Sim4 centromere complex that is required for the recruitment of CenH3/CENP-A in fission yeast. PLoS One **6:**e17761.
269. **Shiu, P. K., N. B. Raju, D. Zickler, and R. L. Metzenberg.** 2001. Meiotic silencing by unpaired DNA. Cell **107:**905-916.

270. **Shiu, P. K., D. Zickler, N. B. Raju, G. Ruprich-Robert, and R. L. Metzenberg.** 2006. SAD-2 is required for meiotic silencing by unpaired DNA and perinuclear localization of SAD-1 RNA-directed RNA polymerase. Proc Natl Acad Sci U S A **103:**2243-2248.
271. **Shivaraju, M., J. R. Unruh, B. D. Slaughter, M. Mattingly, J. Berman, and J. L. Gerton.** 2012. Cell-cycle-coupled structural oscillation of centromeric nucleosomes in yeast. Cell **150:**304-316.
272. **Smith, K. M., J. M. Galazka, P. A. Phatale, L. R. Connolly, and M. Freitag.** 2012. Centromeres of filamentous fungi. Chromosome Res **20:**635-656.
273. **Smith, K. M., P. A. Phatale, C. M. Sullivan, K. R. Pomraning, and M. Freitag.** 2011. Heterochromatin is required for normal distribution of Neurospora crassa CenH3. Mol Cell Biol **31:**2528-2542.
274. **Stajich, J. E., M. L. Berbee, M. Blackwell, D. S. Hibbett, T. Y. James, J. W. Spatafora, and J. W. Taylor.** 2009. The fungi. Curr Biol **19:**R840-845.
275. **Steiner, N. C., K. M. Hahnenberger, and L. Clarke.** 1993. Centromeres of the fission yeast *Schizosaccharomyces pombe* are highly variable genetic loci. Mol Cell Biol **13:**4578-4587.
276. **Stimpson, K. M., and B. A. Sullivan.** 2011. Histone H3K4 methylation keeps centromeres open for business. EMBO J **30:**233-234.
277. **Stoler, S., K. C. Keith, K. E. Curnick, and M. Fitzgerald-Hayes.** 1995. A mutation in CSE4, an essential gene encoding a novel chromatin-associated protein in yeast, causes chromosome nondisjunction and cell cycle arrest at mitosis. Genes Dev **9:**573-586.
278. **Stoler, S., K. Rogers, S. Weitze, L. Morey, M. Fitzgerald-Hayes, and R. E. Baker.** 2007. Scm3, an essential Saccharomyces cerevisiae centromere protein required for G2/M progression and Cse4 localization. Proc Natl Acad Sci U S A **104:**10571-10576.
279. **Strandberg, R., K. Nygren, A. Menkis, T. Y. James, L. Wik, J. E. Stajich, and H. Johannesson.** 2010. Conflict between reproductive gene trees and species phylogeny among heterothallic and pseudohomothallic members of the filamentous ascomycete genus Neurospora. Fungal Genet Biol **47:**869-878.
280. **Sullivan, B. A., and G. H. Karpen.** 2004. Centromeric chromatin exhibits a histone modification pattern that is distinct from both euchromatin and heterochromatin. Nat Struct Mol Biol **11:**1076-1083.
281. **Sullivan, K. F., M. Hechenberger, and K. Masri.** 1994. Human CENP-A contains a histone H3 related histone fold domain that is required for targeting to the centromere. J Cell Biol **127:**581-592.
282. **Sullivan, S. A., and D. Landsman.** 2003. Characterization of sequence variability in nucleosome core histone folds. Proteins **52:**454-465.
283. **Sun, X., H. D. Le, J. M. Wahlstrom, and G. H. Karpen.** 2003. Sequence analysis of a functional Drosophila centromere. Genome Res **13:**182-194.
284. **Sun, X., J. Wahlstrom, and G. Karpen.** 1997. Molecular structure of a functional Drosophila centromere. Cell **91:**1007-1019.
285. **Szewczyk, E., T. Nayak, C. E. Oakley, H. Edgerton, Y. Xiong, N. Taheri-Talesh, S. A. Osmani, and B. R. Oakley.** 2006. Fusion PCR and gene targeting in Aspergillus nidulans. Nat Protoc **1:**3111-3120.

286. **Tachiwana, H., W. Kagawa, T. Shiga, A. Osakabe, Y. Miya, K. Saito, Y. Hayashi-Takanaka, T. Oda, M. Sato, S. Y. Park, H. Kimura, and H. Kurumizaka.** 2011. Crystal structure of the human centromeric nucleosome containing CENP-A. Nature **476:**232-235.
287. **Tachiwana, H., and H. Kurumizaka.** 2011. Structure of the CENP-A nucleosome and its implications for centromeric chromatin architecture. Genes Genet Syst **86:**357-364.
288. **Tachiwana, H., A. Osakabe, T. Shiga, Y. Miya, H. Kimura, W. Kagawa, and H. Kurumizaka.** 2011. Structures of human nucleosomes containing major histone H3 variants. Acta Crystallogr D Biol Crystallogr **67:**578-583.
289. **Tada, K., H. Susumu, T. Sakuno, and Y. Watanabe.** 2011. Condensin association with histone H2A shapes mitotic chromosomes. Nature **474:**477-483.
290. **Takahashi, K., E. S. Chen, and M. Yanagida.** 2000. Requirement of Mis6 centromere connector for localizing a CENP-A-like protein in fission yeast. Science **288:**2215-2219.
291. **Takahashi, K., S. Murakami, Y. Chikashige, H. Funabiki, O. Niwa, and M. Yanagida.** 1992. A low copy number central sequence with strict symmetry and unusual chromatin structure in fission yeast centromere. Mol Biol Cell **3:**819-835.
292. **Takahashi, K., Y. Takayama, F. Masuda, Y. Kobayashi, and S. Saitoh.** 2005. Two distinct pathways responsible for the loading of CENP-A to centromeres in the fission yeast cell cycle. Philos Trans R Soc Lond B Biol Sci **360:**595-606; discussion 606-597.
293. **Takayama, Y., H. Sato, S. Saitoh, Y. Ogiyama, F. Masuda, and K. Takahashi.** 2008. Biphasic incorporation of centromeric histone CENP-A in fission yeast. Mol Biol Cell **19:**682-690.
294. **Talbert, P. B., T. D. Bryson, and S. Henikoff.** 2004. Adaptive evolution of centromere proteins in plants and animals. J Biol **3:**18.
295. **Talbert, P. B., and S. Henikoff.** 2010. Centromeres convert but don't cross. PLoS Biol **8:**e1000326.
296. **Talbert, P. B., R. Masuelli, A. P. Tyagi, L. Comai, and S. Henikoff.** 2002. Centromeric localization and adaptive evolution of an Arabidopsis histone h3 variant. Plant Cell **14:**1053-1066.
297. **Tamaru, H., and E. U. Selker.** 2001. A histone H3 methyltransferase controls DNA methylation in Neurospora crassa. Nature **414:**277-283.
298. **Tamaru, H., X. Zhang, D. McMillen, P. B. Singh, J. Nakayama, S. I. Grewal, C. D. Allis, X. Cheng, and E. U. Selker.** 2003. Trimethylated lysine 9 of histone H3 is a mark for DNA methylation in Neurospora crassa. Nat Genet **34:**75-79.
299. **Tamura, K., J. Dudley, M. Nei, and S. Kumar.** 2007. MEGA4: Molecular Evolutionary Genetics Analysis (MEGA) software version 4.0. Mol Biol Evol **24:**1596-1599.
300. **Tanaka, K.** 2012. Regulatory mechanisms of kinetochore-microtubule interaction in mitosis. Cell Mol Life Sci.
301. **Tanaka, K., H. L. Chang, A. Kagami, and Y. Watanabe.** 2009. CENP-C functions as a scaffold for effectors with essential kinetochore functions in mitosis and meiosis. Dev Cell **17:**334-343.

302. **Tanaka, T. U., and A. Desai.** 2008. Kinetochore-microtubule interactions: the means to the end. Curr Opin Cell Biol **20:**53-63.
303. **Tanizawa, H., O. Iwasaki, A. Tanaka, J. R. Capizzi, P. Wickramasinghe, M. Lee, Z. Fu, and K. Noma.** 2010. Mapping of long-range associations throughout the fission yeast genome reveals global genome organization linked to transcriptional regulation. Nucleic Acids Res **38:**8164-8177.
304. **Therman, E., C. Trunca, E. M. Kuhn, and G. E. Sarto.** 1986. Dicentric chromosomes and the inactivation of the centromere. Hum Genet **72:**191-195.
305. **Tjong, H., K. Gong, L. Chen, and F. Alber.** 2012. Physical tethering and volume exclusion determine higher-order genome organization in budding yeast. Genome Res **22:**1295-1305.
306. **Topp, C. N., R. J. Okagaki, J. R. Melo, R. G. Kynast, R. L. Phillips, and R. K. Dawe.** 2009. Identification of a maize neocentromere in an oat-maize addition line. Cytogenet Genome Res **124:**228-238.
307. **Topp, C. N., C. X. Zhong, and R. K. Dawe.** 2004. Centromere-encoded RNAs are integral components of the maize kinetochore. Proc Natl Acad Sci U S A.
308. **Torras-Llort, M., S. Medina-Giro, O. Moreno-Moreno, and F. Azorin.** 2010. A conserved arginine-rich motif within the hypervariable N-domain of Drosophila centromeric histone H3 (CenH3) mediates BubR1 recruitment. PLoS One **5:**e13747.
309. **Trazzi, S., G. Perini, R. Bernardoni, M. Zoli, J. C. Reese, A. Musacchio, and G. Della Valle.** 2009. The C-terminal domain of CENP-C displays multiple and critical functions for mammalian centromere formation. PLoS One **4:**e5832.
310. **Tsukahara, T., Y. Tanno, and Y. Watanabe.** 2010. Phosphorylation of the CPC by Cdk1 promotes chromosome bi-orientation. Nature **467:**719-723.
311. **Ugarkovic, D. I.** 2009. Centromere-competent DNA: structure and evolution. Prog Mol Subcell Biol **48:**53-76.
312. **Vafa, O., and K. F. Sullivan.** 1997. Chromatin containing CENP-A and alpha-satellite DNA is a major component of the inner kinetochore plate. Curr Biol **7:**897-900.
313. **van Berkum, N. L., E. Lieberman-Aiden, L. Williams, M. Imakaev, A. Gnirke, L. A. Mirny, J. Dekker, and E. S. Lander.** 2010. Hi-C: a method to study the three-dimensional architecture of genomes. J Vis Exp.
314. **Verdaasdonk, J. S., and K. Bloom.** 2011. Centromeres: unique chromatin structures that drive chromosome segregation. Nat Rev Mol Cell Biol **12:**320-332.
315. **Vermaak, D., H. S. Hayden, and S. Henikoff.** 2002. Centromere targeting element within the histone fold domain of Cid. Mol Cell Biol **22:**7553-7561.
316. **Villasante, A., J. P. Abad, and M. Mendez-Lago.** 2007. Centromeres were derived from telomeres during the evolution of the eukaryotic chromosome. Proc Natl Acad Sci U S A **104:**10542-10547.
317. **Walker, G. M.** 1982. Cell cycle specificity of certain antimicrotubular drugs in Schizosaccharomyces pombe. J Gen Microbiol **128:**61-71.

318. **Warburton, P. E., C. A. Cooke, S. Bourassa, O. Vafa, B. A. Sullivan, G. Stetten, G. Gimelli, D. Warburton, C. Tyler-Smith, K. F. Sullivan, G. G. Poirier, and W. C. Earnshaw.** 1997. Immunolocalization of CENP-A suggests a distinct nucleosome structure at the inner kinetochore plate of active centromeres. Curr Biol **7:**901-904.
319. **Watanabe, N., H. Arai, J. Iwasaki, M. Shiina, K. Ogata, T. Hunter, and H. Osada.** 2005. Cyclin-dependent kinase (CDK) phosphorylation destabilizes somatic Wee1 via multiple pathways. Proc Natl Acad Sci U S A **102:**11663-11668.
320. **Watanabe, Y.** 2012. Geometry and force behind kinetochore orientation: lessons from meiosis. Nat Rev Mol Cell Biol **13:**370-382.
321. **Watanabe, Y.** 2006. A one-sided view of kinetochore attachment in meiosis. Cell **126:**1030-1032.
322. **Welburn, J. P., M. Vleugel, D. Liu, J. R. Yates, 3rd, M. A. Lampson, T. Fukagawa, and I. M. Cheeseman.** 2010. Aurora B phosphorylates spatially distinct targets to differentially regulate the kinetochore-microtubule interface. Mol Cell **38:**383-392.
323. **Wendland, J.** 2001. Comparison of morphogenetic networks of filamentous fungi and yeast. Fungal Genet Biol **34:**63-82.
324. **Wieland, G., S. Orthaus, S. Ohndorf, S. Diekmann, and P. Hemmerich.** 2004. Functional complementation of human centromere protein A (CENP-A) by Cse4p from Saccharomyces cerevisiae. Mol Cell Biol **24:**6620-6630.
325. **Williams, J. S., T. Hayashi, M. Yanagida, and P. Russell.** 2009. Fission yeast Scm3 mediates stable assembly of Cnp1/CENP-A into centromeric chromatin. Mol Cell **33:**287-298.
326. **Wratting, D., A. Thistlethwaite, M. Harris, L. A. Zeef, and C. B. Millar.** 2012. A conserved function for the H2A.Z C terminus. J Biol Chem **287:**19148-19157.
327. **Wu, Y., S. Kikuchi, H. Yan, W. Zhang, H. Rosenbaum, A. L. Iniguez, and J. Jiang.** 2011. Euchromatic subdomains in rice centromeres are associated with genes and transcription. Plant Cell **23:**4054-4064.
328. **Xiao, H., G. Mizuguchi, J. Wisniewski, Y. Huang, D. Wei, and C. Wu.** 2011. Nonhistone Scm3 binds to AT-rich DNA to organize atypical centromeric nucleosome of budding yeast. Mol Cell **43:**369-380.
329. **Yamagishi, Y., C. H. Yang, Y. Tanno, and Y. Watanabe.** 2012. MPS1/Mph1 phosphorylates the kinetochore protein KNL1/Spc7 to recruit SAC components. Nat Cell Biol **14:**746-752.
330. **Yan, H., W. Jin, K. Nagaki, S. Tian, S. Ouyang, C. R. Buell, P. B. Talbert, S. Henikoff, and J. Jiang.** 2005. Transcription and histone modifications in the recombination-free region spanning a rice centromere. Plant Cell **17:**3227-3238.
331. **Yeadon, J. P., and D. E. A. Catcheside.** 1996. Quick method for producing template for PCR from Neurospora cultures Fungal Genetics Newsl. **43:**71.
332. **Zhang, H., and R. K. Dawe.** 2012. Total centromere size and genome size are strongly correlated in ten grass species. Chromosome Res **20:**403-412.

333. **Zhang, R., S. T. Liu, W. Chen, M. Bonner, J. Pehrson, T. J. Yen, and P. D. Adams.** 2007. HP1 proteins are essential for a dynamic nuclear response that rescues the function of perturbed heterochromatin in primary human cells. Mol Cell Biol **27:**949-962.

334. **Zhou, Z., H. Feng, B. R. Zhou, R. Ghirlando, K. Hu, A. Zwolak, L. M. Miller Jenkins, H. Xiao, N. Tjandra, C. Wu, and Y. Bai.** 2011. Structural basis for recognition of centromere histone variant CenH3 by the chaperone Scm3. Nature **472:**234-237.